

Progress in Methodologies for the Assessment of Passive Safety System Reliability in Advanced Reactors

*Results from the Coordinated Research
Project on Development of Advanced
Methodologies for the Assessment of
Passive Safety Systems Performance in
Advanced Reactors*

**IAEA**

International Atomic Energy Agency

PROGRESS IN METHODOLOGIES
FOR THE ASSESSMENT OF PASSIVE
SAFETY SYSTEM RELIABILITY IN
ADVANCED REACTORS

The following States are Members of the International Atomic Energy Agency:

AFGHANISTAN	GHANA	OMAN
ALBANIA	GREECE	PAKISTAN
ALGERIA	GUATEMALA	PALAU
ANGOLA	HAITI	PANAMA
ARGENTINA	HOLY SEE	PAPUA NEW GUINEA
ARMENIA	HONDURAS	PARAGUAY
AUSTRALIA	HUNGARY	PERU
AUSTRIA	ICELAND	PHILIPPINES
AZERBAIJAN	INDIA	POLAND
BAHAMAS	INDONESIA	PORTUGAL
BAHRAIN	IRAN, ISLAMIC REPUBLIC OF	QATAR
BANGLADESH	IRAQ	REPUBLIC OF MOLDOVA
BELARUS	IRELAND	ROMANIA
BELGIUM	ISRAEL	RUSSIAN FEDERATION
BELIZE	ITALY	RWANDA
BENIN	JAMAICA	SAN MARINO
BOLIVIA	JAPAN	SAUDI ARABIA
BOSNIA AND HERZEGOVINA	JORDAN	SENEGAL
BOTSWANA	KAZAKHSTAN	SERBIA
BRAZIL	KENYA	SEYCHELLES
BRUNEI DARUSSALAM	KOREA, REPUBLIC OF	SIERRA LEONE
BULGARIA	KUWAIT	SINGAPORE
BURKINA FASO	KYRGYZSTAN	SLOVAKIA
BURUNDI	LAO PEOPLE'S DEMOCRATIC	SLOVENIA
CAMBODIA	REPUBLIC	SOUTH AFRICA
CAMEROON	LATVIA	SPAIN
CANADA	LEBANON	SRI LANKA
CENTRAL AFRICAN	LESOTHO	SUDAN
REPUBLIC	LIBERIA	SWAZILAND
CHAD	LIBYA	SWEDEN
CHILE	LIECHTENSTEIN	SWITZERLAND
CHINA	LITHUANIA	SYRIAN ARAB REPUBLIC
COLOMBIA	LUXEMBOURG	TAJIKISTAN
CONGO	MADAGASCAR	THAILAND
COSTA RICA	MALAWI	THE FORMER YUGOSLAV
CÔTE D'IVOIRE	MALAYSIA	REPUBLIC OF MACEDONIA
CROATIA	MALI	TOGO
CUBA	MALTA	TRINIDAD AND TOBAGO
CYPRUS	MARSHALL ISLANDS	TUNISIA
CZECH REPUBLIC	MAURITANIA, ISLAMIC	TURKEY
DEMOCRATIC REPUBLIC	REPUBLIC OF	UGANDA
OF THE CONGO	MAURITIUS	UKRAINE
DENMARK	MEXICO	UNITED ARAB EMIRATES
DOMINICA	MONACO	UNITED KINGDOM OF
DOMINICAN REPUBLIC	MONGOLIA	GREAT BRITAIN AND
ECUADOR	MONTENEGRO	NORTHERN IRELAND
EGYPT	MOROCCO	UNITED REPUBLIC
EL SALVADOR	MOZAMBIQUE	OF TANZANIA
ERITREA	MYANMAR	UNITED STATES OF AMERICA
ESTONIA	NAMIBIA	URUGUAY
ETHIOPIA	NEPAL	UZBEKISTAN
FIJI	NETHERLANDS	VENEZUELA, BOLIVARIAN
FINLAND	NEW ZEALAND	REPUBLIC OF
FRANCE	NICARAGUA	VIET NAM
GABON	NIGER	YEMEN
GEORGIA	NIGERIA	ZAMBIA
GERMANY	NORWAY	ZIMBABWE

The Agency's Statute was approved on 23 October 1956 by the Conference on the Statute of the IAEA held at United Nations Headquarters, New York; it entered into force on 29 July 1957. The Headquarters of the Agency are situated in Vienna. Its principal objective is "to accelerate and enlarge the contribution of atomic energy to peace, health and prosperity throughout the world".

**PROGRESS IN METHODOLOGIES
FOR THE ASSESSMENT OF PASSIVE
SAFETY SYSTEM RELIABILITY IN
ADVANCED REACTORS**

**RESULTS FROM THE COORDINATED RESEARCH PROJECT
ON DEVELOPMENT OF ADVANCED METHODOLOGIES
FOR THE ASSESSMENT OF PASSIVE SAFETY SYSTEMS
PERFORMANCE IN ADVANCED REACTORS**

COPYRIGHT NOTICE

All IAEA scientific and technical publications are protected by the terms of the Universal Copyright Convention as adopted in 1952 (Berne) and as revised in 1972 (Paris). The copyright has since been extended by the World Intellectual Property Organization (Geneva) to include electronic and virtual intellectual property. Permission to use whole or parts of texts contained in IAEA publications in printed or electronic form must be obtained and is usually subject to royalty agreements. Proposals for non-commercial reproductions and translations are welcomed and considered on a case-by-case basis. Enquiries should be addressed to the IAEA Publishing Section at:

Marketing and Sales Unit, Publishing Section
International Atomic Energy Agency
Vienna International Centre
PO Box 100
1400 Vienna, Austria
fax: +43 1 2600 29302
tel.: +43 1 2600 22417
email: sales.publications@iaea.org
<http://www.iaea.org/books>

For further information on this publication, please contact:

Nuclear Power Technology Development Section
International Atomic Energy Agency
Vienna International Centre
PO Box 100
1400 Vienna, Austria
Email: Official.Mail@iaea.org

© IAEA, 2014
Printed by the IAEA in Austria
September 2014

IAEA Library Cataloguing in Publication Data

Progress methodologies for the assessment of passive safety system reliability in advanced reactors. — Vienna : International Atomic Energy Agency, 2014.
p. : 30 cm. — (IAEA-TECDOC series, ISSN 1011-4289 ; no. 1752)
ISBN 978-92-0-108614-3
Includes bibliographical references.

1. Nuclear reactors — Safety measures. 2. Nuclear reactors — Design and construction. 3. System safety. I. International Atomic Energy Agency. II. Series.

FOREWORD

Strong reliance on inherent and passive design features has become a hallmark of many advanced reactor designs, including several evolutionary designs and nearly all advanced small and medium sized reactor (SMR) designs. Advanced nuclear reactor designs incorporate several passive systems in addition to active ones — not only to enhance the operational safety of the reactors but also to eliminate the possibility of serious accidents. Accordingly, the assessment of the reliability of passive safety systems is a crucial issue to be resolved before their extensive use in future nuclear power plants. Several physical parameters affect the performance of a passive safety system, and their values at the time of operation are unknown a priori. The functions of passive systems are based on basic physical laws and thermodynamic principals, and they may not experience the same kind of failures as active systems. Hence, consistent efforts are required to qualify the reliability of passive systems.

To support the development of advanced nuclear reactor designs with passive systems, investigations into their reliability using various methodologies are being conducted in several Member States with advanced reactor development programmes. These efforts include reliability methods for passive systems by the French Atomic Energy and Alternative Energies Commission, reliability evaluation of passive safety system by the University of Pisa, Italy, and assessment of passive system reliability by the Bhabha Atomic Research Centre, India. These different approaches seem to demonstrate a consensus on some aspects. However, the developers of the approaches have been unable to agree on the definition of reliability in a passive system. Based on these developments and in order to foster collaboration, the IAEA initiated the Coordinated Research Project (CRP) on Development of Advanced Methodologies for the Assessment of Passive Safety Systems Performance in Advanced Reactors in 2008.

The objective of the CRP was to determine a common method for reliability assessment of passive safety system performance. Such a method would facilitate the application of risk informed approaches in design optimization and safety qualification of future advanced reactors, thereby contributing to their enhanced safety levels and improved economics. Five Member States participated, representing seven research institutes and organizations in Argentina, France, India, Italy and the Russian Federation.

This publication is the outcome of the different tasks performed and extensive discussions held in the technical meetings, and summarizes the information provided by the technical experts within the CRP over the four year period.

The IAEA wishes to thank all the experts who contributed to the preparation and review of this publication. The IAEA officers responsible for this publication were M.H. Subki of the Division of Nuclear Power and A. Lyubarskiy of the Division of Nuclear Installation Safety.

EDITORIAL NOTE

This publication has been prepared from the original material as submitted by the contributors and has not been edited by the editorial staff of the IAEA. The views expressed remain the responsibility of the contributors and do not necessarily represent the views of the IAEA or its Member States.

Neither the IAEA nor its Member States assume any responsibility for consequences which may arise from the use of this publication. This publication does not address questions of responsibility, legal or otherwise, for acts or omissions on the part of any person.

The use of particular designations of countries or territories does not imply any judgement by the publisher, the IAEA, as to the legal status of such countries or territories, of their authorities and institutions or of the delimitation of their boundaries.

The mention of names of specific companies or products (whether or not indicated as registered) does not imply any intention to infringe proprietary rights, nor should it be construed as an endorsement or recommendation on the part of the IAEA.

The IAEA has no responsibility for the persistence or accuracy of URLs for external or third party Internet web sites referred to in this publication and does not guarantee that any content on such web sites is, or will remain, accurate or appropriate.

CONTENTS

SUMMARY	1
1. INTRODUCTION.....	3
1.1. Background	3
1.2. Objectives.....	6
1.3. Scope of the CRP.....	6
1.4. Scope of the report.....	8
2. ELABORATION OF REQUIREMENTS TO THE METHOD OF RELIABILITY ASSESSMENT OF PASSIVE SAFETY SYSTEMS	9
2.1. Important issues pertaining to passive system reliability assessment methodologies.....	9
2.2. Goals of the methodology being developed	10
2.3. Steps in the methodology.....	11
2.3.1. Description and characterization of the system	11
2.3.2. Identification of the physical phenomena relevant to the operation of the system	12
2.3.3. Identification of the parameters influencing physical phenomena	12
2.3.4. Identification of components and events influencing the above mentioned parameters.....	12
2.3.5. Identification of failure modes and failure mechanisms, and characterization of the criteria.....	13
2.3.6. Qualification level of analytical tools.....	13
2.3.7. Uncertainty quantification of the parameters influencing physical phenomena	14
2.3.8. Propagation of uncertainties and quantification of reliability	14
2.3.9. Summary of steps in the methodology	14
3. RELIABILITY ASSESSMENT METHODOLOGIES	15
3.1. RELIABILITY METHODS FOR PASSIVE SAFETY FUNCTIONS (RMPS)	15
3.1.1. Definition of accident scenario	16
3.1.2. System characterizations	17
3.1.3. System modelling.....	17
3.1.4. Identification of sources of uncertainty	18
3.1.5. Identification of relevant parameters.....	18
3.1.6. Uncertainty quantification	18
3.1.7. Sensitivity analysis.....	19
3.1.8. Reliability evaluations	20
3.1.9. Integration of passive system reliability in PSA	22
3.2. Enhanced methodology (RMPS+).....	23
3.3. Assessment of Passive System Reliability (APSRA).....	26
3.4. Reliability assessment using generic PSA approaches.....	29
3.4.1. Approach based on independent failure modes	30
3.4.2. Approach based on failure modes of passive system hardware components	31
3.4.3. Functional failure approach	32

4.	VALIDATION OF METHODOLOGIES USING TESTS ON L2 NATURAL CIRCULATION LOOP	34
4.1.	Description of L2 test facility.....	34
4.2.	Validation performed by CNEA, Argentina	35
4.2.1.	Model development	35
4.2.2.	Loop dynamics	40
4.2.3.	Performance indicator	43
4.3.	Validation performed by BARC, India	46
4.3.1.	Nodalization scheme and node sensitivity test	47
4.3.2.	Results & discussions	48
4.4.	Validation performed by University of Pisa, Italy	52
4.4.1.	Application of REPAS/RMPS to L2 natural circulation loop	52
5.	DEVELOPMENT AND APPLICATION OF METHODS TO MINIMIZE NUMBER OF CALCULATIONS	61
5.1.	Introduction	61
5.2.	Adjoint operator approach.....	63
5.2.1.	Adjoint methods for sensitivity and reliability analysis	63
5.2.2.	Adjoint operator formulation	64
5.3.	Algorithmic differentiation	74
5.3.1.	Adjoint/reverse computation methods for response surface generation.....	74
5.3.2.	Automatic differentiation of programs	75
5.3.3.	Monte Carlo sampling with code	76
5.3.4.	Monte Carlo sampling with response surface	78
5.3.5.	Computational efficiency.....	78
5.3.6.	Application to passive heat transport loop.....	79
5.3.7.	Importance of Monte Carlo simulation results	82
5.3.8.	Response surface Monte Carlo simulation results	83
5.4.	Application of response conditioning method to SGDHRs	85
6.	COMPARISON OF DIFFERENT METHODOLOGIES FOR A BENCHMARK PROBLEM OF ISOLATION CONDENSER	101
6.1.	Benchmarking performed by CNEA, Argentina	101
6.1.1.	Models developed	101
6.1.2.	Performance evaluation of IC in case of a station black-out	104
6.1.3.	Performance evaluation of IC and MPIS in case of a SB-LOCA+SBO.....	116
6.2.	Benchmarking performed by BARC, India	129
6.2.1.	Details of the ALWR system	129
6.2.2.	Application of APSRA for reliability assessment of passive decay heat removal system of ALWR.....	129
6.3.	Benchmarking performed by ENEA, Italy.....	148
6.3.1.	Approach based on independent failure modes	148
7.	UNCERTAINTY CALCULATIONS ON PHENIX NATURAL CONVECTION TEST.....	160
7.1.	PHENIX reactor	161
7.2.	Validation performed by CEA, France	163

7.2.1.	Probabilistic model.....	164
7.2.2.	Uncertainty propagation	164
7.2.3.	Characteristics of the output distribution.....	165
7.2.4.	Global sensitivity analysis	167
7.3.	Validation performed by IGCAR, India	178
7.3.1.	1-D Modelling features.....	178
7.3.2.	Analysis of results	178
8.	CONCLUSIONS.....	183
8.1.	Conclusions from BARC, India regarding validation of methodologies using tests on L2 natural circulation loop	183
8.2.	Conclusions from the university of Pisa, Italy regarding validation of methodologies using tests on L2 natural circulation loop.....	184
8.3.	Conclusions regarding application of response conditioning method to SGDHRs	184
8.4.	Conclusions from CNEA, Argentina regarding comparison of different methodologies for a benchmark problem of isolation condenser.....	185
8.5.	Conclusions from BARC, India regarding comparison of different methodologies for a benchmark problem of isolation condenser.....	185
8.6.	Conclusions regarding uncertainty calculations on the PHENIX natural convection test.....	185
APPENDIX I PASSIVE SAFETY SYSTEMS IN ADVANCED SMALL MODULAR REACTORS		
		187
I.1.	AHWR300-LEU (Bhabha Atomic Research Centre, India).....	187
I.2.	CAREM-25 (National Atomic Energy Commission, Argentina).....	190
I.3.	SMART (Korea Atomic Energy Research Institute, Republic of Korea).....	193
I.4.	NUSCALE (NuScale Power, Inc., USA).....	195
I.5.	MPOWER (B&W Generation mPower Inc., USA).....	198
I.6.	ACP100 (China National Nuclear Corporation, China).....	199
I.7.	INTERNATIONAL REACTOR INNOVATIVE AND SECURE (IRIS International Consortium)	200
APPENDIX II SET OF DEFINITIONS FOR RELIABILITY ASSESSMENT OF PASSIVE SAFETY SYSTEMS		
		203
APPENDIX III FRAMEWORK FOR CREATING A DATABANK TO GENERATE PROBABILITY DENSITY FUNCTIONS		
		207
REFERENCES.....		
		216
ABBREVIATIONS.....		
		220
CONTRIBUTORS TO DRAFTING AND REVIEW.....		
		223

SUMMARY

As part of the IAEA's overall effort to foster international collaborations that strive to improve the economics and safety of future nuclear power plants, an IAEA Co-ordinated Research Programme (CRP) on 'Development of Advanced Methodologies for the Assessment of Passive Safety System Performance in Advanced Reactors' was started in 2008. The CRP I31018 was carried out through research agreements or research contracts with participating institutions and included four research coordination meetings (RCMs) held on 31 March – 3 April 2009, 16 – 19 March 2010, 26 – 28 April 2011, and 24 – 26 April 2012 respectively at the IAEA headquarters in Vienna.

A total of eleven (11) experts from the seven research institutes and organization of the five Member States (CNEA, Argentina; CEA, France; UNIPI and ENEA, Italy; BARC and IGCAR, India and OKB Gidropress, Russian Federation) participated in the CRP I31018.

Within the framework of the development of advanced nuclear technologies, the reliability of passive systems has become an important subject and area under discussion, for their extensive use in future nuclear power plants. The efforts conducted so far to deal with and evaluate the reliability of passive safety systems (as the thermal-hydraulic passive systems), being implemented in advanced water cooled reactors design, has aroused an amount of open issues; those need to be addressed. The main objective of the CRP was to determine a common analysis-and-test method for reliability assessment of passive safety systems of advanced small reactors. The specific research objectives of this CRP were:

- To identify the scope of application and common requirements for a technology-neutral methodology for reliability assessment of passive systems for advanced NPPs;
- To work out a consensus set of definitions relevant to reliability assessment of the passive systems and their treatment by PSA;
- To identify a set of common benchmark problems to compare and validate methodologies for reliability assessment of passive systems, including such issues as systematic failure modes and effects analysis (FMEA), component failure rates, treatment of dependencies in fault tree (FT) models, impact from internal and external hazards, etc.;
- To perform trial applications of various approaches to reliability assessment of selected benchmark problems, with evaluation of uncertainties;
- To perform comparative analysis of the results and work out suggestions for a common analysis-and-test based approach;
- To identify necessary R&D, e.g. related to further development and validation of best estimate and computational fluid dynamics codes for passive system performance analysis against experimental benchmarks for natural and mixed convection.

In order to support the above objectives of the following different tasks were performed during the CRP.

- Elaboration of requirements to the method of reliability assessment of passive safety systems;
- Elaboration of a set of definitions for reliability assessment of passive safety systems and their treatment by PSA;
- Validation of methodologies using tests on the L2 natural circulation loop;

- Development of a benchmark problem, and development and application of efficient methods to minimize the number of calculations needed for reliability assessment of passive safety systems;
- Comparison of different methodologies for reliability assessment of passive safety system on the benchmark problem of an isolation condenser of light water cooled reactor (LWCR), developed by ENEA;
- Development of a framework for a databank of probability density functions for process parameters.

The present publication under the title of ‘Progress in Methodologies for the Assessment of Passive Safety System Reliability in Advanced Reactors’ is the outcome of the above tasks performed by the experts within the CRP.

The principal conclusion of this CRP is there is a clear need to obtain more data, especially related to thermal hydraulics. This necessitated additional development, testing and research. It is essential that passive and evolutionary components, Common Cause Failures (CCF) of high redundancy systems and intersystem CCF of such reactors are adequately addressed. The technical challenges for advanced reactors also include the potential need to address very different systems and phenomenology, the potential unavailability of important reliability and experimental data, the potential unavailability of knowledge on new key phenomena, and the potential unavailability of accident analysis models.

The other broad based conclusions are derived from the CRP are as follows:

- Failure of passive components and structures now more important in advanced reactor designs. The new and advanced methodologies described in the report for the assessment of passive safety system reliability are considered as important tools and approaches to achieve improved safety for the future advanced nuclear power plants and particular attention should be paid to the status of development of the methodologies and the obtained results.
- The general consensus was that a more practical approach would be very helpful for the robust design and qualification of advanced nuclear reactors. The further promotion of international collaboration which needs to be enhanced in order to model the unique features of new reactors in key areas such as digital/software based instrumentation and control (I&C) reliability and passive system high degree reliability modelling.
- Passive systems and passive PSA are becoming more and more important as technology evolves. The key element as to furthering development and use of passive systems is the decision to proceed with licensing and construction of an advanced reactor design.
- Facilitate information exchange and promote international collaborative research and development in the area of advanced nuclear reactor technologies needed to meet, in a sustainable manner, the increasing energy demands of the 21st century.

The specific conclusions of the individual analyses/studies are presented inside their concerned topics of the report.

1. INTRODUCTION

1.1. BACKGROUND

Advanced nuclear reactor designs incorporate several passive systems in addition to active one, not only to enhance the operational safety of the reactors but also to eliminate the possibility of hypothetical severe accidents.

While the wording ‘passive safety design options’ denotes various possible combinations of inherent and passive safety features and reasonable combinations of active and passive systems incorporated in reactor design, these are the passive systems, such as those incorporating moving fluids or expanding solid structures, direct action devices, or stored energy sources (i.e. passive systems of categories B, C, and D defined in [1]), that generally require validation and testing to demonstrate and prove their reliable operation and, if necessary, adjust their design. While individual process are well understood, the combinations of these processes, which define actual performance of such systems, may vary depending on changes in the conditions of state, boundary conditions and failure or malfunctioning of components within the system, the circuit or the plant. Therefore, the issue of process performance reliability becomes important for passive systems [2].

Different from category B, C, and D passive system mentioned above, there is a consensus that inherent safety features or category A passive systems (passive components that incorporate no moving fluids or moving solid structures, direct action devices, or stored energy sources), once they eliminate, with a high degree of confidence, the initiating events (IE) of certain accidents or prevent these events from propagating into accidents, or prevent design basis accidents from propagating into severe accidents with major radioactivity releases, are of absolute merit [3, 4].

There are certain accomplishments regarding the testing, construction, licensing and validation of passive systems of B, C, or D types, such as Russian VVER-1000s and the KLT-40S, or the US AP1000 [1, 5]. Experimental-based deterministic approaches to the validation of passive systems including separate-effect tests and integral tests of reactor models with subsequent qualification of analysis models and computer codes have been established and accepted by the regulators in some countries, in line with conventional safety requirements also applied to active safety systems. The indicated deterministic approaches are generally successful with regulators when basic technology involved (e.g. that of water cooled reactors) is evolutionary, i.e. backed by many years of validation and testing and reactor operation experience, and when passive systems are reasonably conventional in their design. When the technology is innovative and passive systems have a somewhat non-conventional design, the application of established deterministic approaches may require multi-year efforts on validation, testing and demonstration of reliable operation of such systems, prior to licensing approval of the corresponding advanced NPP.

The regulations in Argentina, China, France, Germany, India, Japan, the Russian Federation, and the USA already make provisions for accepting the results of probabilistic safety assessments (PSAs) on a complementary or compulsory basis. In order to ensure that the PSA used in the risk-informed decision making (RIDM) process is of acceptable technical quality, the effort is being made in different countries to provide PSA standards that define inherent technical features of PSA acceptable for regulatory body. An example is ASME PRA Standard endorsed by the US NRC. In line with the worldwide trends, the IAEA is developing a series of publications in the Safety Standards Series on PSA and RIDM.

The general trend toward a more risk informed approach to design certification, which is pursued to permit a focus on what is really important from the safety perspective and to achieve a design that is more favourable from the cost–benefit perspective, could potentially result in a more competitive advanced nuclear power plant. To enable a risk informed approach to certification of reactor designs with passive systems, for which there is no operation experience that would provide statistical data for definition of the reliability parameters, a methodology for reliability assessment of the passive systems that would allow quantification of such reliability to treat both active and passive systems within a common PSA approach is required. Several such methodologies are available in France, India, Italy and the USA [6–8]; however, no consensus on a common approach has been established so far among their proponents. What is important from a perspective of the overall risk assessment, these methodologies take into account uncertainties associated with unforeseen physical phenomena that may affect the operation of passive systems, worsening their reliability.

The approach to assessment of reliability of plant systems when component operational data are available is generally established, being based on PSA techniques incorporating fault tree (FT) analysis with failure probability data of components constituting such systems, operator errors, and the uncertainty analysis [9, 10]. For new designs of passive safety systems, there is not operational evidence data that would allow classical statistical reliability analysis, therefore, performance reliability for category B passive systems (and, to varying extent, for category C and D passive systems) can be analysed taking into account the capability of combinations of passive processes to perform a safety function under a possible variation of multiple internal and external conditions that may affect such combinations in a time-dependent way. A notion of probability of failure is generally directly non-applicable to time-dependent variations of many of such conditions; therefore, a new and more complex approach is needed to assess and quantify reliability of such passive systems.

As an example, in the late 1990s, a methodology known as reliability evaluation of passive safety system (REPAS) was developed cooperatively by ENEA, the University of Pisa, the Polytechnic of Milan and the University of Rome in Italy that was later incorporated in the European Union's RMPS project. The RMPS methodology is based on the evaluation of a failure probability of a system to carry out the desired function for a given set of scenarios taking into account the uncertainties of those physical (epistemic) and geometric parameters the deviations of which can lead to a failure of the system. The RMPS approach considers a probability distribution of failure to treat variations of the comparative parameters considered in the predictions of codes.

A different approach is followed in the assessment of passive system reliability (APSRA) methodology developed at BARC, India. In this approach, the failure surface is generated by considering the deviation of all those comparative parameters which influence the system performance. Then, the causes of deviation of these parameters are found through root diagnosis. It is attributed that deviation such physical parameters occurs only due to a failure of mechanical components such as valves, control systems, etc. Then, the probability of failure of a system is evaluated from the failure probability of these mechanical components through classical PSA treatment. Moreover, to reduce the uncertainty in code predictions, BARC makes use of the in-house experimental data from integral facilities as well as separate test effect tests.

During a dedicated IAEA Technical Meeting on 'Status Of Validation and Testing of Passive Systems for Small and Medium-Sized Reactors (SMRs)', June 2006, held with broad

representation of interested stakeholders, it was shown that the above mentioned different approaches seem to show a consensus on:

- The use of the 'functional failure' concept;
- The fact that there are two elements that may contribute to a failure of the expected performance: failure of the components in a system, and failure of a combination of the physical processes (failure of the physical process).

However, at the mentioned meeting, the developers of these two approaches have failed to find a consensus on the definition of a reliability of a thermal-hydraulic passive system according to a given scenario. It was the point of view of the stakeholders of RMPS (representatives from CEA, France) that it has no meaning to define an inherent reliability for a thermal-hydraulic (category B) passive system. BARC (India) thought the opposite. The RMPS stakeholders have expressed interest to analyse and study the definition of an inherent reliability of a thermal-hydraulic passive system if such a definition is proposed. They also commented that the RMPS methodology assumes the following two important facts:

- Even if, at the moment of a thermal-hydraulic passive system start-up, the initial and boundary conditions are beyond the design conditions, it is still possible that a safe state could be reached;
- In the case where, at the moment of a start-up, the initial and boundary conditions are within the design conditions, it is still possible that a safe state could not be reached, because passive phenomena could be very complex.

For the abovementioned two reasons, the RMPS stakeholders have introduced in the PSA model the probability of a physical process failure.

The CEA (France) viewpoint expressed at the IAEA technical meeting (June 2006) is that APSRA and RMPS are complementary in the following:

- APSRA incorporates an important effort on qualification of the model and use of the available experimental data. These aspects have not been studied in RMPS, given the context of this project.
- APSRA includes in the PSA model the failure of those components, which cause a deviation of the key parameters resulting in a system failure, but does not take into account the fact that the probability of failure of a physical process (actually, always of a combination of physical processes) could be different from unity.
- RMPS proposes to take into account in the PSA model the failure of a physical process. It is possible to treat such data (best estimate code plus uncertainty approach is suitable for this purpose).
- In fact, two different philosophies or approaches have been used in RMPS and APSRA, and the two developed methodologies are, therefore, different. At the same time, CEA concludes that certain parts of the APSRA and RMPS could be merged in order to obtain a more complete methodology.

The IAEA technical meeting mentioned previously also included presentations of other distinct approaches for reliability assessment of passive systems, such as the MIT approach

[8, 11], and also identified research teams that willing to participate in further development of such approaches. The general consensus was that a more practical approach would be very helpful for further design and qualification of advanced nuclear reactors.

Reflecting on these developments in Member States, the IAEA recommended coordinating a research project 'Development of advanced methodologies for the assessment of passive safety system performance in advanced reactors'.

1.2. OBJECTIVES

The overall objective was to achieve progress in the development of a common technology-neutral approach to the substantiation and evaluation of the reliability of passive safety systems, which would enable the application of risk-informed approaches to design optimization and safety qualification of advanced nuclear power plants (NPPs), contributing to their enhanced safety level and improved economics.

The specific research objectives of this coordinated research project (CRP) were:

- To identify the scope of application and common requirements for a technology-neutral methodology for reliability assessment of passive systems for advanced NPPs;
- To work out a consensus set of definitions relevant to reliability assessment of the passive systems and their treatment by PSA;
- To identify a set of common benchmark problems to compare and validate methodologies for reliability assessment of passive systems, including such issues as systematic failure modes and effects analysis (FMEA), component failure rates, treatment of dependencies in fault tree (FT) models, impact from internal and external hazards, etc.;
- To perform trial applications of various approaches to reliability assessment of selected benchmark problems, with evaluation of uncertainties;
- To perform comparative analysis of the results and work out suggestions for a common analysis-and-test based approach;
- To identify necessary R&D, e.g. related to further development and validation of best estimate and computational fluid dynamics codes for passive system performance analysis against experimental benchmarks for natural and mixed convection.

1.3. SCOPE OF THE CRP

The CRP was carried out through research agreements or research contracts with participating institutions and included four research coordination meetings (RCMs) held on 31 March – 3 April 2009, 16–19 March 2010, 26–28 April 2011, and 24–26 April 2012 respectively at the IAEA in Vienna. The scope of the CRP includes following different task;

- Elaboration of requirements to the method of reliability assessment of passive safety systems;
- Elaboration of a set of definitions for reliability assessment of passive safety systems and their treatment by PSA;

- Validation of methodologies using tests on the L2 natural circulation loop;
 - Preparatory activities, including issuance of initial problem suggestion and description of tests already performed;
 - Identification of important modifiable parameters and probability density functions (PDFs);
 - Identification of additional tests to be performed ;
 - Performance of tests;
 - Reliability evaluation based on test results;
 - Thermal-hydraulic codes' qualification and nodalization;
 - Identification of PDFs for other parameters (e.g. code uncertainties);
 - Performance of calculations;
 - Reliability evaluation based on calculation results.
- Development of a benchmark problem, and development and application of efficient methods to minimize the number of calculations needed for reliability assessment of passive safety systems;
 - Refine safety decay heat removal (SDHR) model specifications;
 - Elaborate the criteria and the scenario;
 - Selection of codes;
 - Perform automatic differentiation;
 - Perform reliability calculations and procedure results;
 - Explore open source;
 - Assemble and validate open source code;
 - Perform reliability calculations using assembled and validated open source code and produce results;
 - Develop Meta model;
 - Perform subset simulations for importance sampling using Monte-Carlo method;
 - Perform reliability calculations and produce results.
- Comparison of different methodologies for reliability assessment of passive safety system on the benchmark problem of an isolation condenser of light water cooled reactor (LWCR), developed by ENEA;
- Development of a framework for a databank of probability density functions for process parameters.

1.4.SCOPE OF THE REPORT

The present publication under the title of “Progress in Methodologies for the Assessment of Passive Safety System Reliability in Advanced Reactors” is the outcome of the different tasks and discussion performed and summaries the information provided by the technical experts for four years in the CRP I31018 on Development of Advanced Methodologies for the Assessment of Passive Safety System Performance in Advanced Reactors, as part of the IAEA’s overall effort to foster international collaborations that strive to improve the economics and safety of future nuclear power plants. The report also focuses on the different reliability assessment approaches, methodologies, analysis and evaluation of the results and technical challenges in the subject area. This report provides the insights resulting from the analysis on the technical issues associated with assessing the reliability of passive systems in the context of nuclear safety and probabilistic safety analysis, and a viable path towards the implementation of the research efforts in the related areas is delineated as well. The report is written; to facilitate information exchange and promote international collaborative research and development in the area of advanced nuclear reactor technologies needed to meet, in a sustainable manner, the increasing energy demands of the 21st century. The primary users of the report are utilities/operating organizations, governing organizations, researcher and developers, designer, or other who are or will be responsible for the process of selecting an advanced small reactor.

2. ELABORATION OF REQUIREMENTS TO THE METHOD OF RELIABILITY ASSESSMENT OF PASSIVE SAFETY SYSTEMS

2.1. IMPORTANT ISSUES PERTAINING TO PASSIVE SYSTEM RELIABILITY ASSESSMENT METHODOLOGIES

The reliability assessment methods of active components and systems have its origins in the quality control and associated statistical treatment. Failure of systems and components is based on stress-strength concept where a component or system fails if there is an unfavourable mismatch of stress and strength. To elaborate the point, let us consider a mechanical component produced in mass production, designed for certain nominal load using a material of certain nominal strength. Appropriate nominal dimensions required can be arrived using appropriate theory of failure. This does not ensure an absolutely reliable component, as components produced in mass production will have certain variability depending on the tolerances of production process. At the same time, the different components so produced in mass production even with minimal tolerances would not be subjected to identical loading conditions. As a result of this, certain components having unfavourable combination of dimensions and loading will give away during service. To accommodate the effect of variability, the statistical methods were developed that formed the basis for quality control as well as reliability assessment. The most important aspect of this approach is the use of probability distribution to accommodate the variability of parameters. Normal distribution is the one most commonly employed as the parameter owe their variability to multiple random variables like variability of a diameter of a shaft machined on lathe depends on feed rate, depth of cut, tool orientation, wear and tear of tool, operator skill and his state of mind etc. Variability associated with large number of parameters in random manner is considered to be best represented by normal distribution. Application of methods based on these principles is well established and has universal acceptance as far as the performance of mass production components is considered. However, the direct import of such methodology for passive system is disputable due to the very reason associated with causes of their failure.

Passive systems fail to perform their function in a satisfactory manner due to degradation of process conditions which provide the driving force. For example a natural circulation system may fail to remove the required amount of heat, if the system pressure changes beyond a certain value. The early developed methods for reliability assessment of passive systems are based on consideration of a probability distribution function for the various parameters affecting the system performance like geometrical parameters and operating parameters like pressure which is a key parameter. Consideration of probabilistic distribution for the geometrical parameters and material properties may have a rationale, whereas the application of the same for operating state appears untenable. Variation of operating pressure in a system of modern power plant with adequate sophistication cannot be ascribed an arbitrary probability distribution like the dimensions of mass produced component, rather it depends on the performance of various controllers. In view of this, statistical treatment using probabilistic distribution for the operating parameters deserves serious attention in context of passive system reliability assessment.

Another important problem plaguing the reliability assessment of passive system is the treatment of parameters in time domain i.e. application of generic failure frequencies with due consideration of mission time. It is well understood that the failure of passive system can always be traced to the failure of active components/systems like associated controllers, valves, and pumps etc., which lead to degraded conditions of process and reduced driving

force. This allows for assessment of passive system reliability on the basis of failure frequencies of such active components. The failure frequencies of such components are generally associated with the concept of binary state like, for example, a valve that fails to open can have fully open state as success and all other states as failure. However, in practice, a partially open valve may not lead to a failure of the passive system depending on the grace period available. For the shorter mission times, even a partially open valve may lead successful performance of passive system. In light of this, it appears that, a rational and acceptable method of reliability assessment of passive systems must consider the multiple states of active components.

2.2. GOALS OF THE METHODOLOGY BEING DEVELOPED

In view of the developments highlighted in the Introduction (section 1), the present CRP aimed at the development of a methodology to fulfil following requirements:

- To obtain a consensus on methodology for the reliability assessment of passive safety systems, to enable their treatment by PSA and comparison with active safety systems.

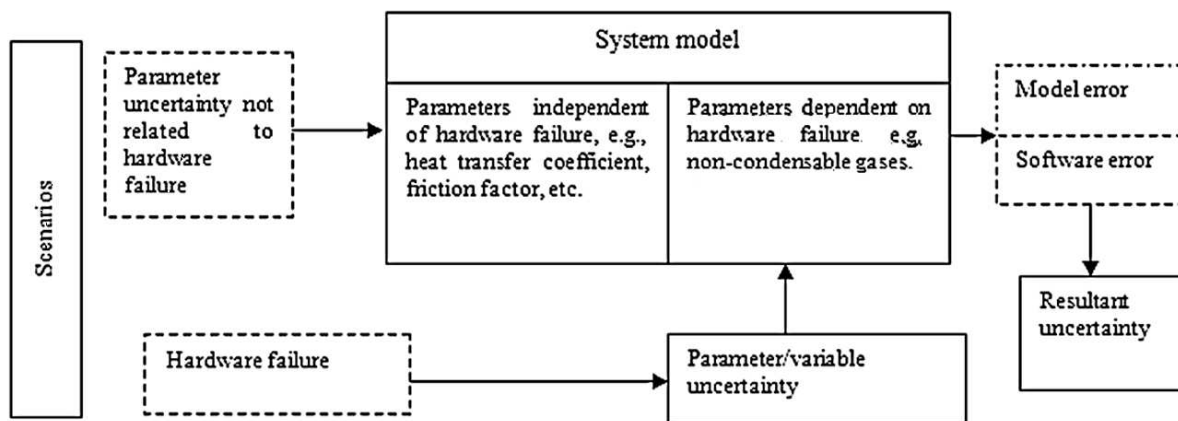
The methodology, being developed for advanced reactors, should:

- Cover all plausible scenarios with a potential of passive safety system functioning.

This is to ensure that not only a typical or more severe scenario is analysed but a range of scenarios which can lead to significant passive function failure needs to be covered. For example, station blackout condition, loss of heat sink, hardware pertaining to passive system failure etc. could be possible scenarios. Each scenario could yield reliability figure which could be combined or a vector of values could be used in applications.

- Take into account different kind of uncertainties in parameters, phenomena, hardware and software.

Since it is implicitly agreed that reliability of passive systems needs to be quantified, variability of key process parameters affecting the system performance should be treated correctly. The uncertainties can arise from a variety of sources for a passive system. Figure 1 is diagrammatic elaboration of the uncertainties and the uncertainty propagation model.



Boxes with dotted line represent statistical/epistemic uncertainty information input. Information from experiments is required to accurately quantify the contents of dotted boxes. Experimental information is thus required to quantify model error and parameter variability. Software error quantification would require tests and models. Hardware failure data is presumed to be available if it is part of conventional PSA activity.

FIG. 1. Uncertainties and uncertainty propagation model.

- Be accurate and efficient.

Easy to use methodologies are preferable as they would facilitate easy analysis and review and will have wider acceptability. However easiest of the methods may not be efficient and accurate. Therefore work needs to be done make efficient and accurate methods easy to use. For example, response surface based methods for uncertainty propagation are easy to use and efficient. They however may not be accurate. Advanced methodologies employing importance sampling and response conditioning are expected to be easy to use and accurate. However wider acceptability for these methods would involve development of automation tools so that they become easy to use.

- When applicable, meet licensing criteria.
- Assist in design optimization.
- Facilitate the application of a risk-informed approach to enable integration of passive system reliability into PSA.

An accurate quantitative metric for passive system performance will be helpful for a risk based application. However, a risk informed application would require more insights into passive system operation. For example sensitivity coefficients and failure margins with respect to most sensitive parameters could be useful.

- Consider time dependence of event sequences.
- Offer reliability indicator(s) allowing a comparison of passive and active safety systems.

The results of method application should allow clear and unambiguous interpretation.

2.3. STEPS IN THE METHODOLOGY

2.3.1. Description and characterization of the system

Description and characterization of the system includes the following necessary sub-steps/requirements:

- Identification of accident scenarios (external, internal events or combinations thereof) for which the interactions between a given passive system and other systems are important;

Knowledge of each scenario helps identifying the specific failure criteria and relevant parameters and the specific quantification of uncertainties. The results obtained in the reliability and sensitivity analyses of the passive system are thus specific to each scenario. A global evaluation of the passive system is obtained by the integration of its unreliability in a PSA, in which all the sequences involving the passive system are considered. This approach is preferred to conservative analyses consisting in evaluating the system reliability for the worst scenario considered or in integrating the larger variability of the uncertain parameters covering all the scenarios involving the system.

- Identification of the mission (safety function) of the passive system under consideration;
- Definition of the initial and boundary conditions.

The passive system under consideration must have a well-defined physical and geometrical configuration and associated objective function. The reliability assessment must be specific to that configuration and associated objective function. The intent is to differentiate the system

reliability under normal conditions from that of accidental conditions associated with impaired configuration.

2.3.2. Identification of the physical phenomena relevant to the operation of the system

Identification of the physical phenomena relevant to the operation of the system includes the following necessary sub-steps/requirements:

- Compilation of a comprehensive list of all phenomena related to the accident scenario;

For example, a buoyancy induced pump which drives natural circulation, operates due to density difference between hot and cold legs. As long as heat source and sinks are available, natural circulation always builds-in. However, the flow rate may not be sufficient to meet the desired objectives of the system, which can lead to:

- Inadequate removal of heat causing rise in clad surface temperature; or
- Occurrence of flow oscillations; or
- Occurrence of critical heat flux (CHF) with or without flow oscillations, etc.
- Adequate modelling of all identified phenomena in the selected code: Analytical tools chosen to simulate the system behaviour under postulated transient conditions must be able to capture the important physical phenomena associated with passive system.

2.3.3. Identification of the parameters influencing physical phenomena

Identification of the parameters influencing physical phenomena includes the following necessary sub-steps/requirements:

- Identification based on present knowledge and available information;
- Determination of inter-dependence of the parameters;
- Sensitivity/importance analysis;
- Basis for identification: codes and tests, expert judgement (EJ).

The methodology must identify the key parameters affecting the system performance. The parameters identified must be independent of each other and must have significant influence on the system performance. Their cause of deviation from nominal operational state must be ascribable. These key parameters must be established by a formal sensitivity analysis or by use of phenomena specific models or by expert elicitation in case of commonly deployed engineering applications.

These sensitivity measures give a ranking of input parameters. This information provides guidance as to where to improve the state of knowledge in order to reduce the output uncertainties most effectively, to steer research and development efforts, or better understand the modelling or to obtain a good confidence in the results.

2.3.4. Identification of components and events influencing the above mentioned parameters

Identification of components and events influencing the above mentioned parameters includes the following necessary sub-steps/requirements:

- Active or passive components that are part of the system;

- Active or passive components that are not part of the system;
- External and internal events and their combinations.

All the associated system and components having bearing on the performance of passive system must be identified like associated controllers, heat exchangers, pumps and valves, malfunction of which could lead to deviation of key parameters affecting passive system from their nominal values.

2.3.5. Identification of failure modes and failure mechanisms, and characterization of the criteria

Identification of failure modes and failure mechanisms, and characterization of the criteria includes the following necessary sub-steps/requirements:

- Options available to identify failure modes (FMEA, HAZOP, codes);
- Success/failure criteria: deterministic or probabilistic.

Appropriate failure criteria consistent with the objective function of the passive system must be assigned. Failure criteria can be established as single-targets (e.g. the system must deliver a specific quantity of liquid within a fixed time) or as a function of time targets or integral values over a mission time (e.g. the system must reject at least a mean value of thermal power during the entire system intervention).

In these cases, the failure criterion is obtained by the comparison between the real performance of the system and the expected value of this performance. In some cases, it is better to define a global failure criterion for the whole system instead of a specific criterion for the passive system. For instance the failure criterion can be based on the maximal clad temperature during a specified period. In this case, it will be necessary to have modelled the complete system and not only the passive system.

Failure criteria definition needs more attention as this step has direct influence on the quantitative results and meaning of the result. That is, whether failure is ultimate failure with respect to radioactivity release or failure with respect to some performance index (serviceability) which is not likely to lead to radio activity release. The failure criteria used for reliability analysis needs to be consistent with the criteria used for deterministic analysis. This is desirable from a review/regulatory perspective as well. Very few transients seen in the life of a reactor may cause temperature limits of critical structure to approach melting point. But many of the transients cause temperature to rise modestly but they may lead to cumulative damage of structures. This aspect may have to be factored in the failure criteria definition.

- Criteria for the selection of adequate performance indicators;
- Provisions for inclusion of human factors.

2.3.6. Qualification level of analytical tools

Qualification level of analytical tools includes the following necessary sub-steps/requirements:

- Range of validation of the code (on the results of both, separate effect and integral tests) should cover the range of parameters under both normal and abnormal conditions;
- All identified phenomena should be adequately modelled in the code;

- Uncertainty of code prediction should be quantified through verification and validation;
- Uncertainty quantification of relationships and physical models used in analytical tools.

2.3.7. Uncertainty quantification of the parameters influencing physical phenomena

Uncertainty quantification of the parameters influencing physical phenomena includes the following necessary sub-steps/requirements:

- A weak point is the absence of unambiguous rules and validated data for the assignment of probability distributions to parameters;
- Inclusion of a formal expert judgement (EJ) protocol to estimate distributions is necessary for parameters whose values are either sparse or not available;
- A data bank to generate probability density functions for parameters would be useful;
- Inter-dependence of parameters;
- Sensitivity analysis;
- Use of the efficient sensitivity analysis techniques is necessary to estimate the impact of changes in the input parameter distributions on the reliability estimates;
- Additional tests to reduce high uncertainty of important parameters.

2.3.8. Propagation of uncertainties and quantification of reliability

Different methods exist for propagating the uncertainties and for quantifying the reliability of a passive safety system (direct simulation, determination of response surface, adjoint methods, first and second order reliability methods, etc.). The selected methods should be:

- Efficient, which means the number of calculations with a thermal-hydraulic code must be minimized.
- Accurate, which means bias or error introduced by methods must be evaluated and results must be given with confidence intervals.

2.3.9. Summary of steps in the methodology

Steps described in sections 2.3.7 and 2.3.8 are the crucial steps differentiating the existing methodologies. RMPS relies on considering uncertainty of the model/code and the key parameters by assigning the probability density function to the key parameters of the system and key variable of the models employed. On the other hand, APSRA considers the uncertainty assessment of code/model on the basis of experimental validation. As far as the uncertainty associated with the key parameters is concerned, APSRA attributes the variability of key parameters to the functional failure of associated active/passive systems riding on the passive system under consideration.

3. RELIABILITY ASSESSMENT METHODOLOGIES

3.1. RELIABILITY METHODS FOR PASSIVE SAFETY FUNCTIONS (RMPS)

Advanced reactor concepts make use of passive safety features to a large extent in combination with active safety or operational systems. According to the IAEA definitions [1], a passive system does not need external input, especially energy to operate. That is why passive systems are expected to combine among others, the advantages of simplicity, a decrease in the need for human interaction and a reduction or avoidance of external electrical power or signals.

Besides the open feedback on economic competitiveness, special aspects like lack of data on some phenomena, missing operating experience over the wide range of conditions, and driving forces which are smaller in most cases than in active safety systems, must be taken into account.

This remark is especially applicable to category B or C passive systems (i.e. implementing moving working fluid, following the IAEA classification [1]) and in particular to the passive systems that utilize natural circulation. These passive safety systems in their designs rely on natural forces to perform their accident prevention and mitigation functions once actuated and started. These driving forces are not generated by external power sources (e.g. pumped systems), as is the case of operating and evolutionary reactor designs. Because the magnitude of the natural forces, which drive the operation of passive systems, is relatively small, counter-forces (e.g. friction) can be of comparable magnitude and cannot be ignored as it is generally the case with systems including pumps. Moreover, there are considerable uncertainties associated with factors, which depend on the magnitude of these forces and counter forces (e.g. values of heat transfer coefficients and pressure losses). In addition, the magnitude of such natural driving forces depends on specific plant conditions and configurations, which could exist when a system is called upon to perform its safety function. All these uncertainties affect the thermal-hydraulic (T-H) performance of the passive systems.

To assess the impact of uncertainties on the predicted performance of a passive system, a large number of calculations with best estimate T-H codes are needed. If all the sequences involving a passive system are considered, the number of calculations can be prohibitive. For all these reasons, it appeared necessary to create a specific methodology to assess the reliability of category B or C passive systems. The methodology has been developed within the framework of a project called reliability methods for passive safety functions (RMPS), performed under the auspices of the European 5th Framework Programme [6]. The methodology addresses the following issues:

- Identification and quantification of the sources of uncertainties and determination of the important variables;
- Propagation of the uncertainties through T-H models and assessment of T-H passive system unreliability;
- Introduction of passive system unreliability in the accident sequence analysis.

The proposed methodology consists of several steps, which are shown in FIG. 2 and are detailed as follows:

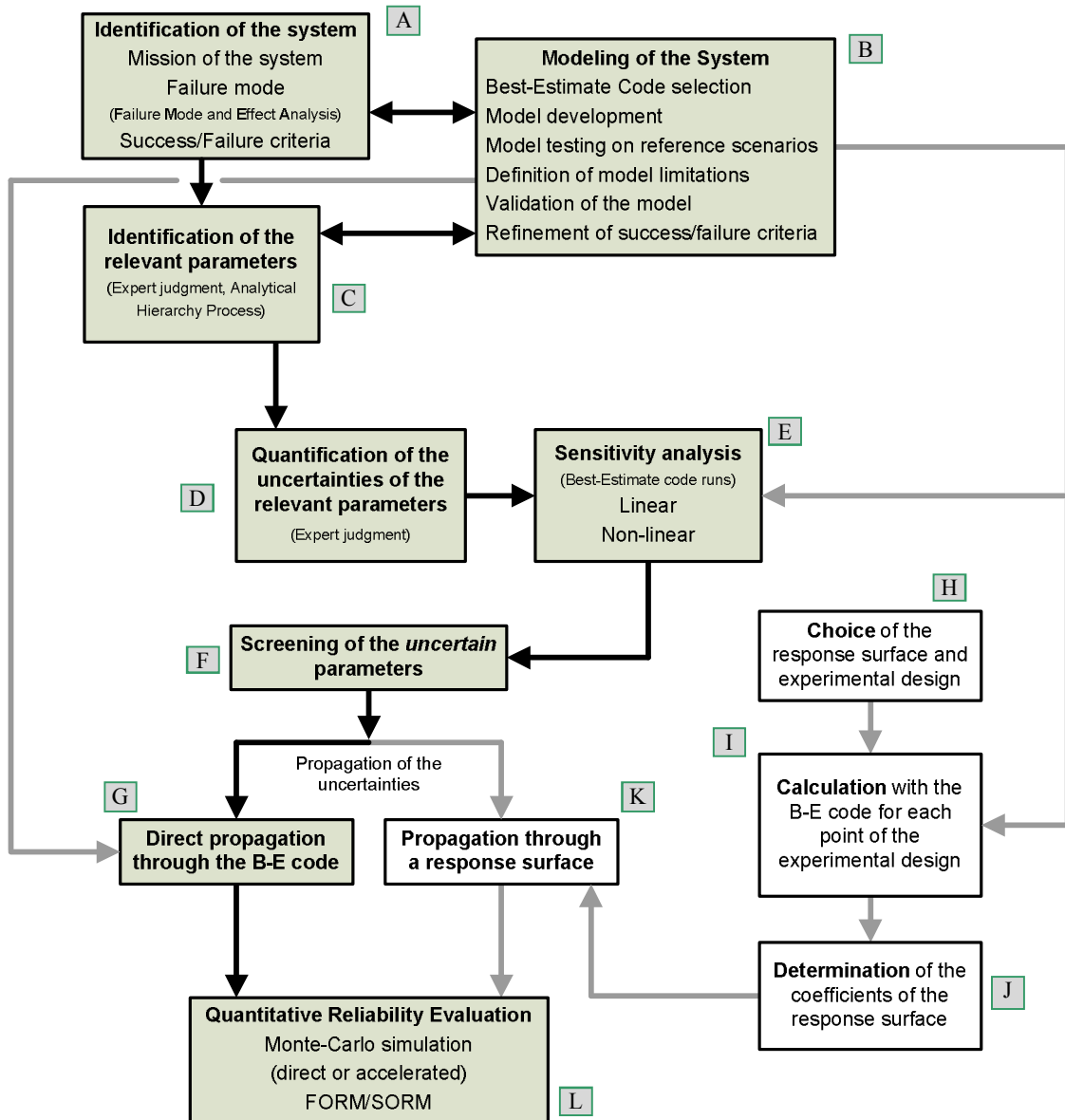


FIG. 2. RMPS methodology flowchart.

3.1.1. Definition of accident scenario

The first step of the methodology is the definition of the accident scenario in which a passive system is expected to operate. Knowledge of each scenario helps identifying the specific failure criteria and relevant parameters and the specific quantification of uncertainties. The results obtained in the reliability and sensitivity analyses of a passive system are thus specific to each scenario. A global evaluation of a passive system is obtained by the integration of its unreliability in a probabilistic safety assessment, in which all the sequences involving a passive system are considered. This approach is preferred to conservative analyses, which evaluate the system reliability for the worst scenario considered or by integrating the larger variability of the uncertain parameters covering all the scenarios involving the system.

3.1.2. System characterizations

The purpose of this analysis is to obtain information on the behaviour of a passive system in an accident scenario occurring during the life of a nuclear reactor, and to identify the failure zones and conditions if it exists. Therefore, the missions of the system, its failure modes and the failure criteria must be defined.

3.1.2.1.Mission(s) of the system

The missions of the system are the goals for which a passive system has been designed and located within the overall system. For instance, the mission of a passive system can be decay heat removal, vessel cooling, pressure decrease of the primary circuit, etc. In some cases, a passive system can be designed to fulfil several missions at the same time or different missions depending on the considered scenario.

3.1.2.2.Failure mode

Due to the complexity of T-H phenomena, and complex interaction between the passive system and the overall system, it is not always obvious to associate a failure mode to the mission of the system. A qualitative analysis is often necessary so as to identify potential failure modes and their consequences, associated with a passive system operation. A hazard identification qualitative method such as the FMEA can be used to identify the parameters judged critical for the performance of a passive system and to help associate failure modes and corresponding indicators of a failure cause. This method can necessitate the introduction of a 'virtual' component, in addition to mechanical components of the system (piping, drain valve, etc.). This component is identified as natural circulation and is evaluated in terms of potential 'phenomenological' factors (such as non-condensable gas build up, thermal stratification, surface oxidation, cracking, etc.), whose consequences can affect a passive system performance.

3.1.2.3.Success/failure criteria

Knowledge of system missions and failure modes allows the evaluation of failure criteria. The failure criteria can be established in terms of exceeding/not exceeding given thresholds set on relevant physical quantities over given time periods (e.g. mission times). Some examples include: exceeding a limit pressure in the primary system during the first 24 hours after the beginning of the scenario, or not removing more than a given fraction of residual energy produced during the same time period. In some cases, it is better to define a global failure criterion for the whole system instead of a specific criterion for a passive system. For instance, the failure criterion can be based on the peak cladding temperature during a specified period. In this case, it will be necessary to model the complete system and not only a passive system.

3.1.3. System modelling

Due to the lack of suitable experimental databases for passive systems in operation, the evaluation must rely on numerical modelling. The system analysis must be carried out with a qualified T-H system code and performing best estimate calculations. Indeed, there is an increasing interest in computational reactor safety analysis to replace the conservative evaluation model calculations by best estimate calculations supplemented by a quantitative uncertainty analysis [12]. Particularly in the present methodology, where the objective is the passive system reliability evaluation, it is important to simulate a passive system performance

in a realistic and not conservative way. At this stage, calculations have to be carried out on the reference case with nominal values of the system characteristic parameters. The results have to be compared with experimental data if exists. During the characterisation process, the modelling and the evaluation of the passive system, new failure modes can be identified (such as flow oscillations, plug phenomena due to non-condensable gases, etc.), which must also be taken into account.

3.1.4. Identification of sources of uncertainty

First of all, the method requires the identification of the potentially important contributors to uncertainty. These contributors are:

- Approximations in modelling physical process: for instance, the treatment of a liquid-steam mixture as a homogeneous fluid, the use of empirical correlations, etc.;
- Approximations in modelling system geometry: simplification of complex geometry features and approximation of three-dimensional systems;
- The input variables: initial and boundary conditions such as plant temperatures, pressures, water levels and reactor power, dimensions, physical properties such as densities, conductivities, specific heats, and thermal-hydraulic parameters such as heat transfer coefficients or friction factors.

This identification of the relevant parameters must be based on expert opinions. Different methodologies have been developed to evaluate the overall uncertainty in the physical model predictions and some efforts have been made for the internal uncertainty assessment capacity of T-H codes [13]. In real applications, the reliability assessment should also include this type of uncertainty.

3.1.5. Identification of relevant parameters

The evaluation of the reliability of a passive system requires the identification of the relevant parameters, which really affect the system goal accomplishment. The tool initially chosen for this task was the analytic hierarchy process [14, 15]. This method consists of three major steps i.e. building of a hierarchy to decompose the problem at hand, the input of pair-wise comparison judgments regarding the relevance of the considered parameters, and the computation of priority vectors to obtain their ranking. Other deductive approaches have been used within the framework of the applications concerning new concepts of reactors under development [16].

3.1.6. Uncertainty quantification

A key issue in this methodology is the selection of distributions for the input parameters. The main objective is that the selected distribution for each input parameter must quantify the state of knowledge and express the reliable and available information about a parameter. The choice of distribution may highly affect the reliability evaluations of a passive system. The following points have to be considered for this quantification:

3.1.6.1. The amount of data

When the data on a parameter are abundant, statistical methods can be used such as the maximum likelihood method or the method of moments to adjust analytical density functions. Different goodness-of-fit tests can be used (Chi square, Kolmogorov, etc.) to find the best

analytical fit to the data. When the data are sparse or non-existent, which is generally the case when we consider the uncertainties affecting a passive system performance, the evaluation of the probability functions of the uncertain parameters must be based on expert judgement. In the case where no preferences can be justified, a uniform distribution can be specified, i.e. each value between minimum and maximum is equally likely. These distributions are quantitative expressions of the state of knowledge and can be modified if there is new evidence. If suitable observations become available, they can be used consistently to update the distributions.

3.1.6.2. Dependence between parameters

If parameters have common contributors to their uncertainty, the respective states of knowledge are dependent. As a consequence of this dependence, values of different parameters cannot be combined freely and independently. Instances of such limitations need to be identified and the dependencies need to be quantified, if judged to be potentially important. If the analyst knows dependencies between parameters explicitly, multivariate distributions or conditional probability distributions may be used. The dependence between the parameters can also be introduced by covariance matrices or by functional relations between the parameters.

3.1.7. Sensitivity analysis

3.1.7.1. Objectives

An important feature of the methodology is to evaluate the sensitivity of reliability driving output variables (pressure, removed power, etc.) with respect to input uncertain parameters. The sensitivity measures give a ranking of input parameters. This information provides guidance as to where to improve the state of knowledge in order to reduce the output uncertainties most effectively. If experimental results are available to be compared with calculations, the sensitivity measures provide guidance as to where to improve the models of the computer code.

3.1.7.2. Qualitative sensitivity analysis

Sometimes the lack of operational experience and significant data concerning the passive system performance forces the analysis to be performed in a qualitative way aiming at the identification, for each failure mode, of both the level of uncertainty associated with the phenomenon and the sensitivity of failure probability to that phenomenon [17]. For example, even if a phenomenon is highly uncertain because of deficiencies in the physical modeling, this may not be important for the overall failure probability. On the other hand, a phenomenon may be well understood (therefore the uncertainty is small), but the failure probability may be sensitive to small variation in this parameter. The worst case is characterized by 'high' rankings relative to sensitivity or uncertainty (e.g. presence of non-condensable gas or thermal stratification), making the corresponding phenomena evaluation a critical challenge.

3.1.7.3. Quantitative sensitivity analysis

The quantitative sensitivity analysis necessitates T-H calculations. It consists of ranking the parameters according to their relative contribution on the overall code response uncertainty and quantifying this contribution for each parameter. To apportion the variation in the output to the different input parameters, many techniques can be used [18], each yielding different measures of sensitivity.

A common approach is to base the sensitivity analysis on a linear regression method, which is based on the hypothesis of a linear relation between response and input parameters. This, in case of passive systems is obviously restrictive. However, the method is simple and quick, and provides useful insights in case of a restricted number of sampling. Three different sensitivity coefficients have been considered and each one providing slightly different information on the relevance of a parameter: standardized regression coefficients (SRC), partial correlation coefficients (PCC) and correlation coefficients (CC). Small differences between the different coefficients may be due to a certain degree of correlation between the inputs and to the system's non-linearity. These occurrences should be analysed, the first one possibly through the examination of the correlation matrix and the second one by calculating the model coefficient of determination R^2 .

Depending on the nature of the model representing the passive system operation and calculating its performances, the use of sensitivity methods developed for non-monotonous or non-linear models are considered to be more accurate.

In case of non-linear but monotonous models, we perform rank transformations and calculate associated indices i.e. standardized rank regression coefficients (SRRCs) and partial rank correlation coefficients (PRCCs). The rank transformation is a simple procedure, which involves replacing the data with their corresponding ranks. We can also calculate a determination coefficient based on the rank R^{2*} . The R^{2*} will be higher than the R^2 in case of non-linear models. The difference between R^2 and R^{2*} is a useful indicator of non-linearity of the model. For non-linear and non-monotonous models, two methods exist i.e. the Fourier amplitude sensitivity test (FAST) and the Sobol method.

The main idea of these methods is to decompose the total variance of the response to express sensitivity through variance, and to evaluate how the variance of such an input or group of inputs contributes into variance of the output. The Sobol indices are calculated by Monte-Carlo simulation. The problem of these methods, and specially the Sobol method, is that a good estimation of these indices requires a great number of calculations (i.e. 10000 simulations). Thus, it is necessary first to calculate a response surface validated in the domain of variation of the random variables. Thus, if the model is really not linear, nor monotonous, we propose to:

- Adjust non-linear models on the data,
- Test the validity of the model (e.g. in calculating R^2 , residues, predictive robustness),
- Use the model as a response surface in order to evaluate the Sobol or FAST indices.

3.1.8. Reliability evaluations

Different methods can be used to quantify the reliability of a passive system once a best estimate T-H code and a model of the system are given. The failure function of a passive system according to a specified mission is given by:

$$M = \text{relevant output variable} - \text{threshold} = g(X_1, X_2, \dots, X_n) \quad (1)$$

Where X_i ($i=1, \dots, n$) are the n basic random variables (input parameters), and $g(\cdot)$ is the functional relationship between the random variables and the failure of the system. The failure function can be defined in such a way that the limit state, or failure surface, is given by $M = 0$. The failure event is defined as the space where $M \leq 0$, and the success event is defined as

the space where $M > 0$. Thus a probability of failure can be evaluated by the following integral:

$$P_f = \int \int \dots \int f_X(x_1, x_2, \dots, x_n) dx_1 dx_2 \dots dx_n \quad (2)$$

Where f_X is the joint density function of X_1, X_2, \dots, X_n , and the integration is performed over the region where $M \leq 0$. Because each of the basic random variables has a unique distribution and because they interact, the integral (Eq. 2) cannot be easily evaluated. Two types of methods can be used to estimate the failure probability i.e. Monte Carlo simulation with or without variance reduction techniques, and first and second order reliability methods (FORM/SORM).

3.1.8.1. Direct Monte Carlo

Direct Monte Carlo simulation techniques [19] can be used to estimate the failure probability defined in Eq. 2. Monte Carlo simulations consist in drawing samples of the basic variables according to their probabilistic characteristics and then feeding them into the failure function. An estimate $\overline{P_f}$ of the probability of failure P_f can be found in dividing the number of simulation cycles in which $g(.) \leq 0$, by the total number of simulation cycles N . As N approaches infinity, $\overline{P_f}$ approaches the true failure probability. It is recommended to measure the statistical accuracy of the estimated failure probability by computing its variation coefficient (ratio of standard deviation to average of estimations). The smaller the variation coefficient, the better will be the accuracy of the estimated failure probability. For a small number of simulation cycles, the variance of $\overline{P_f}$ can be quite large. Consequently, it may take a large number of simulation cycles to achieve a good accuracy. The computational time needed for the direct Monte Carlo method will then be high, since each simulation cycle involves a long calculation (several hours) performed by a T-H code.

3.1.8.2. Variance reduction techniques

Variance reduction techniques offer an increase in the efficiency and accuracy of the simulation-based assessment of passive system reliability for a relatively small number of simulation cycles [18, 19]. Different variance reduction techniques exist, such as importance sampling, stratified sampling, Latin hypercube sampling (LHS), conditional expectation, directional simulation, etc.

3.1.8.3. FORM/SORM

An alternative to the Monte Carlo simulation is the use of first/second order reliability methods (FORM/SORM) [20–22]. They consist of 4 steps:

- Transformation of space of basic random variables X_1, X_2, \dots, X_n into a space of standard normal variables;
- Searching for the point of minimum distance from the origin to the limit state surface (this point is called the design point);
- Approximation by a first/second order surface of the real failure surface near the design point;

- Computation of the failure probability corresponding to the approximated failure surface.

FORM and SORM apply only to problems where the set of basic variables are continuous. For small probabilities FORM/SORM are extremely efficient when compared to other simulation methods. The drawbacks of these methods come from the difficulty in identifying the design point when the failure surface is not sufficiently smooth, and from the fact that, contrary to Monte Carlo method, there is no direct way to estimate the accuracy of the provided estimation.

3.1.8.4. Response surface methods

To avoid the problem of long computational times in the previous methods, it is interesting to approximate the response $Y=g(X)$ given by the T-H code, in the space of the input random variables, by a simple mathematical model $\tilde{g}(X)$ known as response surface. Experiments are conducted with the basic random variables X_1, X_2, \dots, X_n for a sufficient number of times to define the response surface to the level of accuracy desired. Each experiment can be represented by a point with coordinates $x_{1j}, x_{2j}, \dots, x_{nj}$ in an n-dimensional space. At each point, a value of y_j is calculated by the T-H code and the unknown coefficients of the response surface $\tilde{g}(X)$ are determined in such a way that the error is minimal in the region of interest. When a response surface has been determined, the passive system reliability can be easily assessed by using the Monte Carlo simulation. Different types of response surfaces can be fitted such as polynomial, thin plate splines, neural networks, generalized linear model, partial least squares regression, etc. The type of response surface will be chosen depending on the problem [23]. In any case, the response surface is just an approximation to the real model, and the error committed in such approximation should be taken into account in the final reliability estimate.

3.1.9. Integration of passive system reliability in PSA

The objective of this part of the methodology is the development of a consistent approach for introducing passive system reliability in an accident sequence in a PSA. So far, in existing advanced nuclear reactor PSAs, only passive system components failure probabilities are taken into account, disregarding the physical phenomena on which the system is based, such as the natural circulation. In fact, the inclusion of this aspect of the passive system failure in the PSA models is a difficult and challenging task and no commonly accepted practices exist. In a first approach, we have chosen an event tree (ET) representation of the accident sequences. ET techniques allow the identification of all accident sequences deriving from an initiating event. The initiating event is an event (e.g. equipment failure, transient) that can lead to the accident if no protective action is taken by safety systems. Each sequence of the ET represents a certain combination of events corresponding to the failure or to the success of safety systems. Therefore, ET provides a set of alternative consequences. The consequences in the case of Level 1 PSA of nuclear reactors are usually defined as degrees of reactor core damage, including 'safe' state and 'severe' accident state. These consequences are generally evaluated by T-H calculations carried out in a conservative way.

This choice of the event tree representation might seem unsuitable because it does not appear to consider the dynamic aspects of the transient progression including dynamic system interactions, T-H induced failure, and operator actions in response to system dynamics. In fact, we have treated examples where the overall reactor, including the safety systems and in particular the passive system, is modelled by the T-H code. This results in the fact that the

dynamic system interactions are taken into account by the T-H calculations itself. In addition, we have not considered human intervention during the studied sequences, which is coherent with the usual utilization of the passive systems in advanced reactors. So, as a first approach, the event tree representation seems a good and simple representation for the assessment of accident sequences, including the passive systems.

For the sequences where the definition of envelope cases are impossible, events corresponding to the failure of the physical process are added to the event tree and uncertainty analyses are carried out to evaluate the corresponding failure probability. For this purpose, the T-H code is coupled to a Monte-Carlo simulation module. The failure probabilities obtained by these reliability analyses are fed into the corresponding sequences.

3.2. Enhanced methodology (RMPS+)

RMPS+ methodology is developed by CNEA, Argentina. This methodology is based on RMPS methodology, described earlier in section 4.1, and is basically a condensed and improved form of RMPS methodology. The flowchart of the proposed methodology is shown in FIG. 3.

RMPS+ essentially consists of three blocks, which are briefly described below:

- Block 1: includes steps 1, 2 and 3 and is related with the development of the system that is used to perform the assessment.
- Block 2: includes steps 4, 5, 6 and 7 and its objective is to obtain the reliability of the passive system, as well as the sensitivity of this system against the relevant parameters with uncertainty. All these analyses are done based on the results obtained from the best estimate (BE) code.
- Block 3: contains the steps 8, 9, 10 and 11, and the objective is to wisely increase the population of cases evaluated near the failure domain, in order to improve the accuracy of the previous block results.

As can be seen, most of the steps proposed are equal or analogous to the RMPS methodology. For simplicity, the steps of the proposed methodology are numbered (FIG. 3), and the ones of the RMPS methodology are named with the letters (FIG. 2).

The methodology starts characterizing the problem (step 1) through the identification of the passive safety system, which practically is equal to the step A, and consists of identifying the mission that the safety system must fulfill in the proposed scenario, setting up the criteria to determine whether the safety system completes its mission, and defining the performance indicator (PI) that measure (as a continuous function) how far the safety system in each Monte Carlo simulations fails. The last task mentioned is an extra one in comparison with the step A. It is important to remark, that it is essential to choose a PI as linear as possible.

Step 2 is equal to the step B. It basically consists of the model development for the BE code selected, where it is important to follow the well-established international guides and recommendations as well as to use qualified users, computer codes and procedures. The model must be consistent with the information gathered and defined in the previous step. In addition, the definition of the PI must be suitable with the model capabilities.

In step 3, a full definition of the relevant parameters (those which have some importance with respect to the PI, and whose uncertainties are assigned and used in the assessment) must be

performed. First of all, they are identified (as step C) through different techniques (such as the ones shown in [24]), based on the information generated in steps 1 and 2. Then, their uncertainties are quantified (like in step D) through a function (a probability density function) that represents their random nature, showing the impossibility to know exactly their values due to several reasons, like epistemic or random uncertainties. Finally, it is necessary to define the sampling technique that is used to determine the values that every parameter takes (based on their proposed distributions) in each one of the Monte Carlo simulations. In this step, it is also important to perform the screening of the parameters (as they are used in step F) and to define the sampling methods (Latin-hypercube, stratified, random) as well as the techniques to check the sampling goodness (graphical and analytical ones).

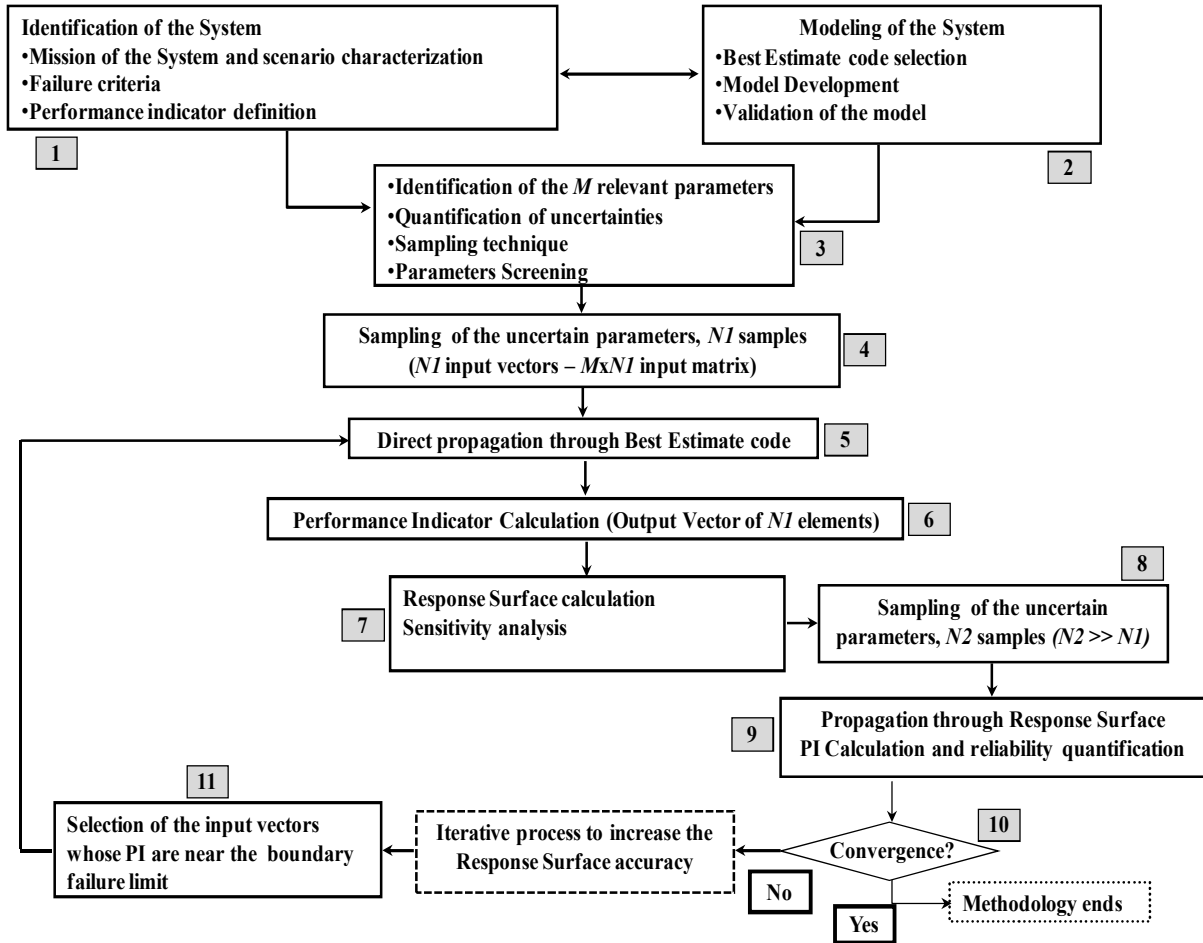


FIG. 3. Proposed methodology flowchart.

Next, in step 4, the sampling of the necessary values for the parameters must be done (where the number of sampling for each one of them is the same, so there are N_1 samples for each one of the M 's parameters). The number of samples is usually determined by the reliability and confidence level that are required (and it is independent of the number of parameters, except for the linear analysis). Then, the j th sample of each parameter is grouped with the others j th samples of the rest of the parameters, to build an input vector. The set of input vectors is called input matrix.

In step 5, the direct propagation through a BE code must be carried out (like in step G). To make this, among many other tasks, values of each set of parameters must be incorporated in the input of the model developed in step 2. By this way, we obtain N_1 'reactor sub models', as

many as input vectors (containing the sampled parameters set) are. It is highly recommended to implement the code input development for each set of parameters values in an automatic manner, as well as the code runs, in order to facilitate and assure the quality of the task.

Next, in Step 6, the calculation of the PI for each one of the N1 reactor sub models is performed, generating the named output vector.

In Step 7 the reliability of the passive safety system is calculated, by using the number of cases whose PI exceeds the design limits (checking if its value violate the success criteria) and the number of runs performed (the same as in step L), taking into account the confidence level that it is required to be assured, and the Wilks's formula [25]:

$$\beta = \sum_{j=0}^{s-1} \binom{N}{j} \gamma^j (1-\gamma)^{N-j} \quad (3)$$

Where:

β : confidence level

N : number of samples

s : position where the sample is located that represents the upper limit in the ordered data

γ probability that samples do not exceed the upper limit. This figure represents the reliability

In case of large sample sizes and non-zero failure cases, implementation of Eq. (3) becomes impractical. For this reason, there are some approximations which are easier to compute and provide results barely conservative.

With the input matrix and the output vector obtained, another task in this step is to make the sensitivity assessment (like step E), which, in this case, consists of calculating the linear regression coefficient from the input matrix to the output vector. The sensitivity coefficients are trivial to obtain once the hyper-plane (response surface) is calculated. Even though it is possible to use a higher order response surface, it is recommended to use linear approximation instead, especially because the response surface is used to extrapolate data. In order to use a hyper-plane, an effort must be invested to define a PI as linear as possible.

The response surface is used later as a model mock-up to calculate the PI, whose evaluation is orders of magnitude faster than the model quantification for the BE code. It is utilized to obtain the performance indicator for a given combination of values of the relevant parameters.

Here appears a difference with the RMPS methodology, because step 1 is omitted, since the results from Step 6 are recycled and used to generate the response surface. And the step J is practically also omitted, because if a hyper-plane is used as response surface, then the surface parameters can be obtained directly from the sensitivity analysis.

The proposed methodology continues with the step 8, where new input vectors are generated (N2, with M elements each one), and therefore produce a sample spectra several orders of magnitude larger than the best-estimate model evaluation. These new input vectors are used to feed the response surface, obtaining the estimation of their respective PI -output vector- (step 9, which is equivalent to the step K). This last step is used to increase the precision of the reliability calculated in the step 7.

Nevertheless, as the hyper-plane is just an approximation of the BE model (which is as close as possible to the real reactor), and its coefficients represent the sensitivity of the PI to the uncertainty of the most relevant parameters, then it results essential to improve its accuracy in the domain of interest, which is the one whose functional image is near the failure zone.

The procedure chosen to improve the surface accuracy is described below, and covers steps 5 to 11.

Step 10 was skipped in the first feedback iteration, but was then used in next iterations to check if the convergence has been achieved.

The improvement procedure starts (step 11) by selecting the subset of the N2 input vectors, whose estimated PI prediction are near to the safety system failure zone. These selected input vectors are used to run the BE model (step 5) in order to obtain the 'true values' for PI.

Next, those input vectors, together with their respective new evaluation of the PI, are added to the ones obtained previously in the step 5. Then, steps 6, 7 and 9 are performed again with this new increased set of values of the parameters, in order to obtain the updated sensitivity coefficients, response surface, and safety system reliability.

This process is repeated as many times as necessary until the convergence is reached, which is checked in step 10.

The convergence criteria used in the proposed methodology was related with the number of failure cases (predicted by the surrogate model). Also, it is useful to check that PI estimation (obtained by the surrogate model) of most of the cases in the failure zone and its surroundings has a good agreement with the ones calculated by the BE code.

When the number of failed cases is too small, it is recommended to define a convergence criterion based on the comparison within the number of BE simulated cases that fail and the number of cases predicted to fail by the response surface, because the convergence is significantly improved. In this case, step 8 should be skipped in the feedback process, because if the samples change in every step then it is hard to know when the convergence is achieved.

3.3. Assessment of Passive System Reliability (APSRA)

In the APSRA methodology, the passive system reliability is evaluated from the probability that the system fails to carry out the desired function. In principle, in a natural circulation system, the operational mechanism of buoyancy driven pump should never fail as long as there is a heat source and sink with an elevation difference between them. However, even though the mechanism does not fail, it may not be able to drive the required flow rate whenever called in, if there is any fluctuation or deviation in the operating parameters even though the system geometry remains intact. In the case of a mechanical pump, the head vs. flow characteristics is not so much susceptible to a slight change or fluctuation in operating parameter to cause the failure of the system unless there is any mechanical failure of the pump itself. Hence, its performance characteristics are well known and can be simulated accurately while assessing the overall safety of the plant. On the other hand, the characteristics of buoyancy driven pump cannot be accurately predicted under all operational conditions or transients due to the inherent complex phenomena associated with natural convection systems. Since applicability of the best estimate codes to passive systems are neither proven nor understood enough, hence, APSRA relies more on experimental data for various aspects of natural circulation. APSRA compares the code predictions with the test data to evaluate the

uncertainties on the failure parameter prediction, which is later considered in the code for prediction of failure conditions of the system. Figure 4 shows the steps followed in APSRA methodology.

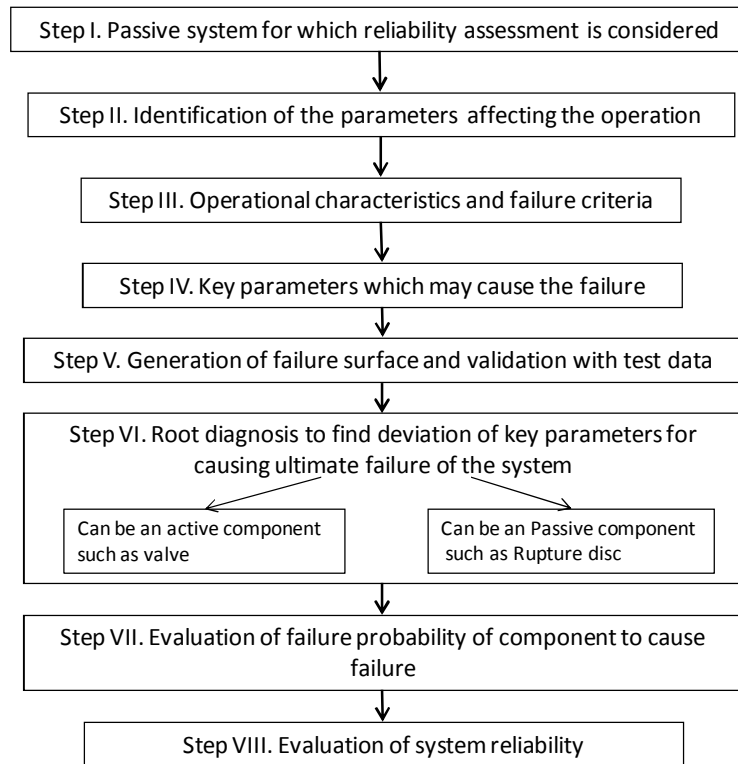


FIG. 4. APSRA methodology.

The steps of the methodology are discussed below in detail.

Step I: Passive system for which reliability assessment is considered

In step I, the passive system for which reliability will be evaluated is considered.

Step II: Identification of parameters affecting the operation

The performance characteristics of the passive system are greatly influenced by some operating parameters. For example, some of the critical operating parameters which influence the natural circulation flow rate in a boiling two-phase natural circulation system are:

- System pressure;
- Heat addition rate to the coolant;
- Water level in the steam drum;
- Feed water temperature or core inlet sub-cooling;
- Presence of non-condensable gases.

Step III: Operational characteristics and failure criteria

In step III, APSRA requires the designer to have a clear understanding of the operational mechanism of the passive system and its failure, i.e. characteristics of the passive system. To judge its failure, the designer has to define its failure criteria. The characteristics of the system can be simulated even with simpler codes which can generate the passive system performance

data qualitatively in a relatively short period. In this step, the purpose is just to understand the system operational behaviour but not to predict the system behaviour accurately. For this, the designer has to use the parameters identified in step II, which can have influence on the performance of the system. Out of them, some must be critical in the sense that a disturbance in these parameters can lead to a significant change in the performance of the system, while others do not. Only a T-H expert can judge this behaviour through parametric calculations, and these parameters must be considered for the reliability analysis of the system.

For example, a buoyancy-induced pump which drives natural circulation operates due to density difference between hot and cold legs. So far as the heat source and sinks are available, natural circulation always builds-in. However, the flow rate may not be sufficient to fulfil the desired objectives of the system, which can be:

- Inadequate removal of heat causing rise in clad surface temperature;
- Occurrence of flow oscillations;
- Occurrence CHF.

The system designer may consider the system to fail if any of the above parameters exceeds the limit.

Step IV: Key parameters which may cause the failure

The studies in steps III and IV are complimentary to each other, in the sense that while the results of step III help in understanding the performance characteristics of the system due to variation of the critical parameters, step IV generates the results for those values of the critical parameters at which the system may fail for meeting any of the criteria given in step III.

Step V: Generation of failure surface and validation with test data

Once the key parameters are identified in step III (deviation of which can cause the failure of the system), the value of these parameters at which the system will fail, are calculated using a best estimate code. Hence there is another requirement for step V, i.e. the results should be generated using a best estimate code such as RELAP5 in order to reduce the uncertainty in the prediction of the failure conditions. The results of step IV generated using a simpler code is only useful in directing the inputs for step V in order to derive the failure conditions rather quickly.

As said before, applicability of the best estimate codes to passive systems are still not well understood. To reduce the uncertainty in prediction experiments for failure data for different passive systems are essential. The programme for benchmarking of the failure surface prediction is shown in FIG. 5.

Step VI: Root diagnosis to find deviation of key parameters for causing failure of system

After establishing the domain of failure, the next task is to find out the cause of deviation of key parameters which eventually result in the failure of the system. This is done through a root diagnosis method.

For example, a reduction in core inlet sub-cooling in natural circulation reactor can be due to reduction of feed water flow rate. This can happen due to:

- Partial availability of the feed pumps;

- Malfunctioning of feed control valves or controller;
- Unavailability/failure of feed water heaters.

A passive system fails to carry out its function not due to failure of its mechanism, but definitely due to deviation of some of the parameters on which its performance depends. These so-called ‘key parameters’ deviate from their nominal values due to failure of either some active components such as a control valve, or an external pump, or electric signal, etc. or due to failure of some passive components such a passive valve, or a relief valve, etc.

Step VII: Evaluation of failure probability of components causing the failure

This is the most critical step in evaluation of reliability of the system. Once the causes of deviation of key parameters are known in step VI, the failure probability of the components can be evaluated using the classical PSA treatment through a clean event/fault tree analysis.

Step VIII: Evaluation of system reliability

The component failure probability is integrated to evaluate the reliability of the system.

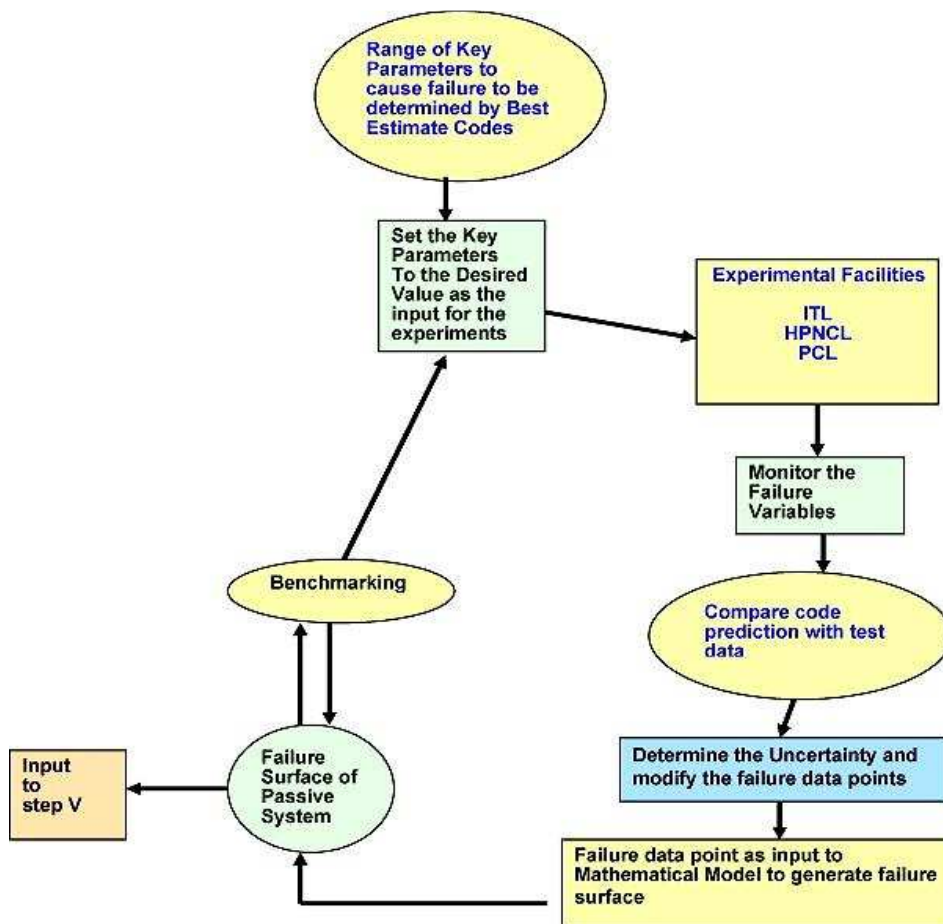


FIG. 5. The programme for benchmarking the failure surface.

3.4. RELIABILITY ASSESSMENT USING GENERIC PSA APPROACHES

Some approaches, commonly used in PSA studies for system reliability estimation, have been developed by ENEA for the reliability assessment of T-H passive systems and more

specifically for the performance assessment of the isolation condenser (IC) system. This section describes some of these approaches.

In the first methodology, the failure probability is evaluated as the probability of occurrence of different independent failure modes, a priori identified as leading to the violation of the boundary conditions and/or physical mechanisms needed for successful passive system operation. In the second, modelling of the passive system is simplified by linking to the modelling of the unreliability of the hardware components of the system. This is achieved by identifying the hardware failures that degrade the natural mechanisms upon which the passive system relies and associating the relative unreliability of the components designed to assure the best conditions for passive function performance. The third approach is based on the concept of functional failure, defined as the probability of the passive system failing to achieve its safety function as specified in terms of a given safety variable crossing a fixed safety threshold. In the following, these methods are presented and analysed.

3.4.1. Approach based on independent failure modes

In this approach, the reliability of a passive system is seen from two main perspectives i.e. 1) System/component reliability (e.g. valves, piping), and 2) physical phenomena reliability. The former calls for soundly-engineered safety components with at least the same level of reliability of the active ones and can be treated in the classical way, i.e. in terms of failures of components. The latter perspective is concerned with the evaluation of the natural physical phenomena underpinning the passive safety function and the long-term effects of the surroundings on its performance/stability. It addresses the critical failures that defeat or degrade the natural mechanisms which sustain the operation of the passive system.

In this view, the passive system failure probability is evaluated as the probability of occurrence of the different failure modes, considered independent, critical for the passive safety function, i.e. which would violate the boundary conditions and physical mechanisms necessary for the successful operation of the passive system [26].

The operative steps of the procedure adopted are:

1. Identify the failure modes affecting the natural circulation phenomenon: For this scope, well-structured and commonly used qualitative hazard analyses may be adopted, e.g. FMEA and HAZOP, specifically tailored to considering the phenomenology of the natural circulation [27]. These analyses must concern both mechanical components and the natural circulation itself, treated as a 'virtual component' whose operation may be disturbed by unexpected mechanical and thermal loads, plugging, non-condensable gas build-up and heat exchange process reduction which generate additional 'physical' failure modes.
2. Identify a set of n critical parameters $x = \{x_1, x_2, \dots, x_i, \dots, x_n\}$ as direct indicators of the failure modes identified in step 1. (e.g. non-condensable fraction, undetected leakage size, valve closure area, heat loss and piping layout).
3. Assuming that all of the failure modes identified in step 1. are independent from each other, select proper probability distributions $\{f_1(x_1), f_2(x_2), \dots, f_i(x_i), \dots, f_n(x_n)\}$ over the ranges of variability of the corresponding critical parameters identified in step 2. The mean (or, alternatively, the median or mode) values can be taken equal to the expected values of the parameters in nominal conditions while the variances represent the uncertainty associated to each mode of failure.

4. Identify the critical intervals $\{F_1, F_2, \dots, F_i, \dots, F_n\}$ defining the failure criteria for all the parameters. If at least one of the critical parameters lies in its critical interval, then the system is failed.

5. Compute the failure probabilities, $Q_i, i = 1, 2, \dots, n$, pertaining to each failure mode by integrating each probability density function, $f_i(x_i)$, over the corresponding range of failure, F_i :

$$Q_i = \int_{F_i} f_i(x_i) dx_i, i = 1, 2, \dots, n \quad (4)$$

6. Under the assumption of independence (step 3.), calculate the overall probability of failure of the natural circulation system, Q , by combining all the failure probabilities for each failure mode, Q_i , as follows:

$$Q = 1 - \prod_{i=1}^n (1 - Q_i) \quad (5)$$

Thus, for a passive system with n mutually independent failure modes, the total failure probability is computed as for a series system with n critical elements, by summing-up all the single failure probabilities.

Once the probability distributions of the parameters are assigned, the failure probability of the system can be easily obtained from Eq. (4) and Eq. (5) if proper failure criteria are assigned in step 4. Unfortunately, difficulties arise in assigning the range and the probability density functions of the critical parameters defining the failure modes, as well as in defining proper failure criteria, i.e. the failure threshold, because of the unavailability of a consistent experimental and operating data base. This lack of experimental evidence forces one to resort to expert/engineering judgments to a large extent, making thus the results strongly conditional upon the expert judgment elicitation process.

3.4.2. Approach based on failure modes of passive system hardware components

In order to overcome the difficulties of the approach highlighted in the previous section, an effort could be made to try to associate to each physical failure mode a failure mode of a hardware component designed to ensure the corresponding conditions for successful passive safety function performance (e.g. vent valves opening for removal of non-condensable, piping integrity, heat exchanger for heat transfer process).

Thus, the probabilities of physical failures that defeat or degrade the mechanisms upon which the passive system relies are reduced to unreliability figures of the components whose failures challenge the successful passive system operation [17]. If, on the one hand, this approach may in theory represent a viable way to address the matter, on the other hand, some critical issues arise with respect to the effectiveness and completeness of the performance assessment over the entire range of possible failure modes that the system may potentially undergo and their association to corresponding hardware failures.

In fact, failure of the physical process is always (eventually) related to failures of active and passive components, not acknowledging any possibility of failure just because of unfavourable initial or boundary conditions.

In addition the fault tree used for the decomposition of the physical process is used as surrogate model for a complex T-H code that models system behaviour. This decomposition is not good in foreseeing interactions among physical phenomena and makes it extremely difficult to realistically assess the impact of parametric uncertainty on the performance of the system.

3.4.3. Functional failure approach

This approach exploits the concept of functional failure to define the probability of failing to successively carry out a given safety function (e.g. decay heat removal). The idea comes from the resistance-stress (R - S) interference model of fracture mechanics (FIG. 6).

In the framework of T-H passive systems reliability assessment, R and S express respectively the safety functional requirement (R) on a safety physical parameter (for example, a minimum threshold value of water mass flow required to be circulating through the system for its successful performance) and system state (S) (i.e. the actual value of water mass flow circulating). Probability distributions are assigned to both R and S to reflect the uncertainties in both the safety thresholds for failure and the actual conditions of the system state. The function of the passive system defines the safety parameter values that define system failure, whose probability is obtained by comparing the state probability density function with that of the defined safety functional requirement [28].

Note that the analysis typically focus on the passive system process variables rather than on the reactor parameters, since these latter are not considered direct indicators of the performance of the system, despite the effect of the surroundings on the performance/stability of the natural circulation.

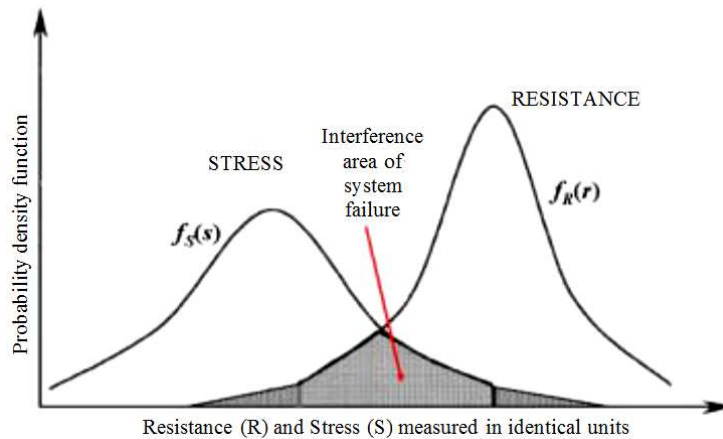


FIG. 6. Resistance-Stress (R - S) interference model.

In the analysis, the states of the system are divided into two sets, the failed and the safe states, separated by a limiting state of the safe set which identifies the safety functional requirement parameter R . Failure then corresponds to the crossing of the system parameter S through the limit state of the safe set [26]. Introducing the random variable limit state function (LSF) or performance function (PF) as $G = R - S$, one defines

$$G = R - S \left\{ \begin{array}{l} > 0 \text{ for function successfully performed} \\ = 0 \text{ at limit state} \\ < 0 \text{ for failure of performing the function} \end{array} \right\} \quad (6)$$

Obviously, the difficulties lie in the definition of the probability distributions $f_R(r)$ and $f_S(s)$ of R and S , respectively, from which the distribution $f_G(g)$ for G is derived. Due to lack of reliable data, engineering judgement must again be used to obtain such distributions.

Then, the failure probability Q is computed as the probability that S is greater than R , i.e. the LSF

(or PF) in Eq. (6) is lower than 0:

$$Q = P(S > R) = \int_{-\infty}^{\infty} \left[\int_{-\infty}^{\infty} f_s(s) ds \right] f_R(r) dr = P(G < 0) = \int_{-\infty}^0 f_G(g) dg \quad (7)$$

It is conceptually worth noting a subtle difference in the treatment of the variables R and S of the resistance-stress model for the reliability assessment of passive systems [28]. In fact, if for example S and R are the actual mass flow rate and its requirement threshold value below which natural convection fails, respectively, the conditions discriminating the safe state region from the failure region in Eq. (7) are reversed: the function is successfully realized when S is larger than R whereas, on the contrary, failure occurs when S is less than R . The same holds in case of consideration of other physical variables as performance outputs, like the pressure differential driving force or the heat removal rate.

In a more general case, failure of the system may occur only when a system actual state parameter S falls below a minimum threshold value or above a maximum threshold; the probability of the two exclusive events of failure must then be summed to give the total probability of failure:

$$Q = \int_{-\infty}^{\infty} \left[\int_S^{\infty} f_R(r) dr \right] f_S(s) ds + \int_{-\infty}^{\infty} \left[\int_{-\infty}^R f_S(s) ds \right] f_R(r) dr \quad (8)$$

4. VALIDATION OF METHODOLOGIES USING TESTS ON L2 NATURAL CIRCULATION LOOP

4.1. DESCRIPTION OF L2 TEST FACILITY

In natural circulation systems there is a heat source and a heat sink, with the former placed lower than the latter, both in contact with a portion of fluid. As consequence of the heat fluxes, the heated part of the fluid becomes lighter and rises, while the cooled part becomes denser and is dropped down by gravity. These combined effects establish circulation. This phenomenon is capitalized to extract heat from the source continuously and establish a natural flow in the closed loop in absence of any active components thereby making the system passive.

This numerical study aims at resolution of flow pattern and stability in single-phase natural circulation in rectangular loops of different inclination and varying heat sink temperatures & comparison of these simulation results with those of experiments performed on L2 facility at Genoa. Brief description of the Genoa test facility is given below.

Two sizes of natural circulation loop (NCL) were experimentally analysed at Genoa: large-scale and mini-scale loops. The study on the large-scale loop (Loop2, 'L2') was focused on the effect of the cooler temperature on the stability of the loop. Additional parameter investigated was the loop inclination, while two working fluids were utilized (water and FC43), characterized by very different thermo-physical properties. The loop inclination was investigated with the purpose of simulating reduced gravity by decreasing the height between the top and the bottom of the loop, and consequently the buoyancy forces acting on the fluid. The experimental apparatus consists of a rectangular loop where the heater is placed at the bottom and the cooler on the top of the loop. The Loop2 is the third NCL realized at DIPTeM labs [29]. Figures 7 and 8 show a scheme of loop.

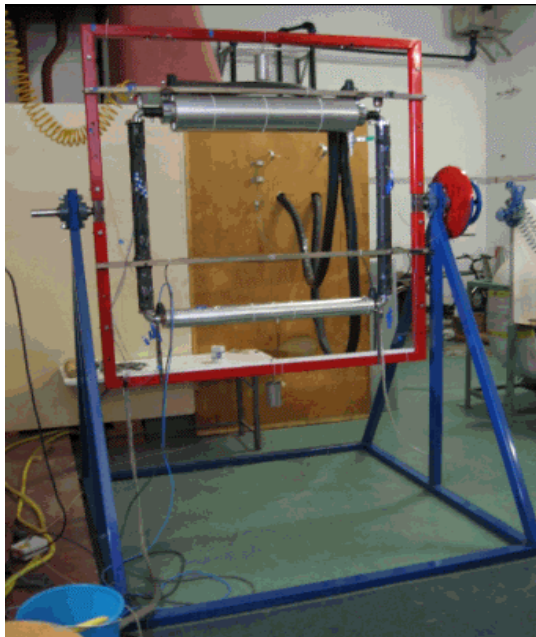


FIG. 7. L2 experimental facility.

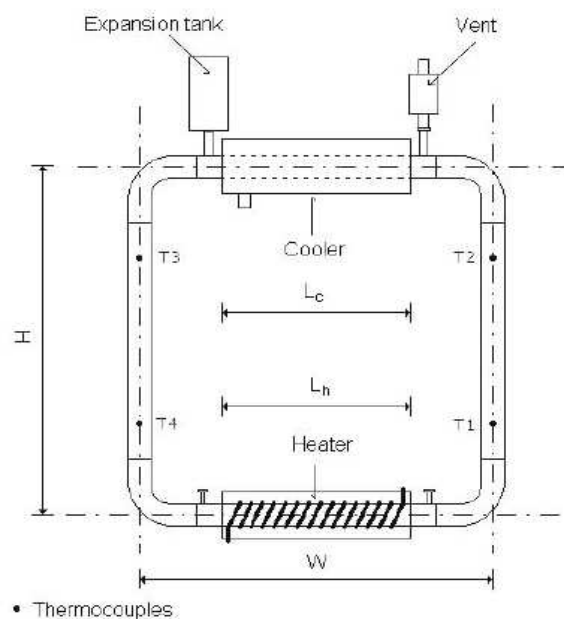


FIG. 8. L2 loop arrangement.

The two vertical tubes were insulated by means of an Armaflex® layer of 2 cm of thickness ($\lambda=0.038$ W/mK at 40°C) and can be considered adiabatic. At the heating section the flux is imposed, while at the cooling section the heat sink temperature (HS Temp.) is imposed. The vertical tubes and the four bends are made of stainless steel AISI 304, while both the horizontal tubes are made of copper (99.9%). The loop internal diameter D is 30 mm and it is constant over the entire loop; the loop height H is 0.988 m and the total length L_t , measured on the tube axis, is 4.100 m, with a L_t/D ratio of 136.7. The heater is made by an electrical nicromel wire rolled uniformly around the copper tube, connected to a programmable DC power supply. On the upper part of the loop a coaxial cylindrical heat exchanger is connected to a cryostat, which is able to maintain constant temperature of -20°C with cooling power of 1 kW, whereas it can remove up to 2.5 kW in a temperature range between -10°C and +30°C. The geometric details of L2 facility are given in Table 1.

TABLE 1. GEOMETRICAL DETAILS OF THE FACILITY

Symbol	Description	Detail (mm)
D	Loop diameter	30
W	Loop width	1112
H	Loop height	988
L_{heater}	Heater length	960
L_{cooler}	Cooler length	900
L_t	Total length	4100
L_t/D	Aspect ratio	136.7
H/W	Geometric aspect ratio	0.88

4.2. VALIDATION PERFORMED BY CNEA, ARGENTINA

4.2.1. Model development

Figure 9 shows the main components and structures that were considered in the modeling of the L2 loop facility, besides the expansion tank, which was connected to the top of the primary side of loop.

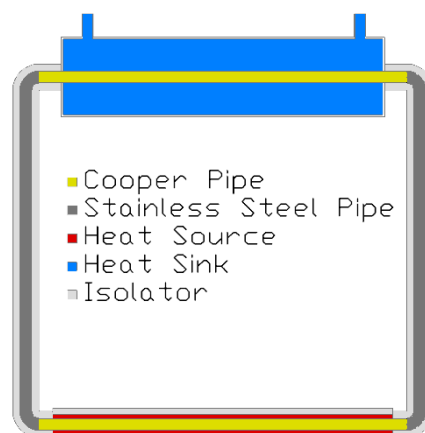


FIG. 9. Main loop components and structures.

The system modeling was performed based on those components shown in the previous figure, and some complementary information provided. The sliced nodalization (the same number and high of nodes in the vertical pipes) was one of the main criteria followed; as well as the criteria that all the nodes should have a length as similar as possible, in order to have similar Courant number. In FIG 10, the final nodalization obtained is shown.

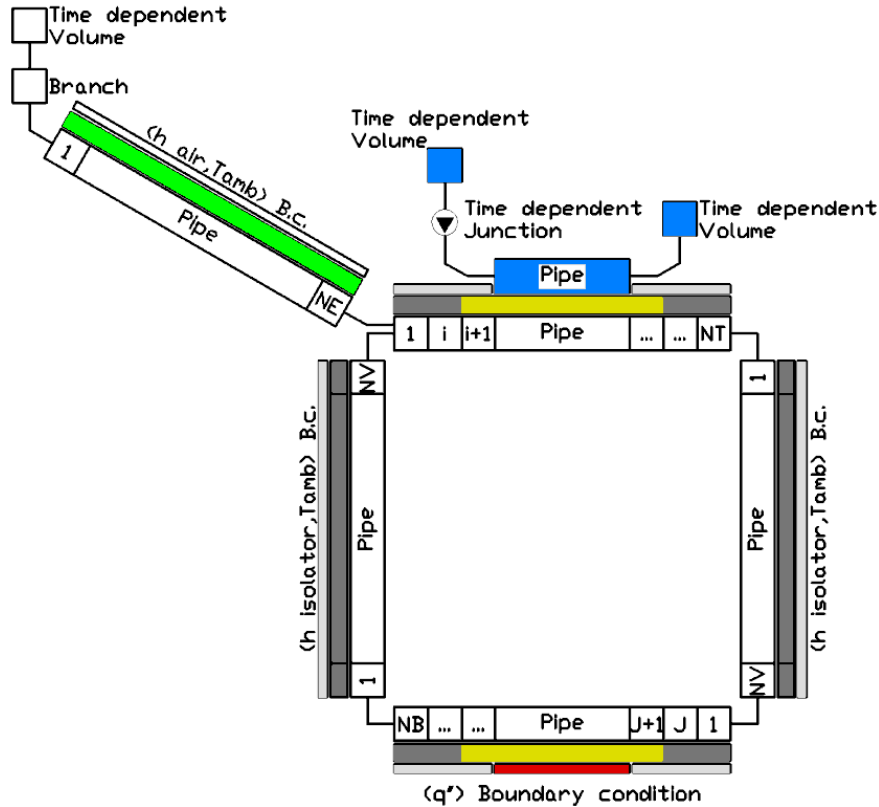


FIG. 10. Nodalization scheme.

As it can be seen, the model is quite simple, and it mainly has two independent circuits, one that corresponds to the water that circulates inside the loop (called primary circuit), and the other one that represents the cryogenic fluid that flows through the outside of the heat sink (named secondary circuit).

In the primary circuit, the thermodynamic property that is externally imposed is the pressure and the initial temperature (that is equal to the room temperature, fixed as right boundary condition of the primary circuit isolated heat structures). The primary mass flow rate and temperatures will be then the result of the dynamic of the system.

In the secondary circuit, the pressure is also fixed, as well as the inlet temperature (which is the parameter that is varied in the experimental runs) and the mass flow rate (which is adjusted in order to take into account the differences between the cryogenic fluid (Glycol-Water mixture) and the water used in the model). Also, the heat transfer coefficient from the heat sink wall to the secondary fluid is externally imposed, through one temperature-dependent table that was calculated based on the Dittus-Boelter correlation, and multiplied by one factor that was used to correct the differences between the correlation and the loop measures.

A systematic assessment was performed in order to tune the model to the experimental results, especially because the model tended to be unstable, even for the cases that the experiments showed a clear stable behaviour.

A spreadsheet based platform was used to assist the tuning process. In this platform, all the parameters were changed as well as the system nodalization and all the intermediate calculations. This allowed us to just change one desired parameters and automatically create the input file for the BE code.

Another platform allowed us to perform automatic parametric BE code runs based in one input file created with the previous platform.

Between the parameters that were modified, there are remarked:

- Node length;
- Time step;
- Heat transfer mesh size;
- Pipe dimensions;
- Heat transfer coefficients;
- Wall roughness;
- Heat loses;
- Heated perimeter;
- Wall thickness;
- Friction loses.

Two indicators were used to qualify the goodness of the model, compared to the experimental measures. One of them, was the hot leg temperature (that also takes into account the mass flow direction; because which of the vertical leg is the hot leg, depending on the mass flow direction), and the other one was the logarithmic mean difference temperature at the heat sink. Both indicators always were calculated for every time step and their values were condensed into a box-plot-like graph for each simulation or experimental run.

The box-plot graphs are commonly used in statistics, and one example of what they represent is shown in FIG. 11. In this case, for example, the 5% value in the box-plot represents the upper limit which assures that the 5% of the measured parameter are below them, and this is commonly named ‘the 5% quartile’. Additionally, the distribution mean value is also showed in this box-plot-like graph.

The procedure used to make the fine tuning of the model was the next:

1. Choice of one parameter to be varied
2. Setting of the parameters between the range provided
3. Performance of parametric simulation, varying the sink temperature between 2°C and 20°C
4. Visual comparison between the measured and simulated figure of merits
5. If the figures don’t match, application of a respective factor to the secondary-side heat transfer coefficient
6. Repetition of steps 3, 4 and 5 until convergence is reached
7. Check if the unstable to stable regime transition fails inside the range of sink temperatures selected

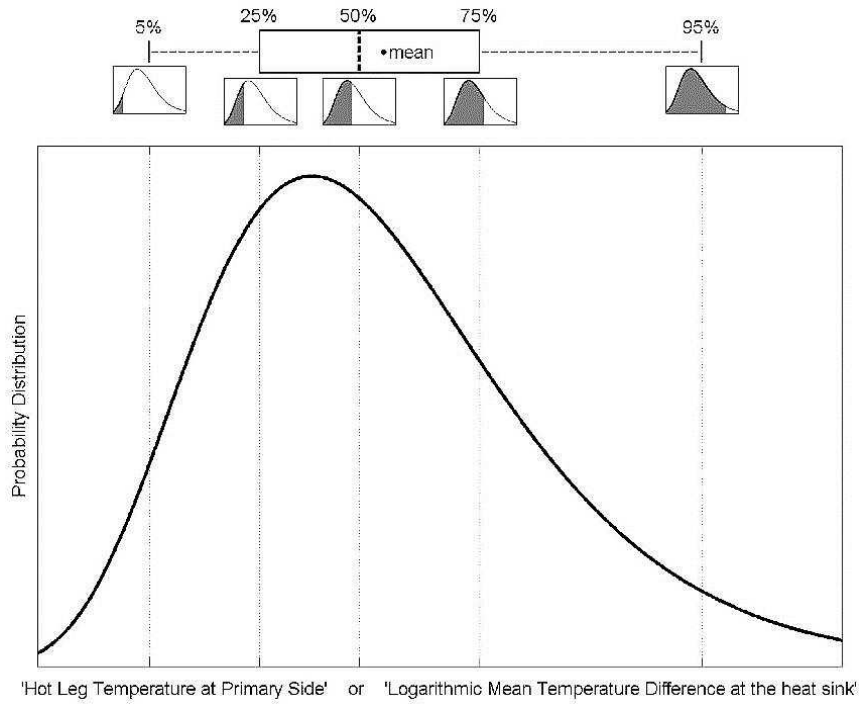


FIG. 11. At top, an example of a Box-Plot like graph. At bottom, the distribution that is represented through this box-plot.

In FIG. 12, it is shown, as an example, the result obtained after the step 7 of this procedure, for some combination of the parameters, and for the first of the model goodness indicator (the one that is related with the hot leg temperature).

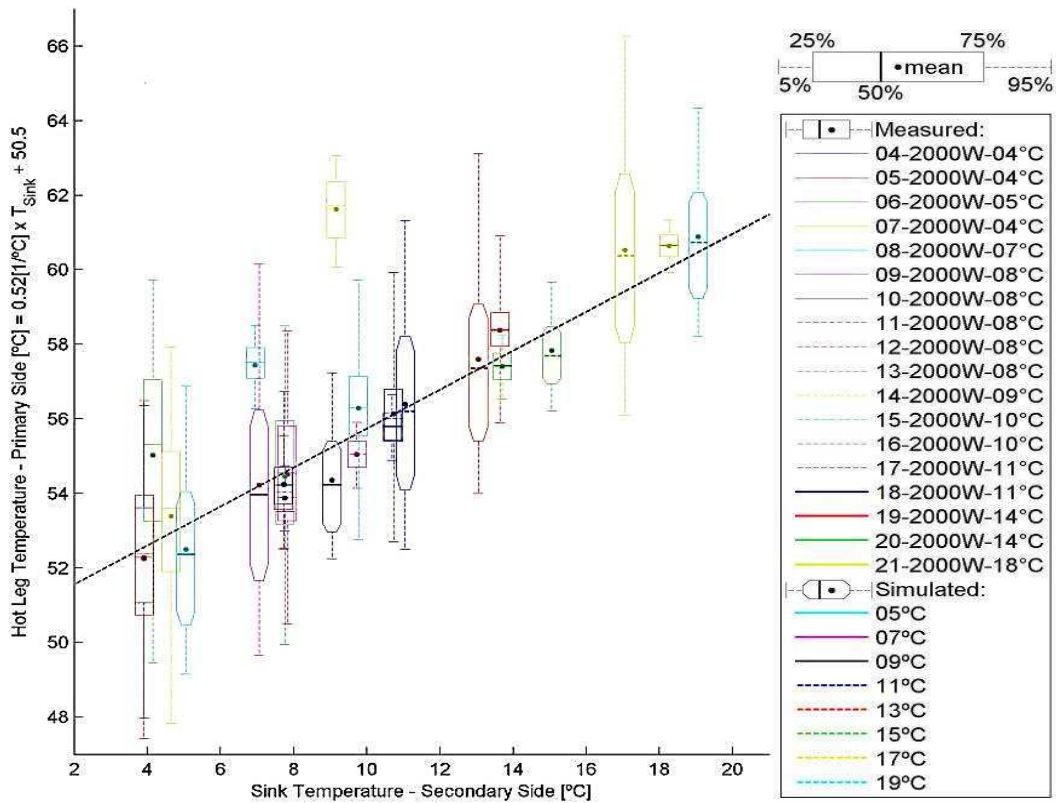


FIG. 12. First model goodness indicator for one model tuning obtained after the 7th step of the procedure.

Each of the box plot shown in the figure, is generated based on one of the experimental runs (which are represented by the rectangular shape) or one of the numeric simulation (which are represented by the ones that has a chamfer made in the corners, in order to visually differentiate them of the experimental runs). The statistics utilized to calculate the box-plot, is obtained taking all the temperature of the top of the hot leg vertical pipe (depending on the flow direction) for every time step, after the system has settled the initial transient.

There is also showed a linear regression, which is obtained based on the runs mean value of only the experimental runs.

Figure 13 shows the second model goodness indicator for the same case utilized in the previous figure. In this case, each of the box-plot are generated based on the statistics obtained from the calculation of the Logarithm Mean Temperature Difference at the heat sink for every time step, after the system has settled. Again, the rectangular ones represent the experimental runs, and the ones with chamfers represent the numeric simulations.

It can be seen that the experimental runs and the simulations have the same trends, as it was required in the 7th step of the tuning procedure. These figures of merits used were also useful to identify 2 experimental runs that can be eliminated.

Finally, it was found that one of the parameter that most affect the displacement of the instability transition was the tube thickness at the heat sink.

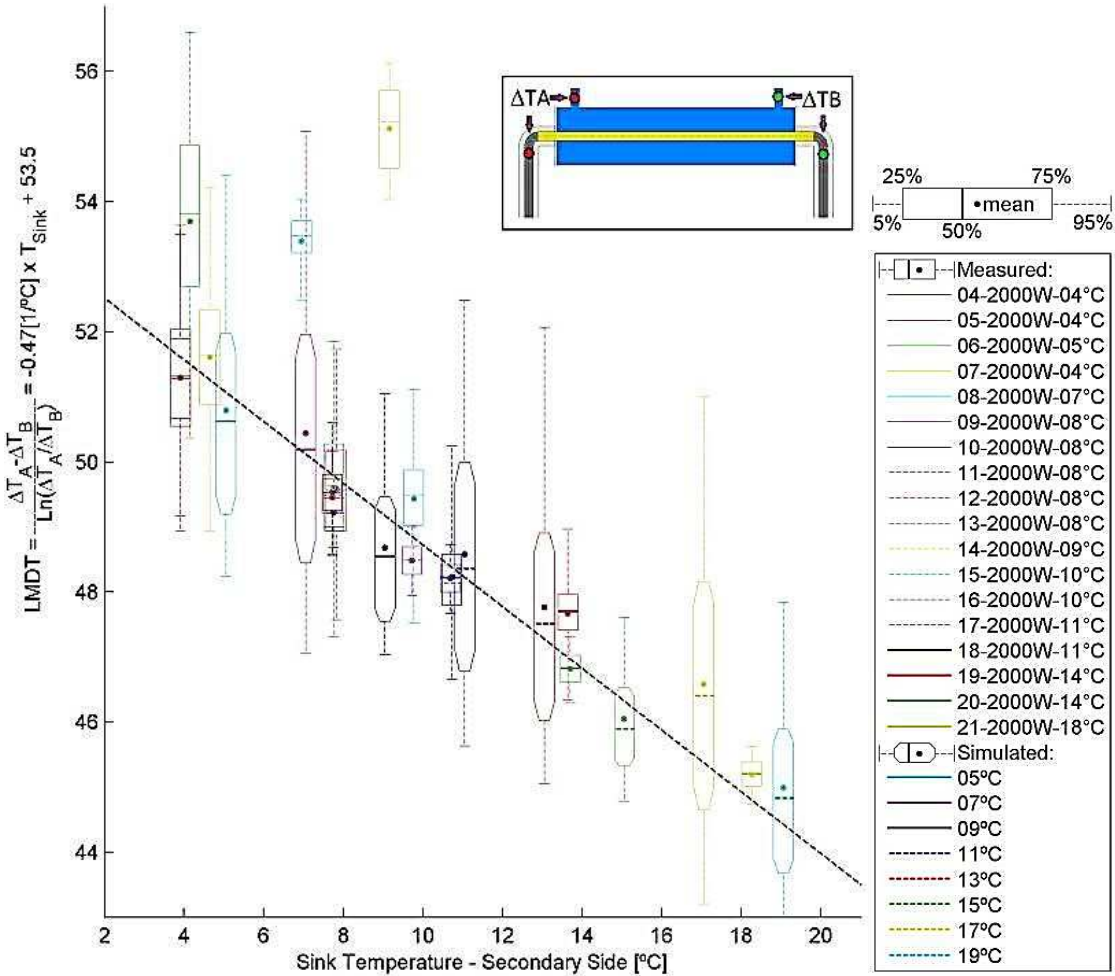


FIG. 13. Second model goodness indicator for one model tuning obtained after the 7th step of the procedure.

4.2.2. Loop dynamics

In order to help us to understand the system phenomenology, a bibliographic research was performed (because this kind of loop was widely studied by the scientific community), as well as several parametric simulations. A specific user interface was developed (which is shown in FIG. 14) to assist the analysis process.

The user interface directly showed the result from some selected RELAP5 restart. It plots, for some selected time and based on one chosen color map, the temperature of the hydrodynamic nodes and their related heat structure, as well as their respective void fraction. It also depicts the primary mass flow rate evolution and the 4 corners nodes temperatures evolution.

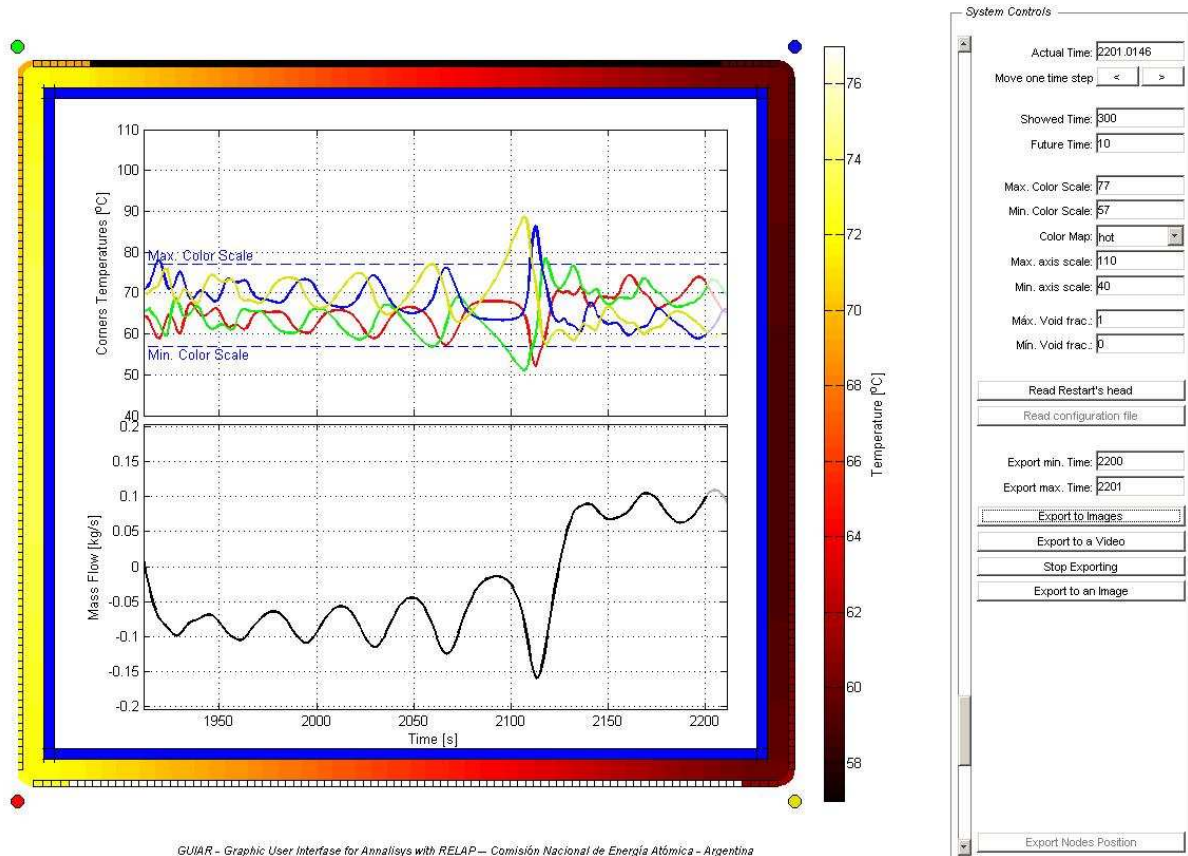


FIG. 14. User interface developed to analyze the loop dynamics.

Figure 15 shows two typical time evolutions of the loop, one supposed stable and other one supposed unstable. As it can be seen, the unstable case always keeps oscillating, and the oscillations amplitude grows up to reach the condition of flow reversal, where the process of oscillation amplification restarts. In contrast, the stable case usually begins as an unstable case, until suddenly reaching a stable condition, where the oscillations amplitude decreases to zero.

The assessment exposed that the loop apparently has a chaotic behaviour. This assumption is partially supported by the results shown in FIG. 16. In this figure, we see the phase diagram (for two faces selected, based on the bibliography [30–33]) of the experimental runs. One phase is the difference of temperature between the two vertical pipes (near the heat sink), and the other one is the mean of those temperatures. In the figures, each point corresponds to the phase state of the system for every time step measured, and all axes have the same limits.

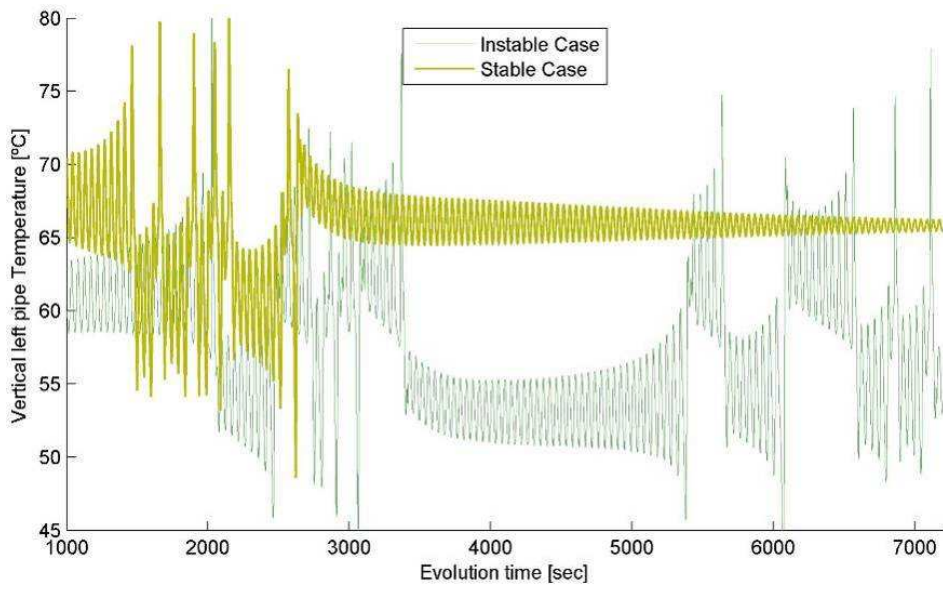


FIG. 15. Typical temperature - time evolution for one stable case and one unstable case.

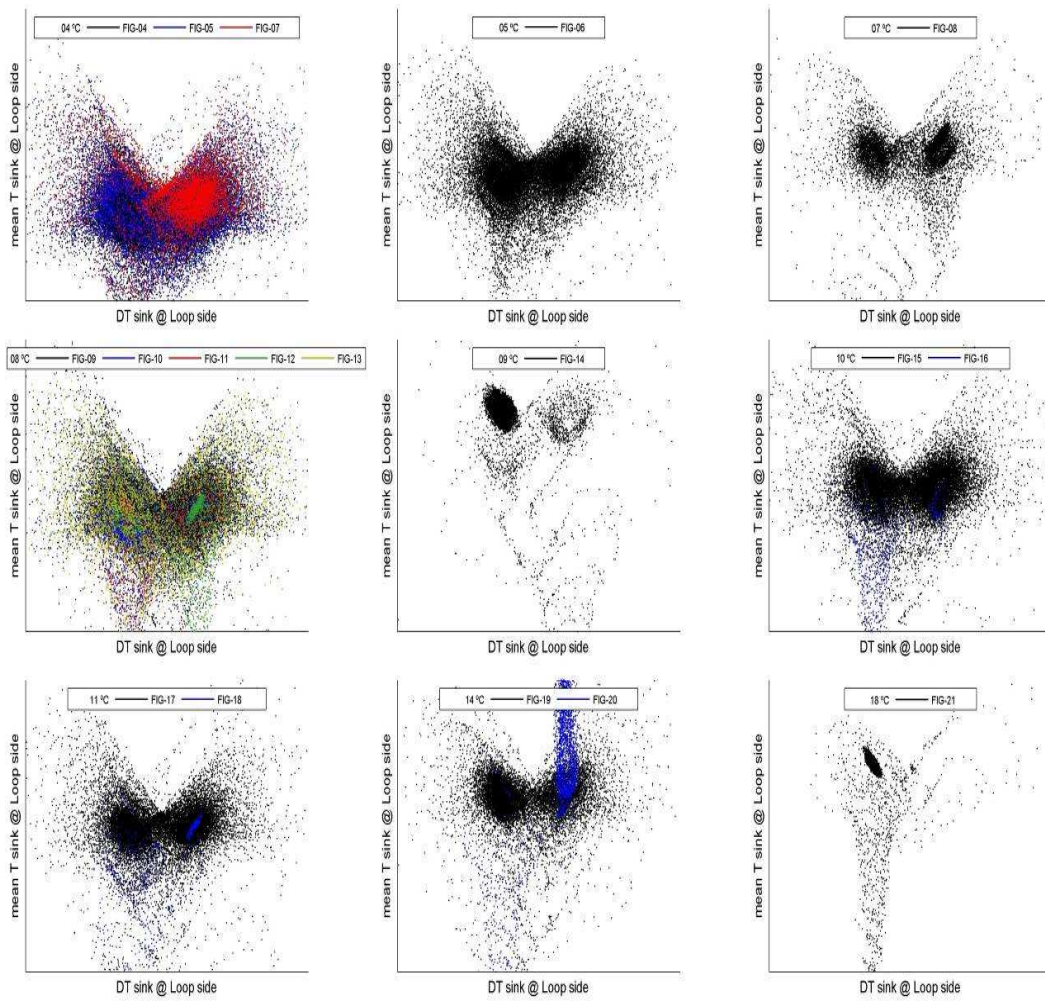


FIG. 16. Phase diagram of the experimental measures, grouped by the sink temperature set point.

The reason for selecting two phases to describe the state of the system is also supported by the study made based on the correlation dimension [34], which gives that the real loop and the modeled one can be described by 2 or 3 dimensions.

Showing the measurement evolution by means of this kind of graphs (instead of time evolution like), allows us to compare them. It also illustrates that the loop dynamics seems to have a butterfly portrait, typical of chaotic systems with two unstable attractors, like the famous Lorenz's attractor.

Besides of the instability nature (which was deeply analyzed by the community, like [32–33] and many others), what can be added after the analysis made, is that the loop always has two stationary conditions, that are the attractors, and there is one for each circulation direction.

In FIG. 17, three possible loop state evolutions are sketched in the phase space (which is also called state space [35]).

In the figure it can be seen that if the state of the system is far enough of one of these points (Case A), then the system will oscillate around it with a divergent orbit until it falls under the influence domain of the other stable point. Otherwise, if the system is close enough to one of these points (Case B or C) then the system will fall to the stable condition, through some kind of convergence spiral.

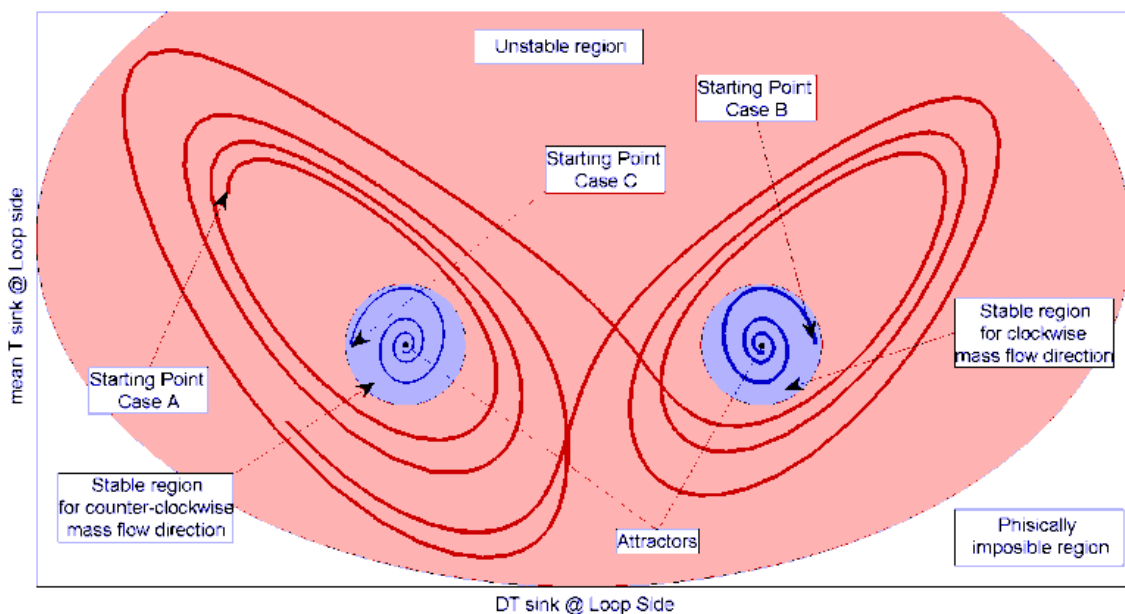


FIG. 17. Example of three possible orbits for the loop dynamics.

If these 'stabilizing regions' are too small, it is possible that the system never falls inside it, or that any minor perturbation removes the system from there. In this case we will say that the system is unstable. Otherwise, if this 'radius' is too big, then it could possibly be physically impossible for the system to fall outside the stable region, then we will say that the system is stable.

This interpretation is quite useful, despite the existence of this frontier (or 'attraction radius', like a potential barrier) is really difficult to prove, because the mentioned radius (which behaves like a threshold) may depend on issues that are usually neglected in the analytical analysis, like 3D effects, heat losses, etc.

Another issue, that supports the assumption that the loop has a chaotic behaviour, is a parametric study performed varying only the time that the heat source and the heat sink are modeled to go from zero to their nominal value. For this study, the model was frozen and the unique parameter that was parametrically varied was the ramp time of the start-up. The results obtained are shown in FIG. 18, where three different ramp times were tested: instantaneous, 6 and 10 minutes. As it can be seen, from the very beginning, the temperature evolution splits and a different behaviour can be observed. When they are compared for long term, the differences are more noticeable. This characteristic, that a minor perturbation in the initial condition produces a major variation in the system evolution, is also typical of chaotic systems.

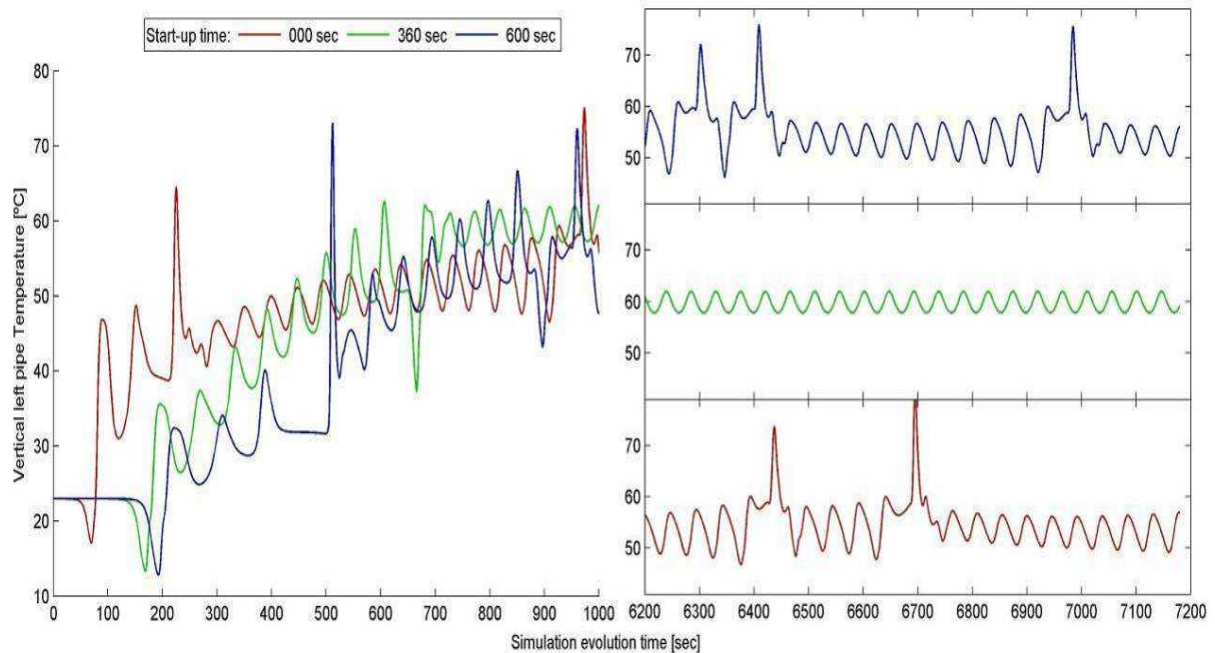


FIG. 18. Time evolution of the loop, obtained from the BE model, and only varying the start-up ramp duration time of the heater and the heat sink pump.

4.2.3. Performance indicator

As it was pointed out in the RMPS implementation for the CAREM like passive safety systems, the definition of the performance indicator is a key point of the methodology. From the PI definition depends on several aspects, such as the extrapolation accuracy of the response surface. Moreover, in order to choose the performance indicator, it is important to understand the system phenomenology.

If the loop dynamics really have a chaotic nature, as it can be presumed from the previous results shown, then it is necessary to be really careful with the definition of the performance indicator. It may happen that the mapping between the input parameters with uncertainties and the PI captures this chaotic behaviour. It means that a bounded change in the input parameters could make an unbounded change in the performance indicator. This remark is relevant, because in order to use the Wilk's formula [36] for the calculation of the failure probability (with the respective confidence level), it is necessary that the PI (black-box model output) has a continuous distribution, which implies [37] a continuous mapping between the input and the output.

Two options for the performance indicators were analyzed, and they can be understood observing again FIG. 15. The first option is the simpler one, and is related to the characteristic amplitude of the oscillations. The second one, is quite more complex to calculate and to understand and it is related with the grow speed of the oscillation amplitude.

a. First option for the performance indicator

One way of testing if the system is unstable or not, is performing one run of the system, and seeing if after same -previously fixed- time, the system is oscillating or not. This procedure is based on what has been previously said, that the system usually orbits around the attractors (in the phase space), inside what we call the 'unstable region', and if we wait the enough time then the system could pass near enough of one of the attractor (into what we call the stabilizing region), and it will converge to them. Therefore, it is possible to know if the stabilizing region exists and is big enough; just waiting the necessary time to the system fall inside this region.

The problem with this testing procedure is that if the system is chaotic, then it is impossible to say how much time it is necessary to wait until the system falls inside the 'stabilizing region', and then we always need to wait an infinite time. This is because of the unpredictability nature of the chaotic systems. But, ignoring this theoretical issue, we could think that the larger the stabilizing region is, the faster the system will fall in it (or more probable is to fall on it), and more stable the system is.

Therefore, following with this concept, what it is proposed as performance indicator is the standard deviation of the last 1000 seconds of the hot leg temperature (taking into account the mass flow direction). Also it is required to run the test during 6 hours. These performance indicators were calculated for each one of the provided experimental tests. They are shown in FIG. 19, where an offset of 0.5C is applied to take into account the possible electronic noise of the measurements.

With the aim to use this performance indicator also in the BE calculations and to compare it with the one obtained with the experimental runs, the following test was proposed. First, several numeric runs are performed with different sink temperatures inside the experimental range. Then, for each sink temperature, several runs are also performed, with the aim of having some statistics. This final task is made doing 51 parametric runs, freezing the whole model, and only varying the start-up ramps of the heaters and the secondary circuit pump, between 0 and 10 minutes. The results obtained for the performance indicators for the different sink temperatures are shown in a box-plot like graph in FIG. 19.

As it can be seen in the figure, the results obtained for the experimental runs and the model are in quite well agreement; showing that for lower temperatures, it is more probable that the system stay in the unstable region of the phase space. On the other hand it shows the problem of this performance indicator, when running a single case, because it just say that the system is stable or unstable (in a binary way), but it can't say how much unstable the system is (in a continuous way).

This performance indicator could be useful if it is used just to say where the transition from stable to unstable regimes is. The cost is to perform several simulations, for each combination of parameters with uncertainties and for each sink temperature and others parameters that could change from one experimental test to another (like the start-up ramp time, initial temperatures, etc.).

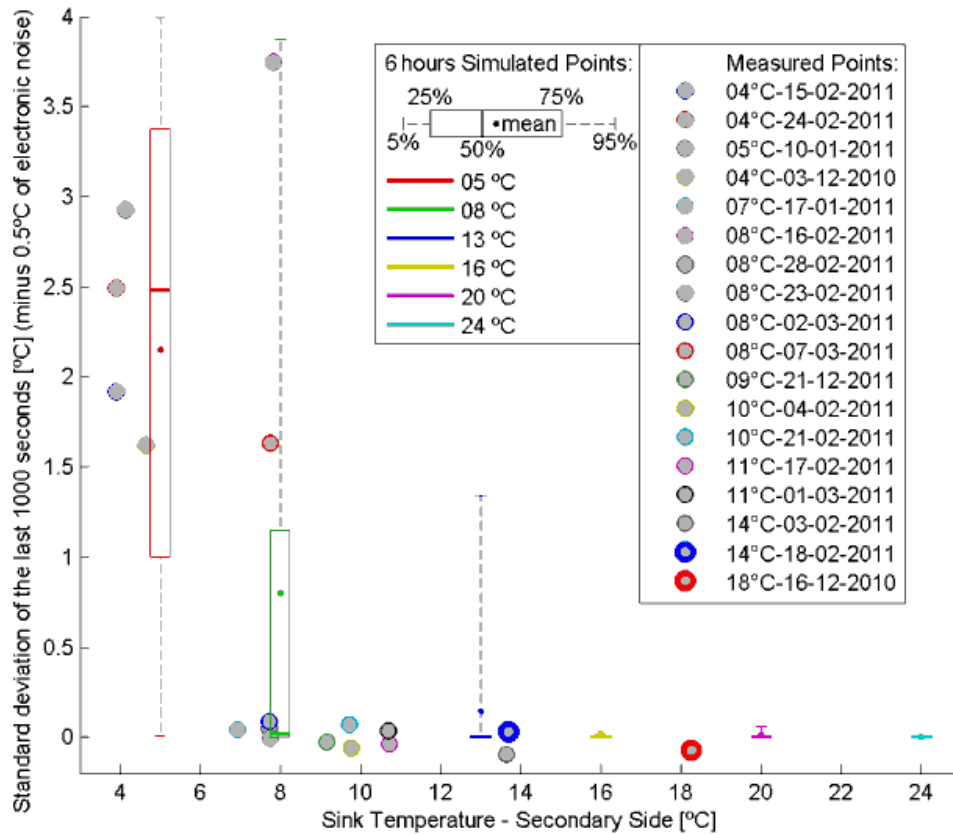


FIG. 19. Results obtained for the implementation of the first performance indicator option, into the experimental runs and into a test performed with the numeric model.

b. Second Option for the Performance indicator

The second selected option for the performance indicator is the one related with the speed of growth of the oscillation amplitude. One of the tools provided by the chaos theory was chosen to measure this, which is named the Lyapunov exponent. This indicator measures how much the distance between two possible orbits of the system varies in the phase space.

The largest one of those exponents is usually studied, which in turns is the dominant one. It gives the idea if the trajectories converge or diverge among them, and how fast it happens. Basically, it is related with the exponential envelope of the oscillation amplitude observed in the evolution, like the one shown in FIG. 15.

It is important to remark that for the calculation of the largest Lyapunov exponent, it is first necessary to reconstruct the phase state of the time series, using the technique of the lag-time and the embedding dimension [38], and then to analyze how fast the orbits approaches or separates.

This performance indicator was calculated for the same experimental test and numerical runs used in the previous option. The results obtained are showed in FIG. 20.

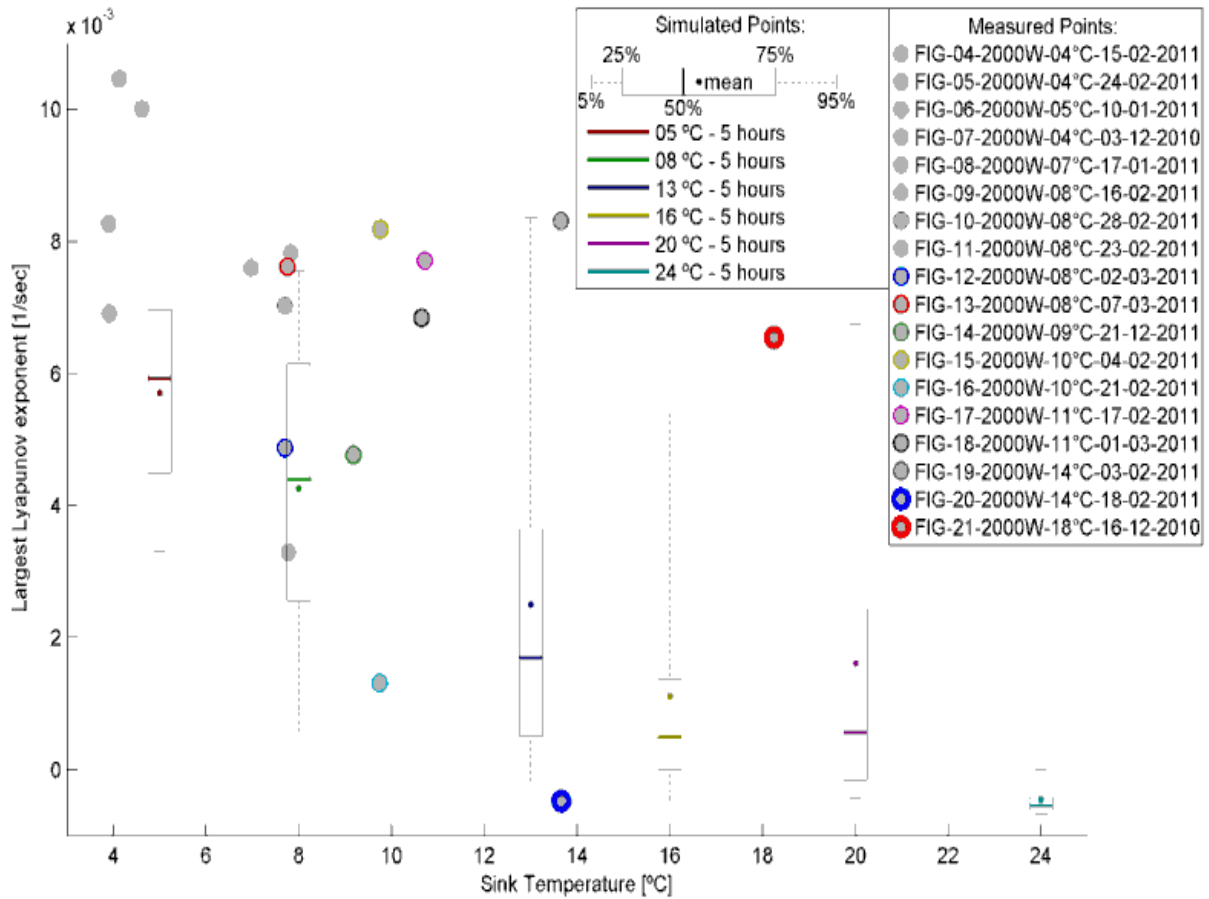


FIG. 20. Results obtained for the implementation of the second performance indicator option, under the same condition of the previous one.

As it can be seen in the figure, this performance indicator gives a continuous idea of how unstable the system is (as the original intention for this option), because it shows a trend, for example in the mean value, to decrease when the heat sink temperature increases. It is important to mention that this performance indicator requires a larger complexity to calculate than the previous one. One of the drawbacks of this indicator, which can be concluded from the figure, is the largest dispersion of the results in the transition zone, which may be located around 13°C. This may happen because when the system is in the transition zone, both regions in the phase space (the stable and the unstable one) have similar sizes. Then, the system evolution is governed by both behaviours (the stable and the unstable one, depending of the distance to the attractors). Consequently two different Lyapunov exponents compete (a positive one that makes the trajectories diverge, and a negative one that makes the trajectories collapse). Therefore it is possible that the algorithm used to calculate the largest Lyapunov exponent, calculates a mean between the two exponents.

4.3. VALIDATION PERFORMED BY BARC, INDIA

The objective of this study was to simulate the Genoa L2 loop using numerical code RELAP5/ MOD3.2 and analyse the effect of heat sink temperature and geometry on the stability and dynamic behaviour of natural circulation loop. The simulation results from this study were compared with experimental results.

4.3.1. Nodalization scheme and node sensitivity test

This section describes the nodalization scheme (FIG. 21) used for the numerical investigation. The RELAP5/MOD3.2 has been used for the analysis presented in this report. It is a one-dimensional best estimate system thermal-hydraulic code which is based on a non-homogeneous and non-equilibrium model for the two-phase flow.

Heater and cooler were modelled as heat structures with 60 nodes in each segment while left and right vertical legs were modelled as adiabatic pipes with 10 nodes in each leg. The heater and cooler were placed slightly eccentric in order to avoid any numerical instability arising due to equal probability of flow in both directions. The temperature distribution and heat transfer in heat structures was calculated using a 1-dimensional heat conduction model. It is mentioned in experimentation manual of the Genoa L2 that the temperature rise in the secondary side flow is less than 1°C . Hence, a high heat transfer coefficient is used as the boundary condition at the cooler side along with the heat sink temperature. One 100 mm ID expansion tank as time dependent volume was also attached with the loop to account for any volume change. It was modeled as two partially filled water columns with interconnecting pipes. Interconnecting pipes were meant to model (if any) flow recirculation in the tank.

The grid independence test for the Genoa L2 facility has been carried out by varying the number of heat structures in the heater and cooler. The problem was solved using three degree of refinement namely, coarse, medium and fine having 40, 60 and 86 heat structures in each case respectively. The results are found to be very close for cases having 60 and 86 nodes for heat structures. Results also reveal that the stability of flow does not depend upon the number of heat structure nodes beyond a certain value which for present case can be taken as 60 nodes. Subsequent analysis for the effect of power, heat sink temperature and gravity (loop inclination) has been carried out with 60 numbers of nodes in heater and cooler.

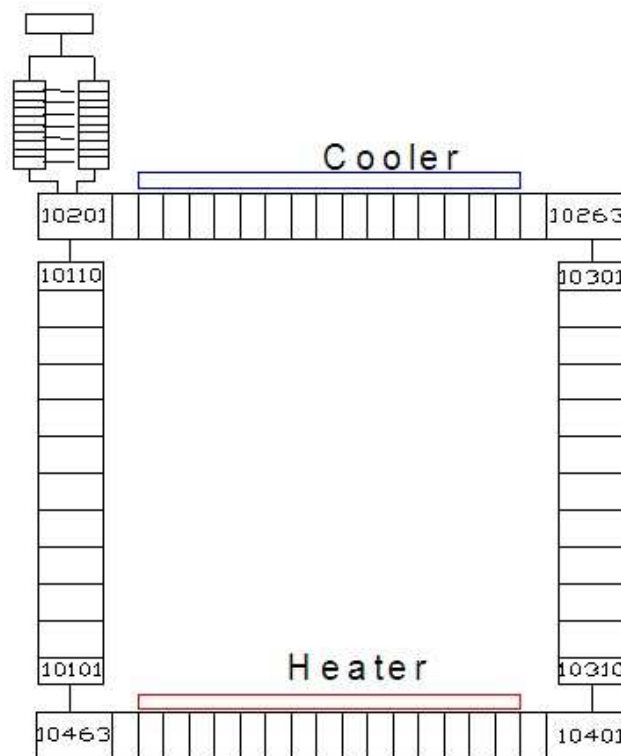


FIG. 21. L2 loop nodalization scheme in RELAP5.

4.3.2. Results & discussions

This section describes the simulation results for numerical studies performed for the Genoa L2 facility. Three independent parameters power, heat sink temperature and loop inclination angle have been varied and their effect on flow stability and fluid dynamics have been discussed. This analysis reveals that the simulation results are in good agreement with experimental results at low heat sink temperature and at lower power while deviates slightly from the same at higher power or high heat sink temperature.

4.3.2.1. Code validation

One sample result has been discussed below to show the validity of the code to predict temperature and flow map in natural convection flow in rectangular loops with circular section pipes.

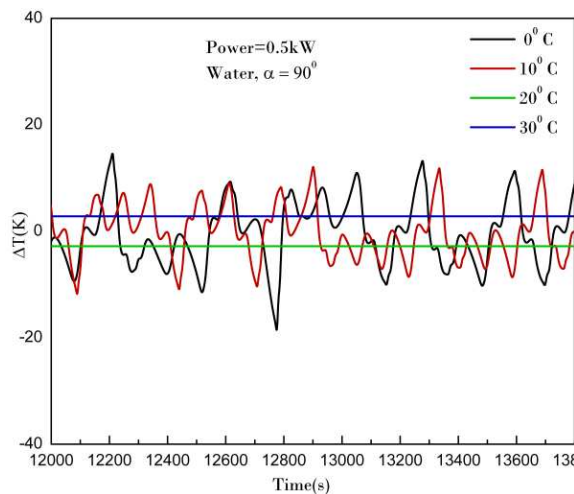


FIG. 22. Simulation results from RELAP5.

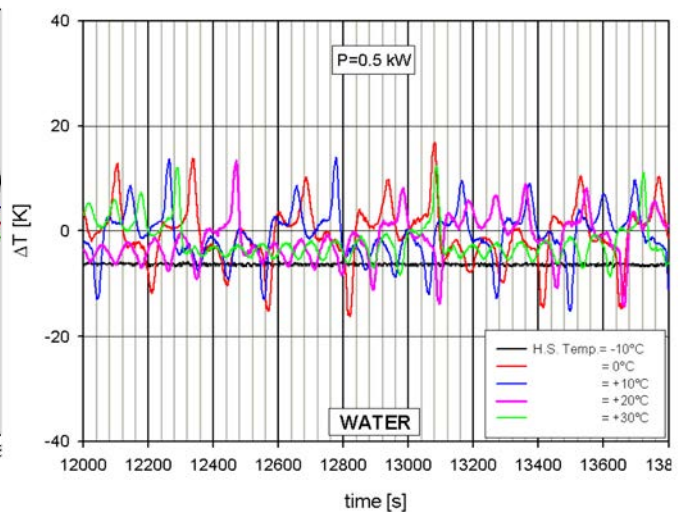


FIG. 23. Experimental results.

Figure 22 and figure 23 show comparison of simulation and experimental results [29].

Here temperature variable (ΔT) is the average of temperature difference across heater and cooler. The above comparison shows a good degree of agreement between simulation and experimental result for 0.5 kW power with water as working fluid in vertical inclination ($\alpha=90^\circ$).

4.3.2.2. Simulation for vertical loop ($\alpha=90^\circ$)

Vertical loop has been investigated for power varying from 0.5 kW to 2.5 kW and heat sink temperature varying from -10°C to 30°C with water remaining in single phase. During experiment the lower temperature limit depended generally on the cryostat cooling capacity and, in case of water at low power, also on the risk of freezing. The upper limit was due to cryostat working range, which excludes high temperatures. Such problems can be managed in numerical study but for the sake of simulation of exact facility, investigations have been restricted to above range. In each run the power is increased gradually from zero to appropriate level, while actual boundary conditions persist from initial time ($t=0$) itself. As mentioned earlier the heater and cooler have been arranged slightly eccentric for numerical calculations in order to make the fluid flow stable in a certain direction during start-up which can otherwise fluctuate in both the directions and thereby lead to spurious instability.

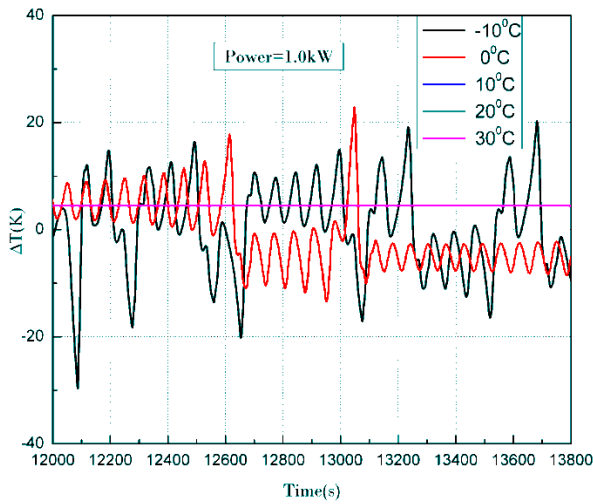


FIG. 24. Simulation results at $P=1.0$ kW.

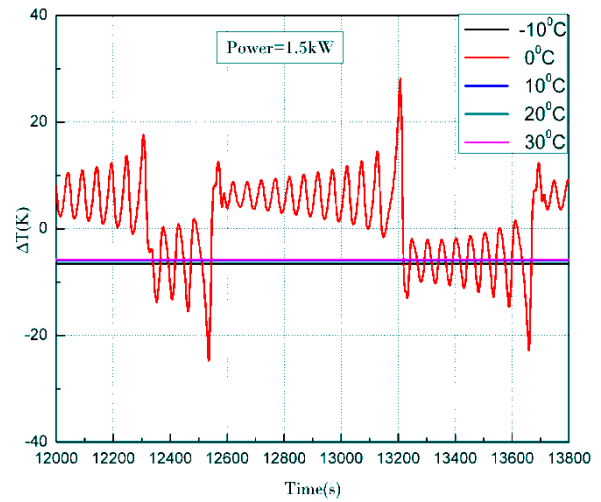


FIG. 25. Simulation results at $P=1.5$ kW.

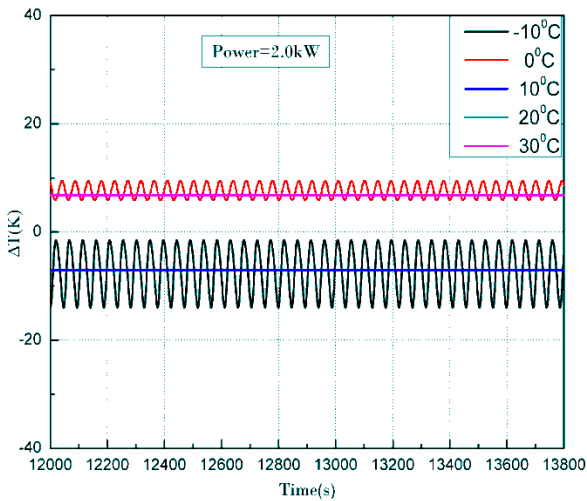


FIG. 26. Simulation results at $P=2.0$ kW.

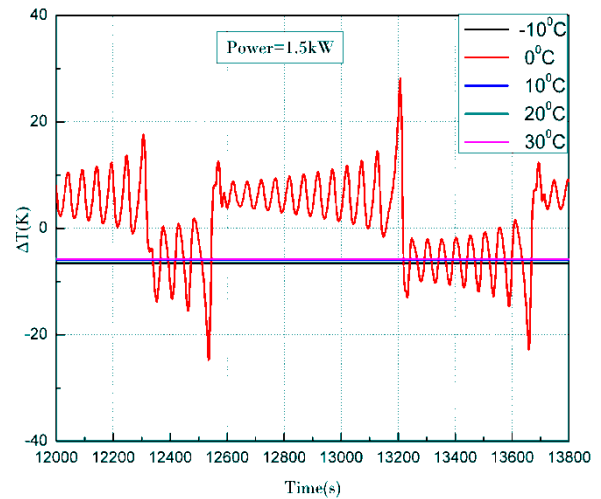


FIG. 27. Simulation results at $P=2.5$ kW.

Figure 24 to Figure 27 show simulation results for ΔT versus time in vertical inclination ($\alpha=90^\circ$) at different heat sink temperatures and power levels; (a) 1.0 kW; (b) 1.5 kW; (c) 2.0 kW; (d) 2.5 kW.

Average of temperature difference across heater and cooler are plotted for a time period of 1800 seconds. It is observed that flow reversals are frequent at low heat flux, with a few small oscillation amplifications. On the contrary, with increasing power, the number of oscillations between two consecutive flow reversals grows too, stabilizing the system at high values of coolant temperature. With increasing power, flow becomes stable even at low heat sink temperatures, which is evident from above figures. However this trend does not follow for the whole regime and for some set of parameters the flow pattern is unexpectedly stable. While the stability characteristics improve with increasing power, they seem to behave rather random with heat sink temperature. However, with increasing heat sink temperature, the average temperature of fluid increases which aids towards stability. When power transferred to the fluid is 2.0 kW flow is oscillatory at -10°C and 0°C . However when the power is increased to 2.5 kW the flow becomes unstable at -10°C but became stable at 0°C . Same is observed for the case of 1.0 kW and 1.5 kW.

4.3.2.3. Inclined loop ($\alpha=60^\circ, \alpha=75^\circ$)

The details of natural convection flow in an inclined loop are presented in this section. The loop inclination angles analyzed were $\alpha = 60^\circ$ and $\alpha = 75^\circ$, other parameters being the same. Figure 28 to figure 31 show the stability behaviour of the inclined loop for different heater power and heat sink temperature for inclination of 60. Similar to the vertical loop, in this loop the flow is found to be stable with increase in power and heat sink temperature. Similar observation is made for loop inclination of 75 as seen from FIG. 32 to 35.

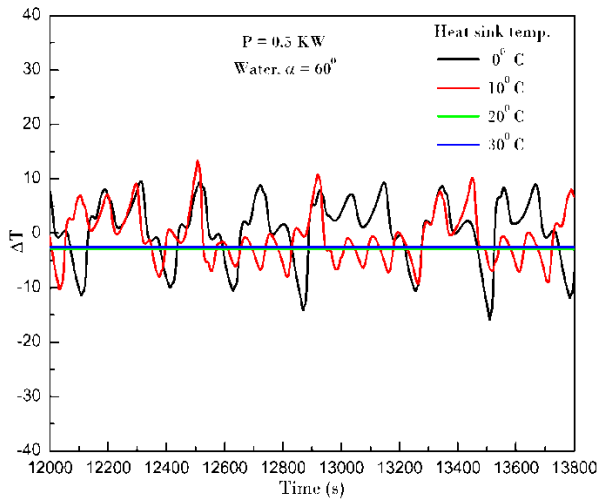


FIG. 28. Simulation results at $P=0.5\text{ kW}$, $\alpha = 60^\circ$.

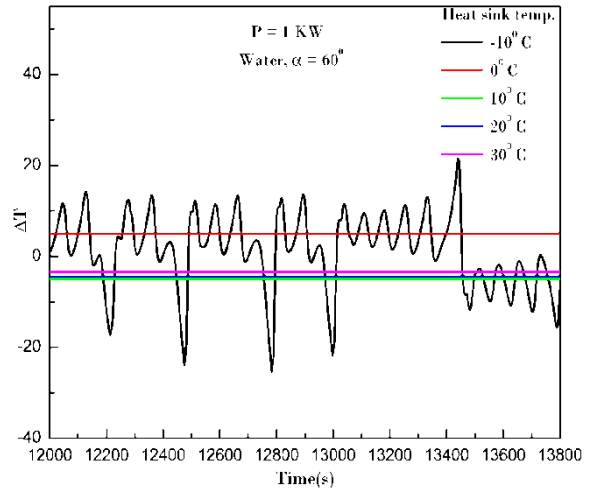


FIG. 29. Simulation results at $P=0.5\text{ kW}$, $\alpha = 60^\circ$.

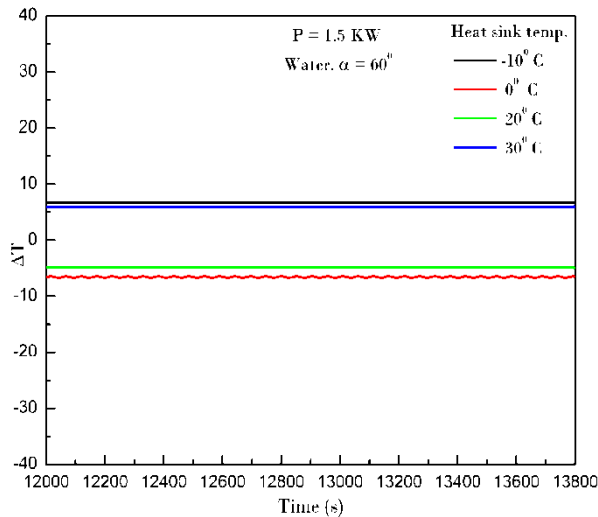


FIG. 30. Simulation results at $P=0.5\text{ kW}$, $\alpha = 60^\circ$.

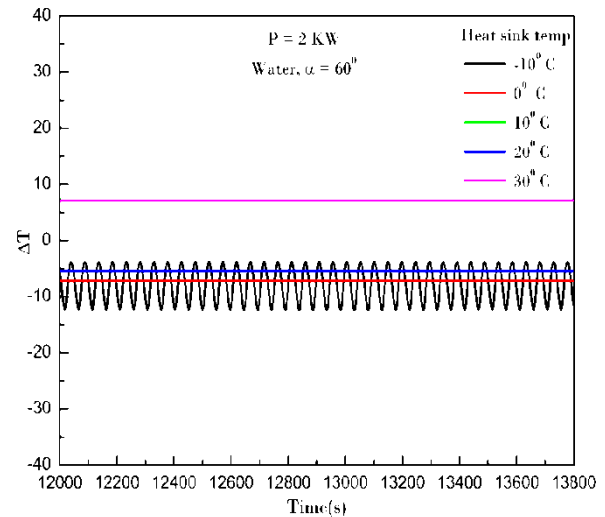


FIG. 31. Simulation results at $P=0.5\text{ kW}$, $\alpha = 60^\circ$.

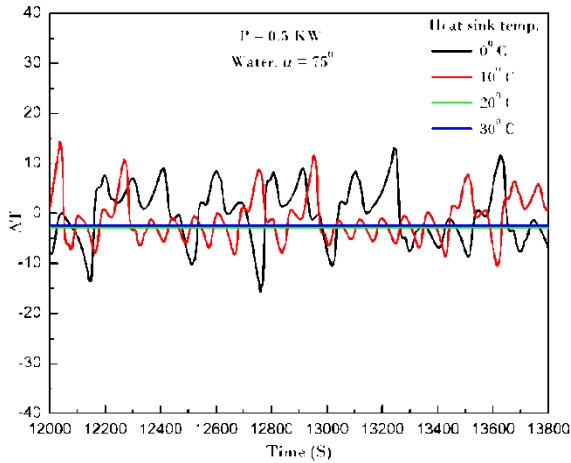


FIG. 32. Simulation results at $P=0.5$ kW, $\alpha = 70^\circ$.

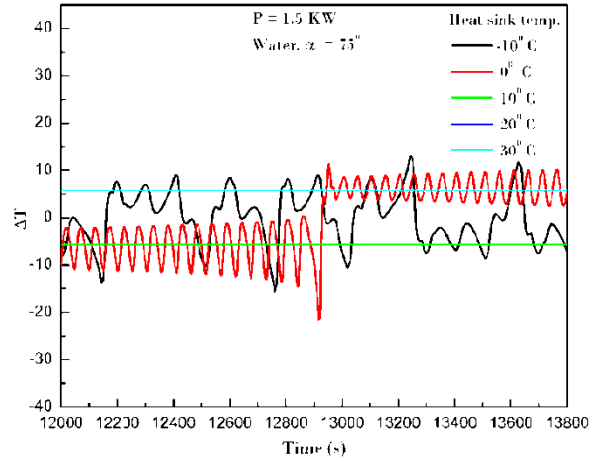


FIG. 33. Simulation results at $P=1.5$ kW, $\alpha = 70^\circ$.

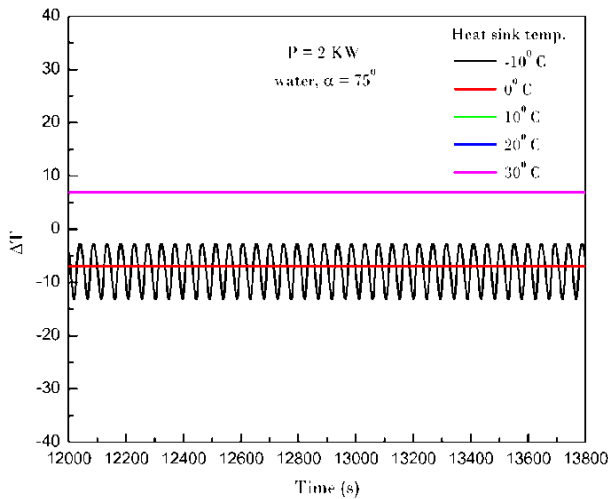


FIG. 34. Simulation results at $P=2$ kW, $\alpha = 70^\circ$.

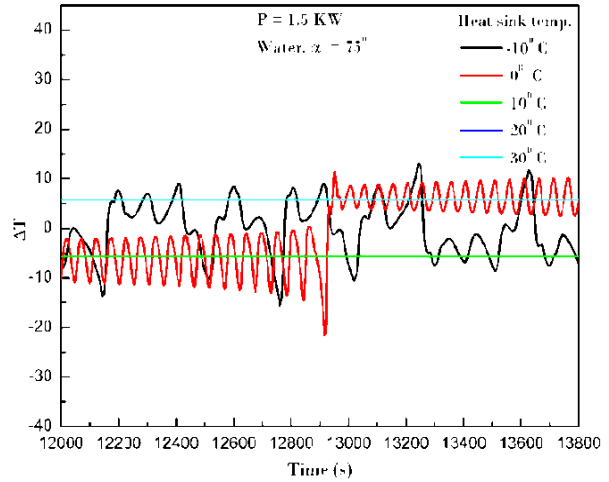


FIG. 35. Simulation results at $P=1.5$ kW, $\alpha = 70^\circ$.

Conclusions

Dynamic behaviour of loop as a function of heat sink temperature, power transferred to the fluid and the vertical inclination was analyzed. It was observed that with increasing power and heat sink temperature the natural circulation flow tends to be more stable. While the stability characteristics improve with power transferred to fluid, it seemed to be rather random with heat sink temperature. Simulation results show that effects of inclination angle on the flow stability are minimal. Different flow regimes such as stable flow, unstable flow, mono directional pulsing and bidirectional pulsing have been observed during the investigation. Comparison between numerical predictions and experiment show that while the results of numerical study are in good agreement at low power and low heat sink temperature but differ at high power and/or high heat sink temperature.

4.4. VALIDATION PERFORMED BY UNIVERSITY OF PISA, ITALY

4.4.1. Application of REPAS/RMPS to L2 natural circulation loop

The application of the REPAS/RMPS foresees a number of steps that for the sake of simplicity have been summarized in FIG. 36. The first block deals with the analysis of the system and the identification of the design goals. The second block deals with the identification of the design parameters of the system under study, their range of variation.

After the completion of the previous steps, the application of the methodology concerns the definition of the limit for the acceptability of the system performance and finally to execute the calculation for observing the variation of the system performances when the parameters are varying inside the established limits. After all the previous steps the reliability of the system can be evaluated.

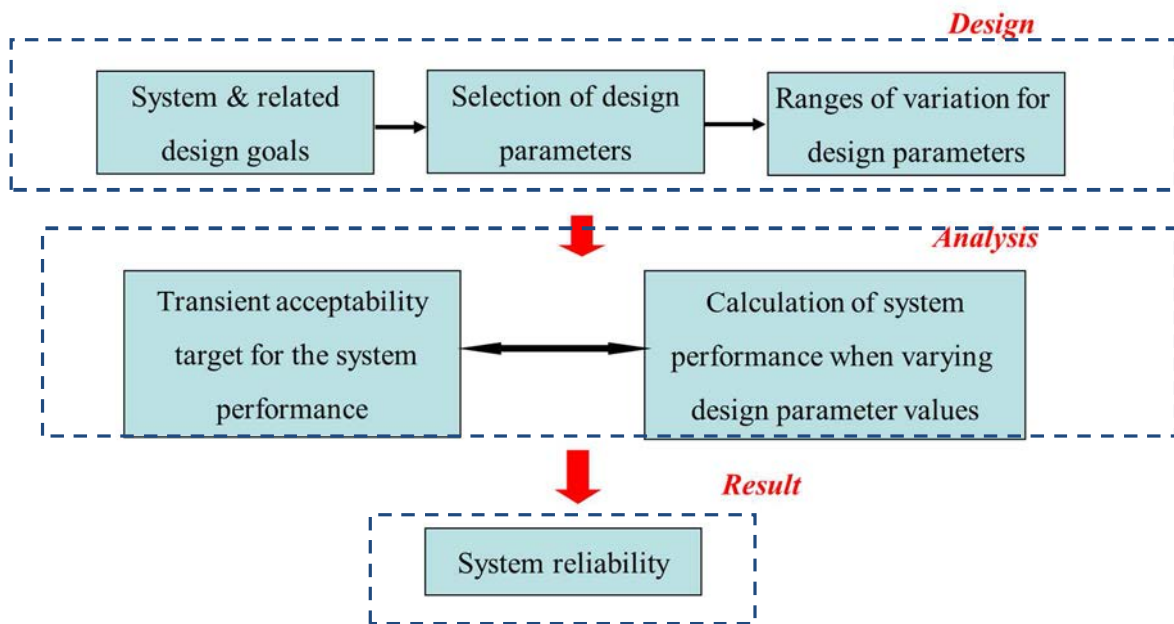


FIG. 36. Simplified REPAS/RMPS flow chart.

Following the road map summarized in FIG. 36, the first step in the application of the REPAS/RMPS is the analysis of the L2 natural circulation loop features. In this case the L2 loop represents a passive system where the natural circulation can be induced. Regarding the mission of the system the following assumptions have been agreed among the participants:

- The mission of the system is to maintain a stable natural circulation;
- The natural circulation is considered stable when the water rotates in the same direction without oscillations;
- During each experiment, the direction of the fluid flow (clock wise or anti-clock wise) is not important for the purpose of the activity.

Once the mission is identified, the parameters that affect the behaviour of the system have to be selected. The characteristics of the L2 loop have been analysed together with the experimental data already available. In addition, a RELAP5/MOD3.3 nodalization has been setup and used to perform sensitivity analysis in order to confirm that the parameters proposed were ok and among them which were the most important that affect the loop behaviour. The results of this activity are described in the next paragraph.

In this case the accuracy of the calculation results is expressed in terms of expert judgement, because the application of tools like the Fast Fourier Transform Based Method (FFTBM) (see Ref. [39–41]) adopted in the Uncertainty Method based upon Accuracy Extrapolation (UMAE) developed at University of Pisa (see Ref. [42–43]) does not give significant results due to the fast oscillation of the phenomenon observed.

An example of these results obtained during the setup phase of the nodalization is reported in FIG. 38. The positions of the thermocouples simulated by the code are reported in FIG. 39.

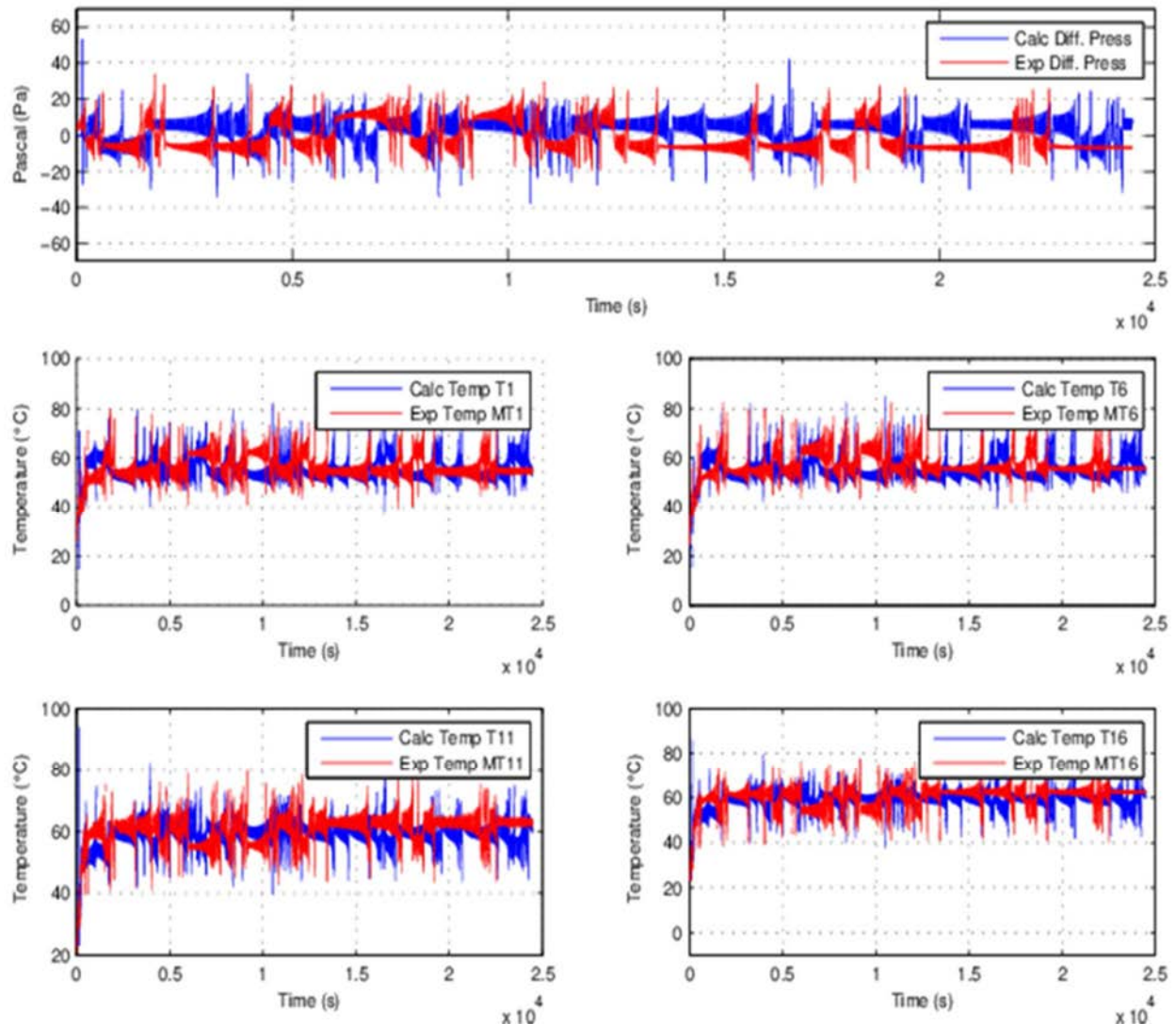


FIG. 38. Comparison Exp-Calc for Differential pressure and temperatures along the L2 loop.

The results show that the code is able to reproduce the main oscillations, their variations in amplitude and time of occurrence. The nodalization that has produced those results has been adopted as the reference for the 800 calculations without any further adjustments.

Once the nodalization was ready, a sensitivity analysis has been conducted aimed at identifying the most important parameters affecting the behaviour of the natural circulation. Several code runs have been executed changing the value of one single parameter a time inside its range of variation and implemented in the nodalization in order to see the effect on the result. Three are the parameters that mainly affect the results:

- Cooler 'inlet temperature';
- Thickness of the tubes;
- Power at heat source.

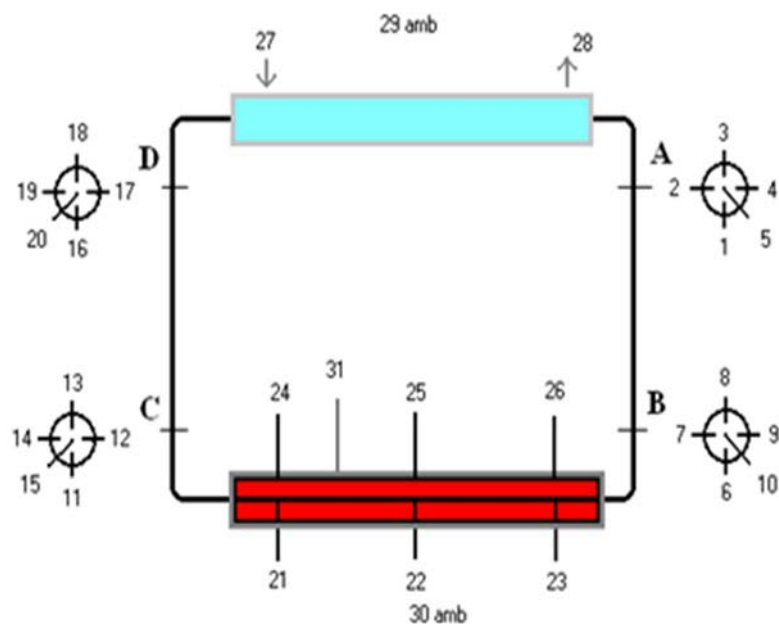


FIG. 39. Position of the thermocouple along L2 loop.

The cooler inlet temperature is important because any oscillation of this parameter affects the temperature of the heat sink and influences the difference between the temperature of the heat sink and heat source. This parameter affects the driving force of the natural circulation.

The thickness of the tube influences the thermal inertia of the system. The variation of this parameter inside the manufacturing tolerances shows a big effect on the results because increasing the thickness there is the effect of smoothing the oscillation, decreasing the thickness the system becomes more unstable and the oscillations increase.

The power at the heat source affects the difference in temperature between the source and the sink. It has an effect similar to the variation of the temperature at the heat sink (HS).

4.4.1.2. Statistical analysis

As prescribed from REPAS/RMPS methodology, once the parameters are selected, their ranges of variation and PDF have to be identified.

For the inlet temperature has been observed that the Gaussian distribution fits the experimental data. In FIG. 40, two examples have been reported for the HS Temp if 4 and 11 °C and it is evident that the experimental data follows a Gaussian shape. For the two temperatures at FIG. 40, the standard deviation is $\sigma = 0.0977$ for HS temperature. 4°C and $\sigma = 0.1158$ for the 11 °C H. S. temperature.

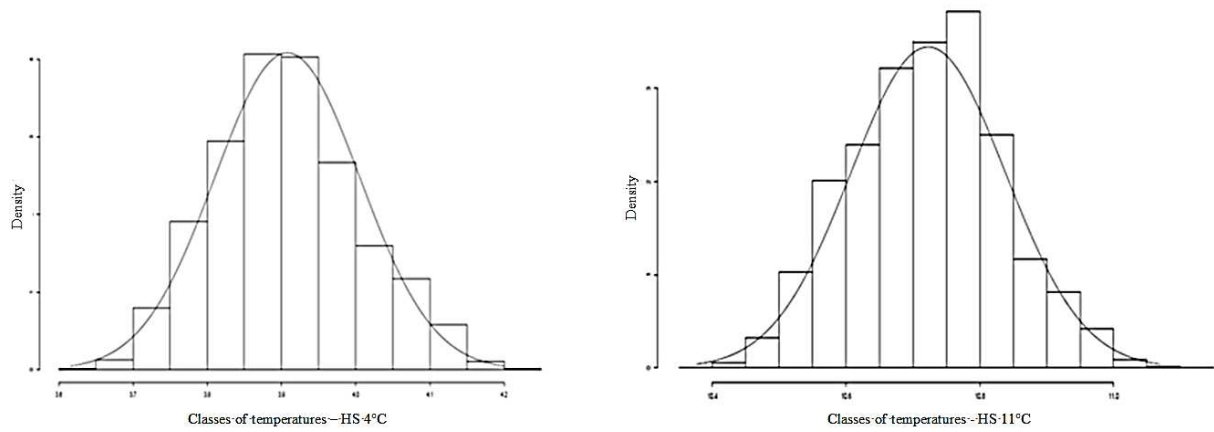


FIG. 40. Histogram at HS Temp 4 °C and HS Temp 11°C.

For the tube thickness, and the power at the heat sink, no data is available from the supplier of the tubes and from the manufacturer of the power system. Furthermore during the experiments there is no registration of the power supplied to the heating resistance. For these reasons, the PDF for both quantities, the Gaussian distribution has been selected by means of engineer judgment (see FIG. 41) with $\sigma = 0.1020$ for the thickness and $\sigma = 1.0204e-3$ for the power.

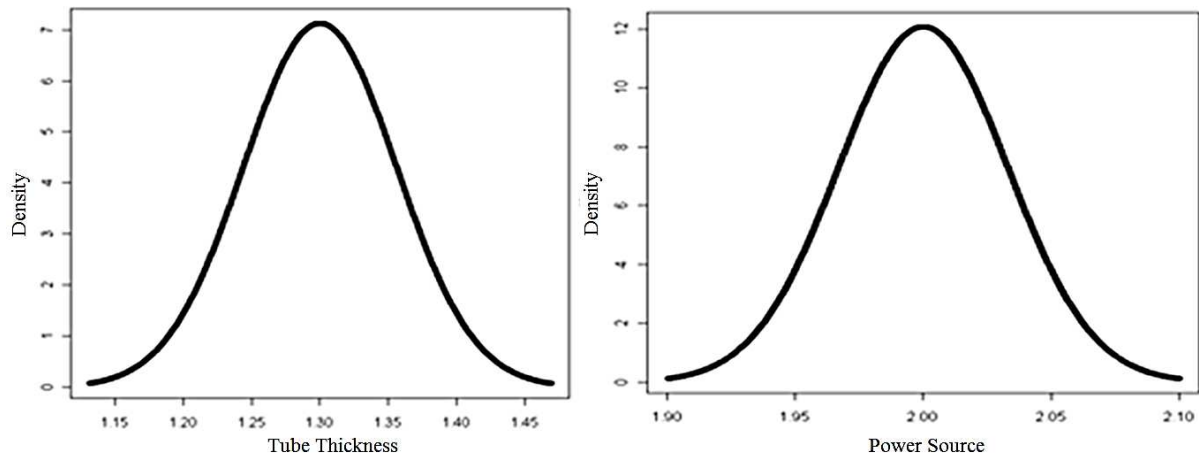


FIG. 41. Gaussian distribution for tube thickness and power at sink source.

A summary of the parameters, their range of variation and the related PDF are reported in Table 2 with the following assumptions for the parameters:

1. The min and the max correspond respectively to the quartile (for example) 2.5% and 97.5%, then the given range of variation corresponds to a confidence interval at 95%;
2. The mean = (min + max)/2 and the standard deviation, $\sigma = (\text{max} - \text{mean})/1.96$;
3. The distribution is truncated at + and - 2*standard deviations (for the temperature) or at their physical limits for thickness and diameter.

Once that the parameters are characterized, the next step is to define the size of the samples for each of the temperatures identified that will be used for performing the code runs.

Among the participants has been agreed that for each of the 8 temperatures of the heat sink identified, a sample size of 100 has been selected. This sample size has been obtained by mean the Wilks' formula that gives the proper number of independent observations of the

random output, minimizing the number of calculations that characterize the system performance.

Each of the samples is obtained selecting 100 sets of triples, one value for the Inlet temperature, one value for the tube thickness and one value for the power of the heat source. The selection has been done by means of Monte Carlo simulation taking into account the PDF and the range of variation of each parameter. One of these triples represents a status of the system and its probability of occurrence is obtained by multiplying the probability of occurrence of each parameter.

Each one of the identified set has been implemented in the RELAP5/MOD3.3 input deck and the calculation has been performed. Totally 800 code results have been obtained. This huge number of calculations has been managed by means of a subroutine that automatically changed the parameter identified inside the nodalization and stored the result of each run.

TABLE 2. L2 NATURAL CIRCULATION LOOP: SELECTED PARAMETERS FOR RELIABILITY ANALYSIS

No.		Parameter	Unit	Setpoint	Max	Min	PDF	Note
1	a	Inlet Temperature	°C	4	5.061	3.578	normal	Experimental Data
	b			7	7.274	6.631	normal	Experimental Data
	c			8	8.137	7.368	normal	Experimental Data
	d			9	9.479	8.879	normal	Experimental Data
	e			10	10.121	9.35	normal	Experimental Data
	f			11	11.12	10.325	normal	Experimental Data
	g			14	14.06	13.32	normal	Experimental Data
	h			18	18.603	17.941	normal	Experimental Data
2	a	Outlet Temperature	°C	4	9.085	4.244	normal	Experimental Data
	b			7	12.307	7.292	normal	Experimental Data
	c			8	13.984	8.027	normal	Experimental Data
	d			9	13.53	9.841	normal	Experimental Data
	e			10	14.433	10.096	normal	Experimental Data
	f			11	15.022	11.111	normal	Experimental Data
	g			14	17.884	14.113	normal	Experimental Data
	h			18	21.799	18.933	normal	Experimental Data
3	a	Tolerance Thickness	mm	1	1.1	0.9	normal	Tolerance 10%
	b	Tolerance Ext. Diameter	mm	31	31.31	30.69	normal	Tolerance 1% Ext. Diameter = 30+1
4	a	Power at the Heat source	kW	2	2.001	1.999	normal	Stability: $\pm 0.05\%$

4.4.1.3. Performance indicator

In order to characterize in analytical way the behaviour of the system and to be able to distinguish among the successful and unsuccessful cases namely the cases in which the mission of the system is fulfilled and the cases were not, a parameter must be selected: the Performance Indicator (PI).

The selection of such parameter for distinguish the cases where the natural circulation is stable from the cases where the natural circulation is unstable is not an easy task.

The proposed one is defined as in the following steps:

1. First of all to select a reference case; namely the limit case from stable and unstable behaviours. Among the calculations performed, the case with T inlet = 18°C the Sensitivity number: 100 has been selected;
2. For the reference case selected to calculate the absolute value of the mean of the difference between the temperatures at point A and D (see FIG. 39);
3. To calculate the integral of the absolute value of the difference T(A)-T(D) minus the value calculated at item 2 in the last 3000 seconds because, as observed in the experimental data, the transient are stable for sure in the last part of the experiment. The system is considered stable if it is stable at least in that range:

$$Z_{ref} = \int_{t=end-3000}^{t=end} |T(A)_{ref} - T(D)_{ref}| - \overline{|T(A)_{ref} - T(D)_{ref}|} dt \quad (9)$$

4. To repeat the step 2 and step 3 for each one sensitivity (Z_i):

$$Z_i = \int_{t=end-3000}^{t=end} |T(A)_i - T(D)_i| - \overline{|T(A)_i - T(D)_i|} dt \quad (10)$$

5. To computed PI for each set point HS Temp., shown in Table 2, following the formula:

$$PI_i = \frac{Z_i}{Z_{ref}} \quad (11)$$

We realized that for a PI>1, the system is unstable, while for 0<PI<1 it is stable.

Once the PIs are evaluated for each status of the system (each code run), they are represented as function of the probability of occurrence of that status.

$$P(\text{Status}) = P(\text{Inlet Temperature}) \times P(\text{Tube Thickness}) \times P(\text{Power source})$$

Once the PIs have been evaluated for each one of the 800 simulations, the same values have to be evaluated for the experimental data as well, because at the end of the process the value of the reliability value evaluated with the REPAS/RMPS methodology has to be compared with the one coming from the experiments, as summarized in the FIG. 42.

The evaluation of the probability of each status of the system cannot be done because the value of the probability for each status experimentally determined is difficult. The probability of the status is obtained multiplying the probability of occurrence of the three parameters selected at the beginning. While for the inlet temperature is possible to have a value for the probability, for the power source and the tube thickness is not possible to know their 'real' values adopted during the experiments.

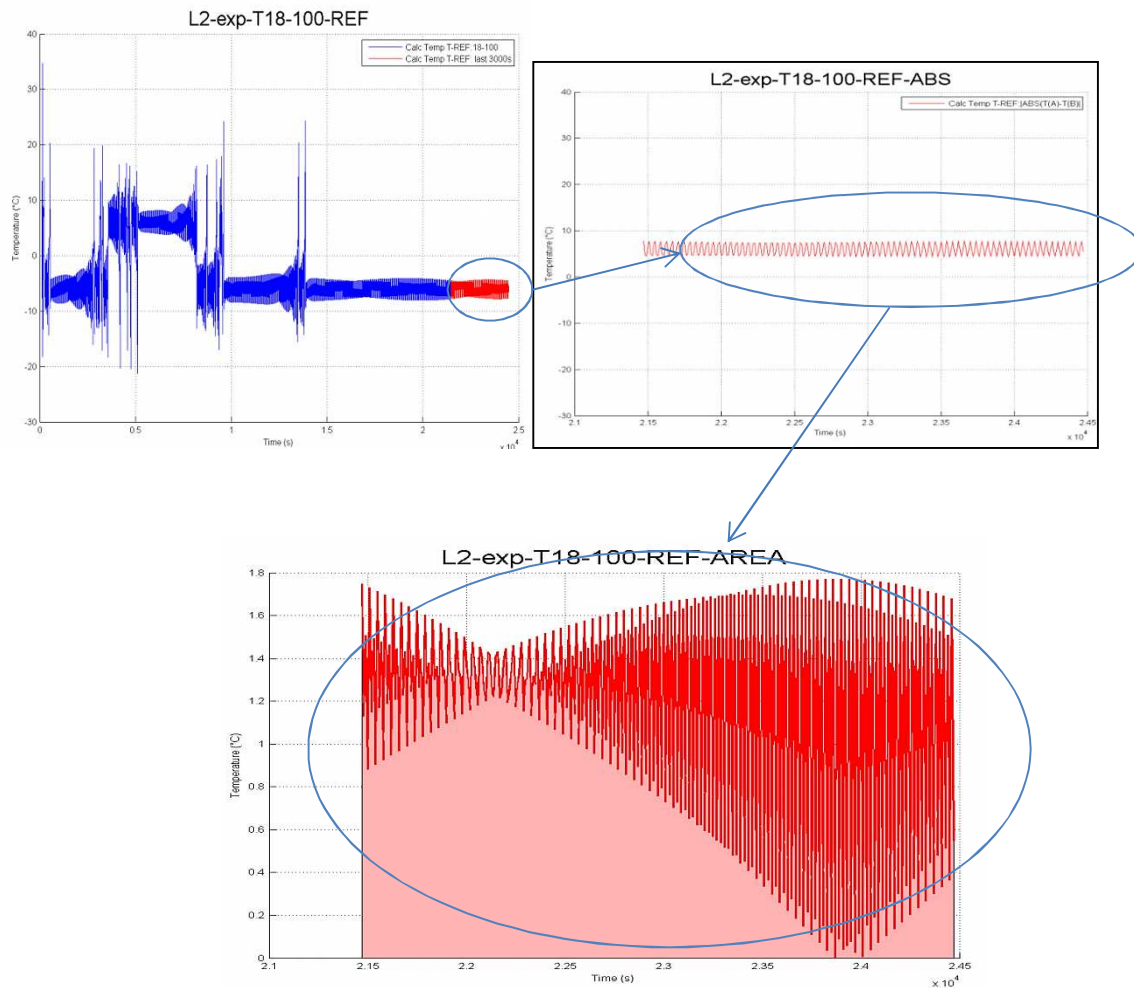


FIG. 42. Reference case ($T=18\text{ }^{\circ}\text{C}$) for PI construction.

For the sake of simplicity, in this case has been decided to consider two values for the probability of the tube thickness and the power source, the lower (in the tail of the curve) and the higher value (the mean value) and to represents these two as bounding cases.

The resulting PIs evaluated by mean the REPAS/RMPS (in light blue) and from the experimental data (yellow and red) have been reported in the FIG. 43.

The PIs evaluated for the experimental data are in yellow for the lower probability (considering the probability in the tail of the PDF) and in red for the values at high probability of occurrence (considering the mean value of the PDF).

It can be noted that:

- All PI of the 800 calculations are contained within the experimental data;
- The curves of merit demonstrate that the stability of the system increases with the increase of the temperature of the HS; the curves of merit are used to judge the system acceptability and provide an indication of the system trend towards stabilization.

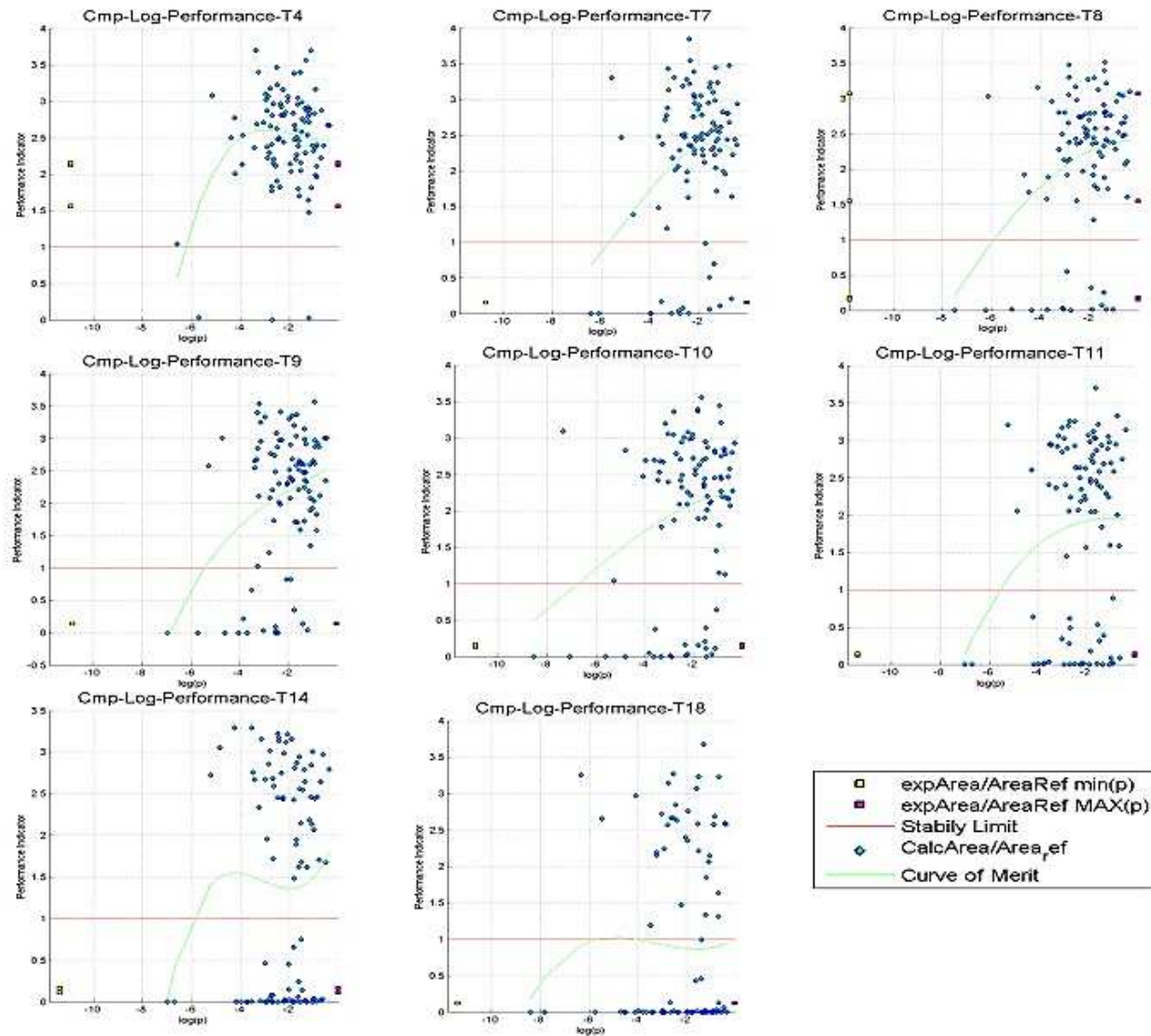


FIG. 43. Comparison PI Exp-Calc and curve of merit.

Conclusions

The application of the REPAS/RMPS has shown that the methodology is able to calculate the reliability of the system, while from the experimental point of view, the lack of some information as the real thickness of the tubes of the facility and the measurement of the power is the reason why the performance indicator of the system cannot be evaluated properly.

At the end is possible to conclude that this activity has a relevant scientific value because the capability of the REPAS/RMPS to simulate the behaviour of the natural circulation loop L2 has been highlighted and from the experimental point of view represents a good test for the design of new future qualification activities.

5. DEVELOPMENT AND APPLICATION OF METHODS TO MINIMIZE NUMBER OF CALCULATIONS

5.1. INTRODUCTION

Reliability of active systems is analyzed by combinatorial methods from known probability of subsystems and components. Whereas, for passive systems in new generation of nuclear reactors such as natural convection based heat transport system or reactor core support structures, the uncertainties in their design performance is a significant contributor to unreliability. The problem of estimating the reliability of passive decay heat removal systems [2] and structures has been an important area of study in probabilistic safety analysis of advanced nuclear reactor designs. The various approaches to the solution of this problem are based on quantifying the margin to failure by uncertainty propagation [44–45]. The analysis framework consists of characterizing the probability density function of important input parameters and then propagating them through a system model to quantify the system response uncertainty [46, 6]. Characterizing the input uncertainty distribution type and model parameters is best done from experimental data. However, characterizing the input uncertainty when the experimental data is scarce is a challenging task and is an active area of research. Techniques like Bayesian Inference and Dempster-Shafer theory are being applied for minimizing subjectivity [47]. The system model might range from simple analytical formula, systems of equations or those represented by complex computable algorithm. Uncertainty propagation could be done by analytical methods when, input parameters are characterized by certain class of distributions like normal distribution and the system of interest is described by simple analytical formula [45]. For more general cases Direct Monte-Carlo methods could be used to construct a probability density function of the response parameter. However, direct Monte-Carlo methods require very large computational time and is due to i) the complexity of the model represented by large computer codes and ii) inherently large number of statistical samples required to estimate small probability of failure (For instance to evaluate a failure probability P_f with fractional error f , the number of samples required by direct MCS, N is $\geq f^{-2}/P_f$). Essentially, the effective time per sample (including any overheads for model reduction) and the number of samples are the two key variables.

For thermal-hydraulic passive systems, the system model is usually a complex computer code, and hence the computational time for each sample could be reduced by constructing a response surface (approximate model) with limited code runs and then use the response surface for propagating the uncertainty. Even here the minimum number of code runs has to be of the order of number of uncertain parameters or more from statistical and model complexity considerations.

In this context, further reducing the number of deterministic code runs and hence the computational effort and cost is an important objective, which will have impact not only for better reliability analysis but also for reliability optimization methods. Sensitivity analysis methods offer good potential for efficiently computing the response surface for a given problem. The sensitivity coefficients are obtained as derivatives of some performance parameter, which is in general some functional of the system response. When the number of response parameters is large and number of input parameters is small the forward solution of the sensitivity analysis problem is efficient. When the number of response parameters is small and input parameters are large in number, the adjoint sensitivity solutions will be efficient [48–51]. With the adjoint operator method all that is required will be one direct computation of the system response and one adjoint computation. From this all parameter sensitivities could be obtained directly or by a subsequent integration procedure. The adjoint operator

method for sensitivity analysis and optimization has been studied in the area of aerodynamic shape optimization [52] and nuclear reactor thermal hydraulics [48] and neutronics [49]. The adjoint theory can be implemented at any of the three different stages during the analysis of a problem, first, at the continuous operator level, second at the discrete operator level and third at the numerical code/program level. Here the application of the adjoint theory, at the first level (referred to as adjoint operator approach) and third level (referred to as automatic differentiation approach) to the functional reliability analysis problem is studied. Figure 44 is diagrammatic elaboration of the uncertainties and the uncertainty propagation model.

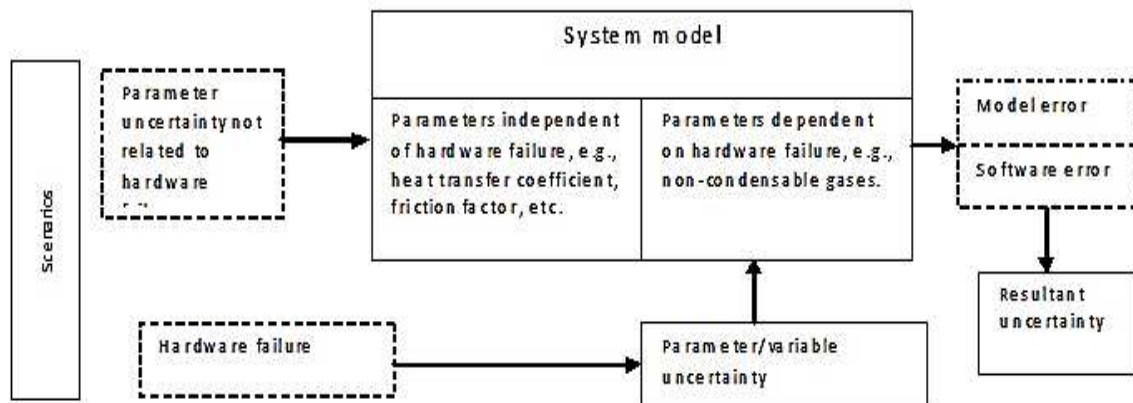


FIG. 44. Uncertainties and uncertainty propagation model.

Within this framework, a new and improved methodology is presented for the functional reliability analysis of a passive thermal hydraulic system by incorporating adjoint theory in the form of adjoint operator technique and algorithmic differentiation technique. In the adjoint operator formalism, the adjoint operators are derived from the continuous integral-differential equations and the adjoint numerical code derived by discretization procedure. In the algorithmic differentiation technique, the adjoint code is derived directly from the best estimate deterministic code. Using any one of these techniques a response surface could be constructed from the generated sensitivity coefficients. This response surface or local gradient information could be used in three different ways to perform a reliability calculation. In the first case, response surface substitutes the original model for Monte Carlo simulation and accurate estimates can be made when the response surface is estimated about the failure point. In the second case, the response surface is used to locate the most probable failure region for the application of important sampling MCS procedures (ex: Metropolis MC-MCS [53]). The third kind of use is when the sampling MCS repeatedly uses gradient information as in Hamiltonian method [53] of Markov Chain Monte Carlo simulation.

The results from the study of the application of above mentioned approaches to the functional failure reliability analysis of a simple thermo-siphon loop for nuclear heat transport applications is presented. The problem studied is transient temperature evolution in critical parts of the system. The efficiency of the approach, for the case of using the response surface constructed about the design point, directly for Monte Carlo simulation and for the case importance sampling MCS by utilizing the information about failure region is compared with direct Monte Carlo method and results presented.

There have recently been studies to speed up Monte Carlo sampling of uncertain parameters, i.e. reducing the number of statistical samples required for a given accuracy, using methods like line sampling [54], especially when the sampling direction is perpendicular to the failure surface and subset simulation [54–55].

5.2. ADJOINT OPERATOR APPROACH

5.2.1. Adjoint methods for sensitivity and reliability analysis

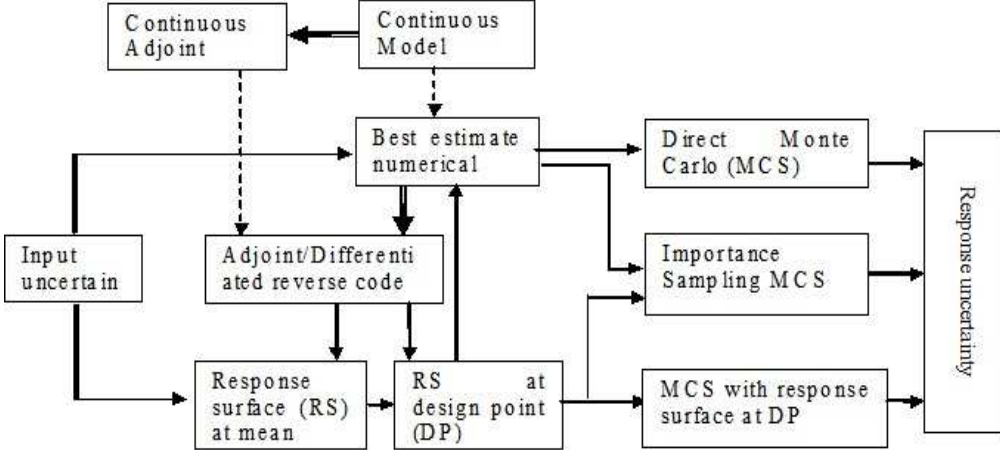


FIG. 45. Schematic showing role of adjoint operator/algorithmic differentiation in the computational methodology for uncertainty propagation.

Figure 45 gives the context of adjoint theory based sensitivity analysis in the passive system functional reliability analysis methodology. The dotted lines indicate discretization step, while double lines indicate adjoint operator/code derivation. The numerical solution of a physical problem is done in three steps. First is the analytical formulation of the problem as an integral-differential equation. Second, the equations are discretized using appropriate numerical schemes. Third is the implementation in a programming language. The adjoint or reverse mode computation can be implemented at any of the three stages. In the first method adjoint differential equations are formulated and solved. In the second method, the continuous differential equations are discretized and the dual operator is derived from the discrete equations. In the third approach, the best estimate code or is differentiated and a dual or reverse mode differentiated program is derived from the forward program. The first approach was applied for the passive system functional reliability analysis problem in [56], which is suitable during code development stage. Here algorithmic differentiation technique is applied to the natural convection system sensitivity analysis. From sensitivity coefficients a linear response surface is constructed about the most probable operating point, which can be used to predict the most central failure point about which importance sampling Monte Carlo simulation could be carried out.

The linear response surface model can be very efficiently generated with the adjoint methods.

This response surface or local gradient information could be used in three different ways to perform a reliability calculation. In the first case, response surface substitutes the original model for Monte Carlo simulation and accurate estimates can be made when the response surface is estimated about the failure point. In the second case, the response surface is used to

locate the most probable failure region for the application of importance sampling MCS procedures (ex: Metropolis MC-MCS). The third kind of use is when the importance sampling MCS repeatedly uses gradient information as in Hamiltonian method of Markov Chain Monte Carlo simulation.

5.2.2. Adjoint operator formulation

5.2.2.1. Direct sensitivity for heat transport in an asymmetrical loop

Forward Equations

The problem considered for the reliability analysis is heat transport through a thermo-siphon loop as shown in FIG. 46 where the working fluid is assumed to be liquid sodium. This is a simplified model of the passive decay heat removal system deployed in fast neutron nuclear reactors. The thermal and hence density gradients interacting with the gravitational field induces fluid flow resulting in increased energy flow from source to sink. The asymmetry of the heater and cooler positions with respect to the gravitational field is essential for the driving force. It is assumed that Boussinesq approximation holds. The equations for the conservation of mass, momentum and energy in one spatial dimension after integration along the thermo-siphon loop length, after simplification, are:

The mass flow rate,

$$W(x,t) = W(t) \quad (12)$$

$$\frac{dW}{dt} + \frac{W^{2-b} \cdot a \mu^b}{2D^{1+b} A^{1-b} \rho_0} = -\frac{A}{\ell} g \beta \rho_0 \int T \cdot \cos \theta \cdot dx \quad (13)$$

The energy conservation equation for the loop is,

$$\frac{\partial T}{\partial t} + \frac{W}{A \rho} \frac{\partial T}{\partial x} + E U(x) T = E q(x) + E U(x) T_0 \quad (14)$$

The boundary conditions are

$$T(x, 0) = T_r \text{ and } W(t=0) = W_0. \quad (15)$$

The flow and temperature sensitivity equations are obtained in the next section.

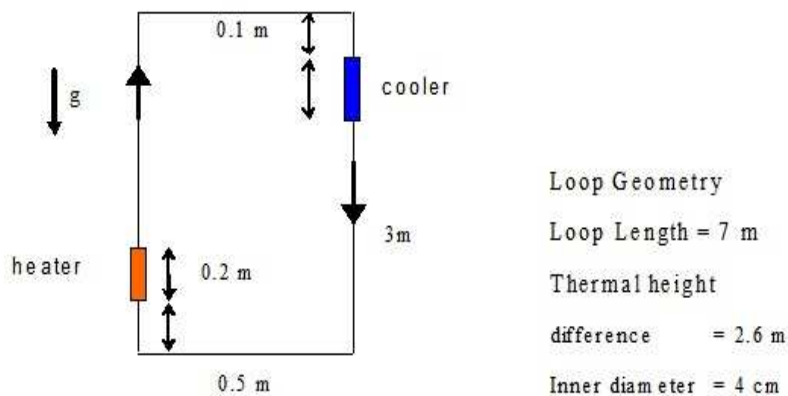


FIG. 46. Simple heat transport loop.

Sensitivity analysis

In sensitivity analysis one is interested in the change in response variables like temperature and flow rate when there is a change in the independent parameters describing the system structure and properties. The response is in general defined as a functional,

$$R = \int_0^{\tau} W(t) g_w(t) dt + \int_0^L \int_0^{\tau} T(x, t) g_T(x, t) dt dx \quad (16)$$

Where g_w and g_T are suitable weighting functions. The sensitivity with respect to parameter α is $S_\alpha = \frac{dR}{d\alpha}$ and normalized sensitivity is defined as $N_\alpha = \frac{\alpha}{R} \frac{dR}{d\alpha}$. (17)

There are several procedures for applying this formula. Simplest but computationally inefficient is to take finite difference as,

$$S_\alpha = \frac{dR}{d\alpha} = \frac{R(\alpha + \Delta\alpha) - R(\alpha)}{\Delta\alpha} \quad (18)$$

and evaluate $R(\alpha + \Delta\alpha)$ and $R(\alpha)$ by two computations of R .

Instead the sensitivity can be obtained by differentiating the original equations and solve them directly to evaluate,

$$S_\alpha = \int_0^{\tau} \frac{dW(t)}{d\alpha} g_w(t) dt + \int_0^L \int_0^{\tau} \frac{dT(x, t)}{d\alpha} g_T(x, t) dt dx + \int_0^{\tau} W(t) \frac{dg_w(t)}{d\alpha} dt + \int_0^L \int_0^{\tau} T(x, t) \frac{dg_T(x, t)}{d\alpha} dt dx \quad (19)$$

The procedure for evaluating the derivatives is shown below. Rewriting the momentum Eq. (13) with

$$B = \frac{\alpha \mu^b A^{b-1}}{2D^{1+b} \rho_0} \quad \text{and} \quad C = \frac{A}{\ell} g \beta \rho_0 \quad \text{we get,}$$

$$\frac{dW}{dt} + B.W^{2-b} = -C \int T \cos \theta dx \quad (20)$$

Differentiating with respect to a parameter denoted by α ,

$$\frac{d}{d\alpha} \frac{dW}{dt} + \frac{d}{d\alpha} B.W^{2-b} = -\frac{d}{d\alpha} C \int T \cos \theta dx, \quad \text{and denoting } \frac{dW}{d\alpha} = S_w$$

$$\frac{dS_w}{dt} + B(2-b)W^{1-b}S_w + C \int S_T \cos \theta(x) dx = -\frac{dB}{d\alpha} W^{2-b} - \frac{dC}{d\alpha} \int T \cos \theta dx \quad (21)$$

with the RHS, denoted by F_w ,

$$\frac{dS_w}{dt} + B(2-b)W^{1-b}S_w + C \int S_T \cos \theta(x) dx = F_w \quad (22)$$

Eq. (22) is sensitivity equation for the flow rate W in terms of the parameter, α which is linear in S_w . All the sensitivity derivatives of parameters appear only on the RHS, namely in F_w . Similar equation for the temperature sensitivity is obtained by differentiating the energy conservation Eq. (14) with respect to α ,

$$\frac{\partial}{\partial t} \frac{\partial T}{\partial \alpha} + \frac{\partial}{\partial \alpha} \left(\frac{W}{A\rho_0} \right) \frac{\partial T}{\partial x} + \frac{W}{A\rho_0} \frac{\partial}{\partial x} \frac{\partial T}{\partial \alpha} + T \frac{\partial}{\partial x} EU(x) + E U(x) \frac{\partial T}{\partial \alpha} = \frac{d}{d\alpha} (E q(x) + E U(x)T_0) \quad (23)$$

with S_T denoting the derivative of T with respect to α , we get

$$\frac{\partial S_T}{\partial t} + \frac{1}{A\rho_0} \frac{\partial T}{\partial x} S_w + \frac{W}{A\rho_0} \frac{\partial S_T}{\partial x} + E U S_T = -W \frac{\partial}{\partial \alpha} \left(\frac{1}{A\rho_0} \right) \frac{\partial T}{\partial x} - T \frac{d}{d\alpha} (E U(x)) + \frac{d}{d\alpha} [E q(x) + E U(x)T_0] \quad (24)$$

denoting the RHS by F_T ,

$$\frac{\partial S_T}{\partial t} + \frac{W}{A\rho_0} \frac{\partial S_T}{\partial x} + E U(x) S_T + \frac{1}{A\rho_0} \frac{\partial T}{\partial x} S_w = F_T \quad (25)$$

The above equations are linear even if the original equations were non-linear because of the wall friction and dependence of the properties on temperature and flow. The left hand side is independent of $\frac{d}{d\alpha}$ terms. The source terms are,

$$F_w = -\frac{dC}{d\alpha} \int T \cos \theta dx - \frac{dB}{d\alpha} W^{2-b} \quad (26)$$

$$F_T = -W \frac{\partial}{\partial \alpha} \left(\frac{1}{A\rho_0} \right) \frac{\partial T}{\partial x} - \frac{d}{d\alpha} (E U) T + \frac{d}{d\alpha} [E q(x) + E U(x)T_0] \quad (27)$$

Finite differencing these equations and solving them numerically would give us the required sensitivity, which could be used in Eq. (19) for any number of responses. However, if the sensitivities are needed for more than one parameter, as many forward solutions as the number of parameters are required and the system of differential equations has to be solved once for each of the parameter with a different source term.

5.2.2.2. Adjoint operator sensitivity approach

Instead of directly solving these direct or forward sensitivity equations if the equations adjoint to them are solved, the parameter sensitivities can be obtained from a single solution of the direct equations and adjoint sensitivity equations. For sensitivity of each parameter further only an inner product operation is involved. The adjoint operator approach is described below.

Adjoint sensitivity equations

The adjoint differential equation is derived by multiplying forward sensitivity equations for the mass flow rate Eq. (22) by Z_W and temperature sensitivity equation Eq. (25) by Z_T and integrating we get,

$$\int_0^{\tau} Z_w \frac{dS_w}{dt} dt + \int_0^{\tau} Z_w B(2-b)W^{(1-b)}S_w dt - \int_0^{\tau} Z_w E \int_0^L S_T \cos \theta dx dt = \int Z_w F_w dt \quad (28)$$

$$\int_0^L \int_0^{\tau} Z_T \frac{\partial S_T}{\partial t} dt dx + \int_0^L \int_0^{\tau} Z_T \frac{W}{A\rho_0} \frac{\partial S_T}{\partial x} dt dx + \int_0^L \int_0^{\tau} Z_T C U S_T dt dx + \int_0^L \int_0^{\tau} Z_T \frac{1}{A\rho_0} \frac{\partial T}{\partial x} S_w dt dx = \int_0^L \int_0^{\tau} Z_T F_T dt dx \quad (29)$$

Integrating by parts and rearranging,

$$S_w Z_w \Big|_0^{\tau} - \int_0^{\tau} S_w \frac{dZ_w}{dt} dt + \int_0^{\tau} S_w Z_w B(2-b)W^{(1-b)} dt - E \int_0^L \int_0^{\tau} S_T Z_w \cos \theta dx dt = \int Z_w F_w dt \quad (30)$$

$$\int_0^L S_T Z_T \Big|_0^{\tau} dx + \frac{1}{A\rho_0} \int_0^{\tau} W S_T Z_T \Big|_0^L dt - \int_0^L \int_0^{\tau} S_T \frac{\partial Z_T}{\partial t} dt dx - \frac{W}{A\rho_0} \int_0^L \int_0^{\tau} S_T \frac{\partial Z_T}{\partial x} dt dx + \int_0^L \int_0^{\tau} S_T Z_T C U dt dx + \int_0^L \int_0^{\tau} S_w Z_T \frac{1}{A\rho_0} \frac{\partial T}{\partial x} dt dx = \int_0^L \int_0^{\tau} Z_T F_T dt dx \quad (31)$$

The sum of RHS of the Eq. (30) and Eq. (31) is:

$$\begin{aligned} & \int_0^{\tau} Z_w F_w dt + \int_0^L \int_0^{\tau} Z_T F_T dt dx = \int_0^L S_T Z_T \Big|_0^{\tau} dx + \frac{1}{A\rho_0} \int_0^{\tau} W S_T Z_T \Big|_0^L dt + S_w Z_w \Big|_0^{\tau} \\ & - \int_0^{\tau} S_w \frac{dZ_w}{dt} dt + \int_0^{\tau} S_w Z_w B(2-b)W^{(1-b)} dt - C \int_0^L \int_0^{\tau} S_T Z_w \cos \theta dx dt \\ & - \int_0^L \int_0^{\tau} S_T \frac{\partial Z_T}{\partial t} dt dx - \frac{W}{A\rho_0} \int_0^L \int_0^{\tau} S_T \frac{\partial Z_T}{\partial x} dt dx + \int_0^L \int_0^{\tau} S_T Z_T C U dt dx + \int_0^L \int_0^{\tau} S_w Z_T \frac{1}{A\rho_0} \frac{\partial T}{\partial x} dt dx \end{aligned} \quad (32)$$

The RHS of this equation can be written as

$$\begin{aligned}
& \int_0^L [S_T Z_T] \Big|_0^\tau dx + \frac{1}{A\rho_0} \int_0^\tau W [S_T Z_T] \Big|_0^L dt + S_W Z_W \Big|_0^\tau - \int_0^\tau [S_W \frac{\partial Z_W}{\partial t} + S_W Z_W B(2-b)W^{(1-b)} + \int_0^L S_W Z_T \frac{1}{A\rho_0} \frac{\partial T}{\partial x} dx] dt \\
& - \int_0^L \int_0^\tau [CS_T Z_W \cos \theta + S_T \frac{dZ_T}{dt} - S_T \frac{W}{A\rho_0} \frac{\partial Z_T}{\partial x} + S_T Z_T CU] dt dx
\end{aligned} \tag{33}$$

The first three terms are boundary terms and the conditions are suitably chosen so that these terms vanish. The remaining terms multiplying S_W and S_T in the integrals are identified as the following adjoint sensitivity equations.

$$-\frac{dZ_W}{dt} + B(2-b)W^{(1-b)}Z_W + \frac{1}{A\rho_0} \int_0^L \frac{\partial T}{\partial x} Z_T dx = g_W(t) \tag{34}$$

and

$$-\frac{\partial Z_T}{\partial t} - \frac{W}{A\rho_0} \frac{\partial Z_T}{\partial x} + EUZ_T - C \cos \theta Z_W = g_T(x,t) \tag{35}$$

The integrals in (25) can now be identified as

$$\int_0^\tau S_W g_W dt + \int_0^L \int_0^\tau S_T g_T dt dx = \int_0^\tau Z_W F_W dt + \int_0^L \int_0^\tau Z_T F_T dt dx \tag{36}$$

The problem is now to solve for Z_T and Z_W . The advantage of computing the adjoint solutions is that, the sensitivity integrals can be computed from one set of direct and adjoint solutions, instead of solving the sensitivity equations for S_W and S_T for different source terms.

5.2.2.3. Adjoint boundary conditions

The terms involving the boundary conditions in Eq. (33) are:

$$\int_0^L [S_T Z_T] \Big|_0^\tau dx + \frac{1}{A\rho_0} \int_0^\tau W [S_T Z_T] \Big|_0^L dt + S_W Z_W \Big|_0^\tau \tag{37}$$

The first term can be made zero if

$$S_T(x, \tau) Z_T(x, \tau) - S_T(x, 0) Z_T(x, 0) = 0 \tag{38}$$

$$\text{Since } S_T(x, 0) = \left. \frac{\partial T(x, t)}{\partial \alpha} \right|_{t=0} = 0, \text{ it is required that, } Z_T(x, \tau) = 0 \tag{39}$$

The second term is zero from continuity of sensitivity at boundary.

$$\text{i.e. } S_T(L,t) Z_T(L,t) - S_T(0,t) Z_T(0,t) = 0 \quad (40)$$

The third term, $S_W(\tau) Z_W(\tau) - S_W(0) Z_W(0) = 0$

$$\text{Since } S_W(0) = \left. \frac{\partial W}{\partial \alpha} \right|_0 = 0 \quad \text{It is required that } Z_W(\tau) = 0 \quad (41)$$

to make the third term vanish.

Discretization of adjoint equations

Having obtained the adjoint equations and boundary conditions for the continuous case, the differential equations are discretized for numerical solution. This is known as discretization of the adjoint procedure (DA). In an alternative approach the continuous forward differential equations are discretized and then its adjoint operator obtained. This is known as adjoint of the discretization. Each of the approach has its merits and demerits [50]. The finite difference formulation of the adjoint set of equations is as follows. Forward difference of Eq. (34) is:

$$Z_w^{n-1} \left(1 + B(2-b)W_{n-1}^{1-b} \Delta t \right) = g_w^{n-1} \Delta t + Z_w^n - f(i, n-1) \Delta t \quad (42)$$

$$Z_w^n = \left[1 + B(2-b)W_n^{1-b} \Delta t \right]^{-1} \left[g_w^n \Delta t + Z_w^{n+1} - \frac{\Delta t}{A\rho} \sum_i Z_{T,i}^n (T_{i+1}^n - T_i^n) \right] \quad (43)$$

Forward differencing equation (28),

$$\begin{aligned} & -(Z_{T,i}^{n+1} - Z_{T,i}^n) + C \cos \theta_i Z_w^n \Delta t - \frac{\Delta t}{\Delta x} \frac{W^n}{A\rho} (Z_{T,i+1}^n - Z_{T,i}^n) + E Z_{T,i}^n \Delta t = g_{T,i}^n \Delta t \\ & Z_{T,i}^n \left(1 + \frac{\Delta t}{\Delta x} \frac{W^n}{A\rho} + E_i \Delta t \right) - Z_{T,i+1}^n \frac{\Delta t}{\Delta x} \frac{W^n}{A\rho} = Z_{T,i}^{n+1} - C \cos \theta_i Z_w^n \Delta t + g_{T,i}^n \Delta t \end{aligned} \quad (44)$$

The forward difference formulas are used for the backward marching solution of the adjoint equations. It is written compactly as

$$Z_{T,i}^n \beta_{i,n} + Z_{T,i+1}^n \sigma_{i,n} = \gamma_{i,n+1} \quad (45)$$

The Eq. (43) and Eq. (45) are solved using Thomas tri-diagonal matrix algorithm [57] and Sherman-Morrison formula. The results are presented in the next section.

5.2.2.4. Numerical results

Direct problem solution for temperature and flow

The solution of the forward Eq. (15) and Eq. (16) are required for solving both the forward sensitivity as well as adjoint sensitivity equations. The flow rate $W(t)$ and $\Delta T(x,t)$ are obtained using numerical procedure as 1.0 kg/sec and 7.68 °C respectively.

Direct discrete and adjoint sensitivities

If sensitivity is required at a particular point x' in the loop at time t' , then we require

$$S_W(t') = \frac{dW(t')}{d\alpha} \quad (46)$$

$$S_T(x', t') = \frac{dT(x', t')}{d\alpha} \quad (47)$$

which means, g_w and g_T are defined as delta functions in $\int_0^\tau S_W g_w dt + \int_0^L \int_0^\tau S_T g_T dt dx$. If the adjoint functions Z_W and Z_T are solved using these delta functions, the sensitivities are obtained by evaluating the right hand side of Eq. (36). Table 3 gives the sensitivity results for the various parameters derived using the adjoint sensitivity operator method. Flow and temperature are the two responses selected. For each of the responses the sensitivity obtained by direct recalculation i.e. by calculating the responses at two different parameter values is given for comparison. The last column gives the assumed standard deviation for the parameters. This standard deviation is used as input for getting the response probability density. The direct flow, adjoint flow sensitivity is given in FIG. 47. The adjoint temperature sensitivity computed is depicted in FIG. 48.

TABLE 3. SENSITIVITY RESULTS WITH DIFFERENT METHODS ($\Delta P/\Delta\alpha$)

Parameter	Sensitivity on W		Sensitivity on T		Std Dev.
	Recalculation	Adjoint	Recalculation	Adjoint	
β	*(2128) 2103.7	2129.7	-8309.9	-8661.1	0.05
a	-0.00753	-0.00782	0.031242	0.031765	0.05
μ	-1506.9	-1563.2	6248.4	6352.9	0.05
D	51.127	50.093	-9353.2	-9799.7	0.01
ρ	0.00113	0.001135	-0.01375	-0.01294	0.05
q	4.94E-05	5.00E-05	0.037886	0.037887	0.1
T_0	-4.40E-006	-4.40E-06	0.99455	0.99455	0.1
U	5.66E-06	6.46E-06	-0.35265	-0.36922	0.1

*by direct differentiation of steady state expression. (7 m, 0.04 m diameter), Mean temperature of the hot leg = 421.5 °C, Standard deviation = 53.2 °C.

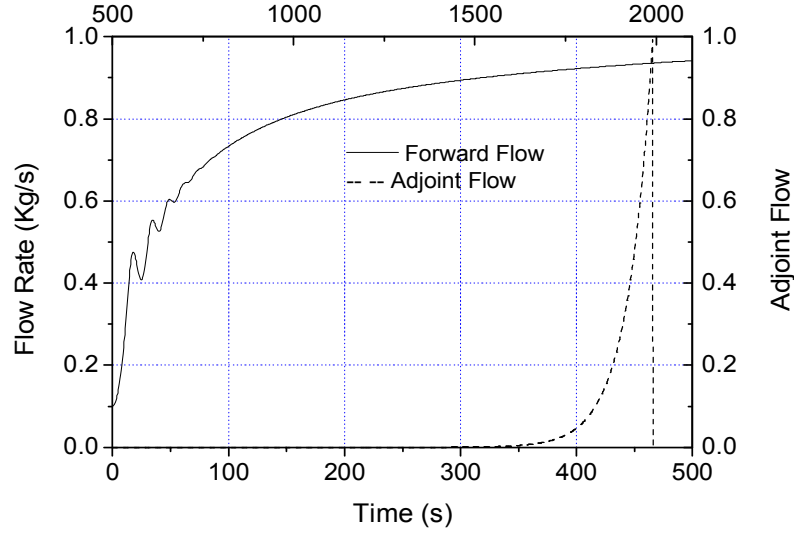


FIG. 47. Transient flow and adjoint flow.

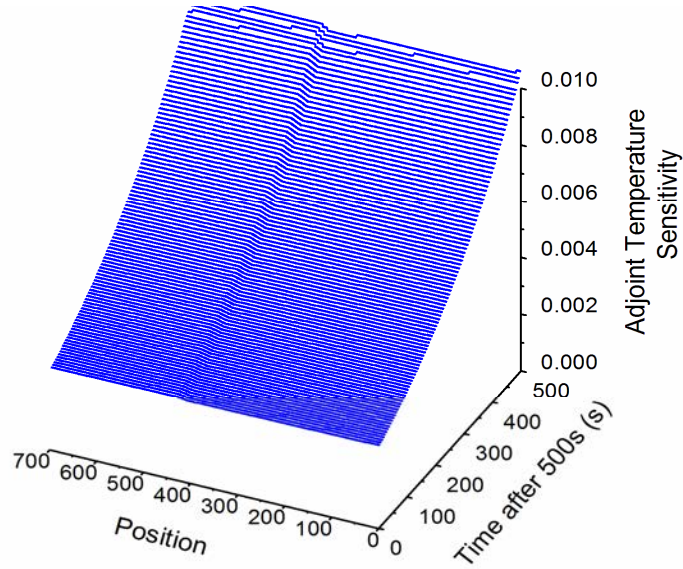


FIG. 48. Adjoint Temperature.

5.2.2.5. Functional reliability calculation

Adjoint sensitivity and moments method

To demonstrate the reliability computation, the limit state function L for the heat transport problem is defined as $L = L(T_L, T_R)$. The parameter dependence is shown explicitl:

$$L(T_L, T, x, t; \alpha) = T(x, t; \alpha) - T_L(x, t; \alpha) \quad (48)$$

where T is temperature response, T_L is limiting value. In general both could be functions of position, time and parameter α . For this problem L is evaluated at a point x' in the hot leg of the loop and time t' , i.e. $L(T_L, T, x', t')$ with $T_L = 500$ and 550 °C as two cases.

Probability of failure is defined as,

$$P(L \leq 0) = \int_{-\infty}^0 p(L)dL \quad (49)$$

Where $p(L)$ is a probability density function for L and it has to be obtained using the relation between L and parameters α and known probability density function of the parameters. If L is expanded in terms of the parameters up to first order as

$$L(\alpha + \delta\alpha) = \sum_i \left. \frac{\partial L}{\partial \alpha_i} \right|_{\alpha} \delta\alpha_i + O(\delta\alpha^2) \quad (50)$$

and comparing the terms with Eq. (13) , the coefficients $c_i = \frac{\partial L}{\partial \alpha_i}$ are the sensitivity terms.

They are obtained from the adjoint operator method and given in Table 4. If the parameters are normally distributed, the probability density function (PDF) of L can be constructed from the first two moments of the parameters as given in equations (44) and (45). That is, the mean of L denoted by $\mu(L)$ is

$$\mu(L) = c_0 + c_1\mu(\alpha_1) + c_2\mu(\alpha_2) \quad (51)$$

The variance of L is

$$\sigma^2(L) = c_1^2 \sigma^2(\alpha_1) + c_2^2 \sigma^2(\alpha_2) + .. \quad (52)$$

The constructed probability density function from these two moments assuming Normal distribution is shown in FIG. 49 as a continuous line; case (i) The accuracy of the reliability result obtained by this approach (referred to as adjoint-response surface-moments) is compared with (ii) adjoint-response surface-Monte Carlo method, where the response PDF is constructed from the response surface by Monte Carlo sampling and (iii) direct Monte-Carlo method, where only repeated code runs are used to generate the response PDF.

5.2.2.6. Adjoint sensitivity and response surface Monte Carlo

In this case (ii) the PDF and probability of function failure $p(L)$ is obtained using the response surface Eq. (50) constructed using the adjoint operator method and subsequent Monte-Carlo sampling of the parameters. The results are shown in FIG. 49 as '+' symbols. The weighted residual error between cases i) and ii) is $\sim 3.6E-3$.

Comparison with direct Monte Carlo method

To validate the new procedure, the PDF and $p(L)$ is obtained using direct Monte Carlo sampling of the parameters and running the numerical code for 10^4 times. The results are shown in FIG. 49 as square dots. There is good agreement between the results from the three methods. The weighted residual error between case i) and iii) is ~ 0.02 . In Table 4, the probability of exceeding a given temperature is presented for two limits (T_L), as computed by different methods. There error is relatively more in the tail region between the direct Monte Carlo method and that obtained using adjoint operator method. Since both variants of the adjoint operator methods (case i and ii) agree closely compared to the direct simulation, the

inference is that results could be improved by generating higher order response surface. However given the large uncertainty in modeling input probability density shape and uncertainty range, the results are acceptable given their efficiency.

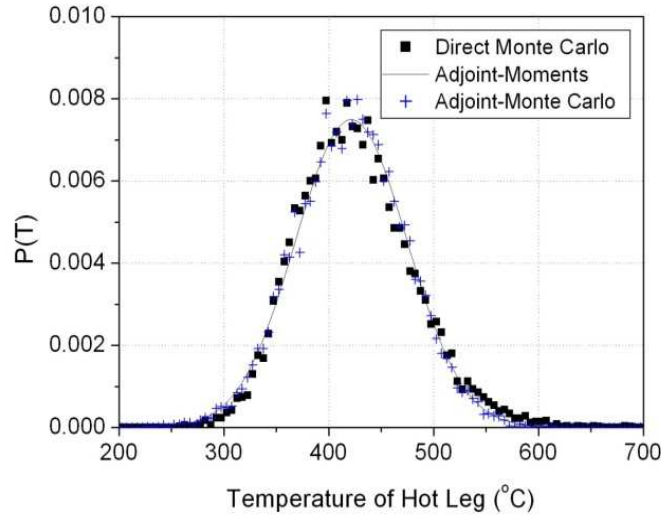


FIG. 49. Probability density function of hot Leg temperature at a given time by three different methods.

TABLE 4. PROBABILITY OF EXCEEDING SPECIFIED VALUES

$P(T > T_L)$	Direct Monte Carlo	Adjoint Sensitivity	
		Monte Carlo	Moments
500	0.09	0.064	0.07
550	2.00E-02	6.80E-03	7.80E-03

There is more error in the tail region between the different methods. Since the adjoint operator method is used to generate a linear response surface about the mean value of response, the failure probability is under predicted, implying that the linear response surface approximation about the mean value is not sufficient. This could be addressed by generating response surface about the most probable failure point, when the failure regions are regular.

Comparison of computational effort

For this reliability estimation problem computational efficiency is obtained by resorting to the construction of response surface by adjoint operator method. Assuming that the number of operations after response surface construction is same but comparatively small for different methods, the speedup achieved by this approach is calculated as follows. The solution of $T(x,t)$ from forward Eq. (13) and Eq. (14) using Thomas algorithm takes about $5M$ operations (multiplications) for M spatial points and for perturbed tri-diagonal system with the use of Sherman-Morrison formula at each time step it is about a total of $11M$ operations. The solution of W at each time step takes M operations leading to a total of about $12NM$ operations for N time steps. Similarly, the solution of adjoint differential Z_T takes about $11M$ operations and solution of Z_W at each time step takes $2M$ operations. For N time steps the total

number of operations are $13.N.M$. Subsequent integration for each parameter-sensitivity require about $N.M$ operations (worst case, best case is N). For k parameters the number of operations required by the adjoint operator method is $k N.M + 25 N M = N M (25 + k)$. The time required by direct method is $NM (12 k)$. In a Pentium 4.3GHz machine for $k = 8$ parameters the direct method takes about 9.7 s and solution by adjoint method takes 3.1 s a speedup by factor 3, for $M= 700$ and $N =2000$. When the number of parameters k is very large, the maximum possible speedup is about 12.

The proposed approach requires formulation of the adjoint equations from the original forward sensitivity equations, discretization and then computer implementation. This procedure will be easy to implement during the computer code development stage or additional routines can developed when modeling equations are readily available. It is not directly applicable to situations where system models are embedded in large computer codes. For those conditions the development of a variant of this approach where, adjoint code is derived directly (automatic differentiation) from the BE code is addressed in the next section.

5.3. ALGORITHMIC DIFFERENTIATION

5.3.1. Adjoint/reverse computation methods for response surface generation

Adjoint operator based methods had been developed and used for sensitivity and uncertainty analysis in nuclear reactor analysis, thermal hydraulics [48] and aerospace applications [50]. The numerical solution of a physical problem is done in three steps. First is the analytical formulation of the problem as an integro-differential equation. Second, the equations are discretized using appropriate numerical schemes. Third is the implementation in a programming language. The adjoint or reverse mode computation can be implemented at any of the three stages.

For passive system functional reliability application, the adjoint operators were formulated at the first stage for the continuous differential equations [56] as presented in the previous sections. Next, the implementation of adjoint transformation at the code level, known as automatic differentiation technique is studied [58]. This process is known as Algorithmic Differentiation and when the program transformation is done with software tools, it is known as Automatic Differentiation (AD). These two terminologies are used interchangeably within this report to refer to the procedure of deriving the adjoint code from direct code either manually or automatically by a tool. This technique is applied to the natural convection system sensitivity analysis. From sensitivity coefficients a linear response surface is constructed about the most probable operating point, which can be used to predict the most central failure point [44] about which importance sampling MCS could be carried out. For the method to work efficiently it is only required to approximately predict the most central failure point as it is expected that the subsequent MCS will sample the entire failure.

Each of the approach has its own benefits and demerits [50]. The first approach was applied for the passive system functional reliability analysis problem in [56] which is suitable during code development stage. Here, automatic differentiation technique is applied to the natural convection system sensitivity analysis. From sensitivity coefficients a linear response surface is constructed about the most probable operating point and is used to predict the most central failure point [44] also known as design point. This information is used for importance sampling Monte Carlo simulation with the forward code or alternatively for MCS with the response surface about the design point, for approximate results. The importance sampling MCS approach provides better estimates of reliability in the tail region of the PDF.

5.3.2. Automatic differentiation of programs

Automatic differentiation is a technique for transforming a computer program that computes a partial function (complex deterministic simulation code) into one that computes the derivatives of that function in terms of input variables [60–61]. In general it is the process of automatically generating the transformed program that computes the Jacobian matrix or higher order derivatives (Hessian matrix). The only requirement that has been assumed for the application algorithmic differentiation is that the functions defined by the program are differentiable. The process of efficiently performing such transformations is still an active area of research.

Let H represent the numerical code of interest. H computes the function $T = H(X)$, (from $R^n \rightarrow R^m$) with X , being the set of input data. Symbolically, with arrow representing a mapping, Automatic Differentiation tool T_F , transforms H as

$$T_F \bullet H \rightarrow G \quad (53)$$

The program G computes the Jacobian $\left. \frac{\partial Y}{\partial X} \right|_{X_0}$. Here, X_0 is the initial set of parameters.

Usually in science and engineering applications, H is an approximation to the analytically defined model M of some problem. In case of a single response variable, G computes the vector dY/dX .

Since, H is a sequence of statements, the differentiated program G is obtained by applying the chain rule for differentiation as follows. If the program or numerical algorithm H has K steps, then it can be decomposed as follows.

$$\text{Let, } H^\ell : Z^{\ell-1} \rightarrow Z^\ell \quad Z^\ell \in R^\ell \quad (54)$$

denote the ℓ^{th} step in the computation and $Z^{\ell-1}$ being the input variables at stage ℓ of computation with $Z^0 = X_0$, $Z^K = Y$, and $\ell = 1$ to K . The functional decomposition of H is,

$$H = H^K \circ H^2 \circ H^1 \quad (55)$$

The derivative of H , is then obtained by successively differentiating each H^ℓ . If we denote the derivative of H^ℓ , by J^ℓ , the elements of J^ℓ , at stage ℓ are,

$$J_{ij} = \left. \frac{\partial H_i^\ell}{\partial Z_j^{\ell-1}} \right|_{Z_0^{\ell-1}} \quad \text{where } Z_0^{\ell-1} = H^{\ell-1} \circ H^{\ell-1} \circ H^1(X_0) \quad (56)$$

The J (Jacobian matrix) is expressed in terms of its elementary steps as,

$$J = J^K \circ J^{K-1} \circ J^1 \quad (57)$$

This step shows that a numerical code, which is a sequence of statements, can be differentiated using the chain rule of differentiation. Computing J in the order of function composition, as in Eq. (57) is known as forward mode of differentiation, implemented by a computer code G . This mode is efficient for computing the derivatives of m response variables in terms of few input variables, i.e. when $m > n$. If the derivatives are required for $n > m$ parameters the differentiated code needs to be run n times for each response variable.

For this situation, when $n > m$, calculation of sensitivities can be done efficiently by carrying out the differentiation in Eq. (57), in the reverse direction, that is from J^K to J^1 , which could

be done by a transformation T_R (a software tool). This is known as adjoint or reverse differentiation generated by the transformation T_R , written for clarity as,

$$T_R \bullet (H, G) \rightarrow B \quad (58)$$

The resulting code B does the adjoint or reverse computation of sensitivity coefficients, which are elements of Jacobian matrix J . As the method operates on programs, Automatic Differentiation approach is advantageous to situations when modeling equations are not available and there is no need for adjoint code development effort.

To see how the abstract notations given above translate in a concrete case, consider two simple program statements,

$$x = a.b ; \quad y = x + c. \quad (59)$$

which is a function of input variables (a, b, c) and output variable y . The differentiated code is obtained as,

$$\delta x = \frac{\partial x}{\partial a} \delta a + \frac{\partial x}{\partial b} \delta b = b \delta a + a \delta b \quad (60)$$

$$\delta y = \frac{\partial y}{\partial x} \delta x + \frac{\partial y}{\partial c} \delta c = \delta x + \delta c \quad (61)$$

To derive the adjoint code, we can express the differentiated code in a matrix form by considering all the input and output variables.

$$\begin{bmatrix} \delta x \\ \delta c \end{bmatrix} = \begin{bmatrix} \frac{\partial x}{\partial a} & \frac{\partial x}{\partial b} & 0 \\ 0 & 0 & 1 \end{bmatrix} \begin{bmatrix} \delta a \\ \delta b \\ \delta c \end{bmatrix} \quad (62)$$

$$\text{and for the second statement, } [\delta y] = \begin{bmatrix} \frac{\partial y}{\partial x} & \frac{\partial y}{\partial c} \end{bmatrix} \begin{bmatrix} \delta x \\ \delta c \end{bmatrix}, \quad (63)$$

$$\text{therefore, } [\delta y] = \begin{bmatrix} \frac{\partial y}{\partial x} & \frac{\partial y}{\partial c} \end{bmatrix} \begin{bmatrix} \frac{\partial x}{\partial a} & \frac{\partial x}{\partial b} & 0 \\ 0 & 0 & 1 \end{bmatrix} \begin{bmatrix} \delta a \\ \delta b \\ \delta c \end{bmatrix} = \begin{bmatrix} 1 & 1 \end{bmatrix} \begin{bmatrix} b & a & 0 \\ 0 & 0 & 1 \end{bmatrix} \begin{bmatrix} \delta a \\ \delta b \\ \delta c \end{bmatrix}$$

$$\text{which is re-written as, } [\delta y] = J_2 J_1 \begin{bmatrix} \delta a \\ \delta b \\ \delta c \end{bmatrix}. \quad (64)$$

Here, as described in Eq. (57) and Eq. (58), $J^T = (J_1^T J_2^T)$, gives the sensitivity coefficients in the adjoint computation mode.

5.3.3. Monte Carlo sampling with code

There have been studies to improve the efficiency of reliability estimates [54, 55, 61]. For reducing the computational cost of Direct Monte Carlo Simulation (DMCS), Latin hyper cube sampling (LHS) is a popular technique. However, LHS is not effective for low failure

probabilities [54]. Efforts have been made to reduce MC simulation time using line sampling [54] and subset sampling [54, 61] procedures for the functional reliability analysis problem with small failure probabilities. The possible approaches that could be adopted to bring down the MC simulation cost is discussed in this and the following section. In one approach, a linear response surface is generated about the most central failure point from the automatic differentiation and an iteration process. Using this one could use probability moments based methods or direct Monte Carlo simulation to make approximate estimates of reliability. Here it is proposed to predict the most central failure point and carry out importance Monte Carlo Sampling about this point to obtain faster but improved estimates of failure probability. (The most central failure point is also known as design point or checking point in FORM and it is defined as the point on the limit state surface at the shortest distance from the most probable operating point). The linear response surface is utilized for predicting the design point in the space of input variables by an iterative procedure as follows. This point is obtained by minimizing the Lagrangian L defined as,

$$L = \left[\sum_i \left(\frac{\delta\alpha_i}{\alpha_i} \right)^2 \right]^{1/2} + \lambda \left(\Delta T - \sum_i \frac{\partial T}{\partial \alpha_i} \delta\alpha_i \right) \quad (65)$$

Where ΔT is the temperature difference between mean and failure limit, α_i represent parameters of interest and $\delta\alpha_i$ are the change in parameters about their mean value. λ is undetermined multiplier.

The solution of which by standard procedures is,

$$\delta\alpha_i = \lambda \alpha_i^2 \chi_i \text{ with } \lambda = \frac{\Delta T}{\sum_i \left(\alpha_i \frac{\partial T}{\partial \alpha_i} \right)^2} \text{ and } \chi_i = \frac{\partial T}{\partial \alpha_i} \quad (66)$$

The most central failure point $\alpha' = \alpha + \delta\alpha$ obtained by iterating the following equation,

$$\alpha'_i = \alpha_i + \theta \delta\alpha_i \quad (67)$$

$$\alpha'^{n+1} = (\theta\lambda)^n \alpha_i^2 \chi_i \quad (68)$$

Where, $\theta = \frac{(T_L - \widehat{T})}{(T(\alpha') - \widehat{T})}$ is a correction factor for λ , required when ΔT is relatively large in Eq. (66).

The computation procedure is as follows. The forward and reverse codes are run once to get the sensitivity coefficients, χ_i . Then Eq. (27) is iterated few times (3 to 4 with a good initial value) using the forward code for convergence in θ . This yields the most central failure point or design point α' .

To estimate low failure probabilities of the order of 1E-2 to 1E-5, both importance sampling MCS and importance sampling MC-MCS is done with joint density function $\psi(X-\alpha')$, where α' determined by Eq. (27). The importance sampling could be further improved, for approximate estimates by considering only the failure region. The total cost of computation is, one forward and reverse computation for sensitivities, 3 to 5 forward runs (iteration) to locate

failure point and N Monte Carlo calculations. Where N is expected to be factor ~ 10 less than that required for DMCS of same statistical error for this probability range.

5.3.4. Monte Carlo sampling with response surface

For approximate but faster estimates, the linear response surface generated about the design point is used in place of the program code for direct Monte Carlo simulation. This is similar to first order reliability methods [44], except for two differences, that is (i) Monte Carlo simulation is used to find P_f instead of standard normal error function ϕ and (ii) the response surface is generated by few forward runs and two runs of reverse differentiated code, making the number of runs independent of the number of parameters. The design point is located using Eq. (27). This procedure requires one forward calculation plus one reverse calculation for computing LRS about most probable operating point. Then 5 to 6 iterations with forward code runs (denoted by f) for locating α' . One reverse calculation (denoted by r) to compute the LRS about the design point giving a total of $\sim 5f+2r$ computations.

5.3.5. Computational efficiency

5.3.5.1. Comparison of direct Monte Carlo and importance sampling methods

Let $T(p, \delta, H_M \mid n, m)$ be the time required to solve a functional reliability analysis problem, to estimate $P_f = p$, with cov or fractional error δ . n is number of input variables, m is the number of response variables. The coefficient of variation cov (δ) is estimated as the ratio of standard deviation of failure probability to its mean. The figure of merit for comparing the different methods is the unitary coefficient of variation, $ucov$ denoted by $\Delta = \delta\sqrt{N}$ [54]. For direct Monte Carlo simulations of N samples,

$T_{MC}(p, \delta, H_M \mid n, m) = T_{MC}(p, \delta, H_M) = N(p, \delta) \tau(H_M)$. where τ is time per forward code run.

For importance sampling with information about the failure region incorporated from the failure surface, N could be significantly lower. Since for direct MCS,

$$\delta \approx \frac{1}{\sqrt{Np}} \quad \text{and} \quad \Delta \approx \frac{1}{\sqrt{p}} \quad (69)$$

$$\frac{\delta\sqrt{N_{MCS}}}{\delta\sqrt{N_{IS}}} = \frac{\Delta_{MCS}}{\Delta_{IS}}, \quad \text{therefore} \quad \frac{N_{MCS}}{N_{IS}} = \left(\frac{\Delta_{MCS}}{\Delta_{IS}} \right)^2, \quad \text{for same } p \text{ and } \delta. \quad (70)$$

where suffix (IS) is for Importance Sampling.

5.3.5.2. Comparison of linear response and adjoint linear response methods

When numerical code H_M is approximated by a response surface L , as $H_M \rightarrow L$,

$$T_{LRS}(p, \delta, H_M \mid n, m) = T(H_M \rightarrow L \mid n, m) + N(p, \delta) \tau(L) \quad (71)$$

where, $\tau(L)$ is time to run response surface model L . Right arrow denotes a map/transformation.

$$= T_{H \rightarrow L}(n) + N(p, \delta) \tau(L), \quad \text{assuming one response variable.}$$

$$\approx (2n + k) \tau(H_M) + N(p, \delta) \tau(L),$$

k is the number iterations for predicting the design point.

$$T_{AD-LRS}(p, \delta, H_M | n, m) = T(M \rightarrow L | n, m) + N(p, \delta) \tau(L) \quad (72)$$

$$= T_{M \rightarrow L}(n) + N(p, \delta) \tau(L), \text{ assuming one response variable.}$$

$$\sim (2 + k) \tau(H_M) + N(p, \delta) \tau(L)$$

$$\sim 1 < T_{LRS} / T_{AD-LRS} \leq (2n+k)/(2+k), \quad (73)$$

Lower limit is applicable when, $(2n+k) \tau(H_M) \ll N(p, \delta) \tau(L)$. For example, when $k = 5$, the ratio is $\sim 0.3 n$, a factor 6 faster with 20 parameters. Here it is further assumed that forward and reverse runs take same amount of time.

5.3.6. Application to passive heat transport loop

System model

To demonstrate the applicability of the method, a simple passive heat transport system has been modelled as shown in FIG. 50. The system consists of a tank and a thermo-siphon loop with one heat exchanger dipped in the tank and the other heat exchanger dissipating the heat to atmosphere. Liquid sodium is the working fluid. The objective of using a simple model is to study and understand the method for this application. The thermal and hence density gradients interacting with the gravitational field induces fluid flow resulting in increased energy flow from source to sink. The asymmetry of the heater and cooler positions with respect to the gravitational field is essential for a stable driving force. It is assumed that Boussinesq approximation holds. The equations for the conservation of mass, momentum and energy in one spatial dimension after integration along the thermo-siphon loop length ℓ and constant area of cross section A are [2],

$$\text{The mass flow rate, } W(x,t) = W(t) \quad (74)$$

Equation for the conservation of momentum is,

$$\frac{dW}{dt} + \frac{W^{2-b} a \mu^b}{2D^{1+b} A^{1-b} \rho_0} = -\frac{A}{\ell} g \beta \rho_0 \int T \cos \theta dx \quad (75)$$

Where, a and b are from the friction factor, $f = \frac{a}{Re^b}$, here θ is the angle between the flow direction and gravitational field. The energy conservation equation for the loop is,

$$\frac{\partial T}{\partial t} + \frac{W}{A \rho} \frac{\partial T}{\partial x} - \kappa \frac{\partial^2 T}{\partial x^2} + E (U_c(x) + U_h) T = E U_h(x) T_h(t) + E U_c(x) T_a \quad (76)$$

The energy conservation equation for the tank is,

$$\rho V C_p \frac{dT_h}{dt} = \pi D \int U_h(x) (T(x,t) - T_h(t)) dx + q(t) \quad (77)$$

where, $\kappa = k / (\rho C_p)$ is thermal diffusivity, $E = 4 / (D \rho C_p)$, U_h and U_c are the overall heat transfer coefficients for the heater and cooler sections, respectively. $T_h(t)$ is the temperature of the hot pool. $q(t)$ is power input to tank of volume V. The boundary conditions are $T(x, 0) = T_r$ and $W(t=0) = W_0$, $T_h(0) = T_{h0}$. The problem simulated with these equations is a transient

temperature evolution in the tank, representing heat removal function on demand after reactor shutdown. Equations (75) to (77) are finite differenced with implicit schemes and implemented in C++. The forward solution code (H) was manually transformed to do the forward (G) and reverse differentiation (B) as per the rules for automatic differentiation.

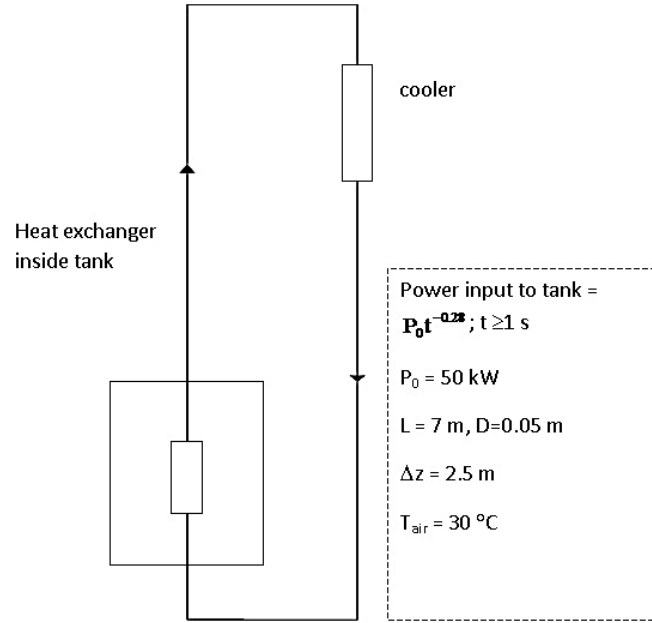


FIG. 50. Simple model of free convection heat transport loop.

To elucidate the application of (AD) to this problem, consider discretization and solution of the momentum equation. The implicit finite difference form of equation (68) is expressed as a polynomial in W^{n+1} which is the mass flow rate at time step ($n+1$),

$$W^{n+1} + C_1(W^{n+1})^{2-b} - C_2 = 0, \quad (78)$$

where C_1 and C_2 involve all other terms of the solution.

The solution of the above equation by Newton-Raphson method is

$$W^{k+1} = W^k - \frac{W^k + C_1(W^k)^{2-b} - C_2}{1 + C_1(2-b)(W^k)^{1-b} - C_2}, \quad (79)$$

Here the time superscript has been dropped and k is iteration index.

The AD approach to derive the linear response compared to other adjoint operator approaches require, only the best estimate source code and information about the input and response variables and need only one forward and reverse code run compared to at least ($n+1$) required with finite difference scheme. For sensitivity calculation for a large number of variables, AD is not only faster but is exact and does not have truncation error as in finite difference way of calculating sensitivity (see Table 5 for formula). Various tools are being developed for the automatic generation of reverse code (B) from the original code (H). The process can become difficult by the requirement to store the variables as they are needed during the reverse computation. Some of the tools for automatic generation of forward and reverse differentiation are [Andreas, 2002] ADIC (C/C++, forward mode), ADIFOR (Fortran77), OpenAD, (Fortran77, Fortran95, C/C++) developed at ANL, USA, TAPENADE (Fortran77, Fortran95) to name a few.

TABLE 5. SENSITIVITY COEFFICIENTS GENERATED BY DIFFERENT METHODS

Parameter	Sensitivity Coefficients			
	Direct Re-Calculation $\frac{T(\alpha + \varepsilon) - T(\alpha)}{\varepsilon}$	Forward Differentiation $\left(\frac{\delta T}{\delta \alpha}\right)$	Reverse Differentiation	
			$\left(\frac{\delta T}{\delta \alpha}\right)$	$\alpha \left(\frac{\delta T}{\delta \alpha}\right)$
β	-1350.57	-1305.23	-1324.4	-0.31124
a	0.19531	0.18248	0.18331	0.18331
μ	162.125	142.985	143.21	0.04583
D	-690.613	-687.656	-692.94	-34.647
ρ	-0.01886	-0.01868	-0.01902	-16.735
Q	0.00114	0.00114	0.00114	56.876
Ta	0.11241	0.11294	0.11294	3.3881
Uh	-0.05631	-0.05621	-0.00172	-12.007
Uc	--	--	-0.05637	-28.185
Time (s) Intel 1.8 GHz Core 2 Duo	49.5	8 x 5.3	9.47	-

Sensitivity results

The temperature evolution in the tank, for the case of 50 kW initial power is depicted in FIG. 51 for a set of samples. The system function is said to fail when coolant temperature in the tank exceeds 350 °C. The sensitivity coefficients obtained by different methods are presented in Table 5.

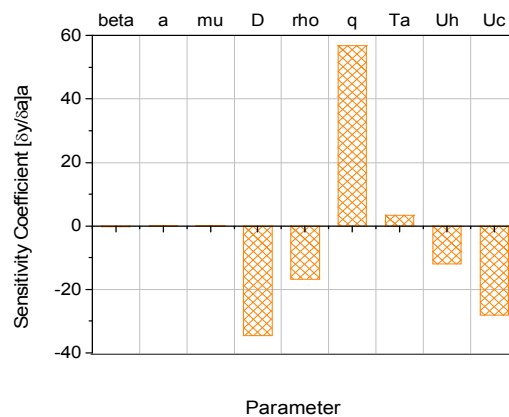
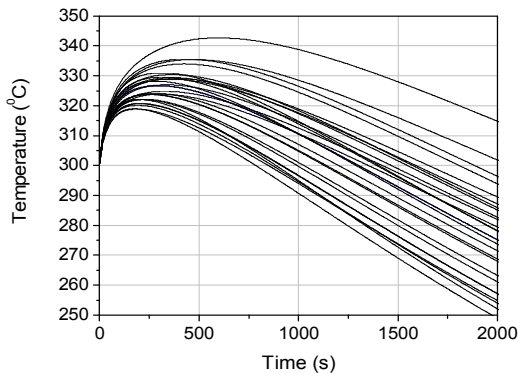


FIG. 51. Tank temperature evolution as a function of time for example samples.

FIG. 52. Normalized sensitivity coefficients.

Direct recalculation by divided difference is done with 2% change of the parameters and is given in second column. Direct re-calculation has round off errors. The forward differentiation is expected to be free from round off errors, but require almost same amount of running time proportional to the number of uncertain parameters. The reverse computation takes only effectively two runs of the original program ignoring the transformation cost. The time taken is presented in the last row of Table. 5. The time required for running the forward problem including forward differentiation is ~ 5.3 s. Time required by adjoint differentiation technique for sensitivity analysis of one response in terms of n input variables is a constant

which is < 2 times the value for one forward run, i.e. ~ 9.5 s. The time required to do this by direct re-calculation is $\sim (n+1) \times 5.2$ s. Therefore the speed up achieved for response surface construction is $\sim (n+1)/2 = 4.5$ for 8 parameters.

The normalized sensitivity coefficients are depicted in FIG. 52. The sensitivity analysis indicates that among the parameters considered for analysis, input power, loop diameter and heat transfer coefficients are sensitive parameters in that order. Heat transfer is governed by cooler heat transfer coefficient than heaters'. These results have been obtained efficiently in one run of the reverse code. This is important for reliability analyses of practical systems where the number of parameters need to be analyzed are numerous.

5.3.7. Importance of Monte Carlo simulation results

Figure 53 and figure 54 depict the convergence of failure probability with sample size for three different runs of importance sampling MCS. Figure 53 is for the case of Markov Chain Monte Carlo importance sampling in the failure region defined by the (LRS) hyper plane, labeled as RS-MC-MCS-HPN. Figure 54 is for the case of MC-MCS about the design point, labeled as RS-MC-MCS-N. Running *cov* is estimated as the ratio of standard deviation to mean of 10 to 20 consecutive samples as a function of time and shown in FIG. 55 and FIG. 56. Figure 55 is for the case of MC-MCS in the failure region defined by the hyper plane and FIG. 56 is for the case of MC-MCS about the design point.

The coefficient of variation *cov* (δ) is estimated as the ratio of standard deviation of failure probability to its mean in 25 runs for each case. The results are summarized in Table 6. The figure of merit for comparing the different methods is the unitary coefficient of variation, *ucov* which is $\Delta = \delta/\sqrt{N}$ [54] corresponding to P_f of $\sim 6.5E-3$, is given in column 5 of Table 6. From the data presented in Table 6 and Eq. (29) it is inferred that a computation time could be reduced by a factor of 7 to 15 using this strategy.

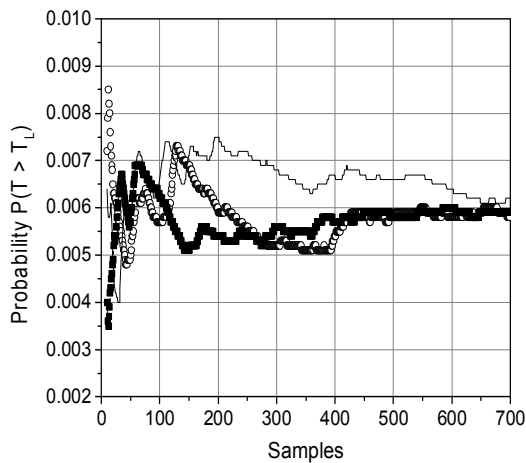


FIG. 53. Failure probability convergence for Markov Chain Monte Carlo importance sampling in the failure region defined by the hyper plane.

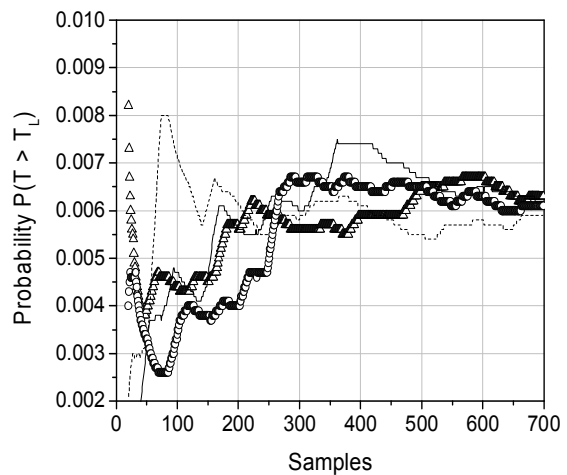


FIG. 54. Failure probability convergence for Markov Chain Monte Carlo importance sampling with PDF shifted to design point.

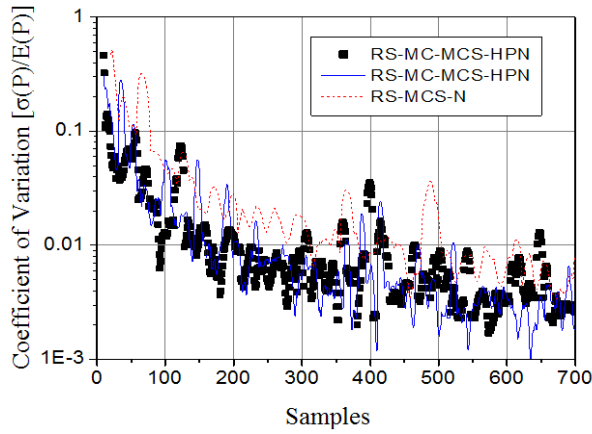


FIG. 55. Running cov for Markov Chain Monte Carlo Importance Sampling in the failure region defined by the hyper plane.

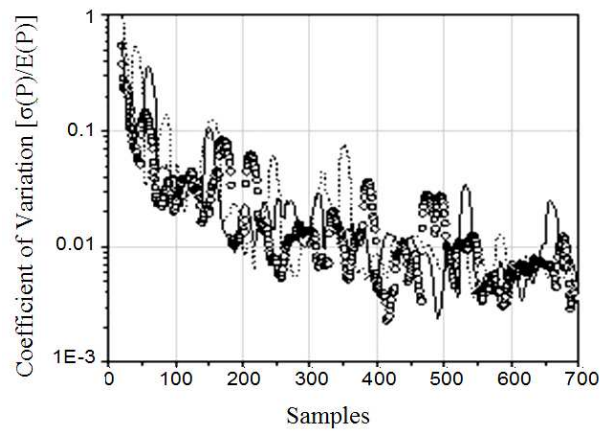


FIG. 56. Running cov for Markov Chain Monte Carlo Importance Sampling with pdf shifted to design point.

TABLE 6. COMPARISON OF COMPUTATIONAL EFFICIENCY FOR DIFFERENT METHODS

Method	Number of simulations	$P_f(T > T_L = 340)$	$P_f(T > T_L = 350)$	$\Delta = \frac{\sigma(P_f)}{E(P_f)} \sqrt{N}$
DMCS	20000	0.056	6.65E-03	12.72
RS-MC-MCS-N	700-1000	-	7.15E-03	4.6
RS-MCS-N	1000	-	7.35E-03	4.7
RS-MCS-HPN	1300	-	6.60E-3*	2.8
RS- MC-MCS-HPN	7001000	-	6.28E-3,6.62E-3*	3.3-3.12

* design point shifted towards mean operating point by a small value.

5.3.8. Response surface Monte Carlo simulation results

Figures 57 and Figure 58 present and compare the probability density function and cumulative probability function for the failure criteria of 350 °C for the peak tank temperature, with two methods, viz., direct Monte Carlo simulation and MCS using the response surface constructed about the mean value. It can be seen from FIG. 58 that for this problem LRS about mean under predicts in the small probability region. The cumulative probability function obtained when the response surface is constructed about the design point is shown in FIG. 59. The P_f value obtained by this method is 7.0 E-3. This figure also compares the PDF obtained from DMCS of 20000 runs ($P_f = 6.7E-3$) and that obtained from Monte Carlo simulation using the response surface constructed about the mean value ($P_f = 1.0E-4$). We have assumed that the parameters are uncorrelated and there is one significant design point about which failure probability is concentrated. In general there could be several ‘design points’ and the failure region may not have a simple structure as assumed here and it remains to be seen if this is true for more complex geometry.

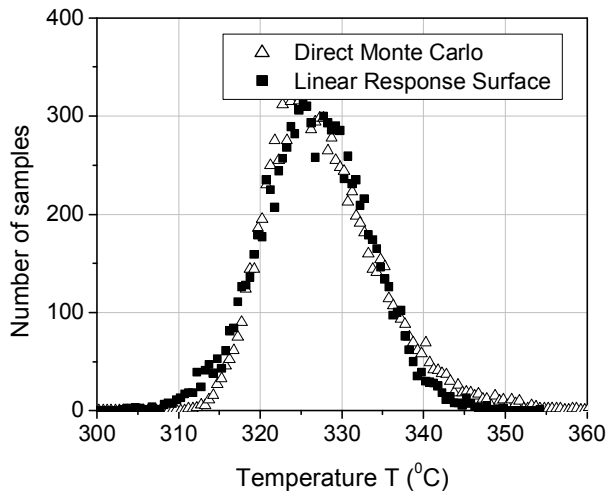


FIG. 57. Probability density function for the failure criteria of 350 °C, with response surface MCS and direct MCS.

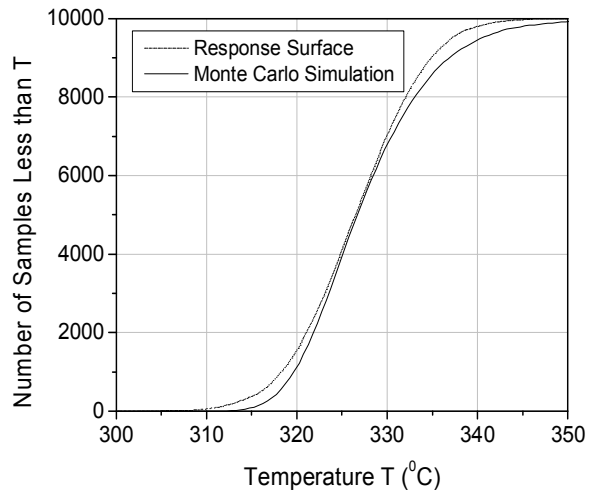


FIG. 58. Cumulative probability function for the failure criteria of 350 °C, with response surface MCS and direct MCS.

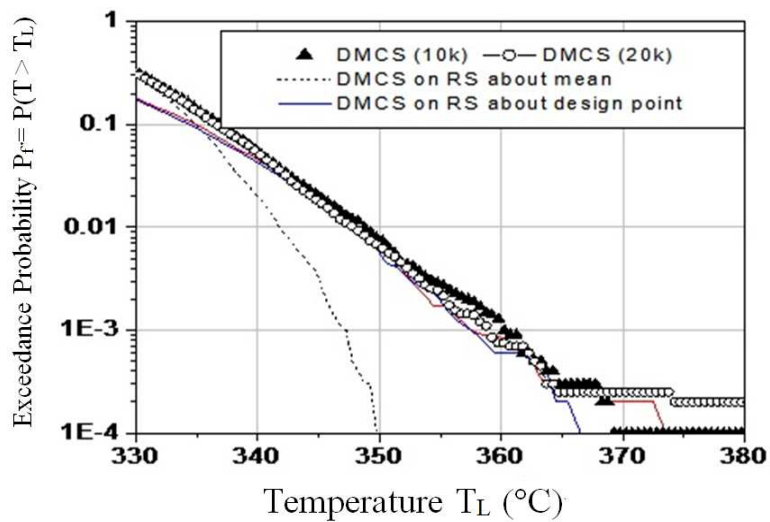


FIG. 59. Probability density function for the failure criteria of 350 °C, with operating point response surface MCS, design point response surface MCS and DMCS.

5.4.APPLICATION OF RESPONSE CONDITIONING METHOD TO SGDHR

Functional failure analysis of SGDHR using the response conditioning method is described in this section. The details on response conditioning method (RCM) can be found in Ref. [61].

5.4.1.1.System description

System components

The systems/sub-systems required for SGDHR are the following as shown in FIG. 60.

- • **Primary Sodium Circuit:** Grid plate, core, two Primary Sodium Pumps (PSP), primary sodium pipe, four Intermediate Heat exchangers (IHX) and sodium contained in main vessel.
- **Intermediate Sodium Circuit:** Sodium to sodium heat exchanger (DHX) dipped in the hot pool of sodium in the main vessel, sodium to air heat exchanger (AHX) placed outside reactor containment building, storage tank, expansion tank and associated piping and valves.
- • **Air Circuit:** Air circuit consists of AHX casing, inlet and outlet ducts, air dampers and a tall stack.

SGDHR consists of four independent loops [62], each having 8 MW heat removal capacity (at a hot pool temperature of 820K). It is a passive system except for the air dampers on the air-side. Heat transfer in the primary circuit, i.e. from core to the DHX is by natural convection. The primary sodium flow path is through core, IHX, PSP and primary pipe and grid plate.

The DHX transfers heat from radioactive primary sodium to non-radioactive intermediate sodium. The AHX dissipates heat from intermediate sodium to atmospheric air. Primary sodium flow is through the shell side of DHX, intermediate sodium flow and air flow are by Natural Convection (NC). Driving force for the NC flows is obtained by the elevation difference between DHX and AHX of ~42 m and by a stack of height 30 m over AHX. In DHX, the top portion of the shell is perforated for sufficient length to permit primary sodium entry even in the event of sodium leak in the main vessel, which is a category 4 event.

AHX casing is provided with 2 dampers in the inlet and 2 in the outlet to enhance the reliability of circuit activation. The air outlet dampers have only full open/ cracked open/ full close control. The inlet dampers are provided with 0–100% open/close capability. On each side one damper is motor operated and the other damper is pneumatically operated, with dedicated class 2 power supply and dedicated air bottles respectively. Provisions are made to open them manually if auto and remote manual opening fails. The signal to initiate SGDHR is SCRAM signal from reactor shutdown system.

Sodium purification is carried out in offline mode from sodium storage tank. Argon cover gas pressure in expansion tank and storage tank during normal operation is kept at 0.3 MPa, from leak before break criteria. Argon supply is provided by the dedicated Argon supply system. Nitrogen supply to AHX casing, in case of fire is provided by dedicated nitrogen supply system. Na leak detectors in 2/3 voting logic monitor leak in AHX. The intermediate circuit is provided with sodium fill and drain lines. There are 2 dump valves in the hot leg and two in the cold leg as shown in FIG. 60. The SGDHR is a typical category B passive system as per IAEA classification [1].

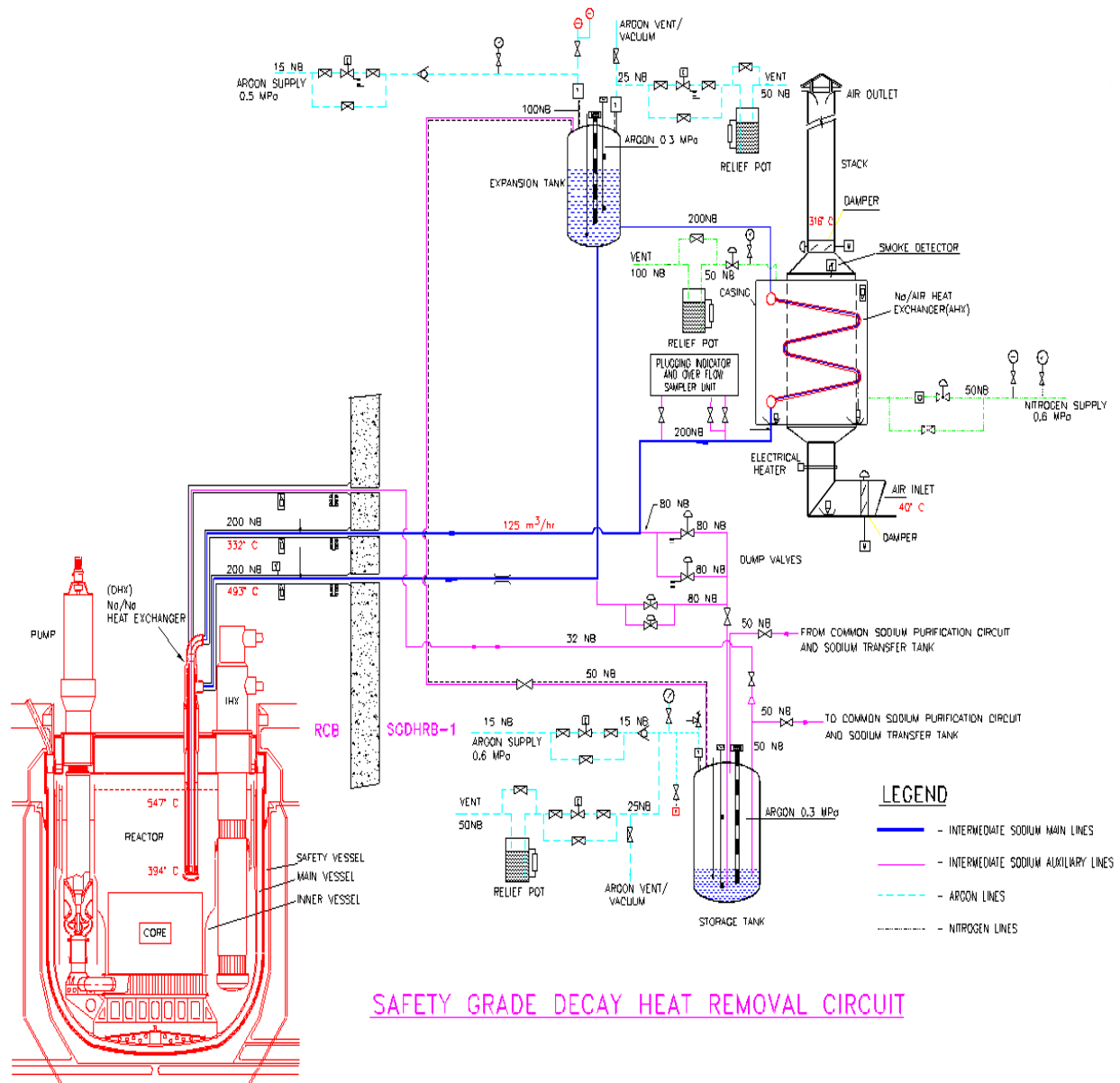


FIG. 60. Safety grade decay heat removal (SGDHR) circuit.

Each primary pump is provided with a main motor and pony motor. The main motor is provided with class III power, while the pony motor gets power from dedicated class II supply. These provisions are for ensuring coolant circulation through core even after off-site power failure or station blackout events. The forced convection in the primary sodium circuit is provided as a defense in depth safety measure. For successful operation of SGDHR, forced convection of primary cooling circuit is not required for meeting design safety limits (DSL) of Category 4 events. The relative locations of PSP, IHX and DHX in the main vessel are shown in FIG. 61 and FIG. 62.

The heat generated (as a function of time up to one year) in the reactor after shutdown is given by the following function [63] (Table 7)

$$P(t) = P_0 a t^{-b}$$

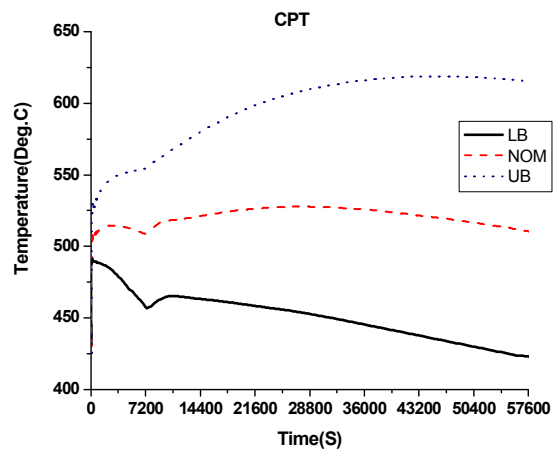
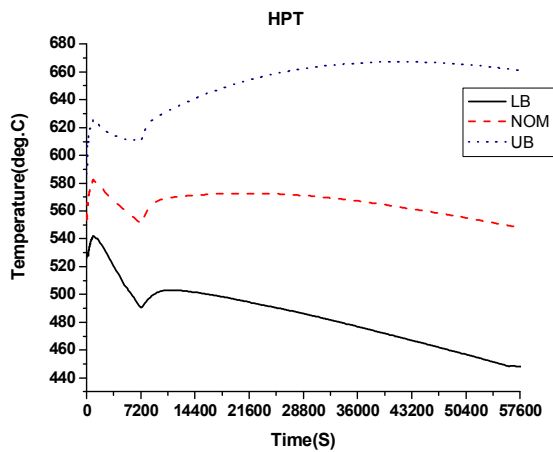


FIG. 61. Evolution of hot pool temperature.

FIG. 62. Evolution of cold pool temperature.

TABLE 7. THE RESIDUAL HEAT FUNCTION PARAMETERS FOR DIFFERENT TIME RANGES

Time	a	b	Error (%)
1s ≤ t ≤ 300s	0.0631	0.1322	± 15
300s < t ≤ 1 d	0.1538	0.288	± 20
1d < t ≤ 100d	0.0061	0.4495	± 30
100d < t ≤ 3y	0.028	0.785	± 30

System function

During operation of reactor all the four loops are in poised state. In this state the four dampers in each loop are in cracked open position allowing about 35% nominal flow in the intermediate loop. This helps to quickly establish natural convection flows when the dampers are opened.

Following a design basis event (DBE) demanding SGDHR, all the dampers are opened (from slightly open to full open) on auto or remote manual or manual mode allowing natural convection in the loops to increase. Forced convection in the core is maintained with PSP (*2/2: F with main and pony motor), such that 15–20% of nominal flow is maintained. When class III power is available, PSP can be run by main or pony motors, otherwise they can be kept running with pony motors driven by battery power. Although for forced circulation with pony motors, both the pumps and their pony motors are required, one pony motor can be run in emergency situations for 4 h. The reactor is not permitted to be on power without the availability of all SGDHR loops. When leak detectors provided for pipes and components detect a sodium leak, the leak is confirmed by other means and then sodium from the loop is drained to the storage tank by opening the dump valves on manual command. In case of

* 2/2: F- 2 out of 2 failures lead to system failure

sodium leak in AHX, 2 out of 3 logic from the leak detectors, gives signal to close the air dampers automatically (if in open position) and nitrogen is supplied to AHX cabin and sodium is drained to the storage tank on manual command. The fail safe position of dampers is the latest operating position.

Design safety limits (DSL)

Design basis events for PFBR are classified into 4 categories. Category 1 includes the events related to the normal operation of the plant. Due to single equipment malfunction or operator error, plant can exhibit abnormal behaviour. Such events are referred as category 2 events. All the events whose categories are greater than 10^{-2} /ry belong to this category. There are events which individually have a very low probability of occurrence, yet there are enough of this type of events that summed together, an occurrence of at least one of these events can be expected. All the events whose frequency of occurrence are less than or equal to 10^{-2} /ry but greater than 10^{-4} /ry belong to this category. For these events mechanical repair of portions of the plant may be necessary and inspection is needed before restarting operation.

The category 4 events are those which are highly hypothetical and occur as a result of incredible set of circumstances with the frequency of occurrences greater than 10^{-6} /ry. The plant integrity may be impaired and restart may not be required following this event. The Design safety limits for each category are given in Table 8 [64].

TABLE 8. DESIGN SAFETY LIMIT FOR FUEL CLAD AND STRUCTURAL TEMPERATURES

Design safety limits for fuel clad and structural temperatures parameters		Event category			
		1	2	3	4
		Temperature (°C)			
Cold Pool Structures		402	540	600	640
Hot Pool Structures		552	600	625	650
Clad Hotspot	Driver SA	700	800	900	1200
	Storage SA	550	600	650	950

5.4.1.2. Functional reliability analysis

The procedure for functional reliability analysis is proposed by the ENEA project called reliability methods for passive safety functions (RMPS). It consists of the following steps.

- Identification and quantification of the sources of uncertainties and determination of the important variables;
- Propagation of the uncertainties through thermal hydraulic (T-H) models and assessment of T-H passive system unreliability;
- Introduction of passive system unreliability in the accident sequence analysis.

The probability density functions assigned are given in the Table 9 and Table 10. The distribution expresses the available information about the parameter i.e. expression of the state of knowledge. The choice of distribution and its range may highly affect the calculated uncertainty bands. In the Table 9, P1, P2 are the function parameters, Nom – is the nominal value and ED1, ED2 and EA denote expert opinion from engineering domain and analysis respectively.

TABLE 9. PARAMETER UNCERTAINTY INTERVALS AND ASSIGNED PROBABILITY DENSITY FUNCTIONS

No	Group	Parameter	Unit	Dist.	P1	P2	Nom	EA	
								L	H
1	Pressure drop cf.	K_{Core}	$\frac{1}{Kg.m}$	Normal	1	0.085	0.012	±15%	-
2	Pressure drop cf.	K_{LHX}	$\frac{1}{Kg.m}$	Normal	1	0.085	0.0049	±15%	-
3	Pressure drop cf.	K_{DHXP}	$\frac{1}{Kg.m}$	Normal	1	0.09	0.473	±20%	-
4	Pressure drop cf.	K_{JC}	$\frac{1}{Kg.m}$	Normal	1	0.085	14	±15%	-
5	Pressure drop cf.	K_{AIR}	$\frac{1}{Kg.m}$	Normal	1	0.085	0.16	±15%	-
6	Secondary flow pressure drop cf.	K_{SEC}	$\frac{1}{Kg.m}$	Normal	1	0.085	*	±15%	-
7	Heat transfer cf.	h_{DHX}	W/(m ² K)	Normal	1	0.06	6211	±10%	-
8	Heat transfer cf.	h_{AHX}	W/(m ² K)	Normal	1	0.06	57.3	±10%	-
9	Heat transfer cf.	h_{CORE}	W/(m ² K)	Normal	1	0.085	21723	±15%	-
10	Heat transfer cf.	h_{RW}	W/(m ² K)	Normal	1	0.085	*	±15%	-
11	Surface Area	A_{DHX}	n	Discrete		0.05, 0.15, 0.8	108	106	108

No	Group	Parameter	Unit	Dist.	P1	P2	Nom	EA	
								L	H
12	Surface Area	A_{AHX}	n	Discrete		0.05,0.15, 0.8	116	114	116
13	Air inlet Temperature	T_{Air}	C	Normal	1	0.1553	30	18	42
14	Decay heat (over RP margin)	P	W	Normal	1	0.05	*	±10%	-
15	FHT- Primary	T_p	s	Discrete	Table 11		8	7	11
16	FHT-Secondary	T_s	s	Discrete	Table 11		4	3	6
17	SCRAM delay	T_n	s	Lognormal	0	0.05	41	37	45
18	Damper opening delay	T_d	Minutes	Lognormal	0	0.23	2.5	2	4
19	Clad conductivity	TC_{CLAD}	W/(K.m)	Normal	1	0.03	21	±5%	-
20	Gap Resistance	H_{GAP}	K/W	Normal	1	0.085	0.0038	±15%	-
21	Initial Power	$P_{INIT.}$	MW	Normal	1	0.05	1253	±10%	-
22	Initial sodium temperature	T_{Na}	K	Normal	1	0.005	397	±1%	-

No	Group	Parameter	Unit	Dist.	P1	P2	Nom	EA	
								L	H
23	Damper cracked open position/Initial air flow	Q_{Air}	kg/s	Normal	1	0.085	0.6	±15%	-
24	Steady State Secondary flow	Q_{SEC}	kg/s	Normal	1	0.03	2921	±5%	-
25	Steady state core flow	Q_{CORE}	kg/s	Normal	1	0.03	6304	±5%	-
26	Fuel conductivity	TC_{FUEL}	W/(K.m)	Normal	1	0.085	3	±15%	-
Thermo physical properties of Sodium									
27	Specific heat	C_p		Normal	1	0.005	*	±1%	-
28	Conductivity	TC_{Na}	W/(K.m)	Normal	1	0.005	*	±1%	-
29	Viscosity	MU	Pa.s	Normal	1	0.005	*	±1%	-
30	Density	RHO	kg/m ³	Normal	1	0.005	*	±1%	-

TABLE 10. DISCRETE PROBABILITY DENSITY FUNCTIONS

Primary FHT (s)	PDF	Secondary FHT (s)	PDF
6.5-7.5	0.1	2.5-3.5	0.1
7.5-8.5	0.5	3.5-4.5	0.6
8.5-9.5	0.2	4.5-5.5	0.2
9.5-10.5	0.12	5.5-6.5	0.1
10.5-11.5	0.06	-	-
11.5-12.5	0.02	-	-

System modelling

The reactor core, SGDHRs, intermediate heat exchangers, sodium pumps, secondary sodium circuit etc., have been modelled by 1 D plant dynamics computer code DHDYN. This is a one dimensional (1D) lumped parameter system analysis code modelling the thermal portions of the core, IHX, DHX and AHX, the hydraulics in the core - IHX primary side - primary pump - inlet plenum and the hydraulics in the DHX primary side. Core thermal model consists of certain number of radial regions and each region is divided into some convenient number of axial nodes. Energy balance is carried over each of the resulting discrete volumes.

For the IHX and the DHX thermal models, the heat transfer length is divided into some convenient number of volumes. Energy balance is done over each set of volumes of primary and secondary side. For defining the primary to secondary side heat transfer, average temperature of each volume obtained as a weighted mean of the respective volumes inlet and outlet temperatures are used. Further simplifying assumption like (i) distribution of tubes and shells material thermal capacities equally between the primary and secondary fluids (so that no explicit equations for the material temperatures are needed) and (ii) negligible axial heat conduction are also made.

The hydraulic model which estimates the transient evolution of the core - IHX and DHX primary side flows are obtained from the integral momentum balance equation over the required segment of flow. Total buoyancy head available in the circuit is obtained by the path integration of the fluid density along the nominal flow direction. The pump developed head is obtained from the homologous characteristics of the pump as a function of the pump speed and flow, wherever present. Transient evolution of free levels (in the hot pool and cold pool) is obtained through the mass balance equation

Modelling of inter-wrapper flow

Here it is assumed that the inter-wrapper flow is only parallel to the vertical faces of SA (Effect of any cross flow heat transport is neglected). For each fuel zone the inter-wrapper sodium space is modelled as an additional node in each axial zone. Then by applying energy balance for each of the axial zone five coupled ordinary differential equations in time are obtained. The mean sodium temperature for subassembly sodium and inter-wrapper sodium are calculated by giving appropriate weight for the inlet and outlet temperatures of that node. The following general assumptions are made on the IWF modelling:

- (i) The inter-wrapper space is modelled as an annular space surrounding each SA

- (ii) The heat transfer from SA sodium to inter-wrapper sodium takes place from all six faces of hexagonal SA. Each SA is associated with a unique IWF channel.
- (iii) All the IWF channels are treated as parallel channels connected to the hot pool at the top and a common IWF inlet plenum at the bottom above the grid plate.
- (iv) Sodium from the hot pool passes through the annular space between peripheral SA and Inner Vessel and mixes with the sodium in the common IWF inlet plenum at the bottom. The common IWF inlet plenum feeds sodium to all IWF channels
- (v) The inter-wrapper sodium after exchanging heat with SA sodium mixes with the bottom region of the hot pool.
- (vi) The driving force for the inter-wrapper flow is purely because of the buoyancy effect.

With these assumptions, governing equations for estimating IWF and core temperatures are obtained.

Failure criteria

The temperatures at four locations that were identified to be important are (1) Hot pool temperature (HPT) (2) Cold pool temperature (CPT) (3) Central sub assembly clad hot spot temperature (CSACHST) and (4) Storage sub assembly clad hot spot temperature (SSACHST). The design safety limits at the above three locations are given in Table 9.

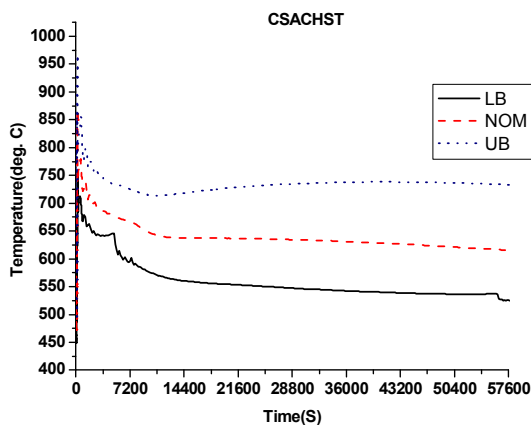


FIG. 63. Evolution of temperatures at critical structures on loss of steam water system (CSACHST).

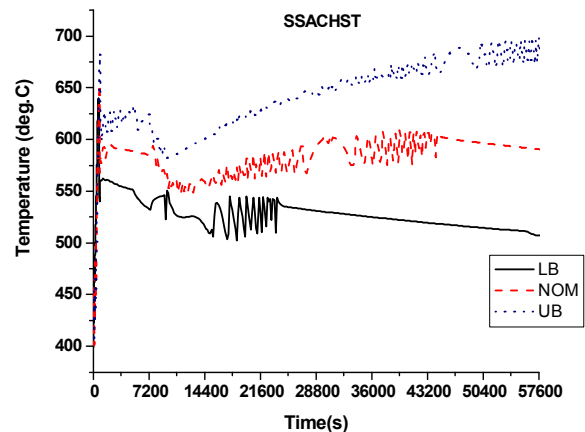


FIG. 64. Evolution of temperatures at critical structures on loss of steam water system (SSACHST).

The system is considered to fail whenever the temperature at any critical structure exceeds the corresponding limit. System performance is assessed based on the ability to meet Category 4 DSL of critical structures. The event simulated is loss of steam water system with simultaneous non-availability of primary and secondary sodium pumps and two loops availability for two hours and then one loop. This is a very conservative initiating event, postulated to assess the functional reliability. The evolution of temperatures at the critical structures for the initiating event considered is given in FIG. 63 and FIG. 64. The three curves in each figure correspond to three sets of input uncertainty parameters based on nominal, upper bound and lower bound. The evolution of hot pool temperatures with time has two distinct peaks. This is shown in FIG. 63 and FIG. 64. The two peaks have been considered as two response variables, viz., hot pool temperature 1 (HPT1) and hot pool temperature 2 (HPT2).

Propagation of uncertainties

Samples of the basic variables were drawn according to their probabilistic characteristics and then fed as input to the code DHDYN. From the code output variables, five quantities HPT1, HPT2, TCP, CSACHST and SSACHST are taken as output response. If the functional failure probability is of the order of 10^{-k} , then T-H code runs of the order of 10^k are required to get one failure. In order to have statistically significant result, very large number of T-H code runs is required, which is a computationally expensive task. The approach followed in this paper to overcome this problem is as follows.

Construction of an approximate response function

Adopting approximate solutions for evaluating system response is a common approach in reliability analysis. Common forms of approximate solutions include empirical formulas, response surfaces and finite element models. Generally, in functional reliability analyses response surfaces are being used as an approximate mathematical model for Monte Carlo simulation. Different types of response surfaces such as polynomial, thin plate splines, neural networks, generalized linear model (GLM) and PLS (Partial least square) regression can be used for functional reliability analysis. In this work, first order linear response surfaces are constructed for all the four responses which are given by,

$$X = \beta_0 + \sum_i \beta_i \theta_i. \quad (80)$$

The regression coefficients β_i are estimated by the method of least squares [65]. This is done by minimizing the sum of squares of the difference between actual response and predicted response, called the residual. The coefficient of determination, R^2 values for all five response surfaces are 0.9942, 0.9769, 0.9519, 0.8596 and 0.3963 respectively. It can be seen from the R^2 values that the fit for SSACHST is poor, as there are oscillations in the flow of these subassemblies (FIG. 63 and FIG. 64). Although system response is expected to non-linear here it is approximated with linear response surface. Response surfaces are taken as a model to approximate the behaviour of a thermal-hydraulic code. Like any model, there is a degree of uncertainty about its predictive capabilities. So in this work, response surfaces are not used directly to estimate functional failure probability. On the other hand, they are used as a conditioning response to generate stratified samples for efficient limited number of T-H code simulations.

Subset simulation using response surfaces

The choice intermediate failure events $\{F_i\}$ play a key role in subset simulation. In order to apply SS to compute failure probability, the failure region F needs to be parameterized with a single parameter so that the sequence of intermediate events $\{F_i: i=1,2,\dots,m\}$ can be generated by varying the parameter. For the failure region F , the critical response variable can be defined as:

$$Y(\Theta) = \max \left\{ \frac{\text{HPT1}}{650}, \frac{\text{HPT2}}{650}, \frac{\text{CPT}}{640}, \frac{\text{CSACHAT}}{1200}, \frac{\text{SSACHST}}{950} \right\} \quad (81)$$

Then the failure region is defined as:

$$F = \{\Theta: Y(\Theta) > 1\} \quad (82)$$

and so the sequence of intermediate failure events can be generated as:

$$F_i = \{Y(\Theta) > y_i\} \quad (83)$$

where $0 < y_1 < \dots < y_m = 1$ is a sequence of intermediate threshold values. Here $Y(\Theta)$ represents the code output for the input parameter vector Θ and $X(\Theta)$ represents the response surface output. Subset Simulation is carried out for X with $p_0=0.1$ and $m=4$ conditional levels. At each conditional levels, $N=10000$ samples are simulated. The total number of evaluations of X (response surface) is

$$N[1+(m-1)(1-p_0)] = 46000. \quad (84)$$

Here a large number of samples is used for the SS to achieve higher quality in the conditional samples of Θ , as they will be used for estimating the failure probabilities of Y . Since the evaluation of X is computationally very efficient, 46000 analyses are a trivial task. The 46000 conditional sample vectors generated by the SS of X is grouped into five bins. Each bin B_i is again subdivided into $N_1=200$ sub bins and one sample is drawn randomly from each sub bin, whose value of Y (code output) is calculated and used for estimating $P(F/B_i)$. The number of evaluations for Y in RCM procedure is

$$N_T = (m+1) \times N_1 = 5 \times 200 = 1000. \quad (85)$$

Calculation of failure probability

The probability $P(Y > y)$ is plotted against y in FIG. 65. In this figure the solid line represents $P(Y > y)$ obtained from 1000 samples using RCM. Whereas the dotted line is for $P(X > x)$ and obtained from the SS of X . The dashed line is the benchmark obtained by 10000 direct MCS of Y . It can be seen that all curves are matching well. The same curves are plotted for a small range ($y: 0.96-1.05$) and given in FG. 66. It is seen that there is significant difference in small probability values calculated by response surface or in other words response surface is not modelling accurately the target response in less probable region.

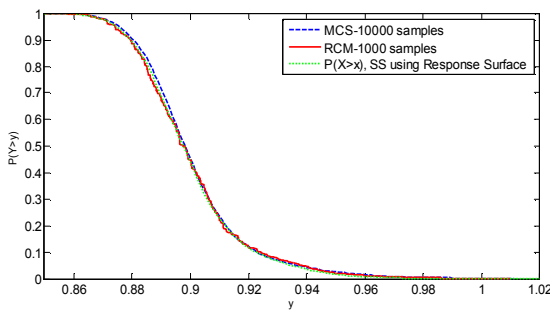


FIG. 65. Probability of Y exceeding y $P(Y > y)$ for $y=0.85$ to $y=1.02$.

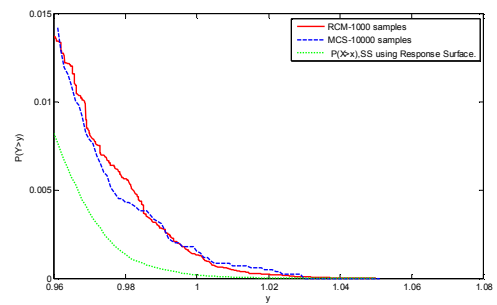


FIG. 66. Probability of Y exceeding y $P(Y > y)$ for $y=0.95$ to $y=1.06$

Conversely, as shown in FIG. 66, probability values derived from response surface by RCM is matching well with benchmark values obtained by direct MCS of 10000 samples. This shows the effectiveness of RCM to incorporate the knowledge obtained from approximate solutions in reliability analysis for obtaining consistent results. The functional failure

probability defined as $P(Y>y=1)$ is obtained as $1.4E-3$ for the presumed conservative initial condition of LSWS and loss of both primary and secondary pumps and 2 loop availability for 2h.

5.4.1.3.Sensitivity calculation

As explained earlier, 1000 DHDYN code runs are made using the conditional samples obtained from subset simulation of approximate response surfaces. Sensitivity of each parameters (θ_i ; $i=1, 2..21$) can be evaluated from the failed set of samples among 1000 conditional samples. An indication can be obtained on how important the parameter θ_i on system failure by comparing the conditional PDF $f(\theta_i / F)$ with the unconditional PDF $f(\theta_i)$. By Bayes' theorem,

$$P(F | \theta_i) = \frac{f(\theta_i | F)}{f(\theta_i)} P(F), \quad i = 1, 2, \dots, n \quad (86)$$

and hence $P(F | \theta_i)$ will be insensitive to θ_i when the conditional PDF $f(\theta_i | F)$ is similar in shape to the unconditional PDF $f(\theta_i)$. For the 30 parameters given in Table 9 (θ_i , $i=1, 2, \dots, 30$), conditional PDF, $f(\theta_i | F)$ can be estimated by identifying the samples in the failure region F. The histograms of the normalized conditional probability distribution of three uncertainty parameters (K_{IC} , P, h_{AHX}) are shown in Fig. 67. The normalized unconditional distribution function of these parameters is also shown in the figure. It can be seen that the conditional distribution function of K_{IC} is similar to its unconditional distribution function. On the other hand, there is significant difference in the distributions of the parameters P and h_{AHX} . As a measure of the sensitivity, the difference ($\rho(\theta_i)$) in the means of normalized conditional and unconditional distributions of each uncertainty parameters are calculated and plotted in Fig. 68.

$$\rho(\theta_i) = \text{mean}(f(\theta_i / F)) - \text{mean}(f(\theta_i)) \quad (87)$$

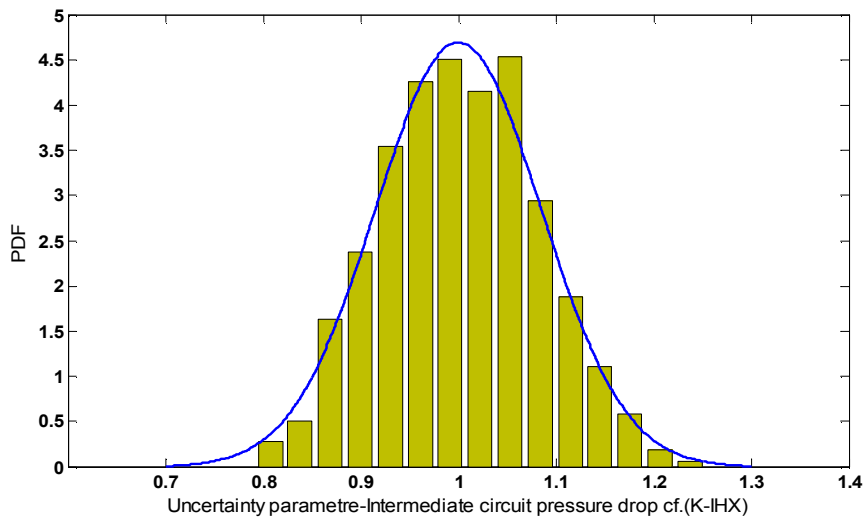


FIG. 67. Comparisons of empirical conditional density function with the unconditional density function (Solid line).

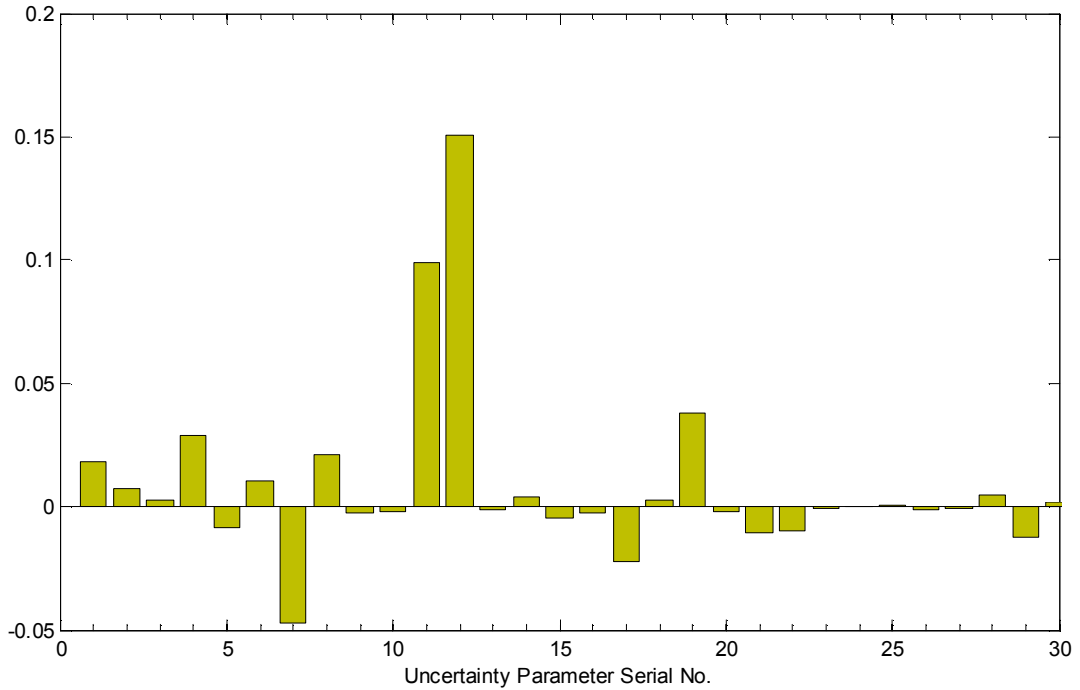


FIG. 68. Sensitivity of critical response to individual uncertainty parameters.

TABLE 11. DESCRIPTION OF PARAMETERS USED IN SENSITIVITY PLOT (FIG. 68)

No.	Parameter	Description	No.	Parameter	Description
1	K_{IHX}	IHX pressure drop cf.	16	T_s	SSP FHT
2	K_{DHXP}	DHX pressure drop cf.	17	h_{CORE}	Core heat transfer cf.
3	K_{IC}	Intermediate ckt pressure drop cf.	18	T_n	SCRAM Delay
4	K_{AIR}	AHX pressure drop cf.	19	T_d	Damper opening Delay
5	h_{DHX}	DHX heat transfer cf.	20	TC_{CLAD}	Clad thermal Conductivity
6	K_{Core}	Core pressure drop cf.	21	h_{Gap}	Fuel pin gap heat transfer cf.
7	h_{AHX}	AHX heat transfer cf.	22	TC_{FUEL}	Fuel thermal Conductivity
8	P_{INIT}	Initial Power	23	C_p	Sodium Specific heat
9	A_{DHX}	No. of tubes in DHX	24	TC_{Na}	Na thermal Conductivity
10	A_{AHX}	No. of tubes in AHX	25	MU	Na Viscosity

11	T_{Air}	Air temperature	26	RHO	Na Density
12	P	Decay Power	27	Q_{SEC}	Secondary flow rate
13	Q_{Air}	Air flow rate/damper position	28	K_{SEC}	Secondary pressure drop cf.
14	T_p	PSP FHT	29	h_{IW}	Inter-Wrapper heat transfer cf.
15	Q_{CORE}	Core flow rate	30	T_{Na}	Initial Na Temperature.

5.4.1.4. Evaluation of functional failure probability on different hardware configurations

Functional failure probability is defined as the probability for the load on the system to exceed the capacity of the system. Since the system capacity depends on system configuration, functional failure probability differs in various system hardware configurations. Using the methodology described in previous sections, functional failure probability is evaluated on various possible SGDHRs hardware configurations with respect to category 3 and category 4 design safety limits and results are reported in Tables 12 and Table 13 respectively.

In Table 12, for the cases 1, 2 and 3, there are two peaks (HPT-1 and HPT-2) in the evolution of hot pool temperature for the event LSWS. The first peak is occurring immediately after the SCRAM and the second peak, HPT-2 is occurring after the hardware failure of one among two functioning SGDHRs loops. The response HPT-2 is the main contributor for functional failure probability with respect to category 4 DSL and the safety margin (Cat.4) for all other responses are too large to contribute. An increase in two SGDHRs loops available time causes a reduction in HPT-2 and this in turn leads to a decrease in corresponding functional failure probabilities. As shown in table 1, for the cases 1 and 2, the availability of primary forced circulation for 4 hours increases functional failure probability. The evolution of hot pool temperature (HPT) with and without primary forced circulation for the case 1 in table 5a is given in FIG. 69.

In the absence of forced circulation in primary, hot pool temperatures are high after the SCRAM and this enhance the natural circulation in intermediate circuit and that in turn remove more heat from hot pool at initial hours. On the other hand, if forced circulation is available immediately after the SCRAM, heat energy will be distributed to cold pool and the heat energy removed through SGDHRs loops in the initial hours is less. This results in an increased hot pool second peak and corresponding high functional failure probability. Conversely, as described earlier, if two loops available time is more, then the peak temperature, HPT-2 decreases and availability of forced circulation for 4h becomes insensitive to functional failure probability.

Even though the results shown in Table 12 indicates that the provision of forced circulation in primary for 4h after the SCRAM is not beneficial for functional reliability with respect two category 4 DSL, forced circulation is necessary to provide sufficient safety margin for CSACHST and SSACHST with category 3 DSL. To make this perception clear, functional reliability is evaluated with respect to category 3 DSL on possible hardware configurations and given in Table 13. Here the high functional failure probability in the absence of forced

circulation corresponds to SSA and CSA temperatures. Since clad temperature peaks are occurring immediately after the SCRAM, these failure probabilities are independent of two loop available time. As shown in Table 13, the availability of forced circulation immediately after the SCRAM decreases the clad temperatures and corresponding functional failure probabilities.

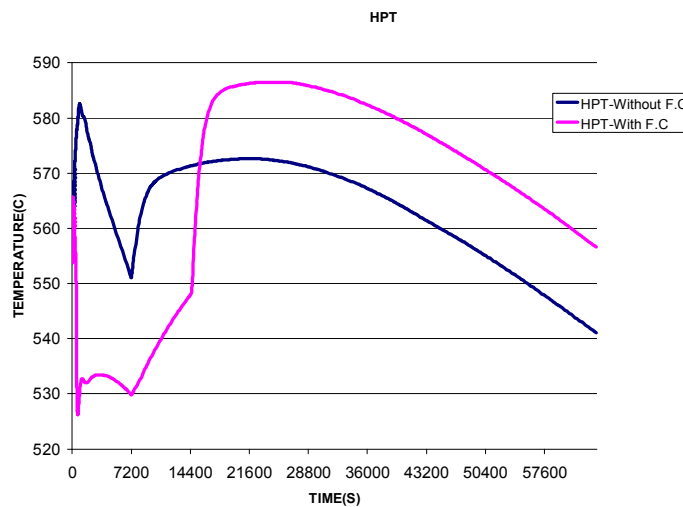


FIG. 69. Evolution of hot pool temperatures with and without primary forced circulation for 4h.

TABLE 12. FUNCTIONAL FAILURE PROBABILITY FOR CATEGORY 4 DSL ON DIFFERENT SYSTEM CONFIGURATIONS

No.	Hardware configuration	Functional failure probability /de	
		Without primary forced circulation	With primary forced circulation
1	2loops 2h then 1 loop	1.30E-03	2.16E-02
2	2loops 4h then 1 loop	6.06E-05	2.00E-03
3	2loops 6h then 1 loop	<E-6	8.20E-06
4	2loops 8h then 1 loop	<E-6	<E-6
5	3 loop full time	<E-6	<E-6
6	4loop full time	<E-6	<E-6

TABLE 13. FUNCTIONAL FAILURE PROBABILITY FOR CATEGORY 3 DSL ON DIFFERENT SYSTEM CONFIGURATIONS

No.	Hardware configuration	Functional failure probability /de	
		Without primary forced circulation	With primary forced circulation
1	2loops 2h then 1 loop	0.8	0.113
2	2loops 4h then 1 loop	0.8	1.40E-02
3	2loops 6h then 1 loop	0.8	1.50E-03
4	2loops 8h then 1 loop	0.8	1.00E-04
4	3 loop full time	1.60E-01	9.40E-07
5	4loop full time	7.10E-02	~E-7

Conclusion

Functional reliability analysis is carried out for the SGDHRs using the overall approach reported in the RMPS. Important parameters that affect the performance of the SGDHRs are identified. Probable ranges of variation of the parameters are estimated and suitable probability distributions were assigned based on experimental data analysis and expert judgment. System failure criteria were identified consistent with the conditions defined for probabilistic safety analysis. The uncertainty in the critical parameters was propagated using the DHDYN code to get the variation in the system response. From a set of 100 code runs multi response surface model for five important responses were constructed. By considering the uncertainties associated with high dimension response surfaces while evaluating small probabilities, here response surfaces are not used directly to evaluate system failure probability. On the other hand, the information obtained from the response surfaces about the system failure region is used to make conditional stratified samples. The system failure probability is evaluated from these conditional samples. The conditional samples are generated by subset simulation of response surfaces.

The probability of functional failure of SGDHRs to limit temperatures of critical structures to their DSL, is dependent on the number and duration of loop availability during the initial few hours of mission. The evaluated functional failure probabilities on various possible hardware system configurations vary from $1.0E-2/de$ to $<1.0E-7/de$ for category 4 design safety limits. Functional failure probabilities are also evaluated with respect to category 3 design safety limits.

6. COMPARISON OF DIFFERENT METHODOLOGIES FOR A BENCHMARK PROBLEM OF ISOLATION CONDENSER

6.1. BENCHMARKING PERFORMED BY CNEA, ARGENTINA

6.1.1. Models developed

In this chapter, a brief description of the two models developed for CAREM-like reactor analysed is presented.

The first model, is highly detailed, and was made for the best estimate plant code RELAP5/MOD3.3.

The second model is an extremely simplified one, with only one component that represents the whole saturated primary system.

The term CAREM-like implies that the model used approximates the design characteristics of CAREM-25 (geometric values, systems layout, etc.) without being actual design values, and further simplifications has been taken into account in order to set-up a definitive model for the development of the task reported here. Despite the above mentioned, CAREM-like represents an accurate model for passive safety function evaluation purposes, and for testing the capabilities of the methodology employed.

Plant code reactor model

The reactor model corresponds to a CAREM-like reactor type, being composed by a primary system (FIG. 83), IC and the medium pressure injection system (MPIS).

The primary circuit is modeled with a one-dimensional nodalization which has been established dividing it into the most relevant components:

- RPV dome;
- Steam generators (SG);
- Down comer;
- Riser;
- Core;
- Lower plenum.

Condensation on control rods hydraulic feed tubes (which are located into the steam dome) and condensation on RPV dome wall due to thermal loss to exterior are modelled since they rule the steam generated in the core, which travels along the riser up to the dome. The amount of steam affects the hot leg density and the buoyancy forces that, together with the pressure losses, determine the primary circuit mass-flow rate.

Down comer and riser are divided into a suitable number of nodes in order to follow properly the thermal fronts. On the other hand lower plenum is modelled with a unique volume aiming to represent the water mixture effect before it comes into the core.

The model of the SG represents the twelve SG with a primary flow and heat transfer areas equal to the sum of all of them.

The core active zone is modelled by only one pipe, axially divided. The reactor power is obtained from point kinetics model, taking into account the feedback due to reactivity coefficients. The decay power is calculated according to ANS79-3 model.

In the model are also included structures like the RPV, barrel and other internals. These heat structures have been modelled keeping the total masses and materials heat capacity.

For the primary system nodalization it was adopted as a general criterion that adjacent volumes have to have the same height.

The IC nodalization includes the following system components:

- Steam line (steam line piping + in header);
- Condensers;
- Return line (return line piping + out header);
- Pool.

Like in the primary system model, the sliced nodalization criterion has been adopted in the steam and return lines regarding also the criterion of same length between nodes of adjacent volumes.

A single valve has been added in the discharge line instead the complete set of two valves.

The MPIS nodalization is the simpler one, and was made based on the accumulator component available in the computer code used.

In the primary system, the upper plenum zone (named dome) has some interesting characteristic: even though it seems to be an innocuous part of the primary system (as it is far away from the core, through it does not circulate the main coolant flow, and it is analogous to the classical pressurizer of the PWR), its modeling highly influence many primary system parameter, like the pressure evolution (parameter of interest in this work).

Thus, special attention was paid to the dome nodalization, in order to allow fluid circulation within the one dimensional path [66]. For its representation, the dome was divided in seven parts (that corresponds with 7 RELAP5's components), which are showed with different colors in FIG. 70. The nodalization showed is named 'Dome 3'.

The steam circulation inside the dome is promoted by the condensation on control rods hydraulic feed tubes (which are located inside the steam dome [3]), and the condensation on the RPV wall due to thermal losses.

In order to evaluate the user-effect in developing a nodalization on the performance indicator, two additional models where developed for the dome zone, which are simpler than the previous one. It was observed that by using these simple models, enveloping results are obtained, from the steady state calculations point of view. In one of these models (Dome 1) the entire dome is modeled with a single RELAP5 volume, which forces the dome to the saturation condition. And the other one (Dome 2), all the dome is modeled with only two vertical volumes: one for the lower region of the dome (in which the primary flow turns from the riser towards the GV) and one for the upper zone (containing the inter-phase between the liquid and the steam, with a stratification regime). In this model an 'uncoupling' within the dome and the rest of the primary circuit (making it extremely sub-cooled) is predicted.

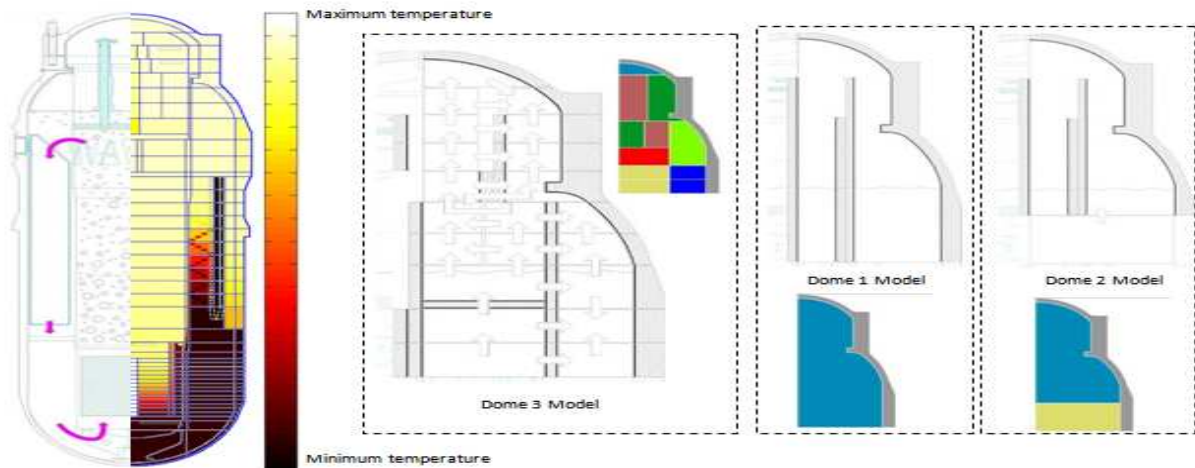


FIG. 70. Primary system nodalization. Left: steady state Temperature of the mean volumes and structures. Right: Dome models with the defined direction of the junctions, and a colorized miniature with the RELAP hydrodynamic components.

Another aspect to remark is that the RELAP5 source code was modified in order to model the uncertainties in the condensation and boiling heat transfer coefficients for the isolation condenser. This task was successfully performed, and the new version of the code accepts the application of some constant coefficients, which internally act as factors that directly affects the desired heat transfer coefficients. These fixed coefficients are simply specified through the standard RELAP5 input, together with the component where it is desired to be applied.

Reactor lumped-parameters model

A simple lumped parameter model to represent the reactor was developed for complementary calculations; this model is used to calculate some performance indicators, when the coolant in the primary system has reached the saturation condition, and using some results of the best-estimate RELAP5 model.

In this reactor model it is assumed that all the primary system is in saturated condition. Therefore, an equilibrium condition is archived. Only two equations are needed: one for energy and one for mass; no momentum equation is solved, as long as it is solved as a zero dimensional problem. Thus, the evolution of the whole system can be described by three state variable, pressure enthalpy and mass –for example-, through their respective balance and closure equations.

To completely define this model, is necessary to adjust several parameters (such as the isolation condenser efficiency in function of the primary pressure, initial primary mass, power decay evolution, etc.) against the events evolution of the plant code.

Figure 71 shows a comparison between the time evolutions of the most representative variables obtained with the RELAP5 model and they respective lumped-parameters reactor model. The evolutions are shown from the time when the system reaches the saturation condition, up to the peak cladding temperature of the hottest fuel reach the 800°C (this model also has the capability to predict a simplified core heat-up, but this feature finally wasn't used in the present work), during a small LOCA + SBO + MPIS failure. As can be seen, there is a very good agreement between the evolutions of the main variables that represents the state of the system.

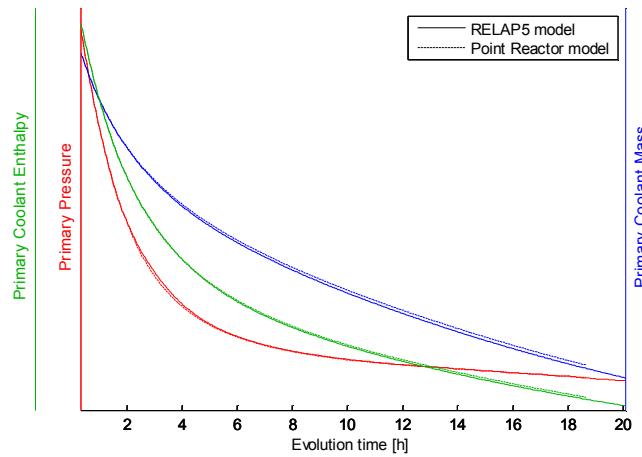


FIG. 71. Evolution comparison between the plant code model results and the lumped-parameters model, in one of the accidents analyzed, after saturation is reached.

6.1.2. Performance evaluation of IC in case of a station black-out

The present work deals with the application of the RMPS methodology to the IC of a ‘CAREM Like’ reactor, in order to verify one of the design criteria for this passive safety system. The aim of this work is to quantify the probability of not verifying that criteria due to uncertainties in engineering and operational parameters, and heat transfer correlations in the IC. This work is based on previous work, which was developed during the CRP of natural circulation in water-cooled nuclear power plants: phenomena, modelling, and reliability of passive systems that utilize natural circulation. At this stage, new parameters, as heat transfer coefficients in IC were considered. Moreover, different models for the reactor dome were developed in order to evaluate the user effect -when modelling a given system- in the functional design reliability calculation.

As can be seen, in this work not only the functional reliability of the system is evaluated, but also the reliability in the prediction of respective efficiencies.

In this chapter, the RMPS’s steps implementation performed is briefly described.

6.1.2.1. Mission of the system and scenario characterization

The scenario proposed for the present analysis is to analyze the IC performance regarding the fulfillment of a design criterion in a station black-out, event which is considered in the design basis. It is conservatively assumed the first shutdown system (FSS) and the IC is not triggered by the SBO signal, but by high pressure signals in the primary system.

The dynamic of primary system pressure, regarding a SBO scenario, is described below. In order to clarify the description, three phases of the transient has been identified (FIG. 72).

Phase I: due to the SBO the SG feed-water is stopped, down-comer temperature increases leading to a decrease in the water density, and consequently a rise in the RPV water level. Therefore, the steam in the dome is compressed increasing the system pressure.

When primary system pressure reaches the correspondent set-point, the FSS is triggered. As consequence of the power reduction, core sub-cooled void generation stops and the pressures decreases temporally. Nevertheless, because there is no power removal, the temperature goes

on increasing in the down-comer and in the whole circuit driving again to the primary circuit coolant expansion with the subsequent primary system pressure increase. During this pressurization phase, the whole primary system remains in a sub-cooled condition.

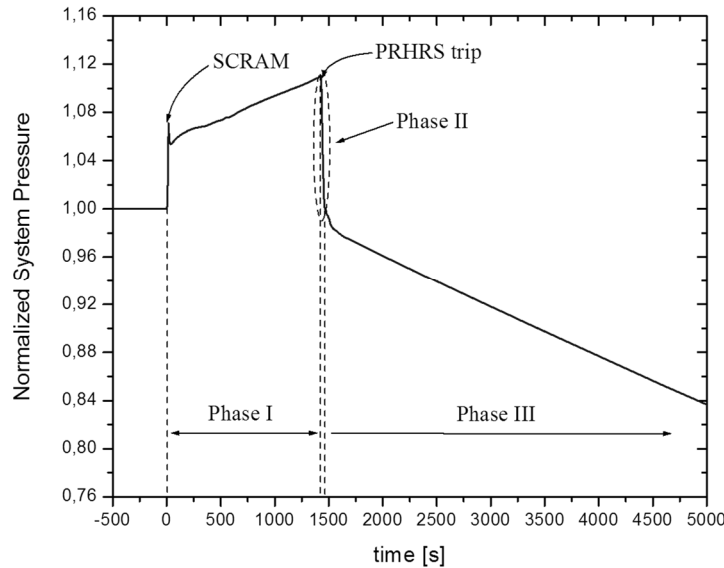


FIG. 72. Short-term pressure evolution for reference (nominal) case. This evolution reflects the condition of higher power removed by IC (in relationship with the core generated power) thus leading to a sustained depressurization after the ending of Phase II.

Phase II: when system's pressure reaches the IC set-point, the system is activated by opening the condensate line valves. As it was explained before, the sub-cooled water drains from the tubes into the RPV and steam coming from dome enters into the tube bundles, condensing on them.

Immediately after the IC actuation a sharp depressurization phase takes place. This behaviour is mainly due to imbalance coming from the steam condensation in the dome without liquid boiling in the primary system. This condition is also accompanied, in a much less extent, by the subcooled water (at pool temperature) coming into the RPV from condensers tubes immediately after the IC actuation.

Phase III: once the primary system reaches again its saturation condition the sharp depressurization ends and from this moment on, pressure begins to be ruled by steam reposition into the steam dome and steam condensation in the IC. Steam is generated in the core and the primary system goes on depressurization, by flashing.

The main phenomena associated to each one of its phases are summarized in Table 14.

TABLE 14. DESCRIPTION OF LOHS FOR REFERENCE (NOMINAL) TRANSIENT

Phase ID	Descriptor	Main phenomenological condition
I	Pressurization phase	Primary system sub-cooled condition
II	Sharp depressurization phase	Steam condensation in the dome without liquid boiling in the primary system
III	IC operation phase, with primary system depressurization	Primary system near saturation equilibrium condition

The (system mission) safety function to be performed by this system is to remove the decay heat (and the energy stored in the primary system) during a SBO event, thus reducing the pressure in the primary system.

For this study case, only the short term design goal is considered that is, after the IC demand, the primary system pressure should be controlled and reduced in order to avoid reaching the RPV safety valves opening set-point. Therefore from this point of view (design) the system is said to fail (failure criteria) if the safety valve opens.

6.1.2.2. Performance indicator definition

The performance indicator (PI) or observable should characterize the passive system behaviour regarding the failure criterion (i.e. safety valve opening). Considering this, the observable must reflect ‘distance’ between the primary system pressure and the safety valve opening set-point, after the isolation condensers demand. In this sense, the performance indicator is a measure of the IC ability to perform its safety function. It is required that the PI must also be a continuous function, among others mathematical goodness.

For this application the following performance indicator (*PI*) is adopted:

$$PI = \frac{\eta_{no\ min\ al}}{\eta_{Fail}}$$

Where, $\eta_{no\ min\ al}$ = actual removed power by the isolation condensers (which actually is a factor that scales the functional dependence between the power removed by the IC and the primary pressure) and η_{Fail} = minimum removed power needed to avoid the safety valve opening set point.

From this definition, PI represents an inverse factor, which affects the actual removed power by the isolation condensers. This factor, tells how much $\eta_{no\ min\ al}$ has to be reduced (or eventually increased, when the passive safety system couldn’t meet its design goal) in order to meet the failure criterion (i.e. if $PI \geq 1$, then the functional design reliability is successful).

The value of η_{Fail} was estimated through a parameterization of $\eta_{no\ min\ al}$; performing stepwise calculations, using the reactor lumped parameter model, that is adjusted based on the simulations performed for the actual relevant parameters combination or set. The stepwise calculation consist on reducing (or eventually increasing, if the nominal power wasn’t enough to accomplish the design criteria) the efficiency of the isolation condensers (obtained from the BE calculation for the respective set of relevant parameters). It is made applying a factor (to the fitted curve of the power removed by the IC versus the primary saturation temperature) and then recalculating by an analytical formula (thus, using the lumped parameters model) the pressure evolution of the primary system from the time of the isolation condensers demand. The process is repeated up to the efficiency reduction is such that the maximum primary system pressure reached is equal to the safety valve set point.

A sketch of this stepwise process is shown in FIG. 73; on each step only $\eta_{no\ min\ al}$ is changed, keeping the rest of the system variables constant.

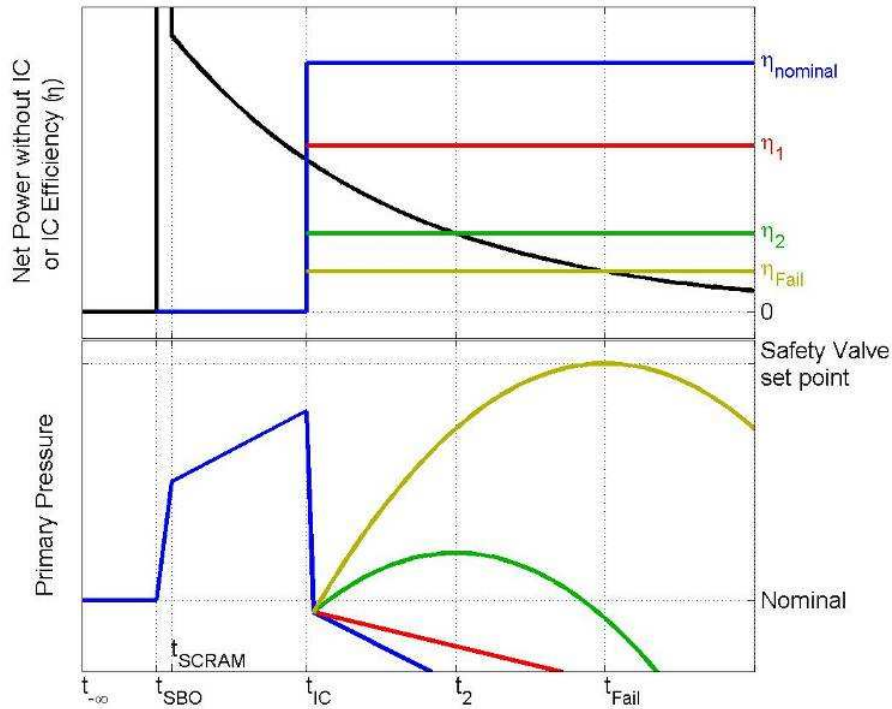


FIG. 73. Qualitative evolutions of net power, and primary pressure regarding four different conditions of removed power by the IC. The stepwise process starts with nominal condition and ends at fail condition when the safety relief valves set point is reached.

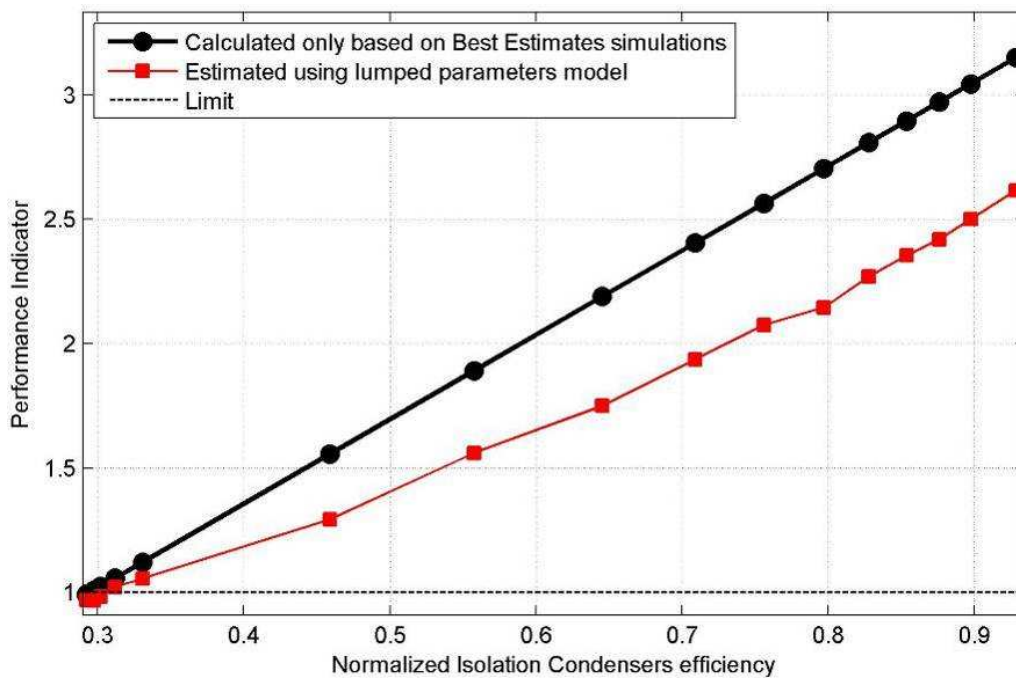


FIG. 74. Example of the relation between the performance indicator and the power removed by the isolation condenser. Comparison between the different approximations made in their estimation.

Figure 74 shows the performance indicator when varying parametrically the power removed by the isolation condensers (reducing the heat transfer coefficient HTC); up to the point when

the failure condition is reached. The figure shows a comparison of two calculations: the PI calculated based on BE simulations, and the estimation using the lumped parameter model. The first one is just obtained from the relation between the power removed by the IC for same HTC and the power removed by the IC when it has their functional failure.

The figure shows a good agreement between the two calculations, being the lumped parameters model more conservative, as long as it is closer to the failure limit.

One of the main advantages of this PI is that it varies linearly with the IC efficiency, as can be seen in the FIG. 74. This allows a reasonable extrapolation to the failure limit, by linearly interpolating, as can be seeing in the Figure. This is not the case for any PI: for example, the maximum pressure would be the IC set point for a wide range of IC efficiency,; for this reason the maximum pressure cannot be used as a PI.

6.1.2.3.Relevant parameters selection and quantification

A key point of the methodology is the identification of relevant parameters and their uncertainty quantification (i.e. assignation of probability distribution functions, nominal values and range of variation). Relevant parameters are those related to the nominal system configuration (design parameters) and physical quantities (critical parameters) that may affect the mission of the passive system.

Usually, during a reliability analysis, the uncertainties pertaining to the code are not accounted for, focusing the attention on the uncertainties relative to the input parameters characteristic of the passive system or the plant. One of the objective proposed to the present application of RMPS methodology to an isolation condenser (a passive residual heat removal system), is not only considering engineering parameters uncertainties, but system code uncertainties originated in empirical heat transfer correlations and in the model development, well known as user-effect. This last issue is addressed in this work by developing and using different models for the RPV dome, which are diverse approaches to its representation by the plant code.

6.1.2.4.Identification and quantification of uncertainties of the relevant parameters

This step was carried out by means of EJ. The selected parameters, whose uncertainties influence the isolation condensers performance, are listed in Table 15.

The three above mentioned reactor dome models will be used to propagate the uncertainties of the selected seventeen parameters. By this way three groups of results for the performance indicator will be obtained.

It is important to note that the non-condensable gases where not taken into account. This is because limitations in RELAP5 models. Nevertheless, it was observed that they would have a minor influence in the performance of the IC in this scenario, at least during the time window of the present analysis [67].

TABLE 15. LIST OF SELECTED PARAMETERS (THE NOMINAL VALUES AND RANGE OF VARIATION ARE NORMALIZED AND DISTRIBUTIONS ARE TRUNCATED AT RANGE LIMITS)

Parameters		Normalized Nominal value	Range		Distribution
1	Reactor power	1	0.95	1.05	TNORMAL
2	SCRAM delay	1	0.68	1.6	TLOGNORMAL
3	SCRAM: safety rods total drop time	2	1.2	4	TLOGNORMAL
4	Decay power factor (ANS79-3)	1	0.85	1.2	TLOGNORMAL
5	Reactor nominal pressure	1	0.99	1.01	TNORMAL
6	SCRAM: pressure set point	1.06	1.05	1.07	TNORMAL
7	IC: pressure set point	1.11	1.1	1.12	TNORMAL
8	RPV dome water level	1	0.75	1.25	TNORMAL
9	Primary circuit mass flow rate	1	0.96	1.04	TNORMAL
10	IC pool temperature	1	0.55	2.38	TLOGNORMAL
11	IC tube thickness	1	0.89	1.11	TNORMAL
12	IC fouling	5.71 10 ⁻³	0	5.71 10 ⁻²	TLOGNORMAL
13	RPV dome (steam zone) heat losses	1.00 10 ⁻³	5.00 10 ⁻⁴	1.50 10 ⁻³	TNORMAL
14	Safety Valves Set-Point	1.14	1.13	1.15	TNORMAL
15	IC pool's boiling heat transfer coefficient	1	0.5	1.5	TNORMAL
16	IC tube's condensation heat transfer coefficient	1	0.5	1.5	TNORMAL
17	Feedback reactivity coefficients	1	0	1.05	UNIFORM

6.1.2.5.Sampling

In order to obtain the relevant parameters samples, simple random sampling (SRS) method was adopted. In this method, every value of the sample is randomly generated from the respective parameters distributions.

The number of code runs - the sample size- was selected aiming to satisfy the Wilks' formula [7]. Based on the hypothesis that nothing is known about the output distribution function except that it is continuous, Wilks' formula gives the proper number of independent observations of the random output (Y) in order to fulfill, for a one-sided tolerance interval:

$$P[P(Y \leq y_{MAX}) > \alpha] \geq \beta$$

Where α = reliability; β = confidence level; and y_{MAX} = maximum output sample value

The selection of one-side tolerance interval is justified since the problem addressed (concerning the failure criterion definition) can be understood as problem of excess from a given value, as long as the failure criteria is associated with the compliance of only one limit for the PI, therefore does not exist a left tail of the output distribution function.

The number of independent observations of the output variable (i.e. number of code runs) for the one-sided tolerance interval can be calculated by means of next equation,

$$1 - \alpha^N \geq \beta$$

Where N = nearest higher integer to the calculated value.

The selected sample size (100 samples) satisfy the 95%/99% criteria (reliability = 95%, confidence level= 99%) for one-sided tolerance interval.

The values obtained in the sampling are presented in the FIG. 75 through a cobweb plot. It depicts all the inputs vectors determined from SRS (and their histogram compared with the respective proposed distribution) and shows the Input Matrix coverage degree of.

From visual inspection, it can be seen that the sample population achieved is well representative.

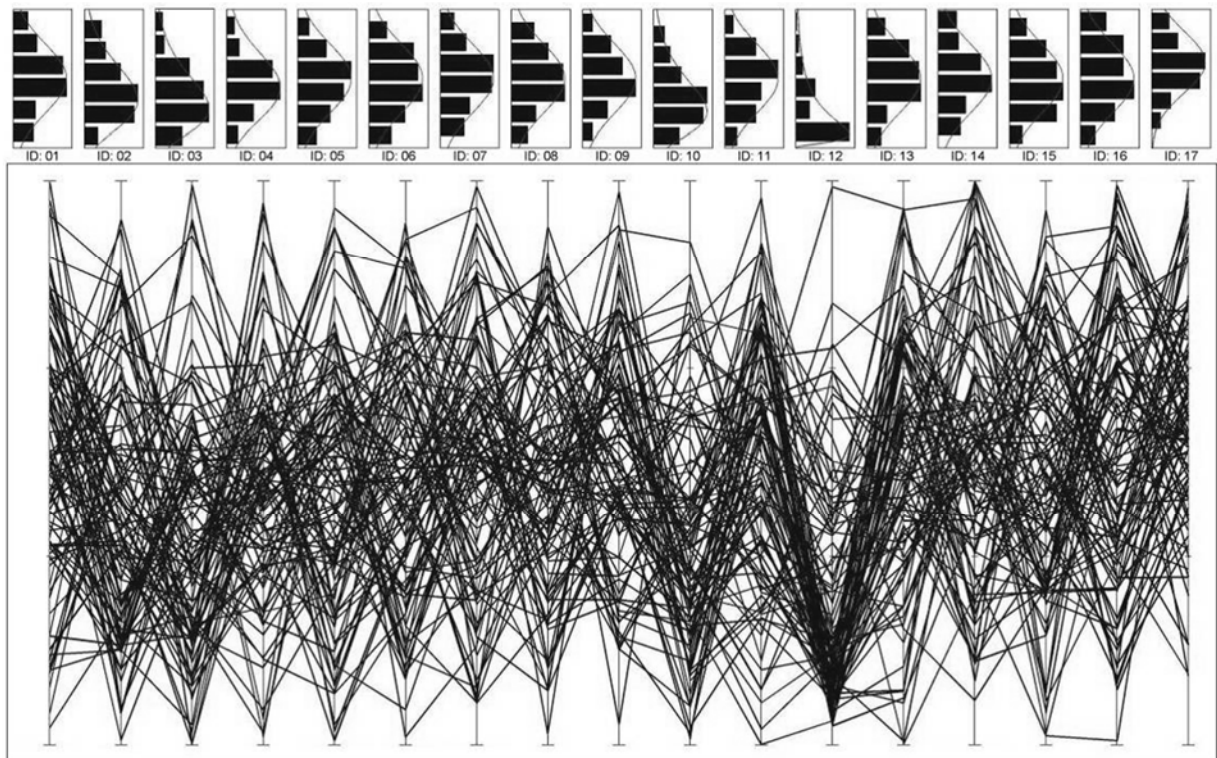


FIG. 75. Cobweb plot of the 100 values sampled for the 17 parameters.

6.1.2.6. Direct propagation of uncertainties through BE code

The aim of direct Monte Carlo simulation is to propagate the representative parameters uncertainties through a plant code (RELAP5/MOD3.3) in order to obtain a model response (set of code run results), which will be evaluated regarding the failure criteria associated to the passive safety function under analysis.

Figure 76 shows the results obtained by Direct Monte Carlo simulation, for the three RPV dome nodalizations. Each result corresponds to the pressure evolution calculated with the BE code for the associated input vector (built with the value of each parameter). It can be observed, that none of the cases reaches the design failure criterion (i.e. none of the cases exceed the RPV safety valve pressure set point, a band is shown because of the uncertainties assumed in the set point).

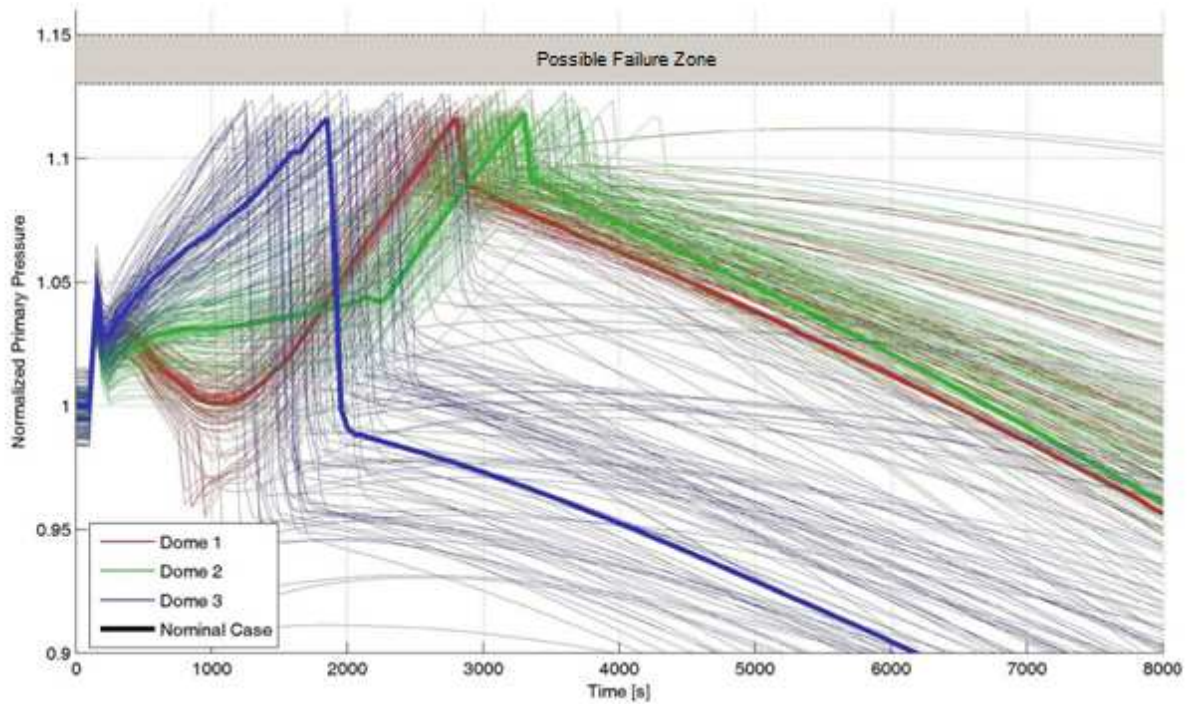


FIG. 76. Short-term Pressure evolution for the 100 BE-runs for the three dome models as well as their nominal case.

The performance indicators for the three dome models compared with the limit value are plotted in FIG. 77.

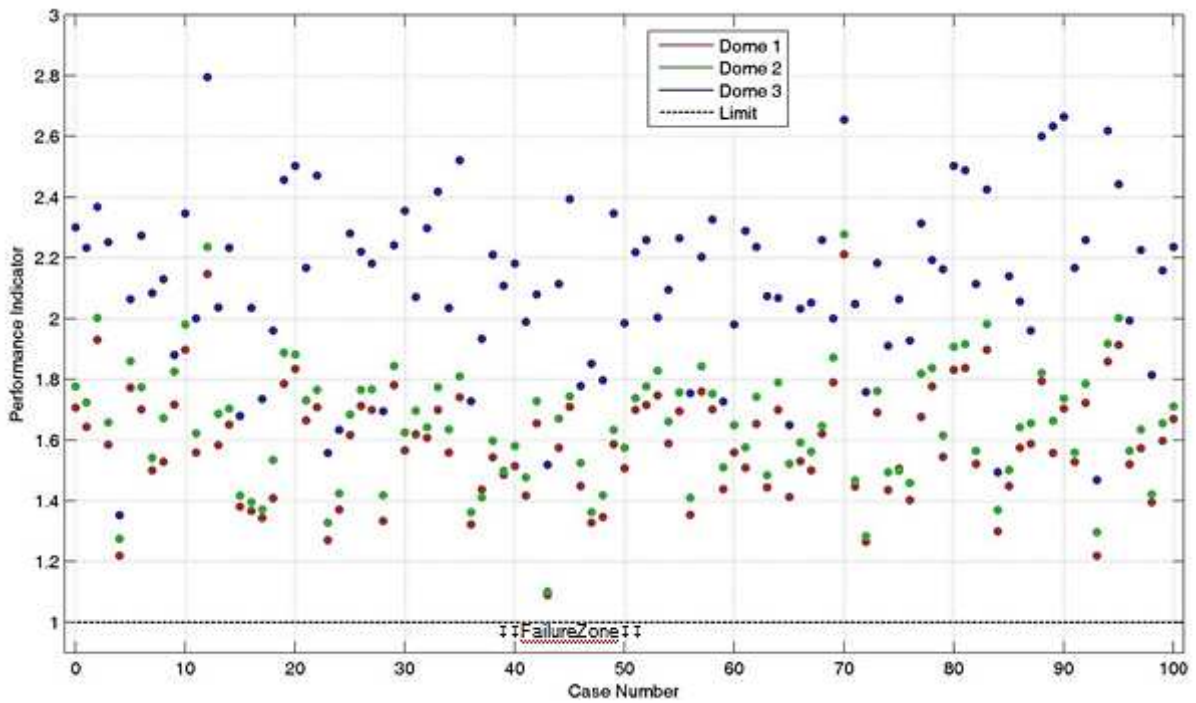


FIG. 77. Performance Indicator obtained for the 100 BE-runs for the three dome models.

As long as all simulated cases successfully accomplish the proposed design safety criteria, it can be assured that the reliability of the Isolation Condensers is, at least, of 95%, with a 99% of confidence, according with the Wilks formula for order N^{th} .

6.1.2.7. Response surface calculation

The selected method to build the response surface was the hyper-plane type, which means that a linear analysis was performed. Then, the assumption of linear relationship between the output observable ($Y = PI$) and the input parameters (X_i), is posed:

$$Y = \beta_0 + \sum_{i=1}^N \beta_i X_i$$

Where, N = number of relevant parameters; β_0 and β_i = regression coefficients; and X_i = values for the selected parameters.

As it was mentioned when the RMPS+ methodology was described, an iterative procedure was implemented in order to increase the accuracy of the surrogate model, which is also directly related with the sensitivity coefficients.

Several mathematical checks were done for each obtained coefficient. It is interesting to remark that the values archived in the determination coefficients are higher than 0.9, which helps to validate the linear hypothesis [68]. The obtained values in the final iteration step are summarized in the Table 16.

TABLE 16. DETERMINATION COEFFICIENTS OBTAINED IN THE LAST ITERATION STEP

Dome	Dome 1	Dome 2	Dome 3
R^2	0.982	0.985	0.976
R^{*2}	0.941	0.945	0.930

Figure 78 shows the performance indicator obtained for the original 100 set of values of the parameters, and with the addition of those obtained from combination of parameters values (within the population of 10^6 samples) that make the isolation condensers to be as near as possible to the failure zone boundary (but without reaching it). It is important to remark that all the points were obtained based on calculation performed with the best estimate code, and that the response surfaces were only used to assist the selection of the news points. Besides, these points were used to update the response surface.

In addition, FIG. 79 shows the respective pressure evolution for those added points, and their comparison with the nominal cases. It can be seen that some of these cases reach a maximum pressure greater that their respective IC pressure trip set point, and even more, some of them are actually near to the design failure criterion (because they pressure evolution enter into the 'possible failure zone', but without reaching their respective safety valve set point, also randomly selected).

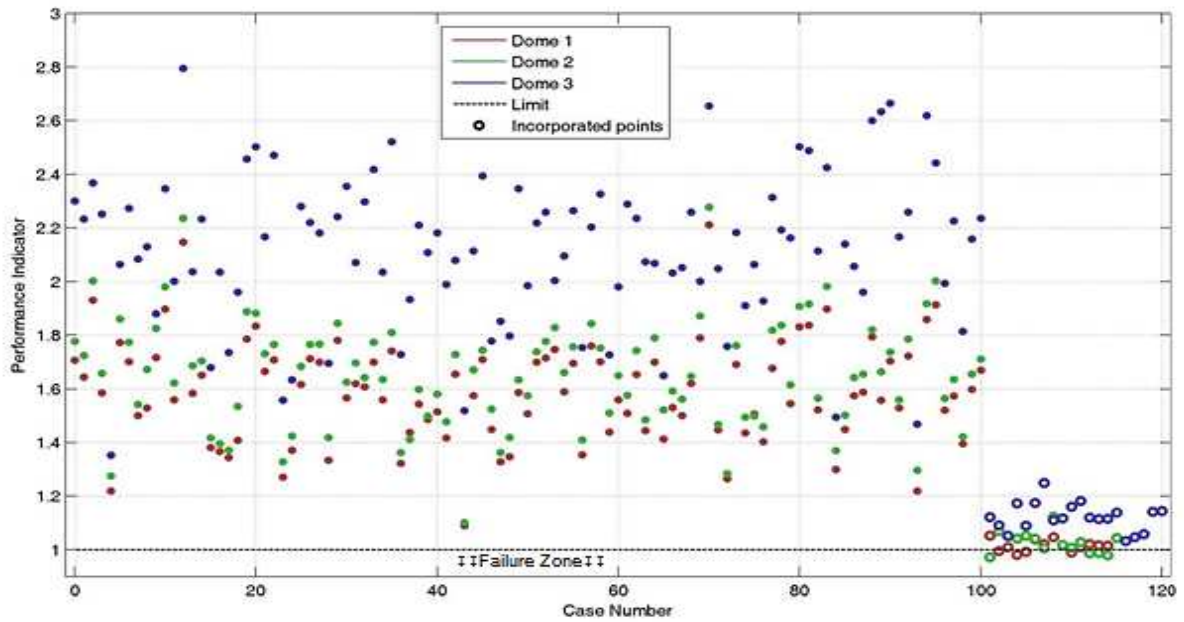


FIG. 78. Performance indicator obtained for the 100 (plus the cases nearest of the failure zone boundary) BE runs for the three dome models.

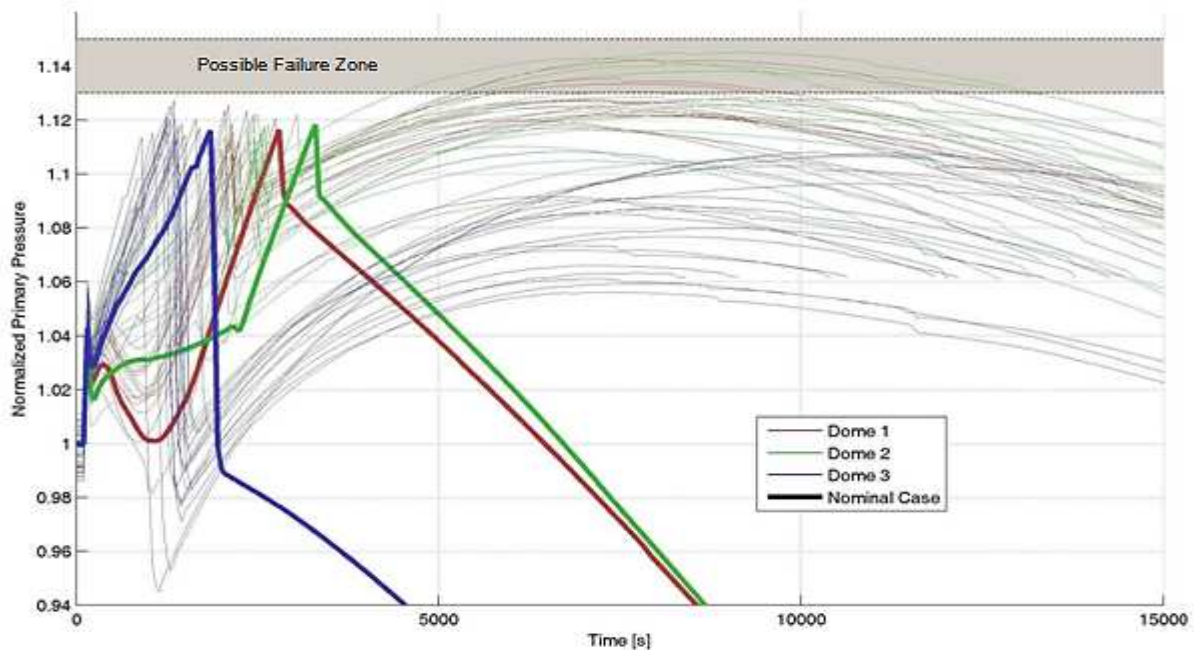


FIG. 79. Short-term Pressure evolution for the BE-runs nearest of the failure zone boundary for the three dome models as well as their nominal case.

Figure 80 shows the performance indicator distributions of the 10^6 cases (or set of relevant parameters), using the response surfaces obtained after each iteration step, and for the three Dome model. There can be seen a trend to convergence in the distributions of the same dome model, but not between them (as can be observed watching the modes). Here can be seen one more time the importance of qualified users and nodalization effect.

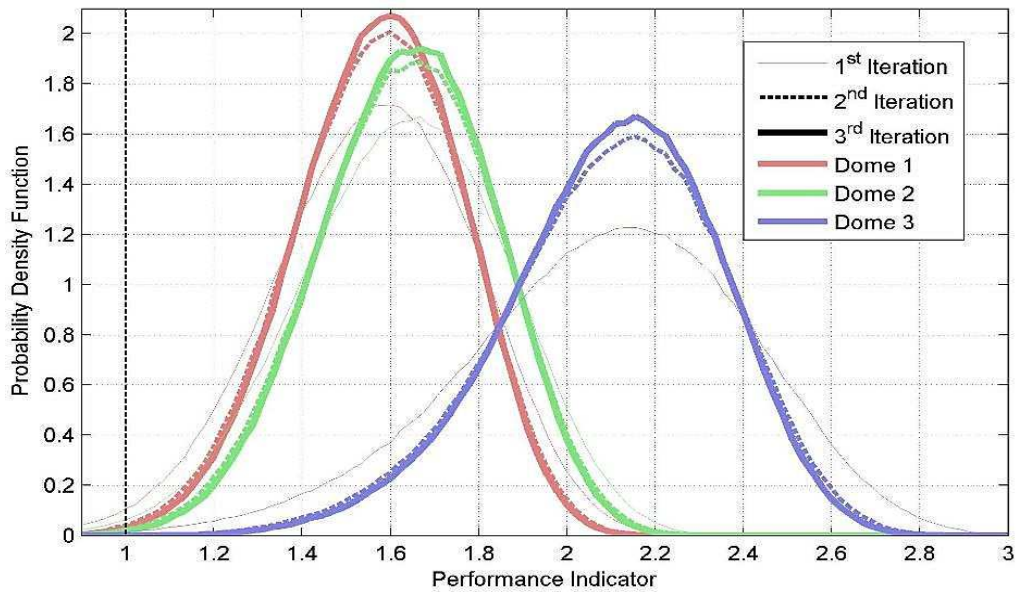


FIG. 80. 10^6 cases distribution, for the three dome model and the three respective iterations.

Table 17 shows the number of cases that are predicted to fail (i.e. those whose PI are equal or lower than one), according with the response surface (surrogate model) calculation, and the number of feedback steps performed, for the three Dome models.

TABLE 17. NUMBER OF FAILURE CASES PREDICTED BY THE SURROGATE MODEL

Number of feedback steps	Dome 1	Dome 2	Dome 3
1	8875	4965	1407
2	2193	1183	20
3	1416	784	3

It can be seen that the number of cases that are predicted to fail, are highly reduced on the feedback process. Even more, it was checked that for the model Dome 3 (the most realistic approach of the three evaluated), there are only 2 cases that truly fail (according to RELAP calculation), between the millions of cases. Its shows the grade of accuracy reached with this method. The difference between the 3 cases predicted by the response surface, against the 2 ones obtained through the best estimate calculations, are just a resultant of the conservatism of the Performance Indicator estimation, and fits precision.

Finally, Table 18 shows the failure probability of the IC to fulfill the selected design criterion for the last iteration feedback step and for the three RPV dome models. These values have been obtained utilizing the Wilks formula of order N-M, with N the number of values sampled (that in this case was equal to 10^6), and M the number of cases that have failed.

TABLE 18. FAILURE PROBABILITY WITH A 99% OF CONFIDENCE, FOR THE THIRD FEEDBACK STEP

Dome 1	Dome 2	Dome 3
1.50E-03	8.80E-04	1.00E-05

These results clearly also show the influence of the user-effect on the performance indicator, for the present analysis.

As can be seen, the Dome 1 and Dome 2 models predict a lower reliability of the ICs. These models have problems, due to poor modeling details, on predicting the flow and heat transfer regimes in the steam zone of the dome. Because of this the code calculates the presence of a mixture of liquid and steam in the IC inlet, producing their partial flooding, with performance degradation. Otherwise, Dome model 3, shows a more realistic behaviour in every aspect that was analyzed, mainly in predicting liquid stratification in large volumes with low flow velocities.

6.1.2.8.Sensitivity analysis

For the present study case, a sensitivity analysis was performed to determine those parameters that mostly influence the model response and thus, the passive safety function.

The selected hyper-plane fit procedure allows calculating the standardized regression coefficients (SRC) and partial regression coefficients (PRC) sensitivity indices. The linear hypotheses have been validated throughout the determination coefficient R^2 .

It is important to remark that SRCs and PRCs provide related but not identical measures of the parameters importance; but in case that the input variables are uncorrelated, the order of variable importance based either on SRCs or PRCs (in their absolute values) is exactly the same, condition that corresponds to the present study case.

The final SRCs obtained for each Dome model are showed in FIG. 81. The negative coefficients are presented in pale colors (their increment produces a detriment in the IC performance), while the positive coefficients are graphed in light colors. The obtained PRCs are not showed because the archived rankings are the same.

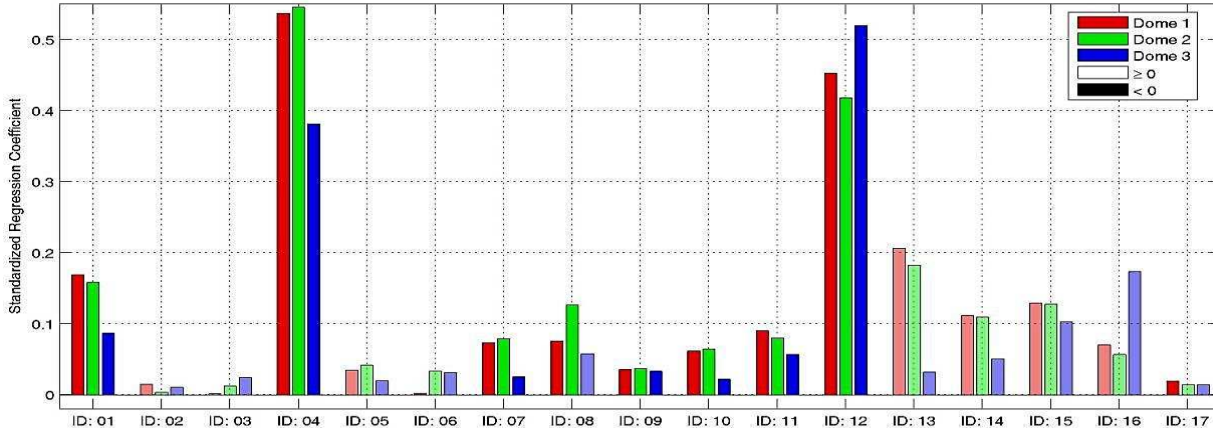


FIG. 81. Standardized regression coefficients finally archived.

It can be seen that, for the case of Dome 3 model, the Decay Power Factor (04) and the Fouling (12) are the parameters whose uncertainty most affect the Isolation Condensers performance. Besides, the Isolation Condenser performance indicator depends intermediately on condensation (16) and boiling (15) heat transfer coefficients, ranked in the 3rd and 4th position, respectively.

Another important result to remark is that the dome model (this means, the user effect) has a great influence on the results obtained, because it can significantly change the parameters influence, and the reliability evaluation (as it was showed in the previous section) as well.

6.1.3. Performance evaluation of IC and MPIS in case of a SB-LOCA+SBO

The aim of this second analysis is to perform another application of the RMPS+ method in a different scenario where dependence between two passive safety systems is present. The chosen scenario is a very small break in a pipeline connected to the RPV (1/2" equivalent diameter) with a station black-out. This implies that the process systems can neither cool the core nor inject water into the RPV. This DBA shall be mitigated by the passive safety systems during the grace period (IC and MPIS).

In this case the primary system needs to be depressurized by the IC in order to let the MPIS (accumulators) to inject into the RPV to keep the core cover during at least the grace period. For breaks with equivalent diameter larger than 3/4", the IC is no longer necessary to reach the MPIS pressure set point.

This combination of events, a small break event and a blackout, when comparing with larger breaks, is the one where the minimum collapsed water level gets closer to the top of the core, that happens just after the accumulators discharge (as can be seen in FIG. 82).

The main objective of this work is to address the selection of the injection pressure of the MPIS accumulators, using a safety related indicator, like water level margin over the core, based on uncertainties analysis using RMPS+.

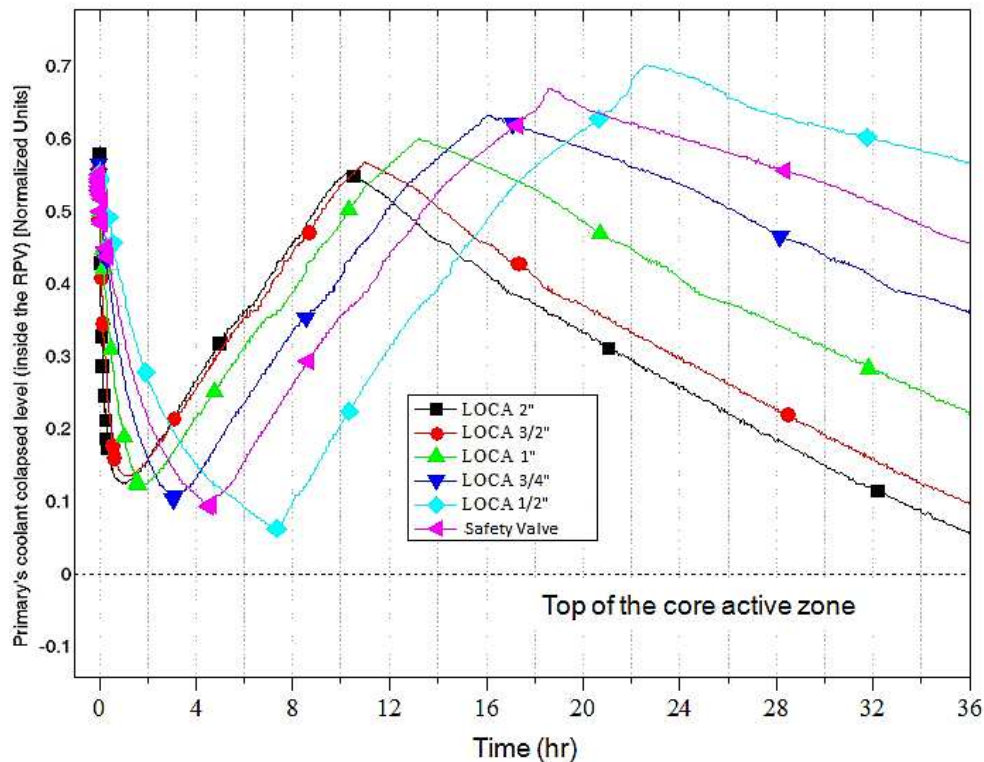


FIG. 82. Parametric variation of the LOCA+SBO break size.

6.1.3.1. System mission and scenario characterization

As it was previously mentioned, the scenario is a SB-LOCA, with a station black-out condition just when the reactor is shutdown. It is assumed that the FSS is trigger by low level or pressure signals. In this scenario the IC mission is to reduce the primary system pressure

below the MPIS injection pressure and the MPIS is to deliver water into the RPV with a given mass flow rate and volume in order keep the core uncover during the grace period.

Due to the initial loss of coolant the primary systems depressurizes rule by flashing in hot leg. Reactor SCRAM is demanded by low water level. At the same time, a SBO is conservatively assumed.

The primary system depressurization increases due to the reactor shutdown, continues (because the enthalpy that is loss through the break is greater than the decay power heat) up to the whole primary system reach the saturation condition and a slower depressurization is observed because a greater steam generation.

All this process is accompanied with a decrease of the primary system water level. When the pressure reaches a given value the MPIS starts to deliver water to the primary system and water level starts to increase until the accumulators get empty, starting decreasing again, keeping the core cover during the grace period (36 hours in the prototype) with one redundancy. Then, to reach the final safe state, the plant shall be controlled by redundant safety related systems, supported by the off-site power or the diesels generators (if recovered). In case of failure of energy supply, water can be injected into the RPV, via the MPIS or others systems, by the fire extinguishing system.

Therefore according to this scenario, the mission of the IC is to depressurize the primary system in order to allow the MPIS injection and the one of the MPIS to refill the RPV avoiding core uncover.

The design related acceptance criterion for this case is that the primary coolant collapsed level must always be over the top of the core active zone. Clearly, this is a very conservative approach and the violation of this criterion doesn't imply a direct commitment in the cladding. But one of the advantages of this criterion is that it is easier to calculate and is useful to be utilized in design assessment, taking credit of the high inertia of the primary systems and the robustness of CAREM like integral reactor.

Another criterion that could be used is the peak cladding temperature (cladding temperature in the hottest point) must always be below 800°C. This criterion is less conservative that the previous one, because when the core starts uncovering less steam is produced and the pressure decrease rate increases. The MPIS could inject if the pressure wasn't lower enough previous to the onset of core uncovering, refilling the core. This performance indicator increases the success domain but implies more refined calculations like heat transfer by radiation and cladding re-wetting.

For the present work the first success criterion is used and the required number of the IC redundancies used in this work is 2 out of 4, that is the design criterion.

6.1.3.2.Parameters identification and quantification

The methodology utilized for the definition of the relevant parameters with uncertainties, was the same that the used in the previous case. The new set of selected parameters with uncertainties includes the previous IC set with the addition of others related with the MPIS and its trigger set point signal (low pressure). In Table 19, the set of relevant parameters are summarized.

TABLE 19. SELECTED PARAMETERS FOR SB-LOCA+SBO. THE NOMINAL VALUES AND RANGE OF VARIATION ARE NORMALIZED AND DISTRIBUTIONS ARE TRUNCATED AT RANGE LIMITS

Parameters		Nominal value	Range		Distribution
1	Reactor Power	1	0.95	1.05	Normal
2	Decay power factor (ANS79-3)	1	0.87	1.2	LogNormal
3	Reactor nominal pressure	1	0.98	1.02	Normal
4	RPV dome water level	1	0.75	1.25	Normal
5	Primary circuit mass flow rate	1	0.94	1.06	Normal
6	RPV dome (steam zone) heat losses	1	0	2	Normal
7	Feedback reactivity coefficients	1	0	2	Uniform
8	IC low primary pressure set point	0.922	0.913	0.932	Normal
9	IC low primary water level set point	1	0.99	1.01	Normal
10	SCRAM signal delay	1	0.68	1.6	LogNormal
11	SCRAM safety rods total drop time	1	0.599	2	LogNormal
12	SCRAM pressure set point	0.955	0.946	0.965	Normal
13	SCRAM water level set point	1	0.99	1.01	Normal
14	IC pool temperature	1	0.568	2.222	LogNormal
15	IC tube thickness	1	0.89	1.11	Normal
16	IC fouling	1	0	10	LogNormal
17	IC pool's boiling heat transfer coefficient	1	0.5	1.5	Normal
18	IC tube's condensation heat transfer coefficient	1	0.5	1.5	Normal
19	MPIS rupture disk differential pressure	1	0.9	1.1	Normal
20	MPIS Liquid Volume	1	0.8	1.2	Normal
21	MPIS Height	1	0.8	1.2	Normal
22	MPIS Friction Losses	1	0.8	1.2	Normal
23	MPIS Accumulators Pressure	1	0.8	1.2	Normal
24	MPIS Volume	1	0.8	1.2	Normal

For all the parameters with normal distribution, the range limits are the nominal value minus or plus two standard deviation, except for heat transfers coefficients, where one sigma was utilized. Simple Random Sampling was also utilized in this methodology application.

6.1.3.3. Performance indicator definition

As was mentioned previously, the performance indicator selection is a key issue in the methodology implementation, because not only have to be continuous and sensible to the parameters, but also must be suitable to the response surface selected as surrogate model. The hyper-plane kind was chosen for the response surface, then, the performance indicator must be as linear as possible respect to the parameters selected.

Based on the previous assessment made, it can be presumed that the parameters that affect the IC efficiency might be between the most important parameters in the scenario proposed. Then

it is recommended to have a linear relationship between the IC efficiency and the performance indicator selected.

In order to obtain this linear relationship, several options for the performance indicator are selected and plotted against the IC performance variation for the most probable combination of the parameters. The results obtained are shown in FIG. 83.

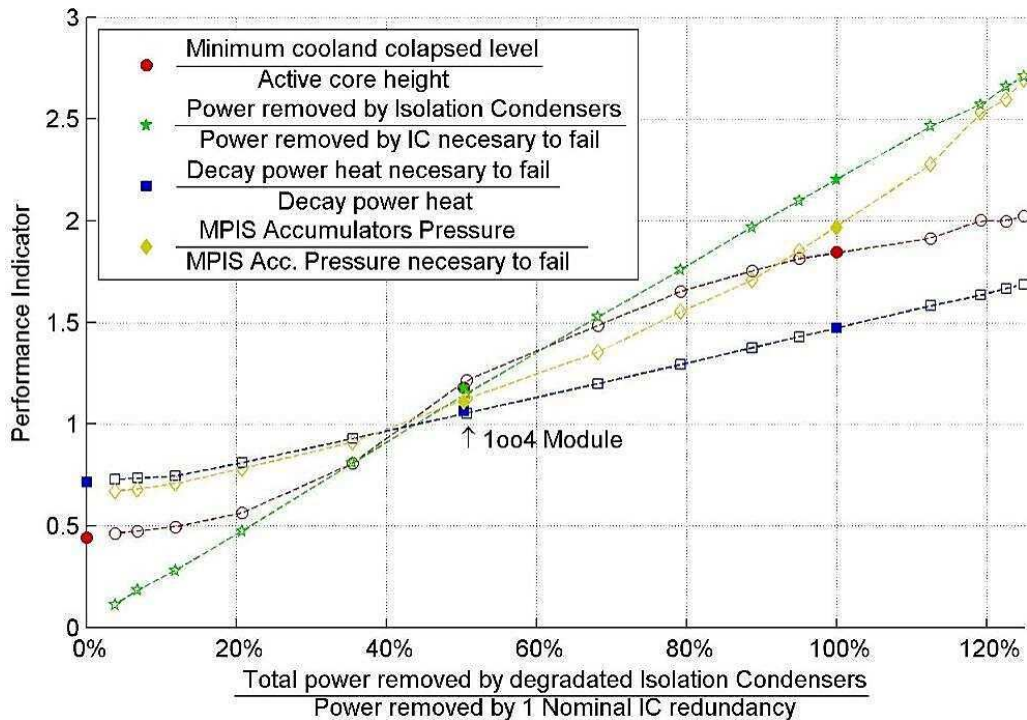


FIG. 83. Comparison of 4 performance indicator definitions, against the power removed by the IC.

The most direct, representative and easy to calculate definition for the performance indicator (PI), is the one related with the minimum level that reach the primary coolant collapsed level, during the accident evolution. In order to make it comparable with other performance indicator, the minimum coolant collapsed level reached is divided by the height of the core active zone. Then, a value higher that one implies that the coupled passive safety function of the passive safety systems do not fail for that combination of the parameters, fulfilling the core cooling safety function.

The result obtained for this option is represented by red circles. As it can be seen, this definition doesn't have a linear relationship with the power removed by the IC, and even more, at least a third order response surface might be necessary to reproduce this behaviour.

Besides this PI definition is not useful to be used for the response surface generation, it was helpful to check if the others PI options were consistent in their cross of the boundary failure domain.

For the following performance indicator definition options that were chosen, there was necessary to perform stepwise simulations. Those stepwise simulations were executed after

each BE simulation with their respective parameters combination. They were made using the lumped-parameters reactor model, which was tuned with their respective BE simulation.

The next option proposed for the IC definition, is practically the same that the previous one, but instead of applying a factor to the power removed, that factor is applied to the power generated. Then, it is how much the decay power factor must be increased in order to the system approaches as much as possible to the functional failure condition. The results obtained are shown in blue squares. As can be seen this option also is highly linear, except for very low powers removed by the IC, where this performance indicator becomes almost insensible.

Finally, the last option proposed for the PI definition, is one related with the pressure, instead of the power. It is the ratio between the nominal MPIS pressure (and consequently its set point) and the MPIS accumulators pressure (reduced by a factor) that allows the MPIS effectively deliver water to the primary coolant system just before the coolant collapsed level reaches the top of the core active zone. The results obtained are shown in yellow diamonds. As can be seen, this definition is less linear that the previous two (which were related with the power removed or generated) but is more linear that the first options, and it has a lower order and any extrapolation will be conservative because of their upward concavity.

As following, the first option and the last one are analyzed in a numerical test. It consists of varying the pressure set point of the MPIS accumulators, by discrete steps and using BE code for the simulations. The collapsed water level evolutions obtained for this test are shown in the FIG. 84. There can be seen that the decrease of the MPIS accumulators in regular pressure steps, produces an increment between each case because the primary system depressurization rate decreases with time.

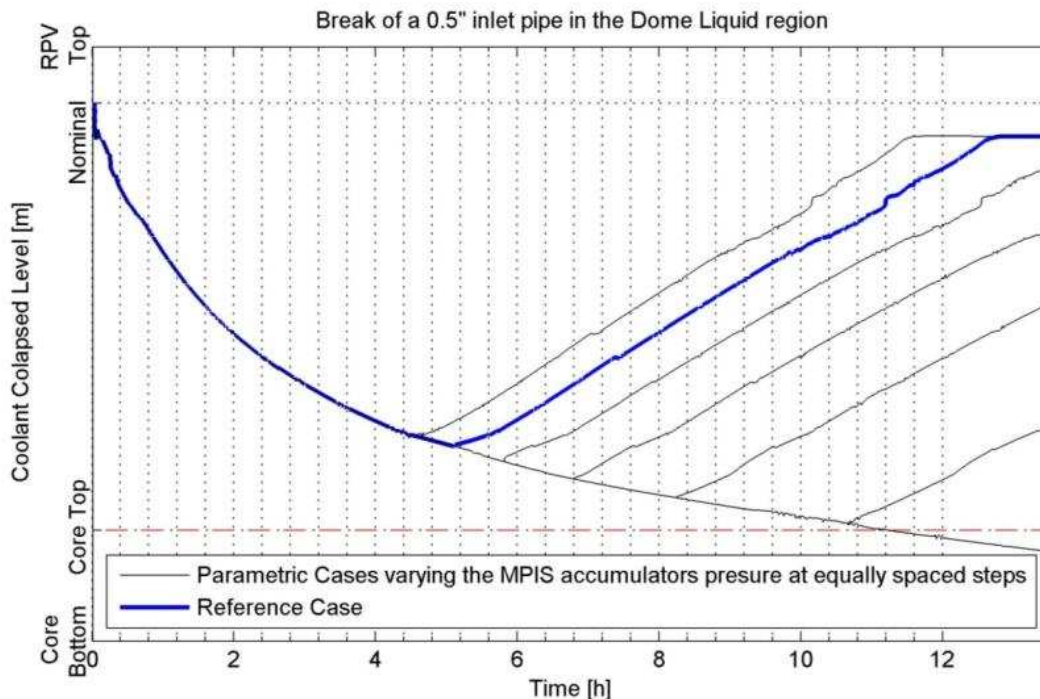


FIG. 84. Parametric variation of the MPIS Accumulator pressure.

In FIG. 85, the performance indicators values obtained for each simulation are shown. It can be clearly seen that the first option has not a linear trend, while the last option has.

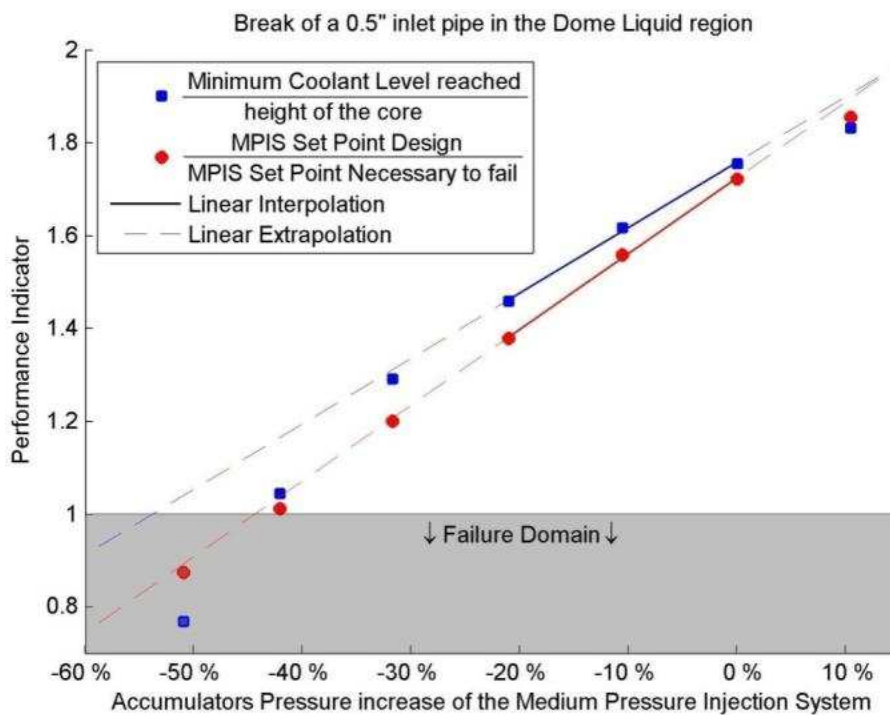


FIG. 85. Comparison of 2 performance indicator obtained from the parametric variation presented previously.

Even more, it is shown how a linear extrapolation made using the first option and based on the nominal point, can give a non-conservative estimation.

Therefore, based on the two parametric test performed, the best PI definition option is the one derived from the MPIS pressure ratio between the actual and the degraded ones.

6.1.3.4. Reliability improvement

The reliability improvement using RMPS has been made in two phases.

In the first phase, a coarse approach to the optimum point was made (using the response surface without the optimization process near the failure zone), and using two options for the break location.

Then, in the second phase, the nominal MPIS accumulator pressure was set to the optimum point previously obtained, the worst break location was selected, and a new RMPS application was made, but now using the optimization routine (improvement of the response surface with additional selected BE cases), and thus obtaining a more accurate optimization curve.

In the next two sections, these phases are shown.

Phase I

There were two main objectives in this phase. The first one was to select which location pipe is the worst to break. The second one was to coarsely find how much must be increased the MPIS accumulator pressure, in order to considerably improve the functional reliability.

To select the worst pipe to break, there is important to know (besides the size, which was selected the smaller one, based on FIG. 82 (the position of the penetration to the RPV. So, to decide which position is the worst, there were selected to test the lower one (which penetrate into the liquid zone of the RPV Dome region) and the higher one (which penetrate into the pure steam Dome zone) as evolving cases.

There are many options that can be used to find the MPIS accumulators pressure increase in order to improve its functional reliability. For this assessment, it was used the response surface obtained in the RMPS application, because it can be seen as a surrogate model that gives the functional reliability for each selected value of the accumulators pressure (supposing that all the parameters are kept fixed but the MPIS accumulators pressure).

Figure 86 shows the primary coolant collapsed level evolution obtained for the 100 random cases of the Monte Carlo BE simulations, and for the two options of break location. It is also plotted the most probable case for both options, and the evolution of one reference case which corresponds to a conservative evolution, based on expert judgment.

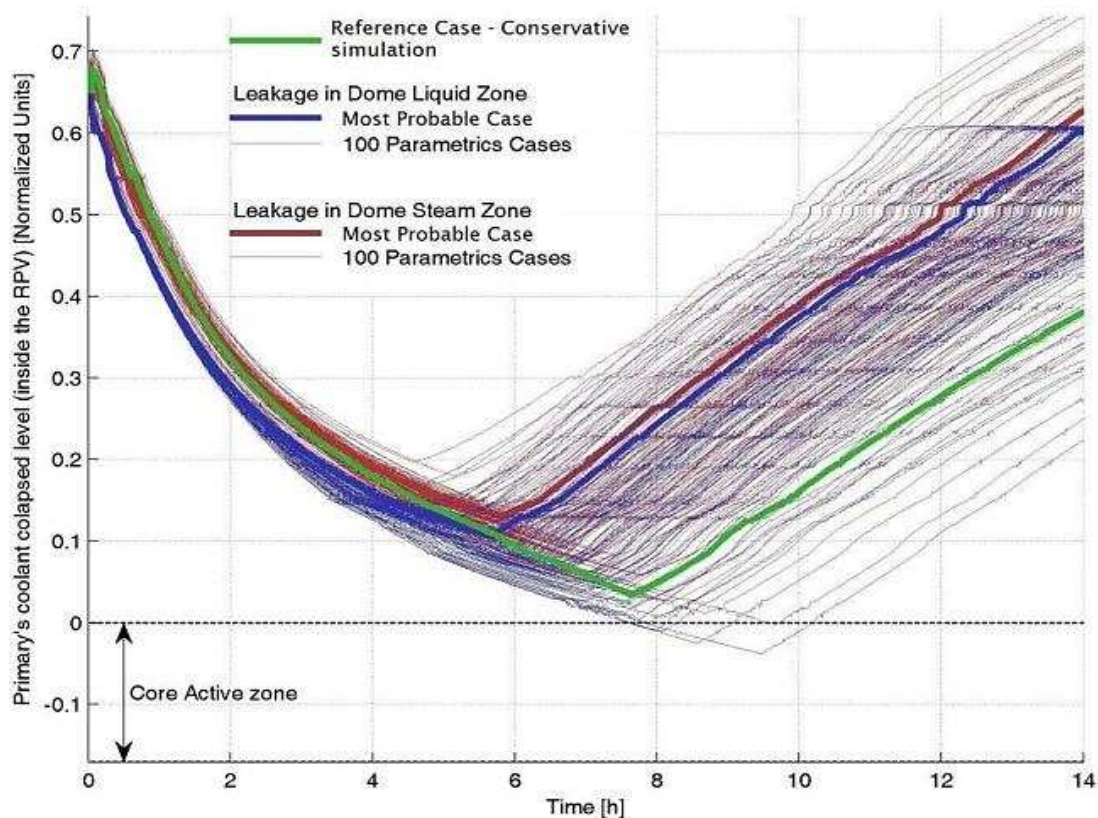


FIG. 86. Monte Carlo BE simulation for 100 cases for the actual MPIS design and for two break locations.

It can be seen that if the broken pipe penetration is in the Steam Dome zone, then 1 of the 100 cases fails. On the other hand, if the penetration is in the liquid region, then 5 cases will fail. From these results it can be presumed that the worst possible break is a small pipe connected to the Dome Liquid region. Then, this penetration location is used in the next phase of the assessment.

It can also be observed that the conservative case doesn't cover all the combinations of parameters simulated; more precisely it doesn't cover the 95% of all the possible combinations of parameters (with 99% of confidence).

In FIG. 87, the standardized regression coefficient for all the parameters and for the two location of break simulated are shown. It is important to remark that all the MPIS related parameters were condensed into one parameter, for this graph.

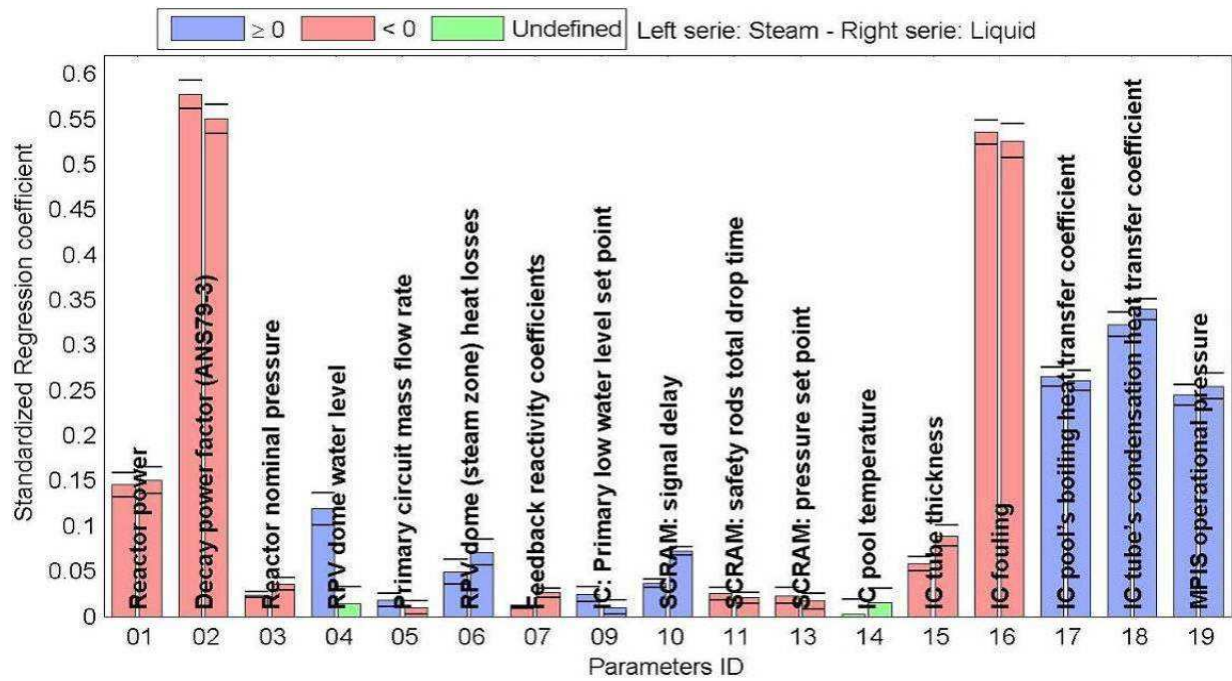


FIG. 87. Standardized regression coefficients obtained for the nominal MPIS design, and for the two breaks locations.

Figure 1: It can be seen that, in general, the importance ranking of the parameters is almost the same that the one obtained in the previous RMPS cases, plus the MPIS related parameters, that also are into the most important ones. It can be also observed that for both tested break positions, the values of the sensitivity is almost the same, with the remarkable exception of the RPV dome water level which is almost insensible in the case of the break located at the Dome liquid region.

Then, in FIG. 88 a cobweb-plot for the most important parameters and with the performance indicator are shown. The performance indicator shown is the one that corresponds to the break at the Dome liquid region. In this case, the lines that join the parameters combinations are colored, so, this graph not only shows that the parameters were well sample, but also shows which was the combination of parameters that makes fail the system. The red lines correspond to the parameters that that makes functionally fail the system. The yellow lines correspond to those which performance indicators are in-between the failure condition and the respective performance indicator of the conservative reference case. The green light ones are for the rest. Finally, the blue one corresponds to the most probable case.

As it can be seen, in general for the failure cases, the parameters that have positive standardized regression coefficient are usually under their respective most probable parameter value, and vice versa. This is because a positive coefficient means that improve the performance indicator, so the system is farther from the failure domain.

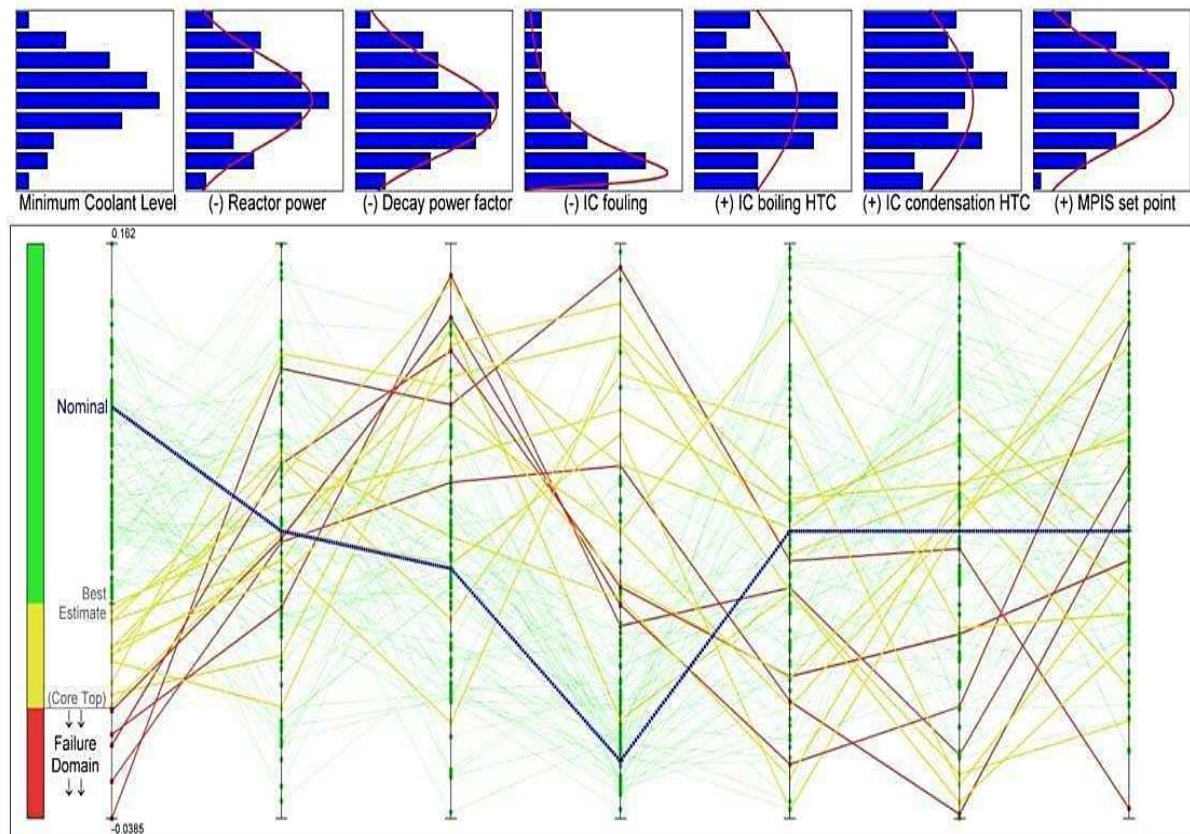


FIG. 88. Most important parameters CobWeb plot, with the PI obtained addition. The parameters combinations are colored based on their respective PI. The most probable case is also shown as nominal. Break is in the dome liquid region.

Finally, the responses surfaces obtained for each break location were used to generate the respective desired design curves, and they are showed in the FIG. 89. The curves represent the functional design failure probability, for each value of the nominal MPIS accumulator pressure.

Each of the failure probability value is obtained feeding the respective response surface with 10^6 random values for each relevant parameter (i.e. 10^6 input vectors, based on their respective distribution), with the particularity that the MPIS accumulator pressure distribution is shifted increasing or reducing the nominal value of the distribution. And then, this process is repeated varying parametrically the shift value.

It is important to remark that both axes were normalized respect the nominal design value, for the case of a break in a pipe connected in the liquid region of the Dome (red star).

As can be seen in this figure, the functional design failure probability can be reduced around of one order of magnitude just increasing a 25% the pressure of the MPIS Accumulators.

There can also be observed that, when the break is in the liquid region, the functional failure probability is systematically higher than when the break is in the steam region.

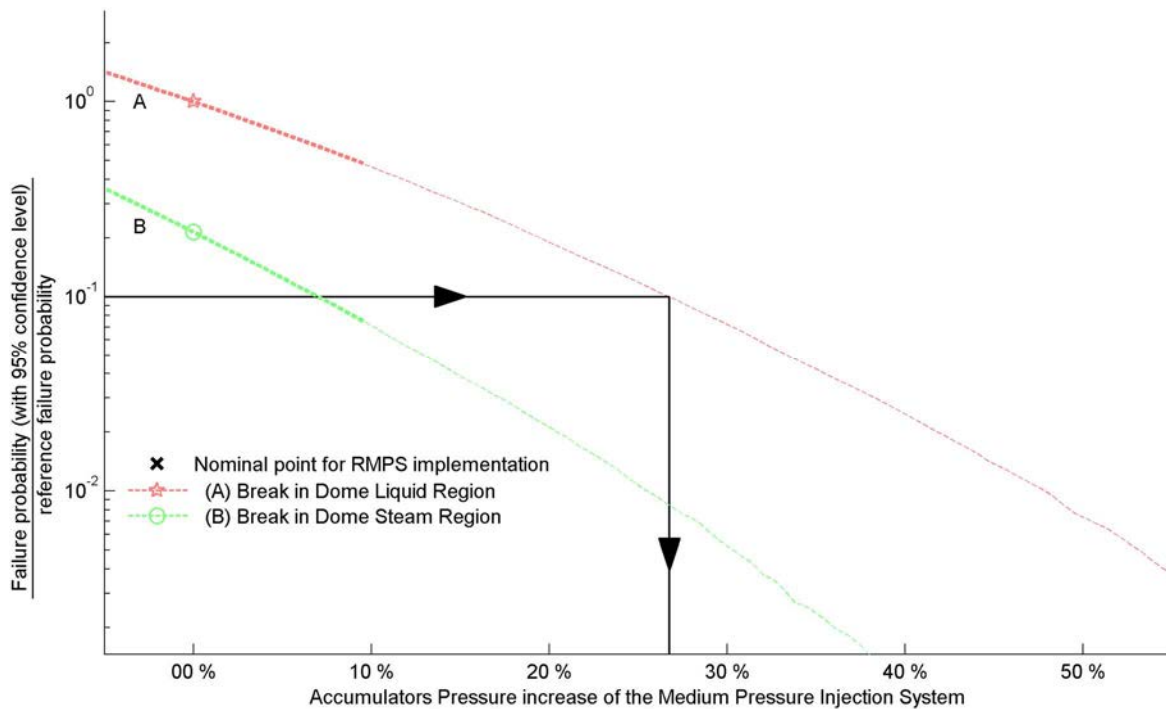


FIG. 89. MPIS accumulator pressure design curve obtained for both break locations.

Phase II

In phase I, it was obtained that the worst break location in the Dome liquid region.

It was also obtained (using the response surface that corresponds to the break in the liquid region, and varying the mean value of the MPIS accumulators pressure distribution) that a 25% increase of the MPIS pressure might reduce one order of magnitude the functional failure probability.

Then, in this second phase, the whole RMPS feedback process was performed, using the worst break and the 25% of MPIS pressure increase. This implies the redefinition of the MPIS accumulators pressure mean value, the parameters sampling of $N=100$ values, the evaluation of this new 100 reactor BE sub-models, and to perform of rest of the feedback process, in order to improve the response surface accuracy.

The feedback process was done twice. The first one was done using the 20 worst cases predicted by the response surface based on the 100 random cases. And the second one was done using 10 additional cases that are closer of the failure boundary domain, predicted by the response surface based on the previous 120 ones.

The RPV collapsed water level evolutions obtained for these 130 cases are shown in FIG. 90.

As it can be seen, after an increase of 25% in the MPIS Accumulator Pressure, none of the 100 random has functionally failed, against the 5 of the nominal pressure value. It can also be observed that the BE evolution of the 20 worst cases predicted by the response surface (generated using the 100 random cases) effectively have the lowest collapsed water levels resulting from a conservative response surface. And that the 10 additional cases (selected

from the improved response surface -120 BE simulations -, second iteration) have a lower number of failure cases and that their respective collapsed water level are higher than in the first iteration.

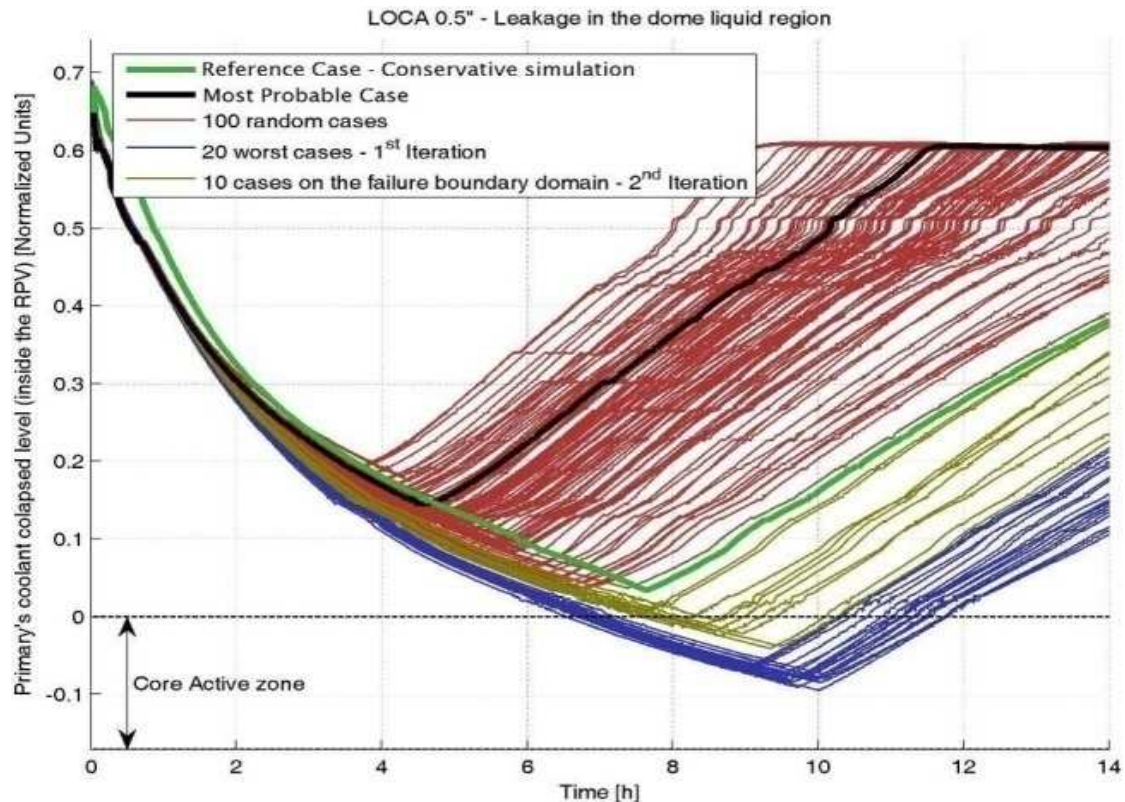


FIG. 90. BE simulation for 100 random cases plus 30 cases obtained in the RMPS optimization routine. The MPIS accumulators' most probable value is the one optimized in the phase I.

Figure 91 shows the respective PI of the BE simulation showed in the previous figure, but not the ones predicted by any of the response surfaces.

These PI clearly reflects the same trends that can be seen in the previous figure. It is important to remark the evaluation of the PI, based on the BE model, is slightly conservative, and for this reason, the last 10 cases are all below the failure limit, despite what can be seen in the collapsed level evolution where some of them show no failure.

Finally, in FIG. 92, the last (and more accurate) standardized regression coefficients obtained are shown. Then, the response surface used to construct the design map is based on these coefficients.

It can be observed that the most important parameters are those related with the generated power, the power removed by the IC (through the fouling and the heat transfers coefficients), and the MPIS Accumulators pressure.

Once, by means of RMPS methodology including the feedback process, the most accurate response surface is obtained. Then it can be used as a surrogate model (which give the performance indicator for any desired parameters combination, whereas the linear hypothesis remains valid) to evaluate the functional failure probability given the selected relevant parameters and their uncertainty distributions.

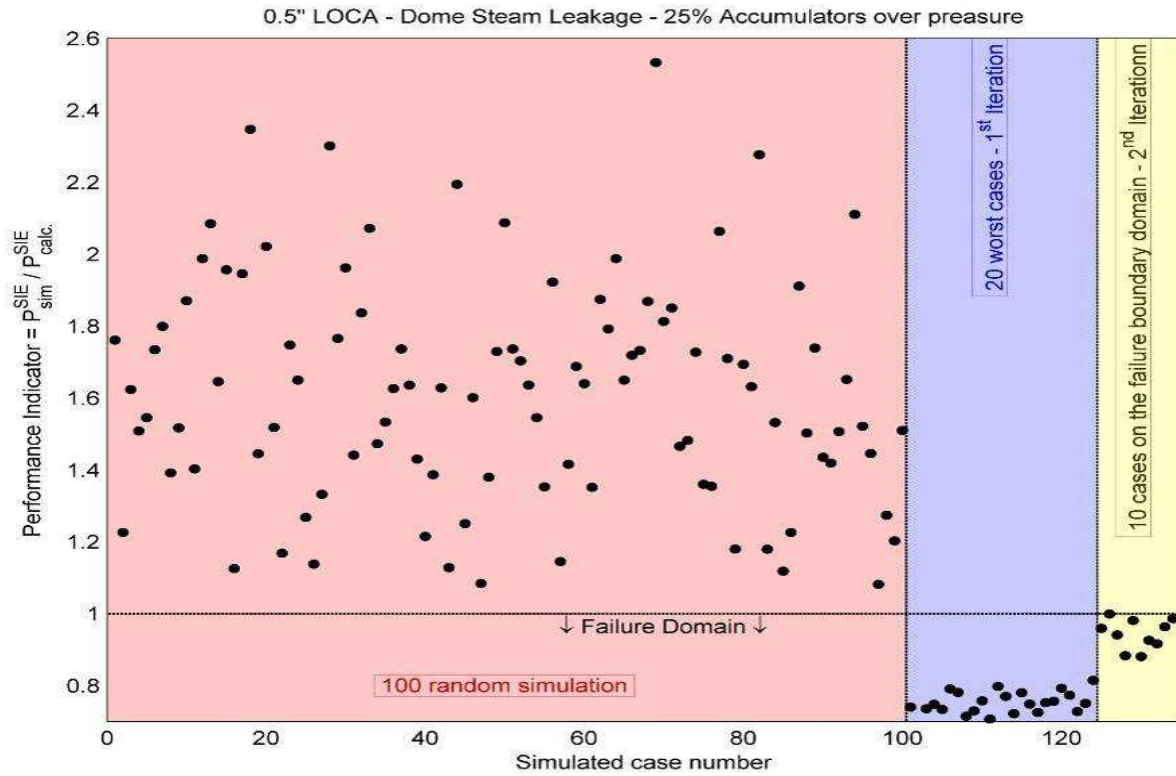


FIG. 91. PI obtained for the BE simulations showed in FIG. 90.

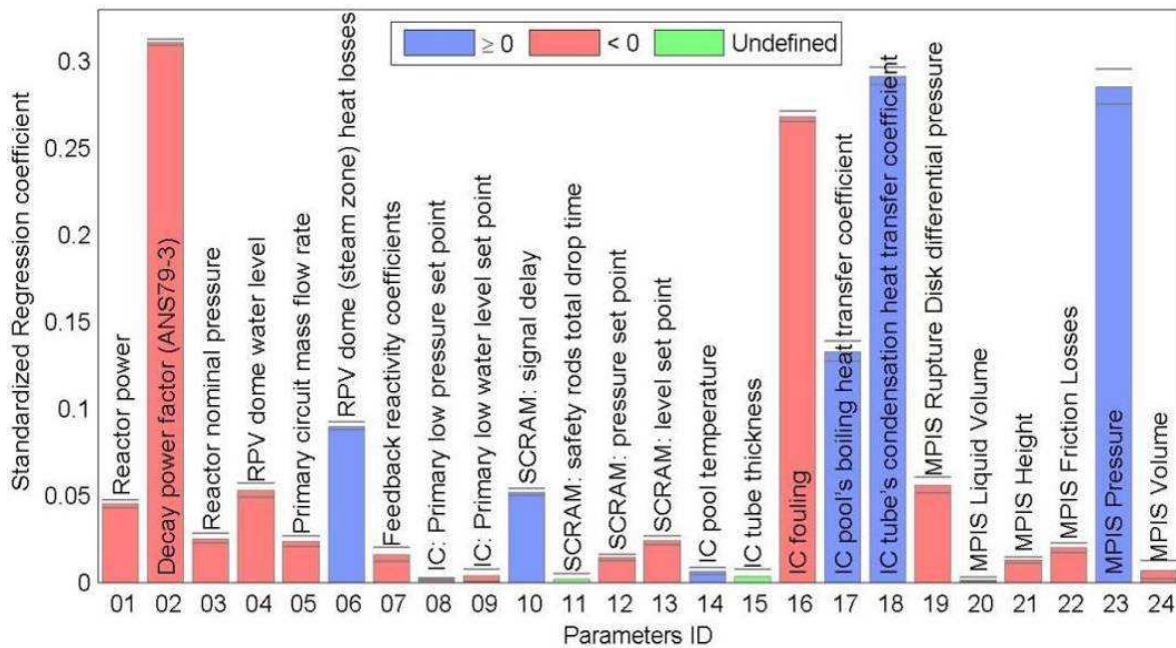


FIG. 92. Standardized regression coefficients finally archived, after the RMPS optimization routine and for the MPIS accumulators optimized in the phase I.

In this case, what we have been done again was to fix the distribution of all the parameters, except for the mean value of the MPIS accumulators pressure, then we find a relationship between this value and the functional failure probability, by parametrically varying the

pressure, feeding the parameters distributions to the response surface (using 10^6 samples for each relevant parameter) and finally evaluating the respective functional failure probability.

The curves obtained for each response surface calculated in the phase I (curves A and B) and II are showed in FIG.93.

In this figure, the curves are showed in continuous lines, and the dots (asterisk, diamond, square, circle and star) represent the pressure at which the respective response surface was generated (which means that the maps are more accurate in the surrounding of each these point).

It is important to remark that both axes were normalized respect the nominal design value, for the case of a break in a pipe connected in the liquid region of the Dome (red star).

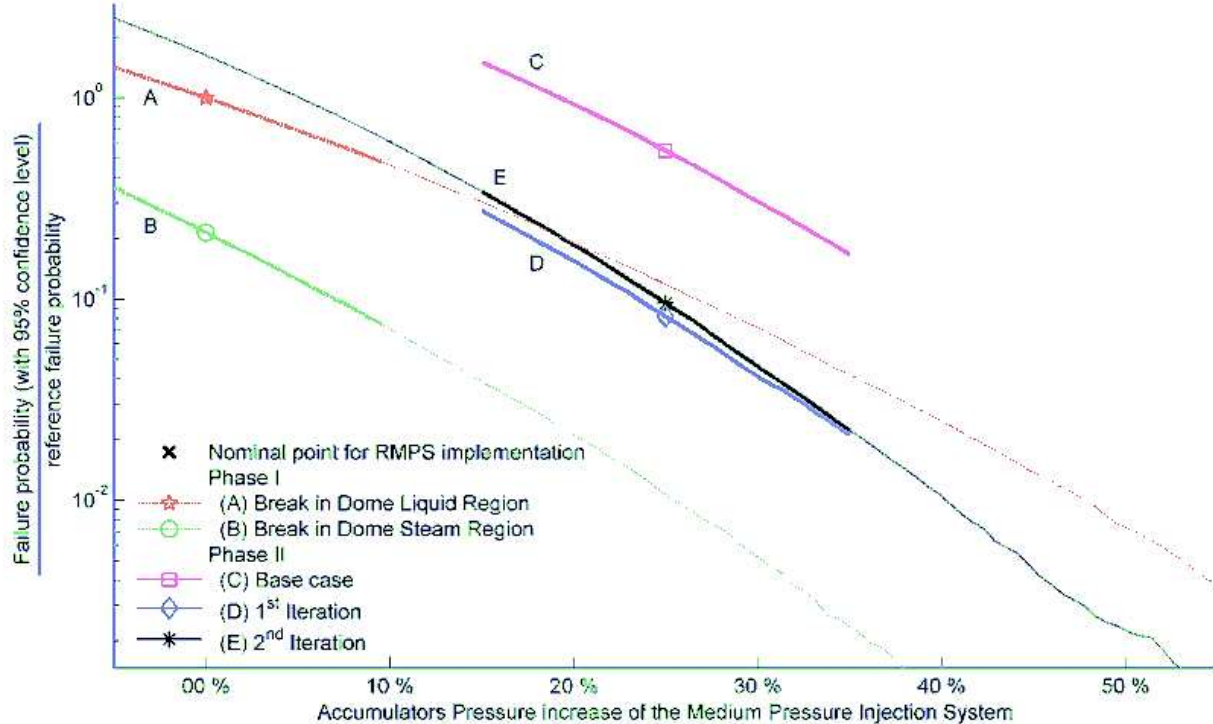


FIG. 93. MPIS accumulator pressure optimization map obtained for each step performed.

In the phase II, it can be seen how the maps converge to the map generated in the previous phase. It can be appreciated that due the conservative assumption made in the technique used to estimate the performance indicator and because the proposed design is more distant to the failure domain boundary, the base shows higher failure probability.

Finally, it can be observed that an increase of a 25% in the design MPIS accumulator’s pressure makes a reduction of one order of magnitude in the failure probability. In order to obtain the optimum value of pressure increase, there is necessary to include the related increase in the investment and the profit obtained through the safety improvement.

Conclusions

The RMPS methodology was improved, tested and used to probabilistically quantify the performance of passive safety systems in order to verify the fulfillment of design criteria.

A sensitive point observed in the methodology is the selection of the performance indicator (i.e. output observable). Its adequacy sustains the results from direct Monte Carlo simulations and the calculations based on surrogate model; therefore, the performance indicator must be strictly linked to the design failure criteria and its definition have to assure that the correct system's phenomenology is encompassed. Then the performance indicator definition is not a straight forward task, and is important to dedicate them a considerably effort.

Finally we can conclude that the improved methodology (RMPS+) was very useful in order to accomplish the objectives proposed for the present work.

6.2. BENCHMARKING PERFORMED BY BARC, INDIA

6.2.1. Details of the ALWR system

The reactor system consists of the following:

- Reactor pressure vessel (RPV);
- Isolation condenser (IC);
- Water pool.

The ALWR system consists of a reactor pressure vessel (RPV) and an isolation condenser (IC) immersed in a pool. The IC is a submerged heat exchanged located at higher elevation than the reactor core, thus establishing a natural circulation loop for decay heat removal. The selected configuration, as well as the operating conditions is typical of those expected for the operation of the IC that is a part of the ALWR design [69]. Figure 94 shows the RELAP5/MOD3.2 nodalization of the system. The transient analyses were started with different initial conditions for the above mentioned parameters and continued for 15000 s.

6.2.2. Application of APSRA for reliability assessment of passive decay heat removal system of ALWR

Step I: Passive system considered—passive decay heat removal system (PDHRS) of ALWR.

Step II: Parameter that may influence the performance of passive decay heat removal systems are considered same as those specified for reliability assessment by RMPS. The parameters are as following:

1. RPV Pressure
2. RPV collapsed level
3. Pool Level
4. Pool initial temperature
5. Non-condensable fraction at the inlet to IC piping
6. Partially open valve in the IC discharge line
7. RPV non-condensable fraction
8. Inclination of the IC piping on the suction side
9. Heat losses piping – IC section
10. Initial condition liquid level- IC tubes, inner side
11. Undetected leakages

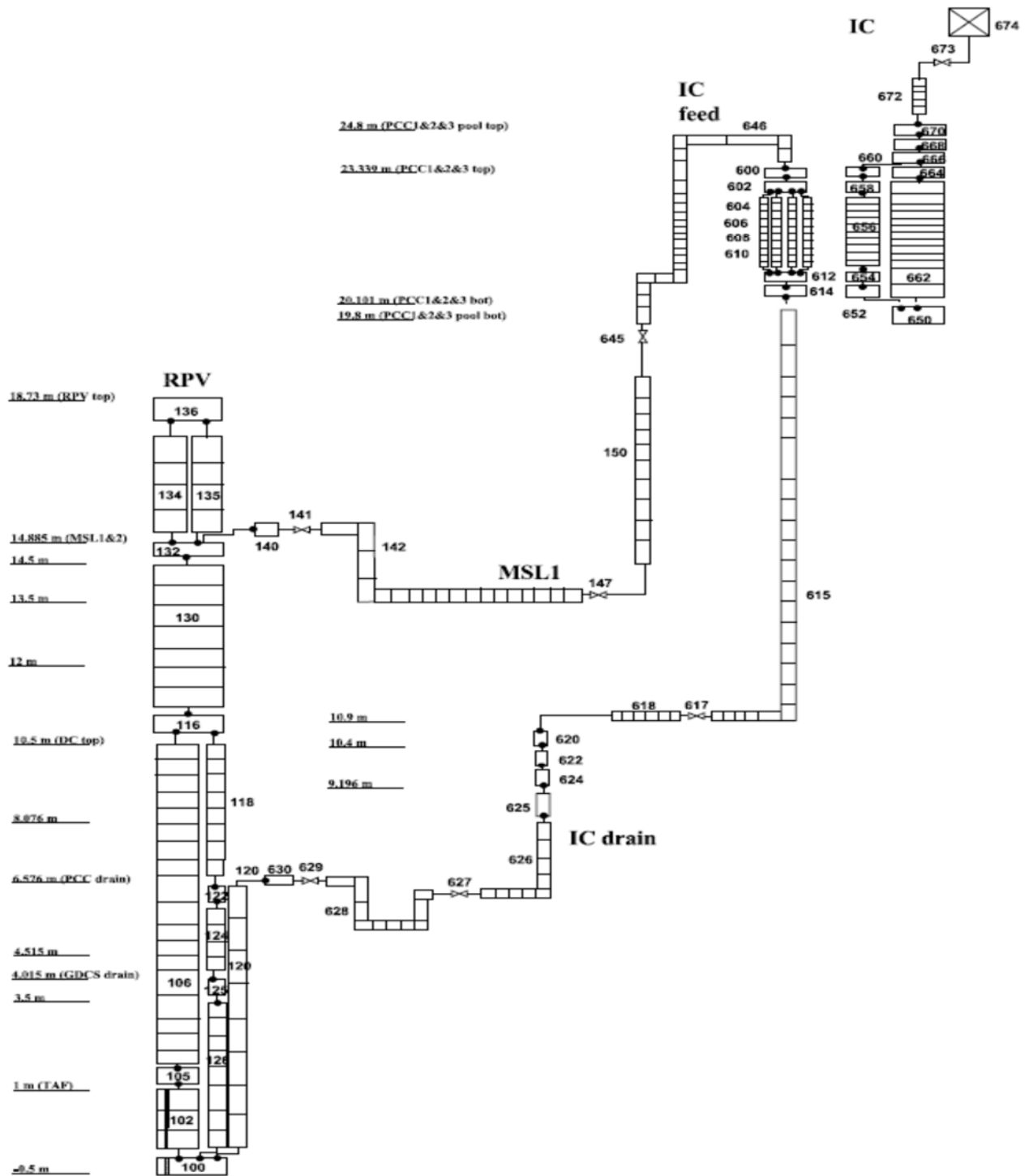


FIG. 94. RELAP 5 Nodalization of the passive system selected for PSA analysis.

Step III: To understand the operational characteristics of the passive system under consideration, the behaviour of system is examined for the effect of various parameters identified in previous step. The computer code RELAP5/MOD3.2 has been used for the purpose. APSRA requires the set of independent process parameters to establish the domain of failure and success. Some of the parameters considered in Step-II may not be completely independent, for example, the system pressure and collapsed level may not be truly independent as system pressure is expected to fall with reduction in system inventory.

Similarly, the non-condensable in RPV and IC line may not be independent as the IC is always in communication with RPV. However, for sake of demonstration of APSRA methodology for reliability assessment of passive systems, the identified parameters and their ranges are considered. The identified parameters are varied over a range as given in Table 20 and Table 21 and their effects on system behaviour are described below:

TABLE 20. RANGE OF DESIGN PARAMETERS OF THE PASSIVE SYSTEM

Parameter		Unit	Nominal value	Range	Discrete Initial value				
P1	RPV pressure	MPa	7	0.2-9	0.2	1	3	7	9
L1	PRV collapsed level	M	8.7	5-12	5	7	8.7	10	12
L3	Pool Level	M	4.3	2-5	24.35				
Tp(0)	Pool initial temperature	K	303	280-368	280, 303, 368				
-	System geometry layout	-	*	Not assigned	-				

TABLE 21. RANGE OF PROCESS PARAMETERS OF THE PASSIVE SYSTEM

Parameter	Discrete values						
X2 non-condensable fraction at the inlet of IC piping (-)2	0	0.01	0.1	0.2	0.5	0.8	1
Q inclination of the IC piping on the suction side (-)3	0	1		5		10	
UL undetected leakage	0	1.0E-5		5.0E-5		10.0E-5	
Initial condition liquid level-IC tubes, inner side	0	50		100			
Partially opened valve in the IC discharge line	0	1	10	50		100	

Sensitivity Study

The system behaviour is assessed in term of system failure criteria postulated for application of RMPS. To analyse the performance of the system, a performance parameter is defined as follows:

$$(Z-Z_{ref})/Z_{ref}$$

where, Z may be either thermal power exchanged across the IC (W_2) or mass flow rate at the IC inlet (G_2) and 'ref' is related to the reference values. The reference values of heat exchanged through and mass flow rate through IC are corresponding to the values at nominal operating conditions.

Effect of RPV Pressure

Pressure of the system is among the most important parameters governing the heat transfer through isolation condenser where flow is established by natural circulation. Figure 95 shows the effect of pressure on normalized thermal power exchanged across IC at pressure 5 MPa

and 9 MPa, whereas corresponding normalized mass flow rate through IC is shown in FIG. 96. It can be seen that both the parameters depend strongly on the RPV pressure.

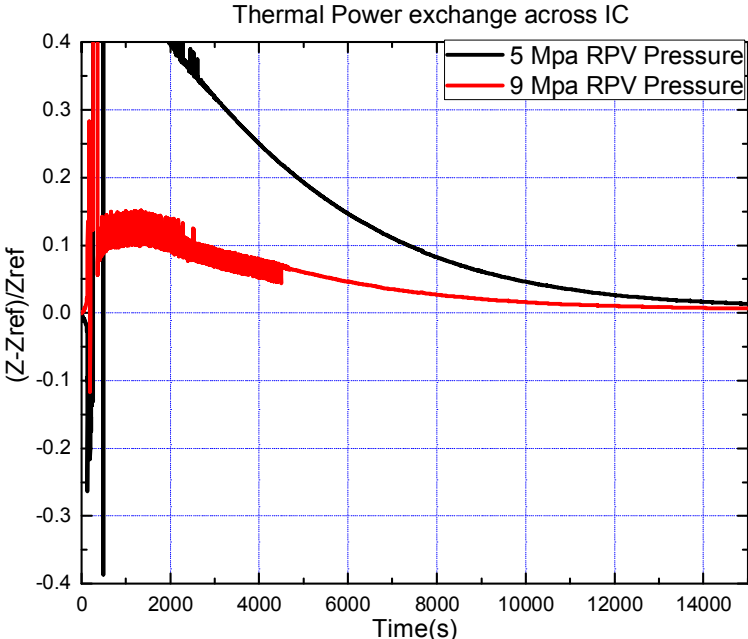


FIG. 95. Thermal power exchange across the IC at different pressures.

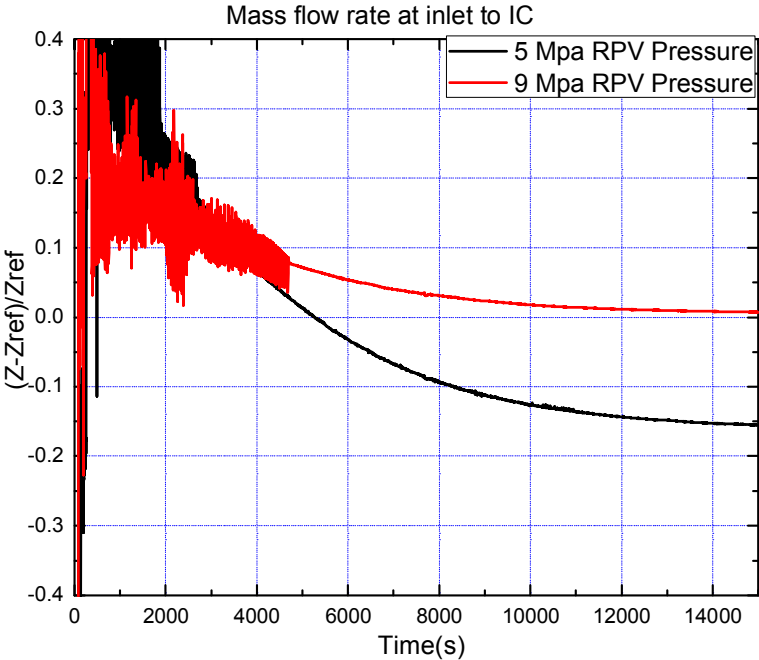


FIG. 96. Mass flow rate inlet to IC at different pressures.

Effect of RPV collapsed level

RPV Collapsed level is another design parameter that could have effect on passive system behaviour. It can be seen in the FIG. 97 and FIG. 98 that collapsed level has significant effect on system behaviour.

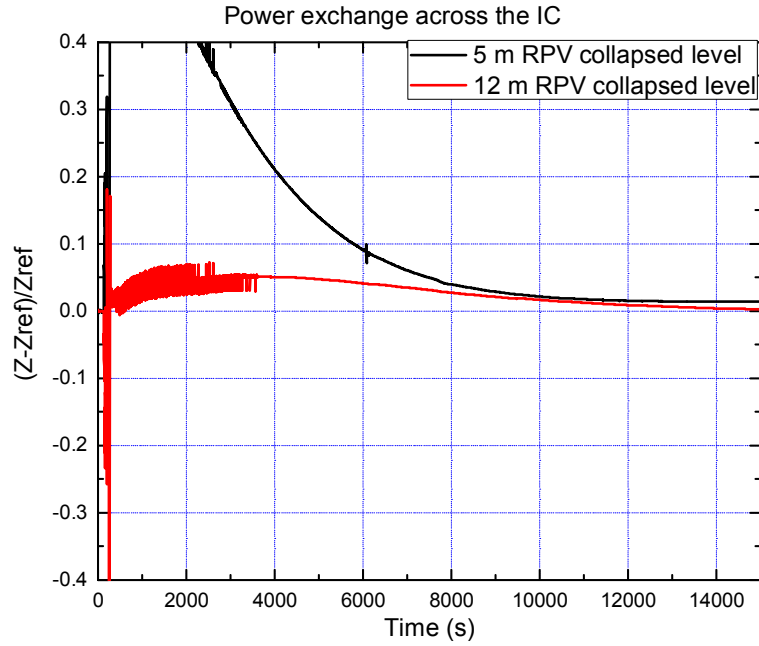


FIG. 97. Thermal power exchange across the IC at different RPV level.

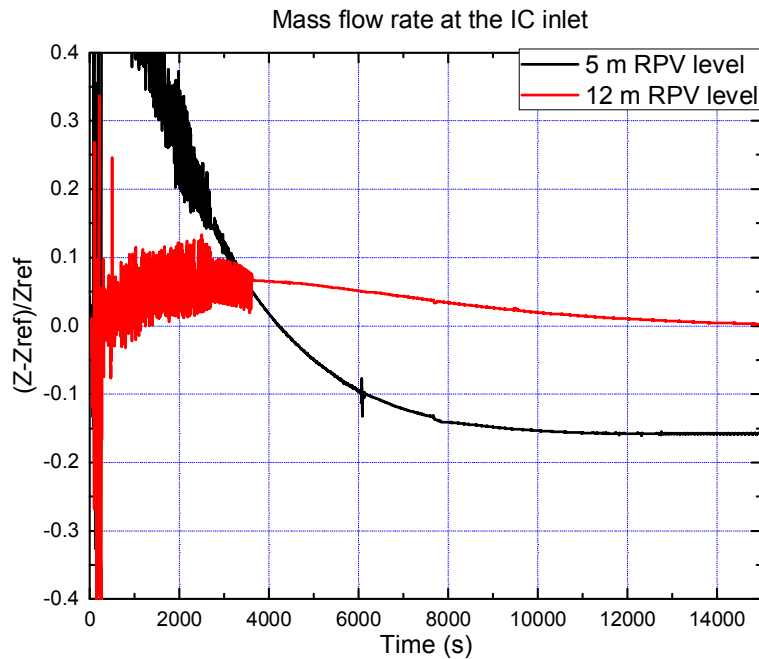


FIG. 98. Mass flow rate inlet to IC at different RPV level.

Effect of Pool Level

Water pool forms the heat sink for the system. The decay heat is transferred to the pool using submerged IC. As the pool water level reduces, the heat transfer capability of IC gets impaired. Figures 99 and 100 show that with reduced pool level thermal power exchanged through IC as well as mass flow rate through it are significantly reduced particularly during the initial phase of transient.

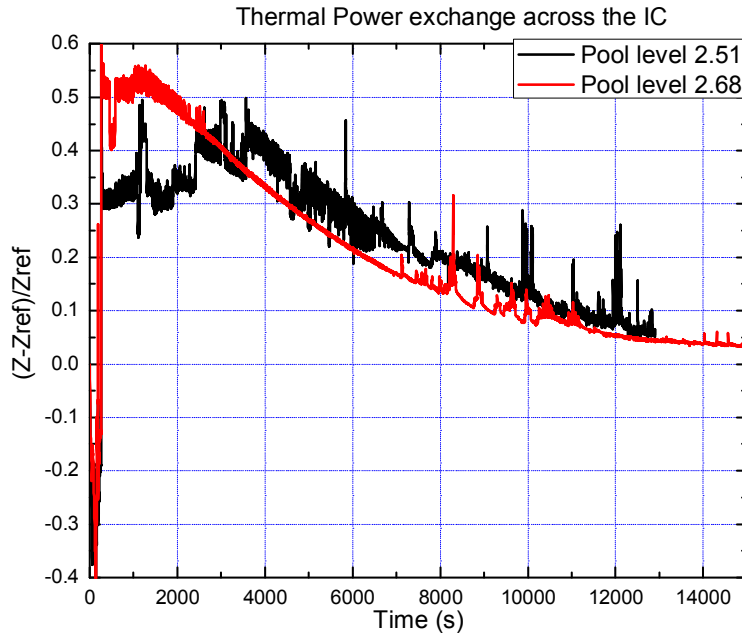


FIG. 99. Thermal power exchange across the IC at different Pool level.

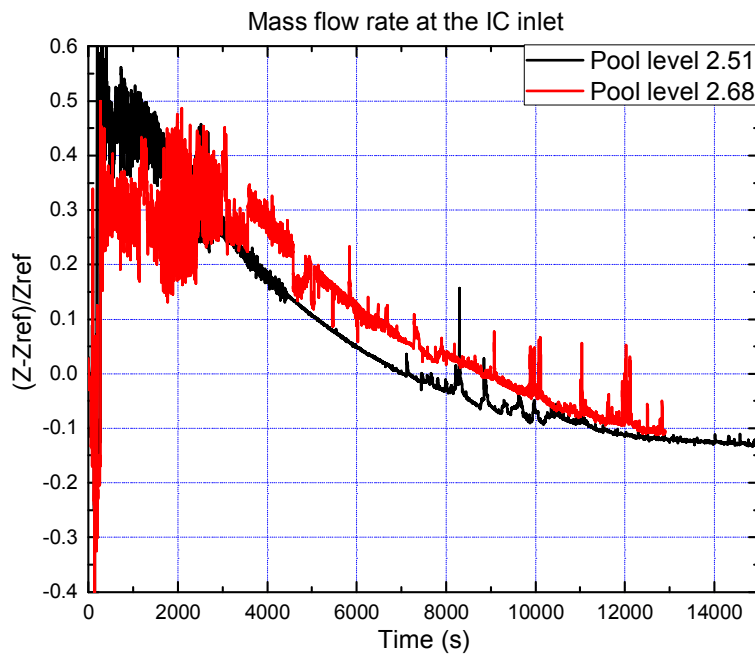


FIG. 100. Mass flow rate inlet to IC at different Pool level.

Effect of Pool initial temperature

The initial temperature of the water pool is very important for performance of passive decay heat removal. Figures 101 and 102 show that with rise in pool initial temperature, thermal power exchanged through IC as well as mass flow rate through are substantially reduced.

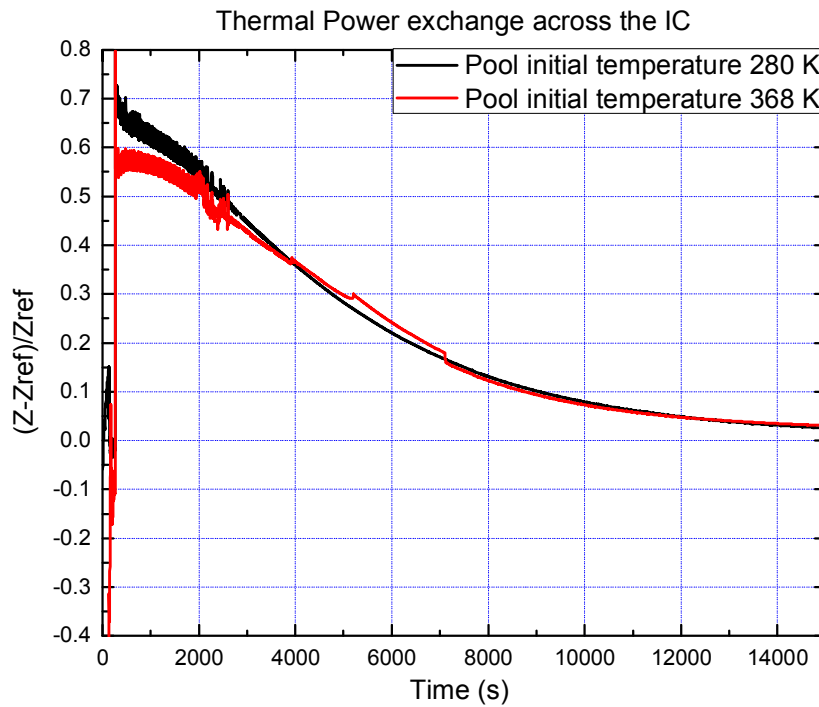


FIG. 101. Thermal power exchange across the IC at Pool initial temperature.

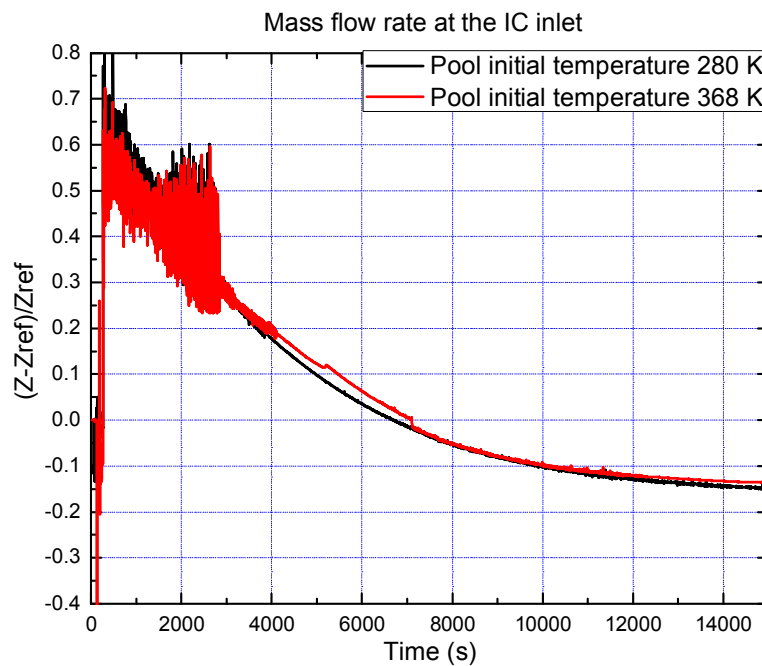


FIG. 102. Mass flow rate inlet to IC at Pool initial temperature.

Effect of Non-condensable fraction at the inlet to IC piping

As the mode of heat transfer inside the IC tubes is condensation of steam, the presence of non-condensable in the system could severely degrade the heat transfer performance. As the RPV and IC are always in communication, the effect of non-condensable can be appropriately captured by considering the non-condensable in IC alone which is at higher elevation than

RPV. Over a period of time, the non-condensable from RPV will flow to IC, thus there may be only some delay in degradation of heat transfer if non-condensable are considered in RPV alone. Hence, for the purpose of this analysis, presence of non-condensable is considered in IC only. The effect of presence of non-condensable in IC can be seen in FIG. 103 and FIG. 104.

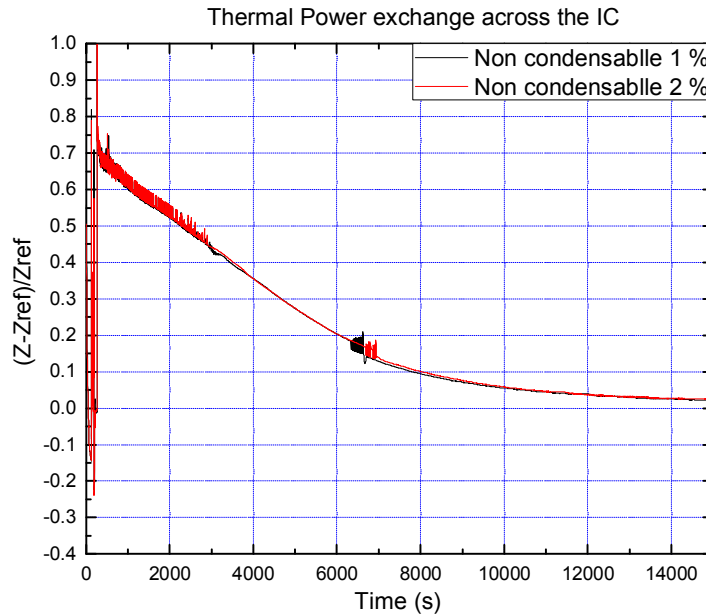


FIG. 103. Thermal power exchange across the IC at different non condensable percentage.

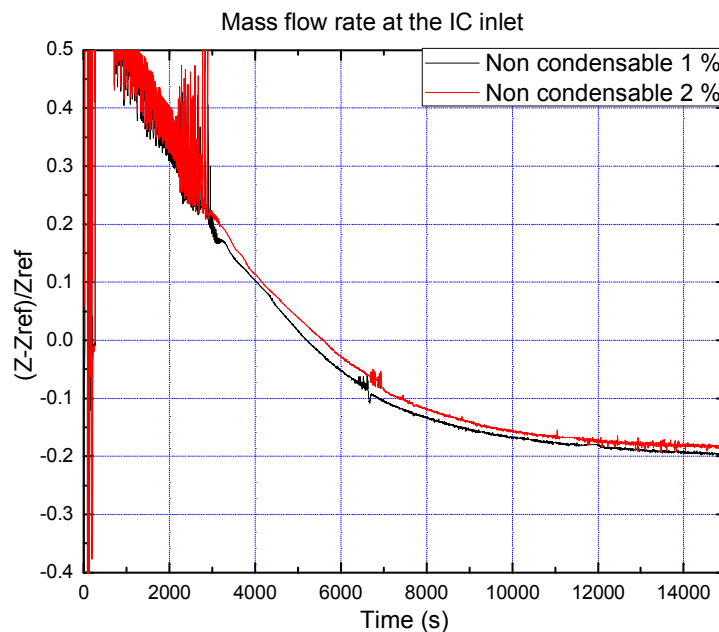


FIG. 104. Mass flow rate inlet to IC at different non condensable percentage.

Effect of Partially open valve in the IC discharge line

The establishment of required natural circulation flow through IC requires the unobstructed return path for condensate from IC to the RPV. Hence, the system performance also depends on the opening of valve downstream of IC in the condensate return line. The effect of valve opening can be seen in the FIG. 105 and FIG. 106.

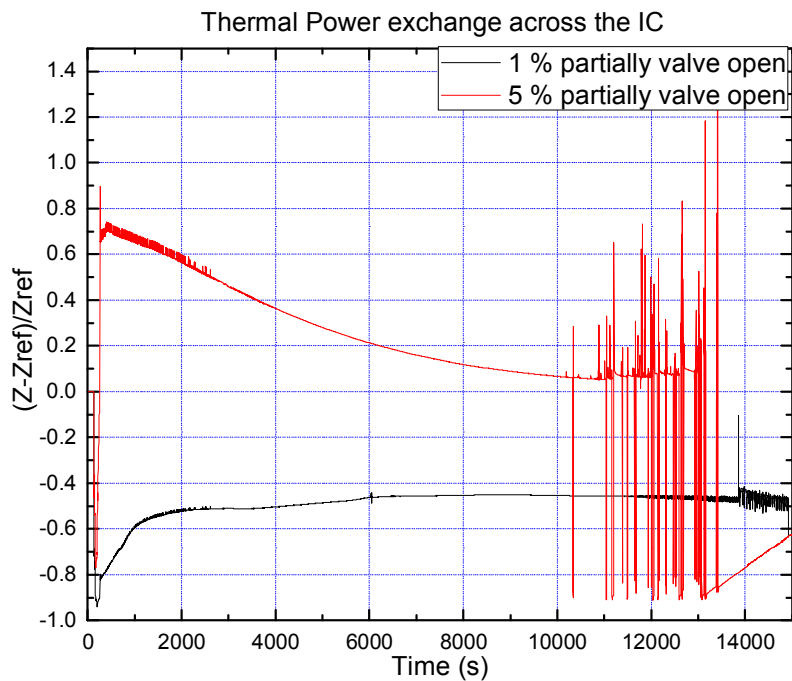


FIG. 105. Thermal power exchange across the IC at different valve opening.

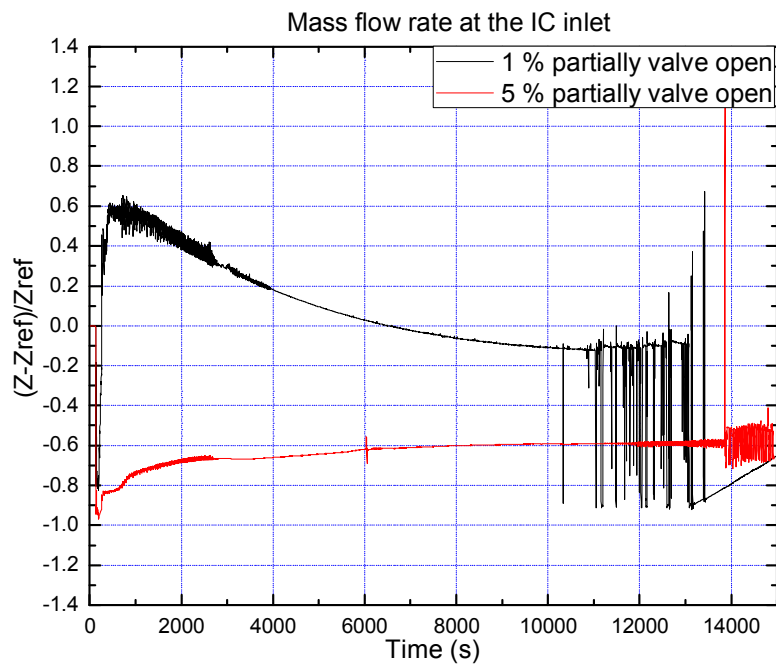


FIG. 106. Mass flow rate inlet to IC at different valve opening.

Effect of Inclination of the IC piping on the suction side

Figure 107 and figure 108 show that inclination of pipe does not have substantial effect on the performance. Also, variability associated with pipe inclination can be neglected as the reactor components are fabricated with narrow tolerances and undergo stringent quality checks.

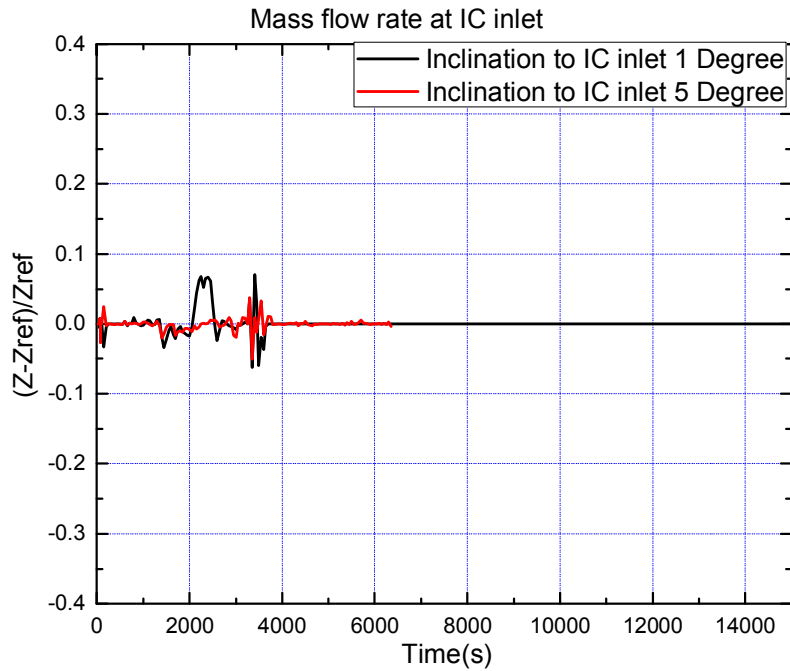


FIG. 107. Thermal power exchange across the IC at different inlet inclination.

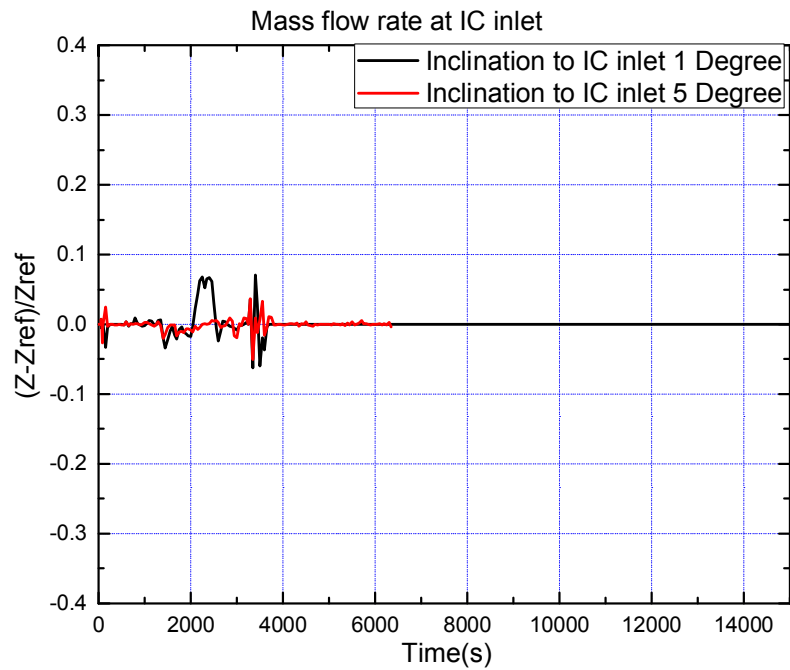


FIG. 108. Mass flow rate inlet to IC at different inlet inclination.

Effect of Heat losses piping – IC section

Heat losses from piping are also not critical to the performance of the system, as the heat losses being considered are very small compared to the decay heat (FIG. 109 and FIG.110).

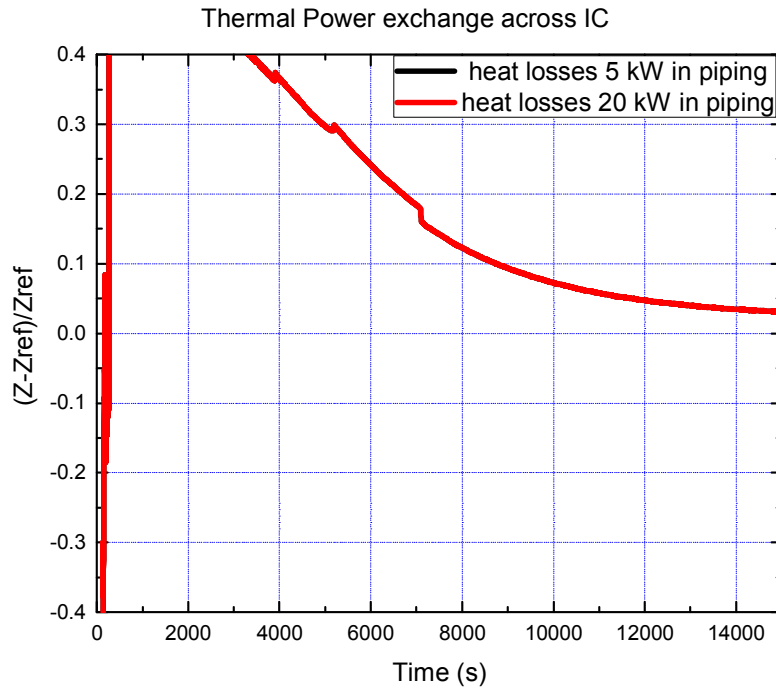


FIG. 109. Thermal power exchange across the IC at different heat loss at piping.

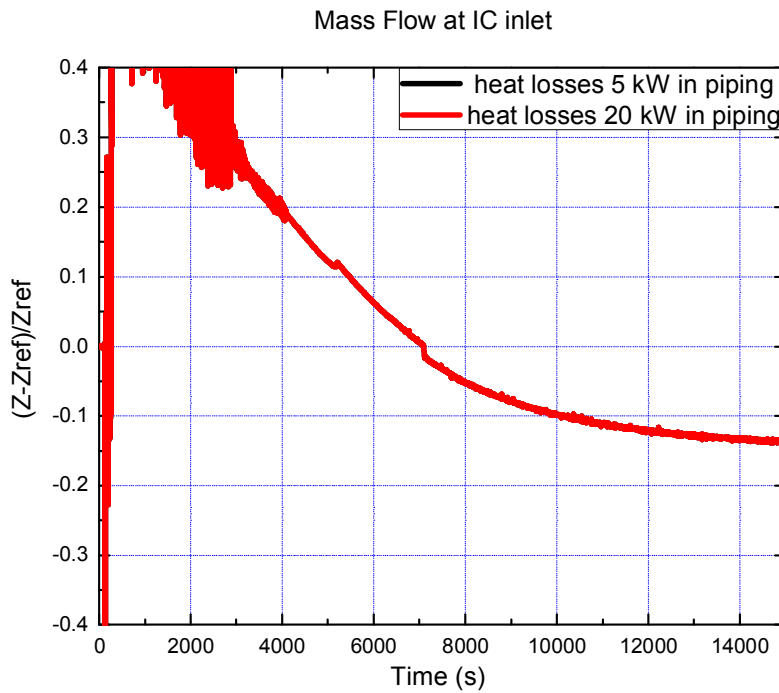


FIG. 110. Mass flow rate inlet to IC at different Heat loss at piping.

Effect of Initial liquid level- IC tubes

Although the IC tubes may have different water level at the initiation of transient, its effect on the system behaviour is negligible, because once the IC valves are closed, the water drains back to RPV (FIG. 111 and FIG. 112).

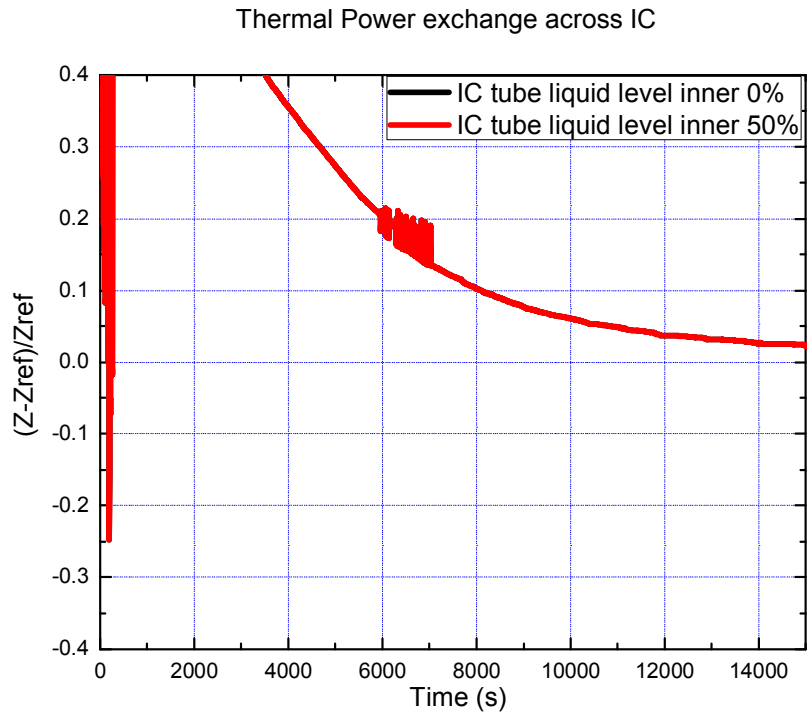


FIG. 111. Thermal power exchange across the IC at different liquid level- IC tubes.

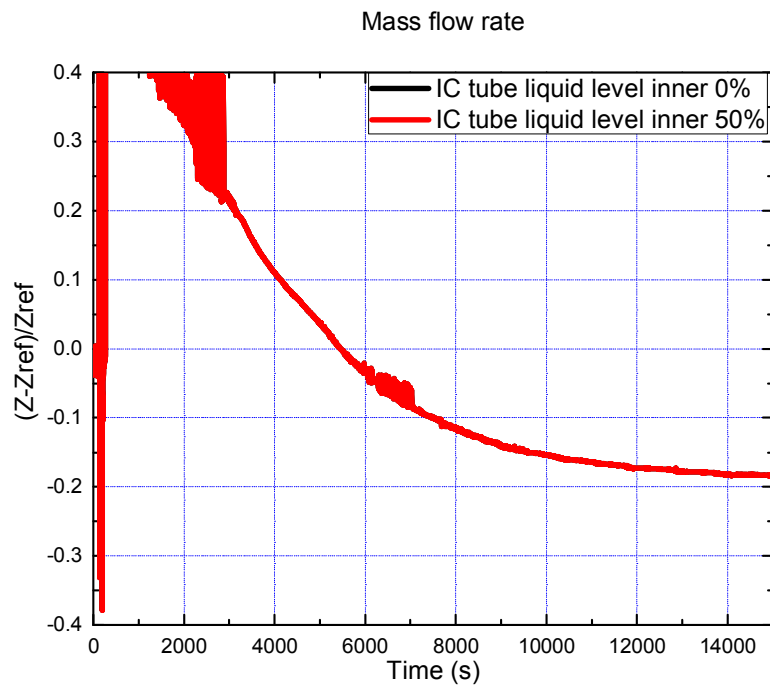


FIG. 112. Mass flow rate inlet to IC at different liquid level- IC tubes.

Effect of Undetected leakages

Effect of small undetected leakage on the performance is as shown in FIG. 113 and FIG. 114. It was found that undetected leakages do not have significant effect on system performance.

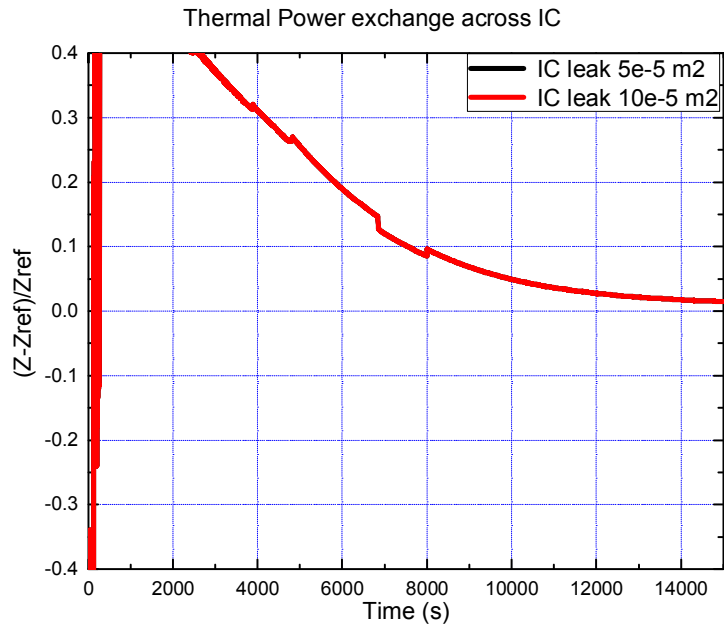


FIG. 113. Thermal power exchange across the IC at different IC tubes leak.

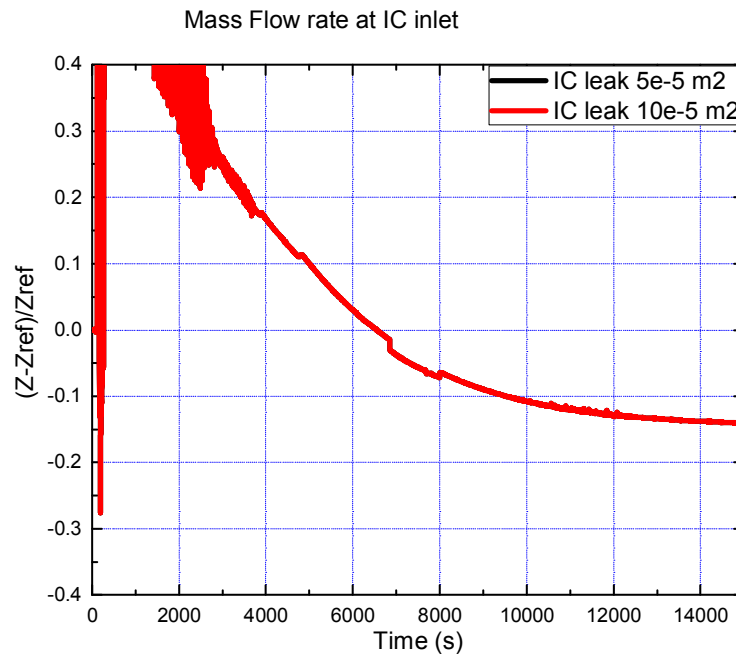


FIG. 114. Mass flow rate inlet to IC at different IC tubes leak.

Identification of failure

Failure criterion followed for this analysis is considered same as that used for reliability assessment by RMPS, given as:

$$(Z-Z_{ref}) / Z_{ref} < (-0.2) \text{ continuously for a time interval greater than } 100s$$

Step IV: Key parameters causing the failure

The assessment of operational characteristic in the previous step reveals that the key operating parameters that may contribute to the failure of the system are as following:

1. RPV Pressure;
2. Pool Level;
3. Pool initial temperature;
4. RPV collapsed level;
5. Non-condensable fraction at the inlet to IC piping;
6. Partially open valve in the IC discharge line.

The system behaviour is analysed by considering the variation of above parameters in the prescribed range to establish the set of condition which will lead to the failure of system consistent with failure criteria. To arrive at the failure domain, initially the parameters are varied one at a time to identify the threshold value for failure. However, deviation of many parameters from their nominal values can be more detrimental to the performance of system, hence, more failure point are established considering the simultaneous variation of parameters from their nominal values. Table 22 shows summaries of failure threshold of various important key parameters causing failure of the system.

TABLE 22. FAILURE THRESHOLD WITH VARIATION OF VARIOUS KEY PARAMETERS

Pressure (MPa)	Pool level (m)	Pool initial temperature (K)	Valve opening %	Non condensable at IC inlet %	RPV level (m)
2.5	4.3	303	100	0	8.7
7	2.33	303	100	0	8.7
7	4.3	325	100	0	8.7
7	4.3	303	1	0	8.7
7	4.3	303	100	10	8.7
5	2.35	303	100	0	8.7
3	3.2	303	100	0	8.7
3	4.3	368	100	0	8.7
5	4.3	315	100	0	8.7
7	2.68	325	100	0	8.7
5	2.68	303	100	5	8.7
5	4.3	315	100	5	8.7
7	2.68	325	100	5	8.7
3	4.3	303	100	0	12

Step V: Failure surface generation

The loci of all failure points, shown in Table 22, can be joined to generate the failure surface in terms of RPV pressure, pool initial temperature and pool level, as shown in FIG. 115. However, consideration of other critical parameters like non-condensable in IC line, partial valve opening and RPV collapse level, results in a modified failure domain as represented in

FIG. 116, showing reduction in success zone. FIG. 117 shows comparison of failure surfaces considering three and six parameters simultaneously.

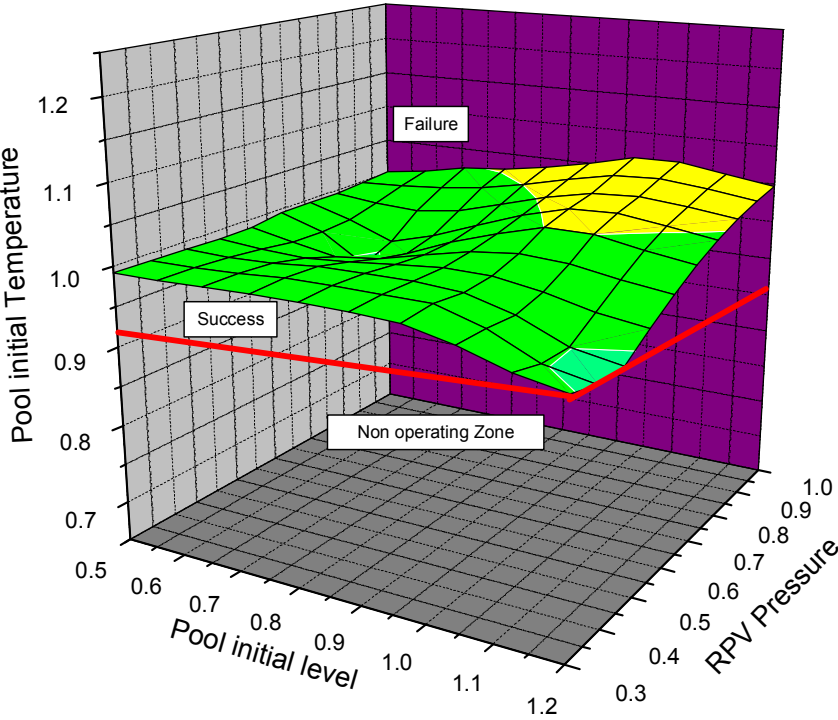


FIG. 115. Failure Surface with all three parameter.

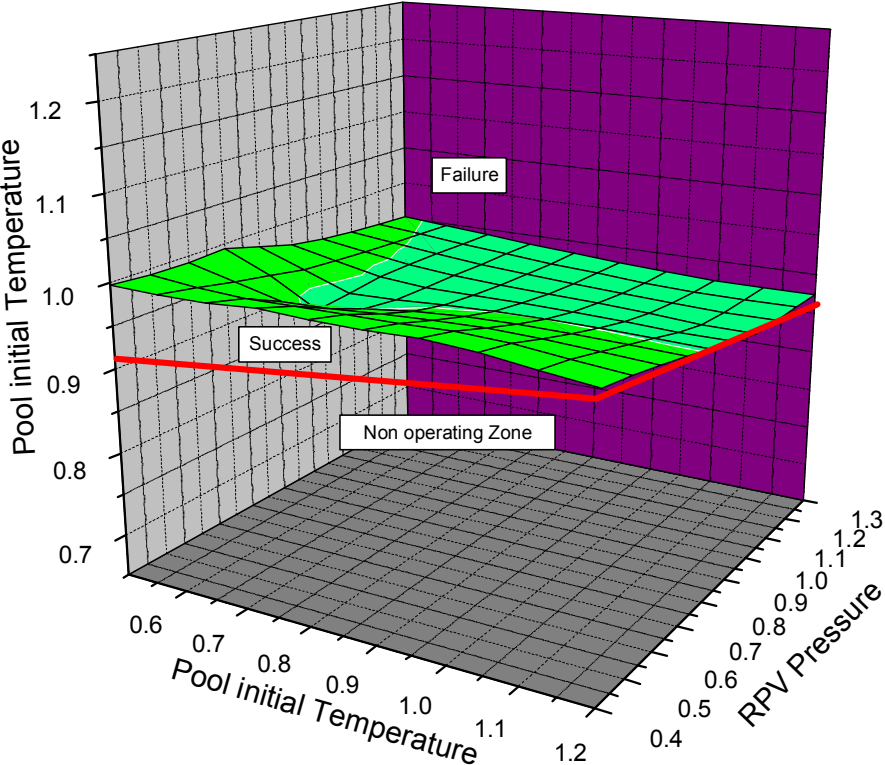


FIG. 116. Failure Surface with all six parameter.

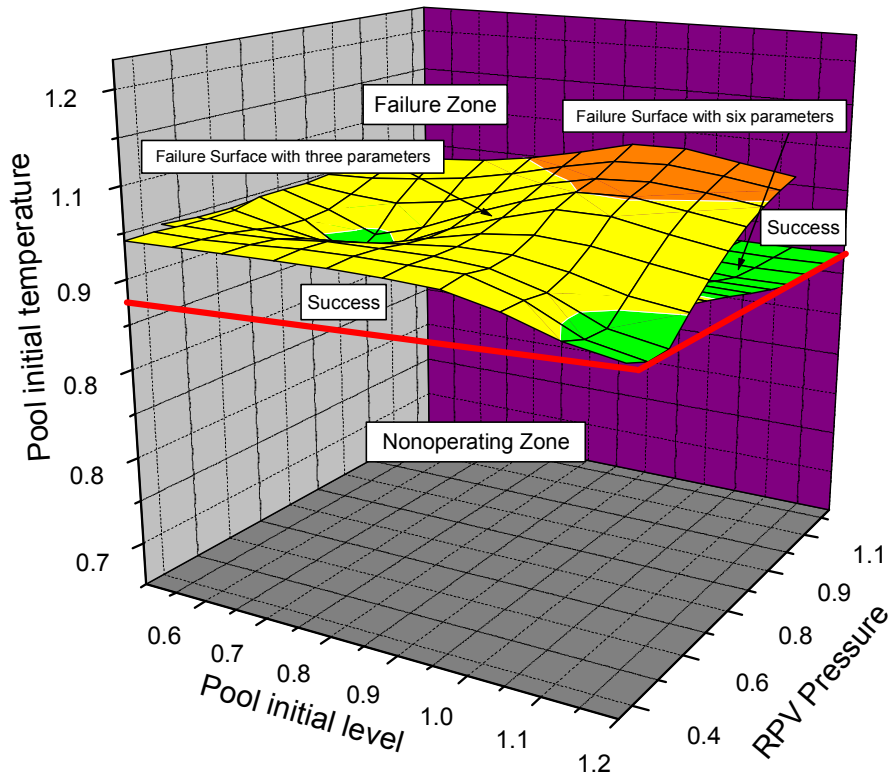


FIG. 117. Comparison of failure surface with and without critical parameters.

Step VI: Root diagnosis

The root causes for the variation of the process parameters are not known for ALWR, hence, the causes for failure are assumed for demonstration of APSRA methodology. The failure probability of the decay heat removal system depends on the variation of various key process parameters as identified in step IV. The fault tree for deviation of process parameters is as shown from FIG. 118 to FIG. 122. Each of the key parameter deviation was analysed for their cause using FMEA as shown in table 23.

TABLE 23. FMEA FOR PARAMETER DEVIATIONS IN IC SYSTEM

No.	Deviation	Causes
1	RPV Low pressure	<ul style="list-style-type: none"> • Pressure controller failure • Pressure transmitter failure • IC tube leakage
2	High RPV level	<ul style="list-style-type: none"> • Mal functioning of Level Control Valves • RPV level transmitter failure • RPV level controller failure
3	Low pool level	<ul style="list-style-type: none"> • Failure of level transmitter • Failure of level controller • failure of makeup circuits
4	Make up circuit failure	<ul style="list-style-type: none"> • Failure of valves

No.	Deviation	Causes
		<ul style="list-style-type: none"> • Failure of pump • Check valve failure
5	High Pool Temperature	<ul style="list-style-type: none"> • Pool cooling system failure (Heat exchanger failure)
6	Presence of non-condensable gases	<ul style="list-style-type: none"> • Failure of Vent valves

Fault tree modelling was carried out for following enveloping combinations of parameter deviations:

- (i) Decrease in pool level;
- (ii) Increase in pool temperature;
- (iii) Opening of valve;
- (iv) Presence of non-condensables in IC >10%;
- (v) Low pressure in RPV along with decrease in pool level;
- (vi) Low pressure in RPV along with increase in pool temperature;
- (vii) Low pressure and high level in RPV;
- (viii) Decrease in pool level along with increase in pool temperature.

The scenario of ‘low pressure in RPV’ resulting in system failure occurs below 2.5 MPa, seems to be unrealistic and hence not modelled as a single event. The fault trees for all the above combinations are given below.

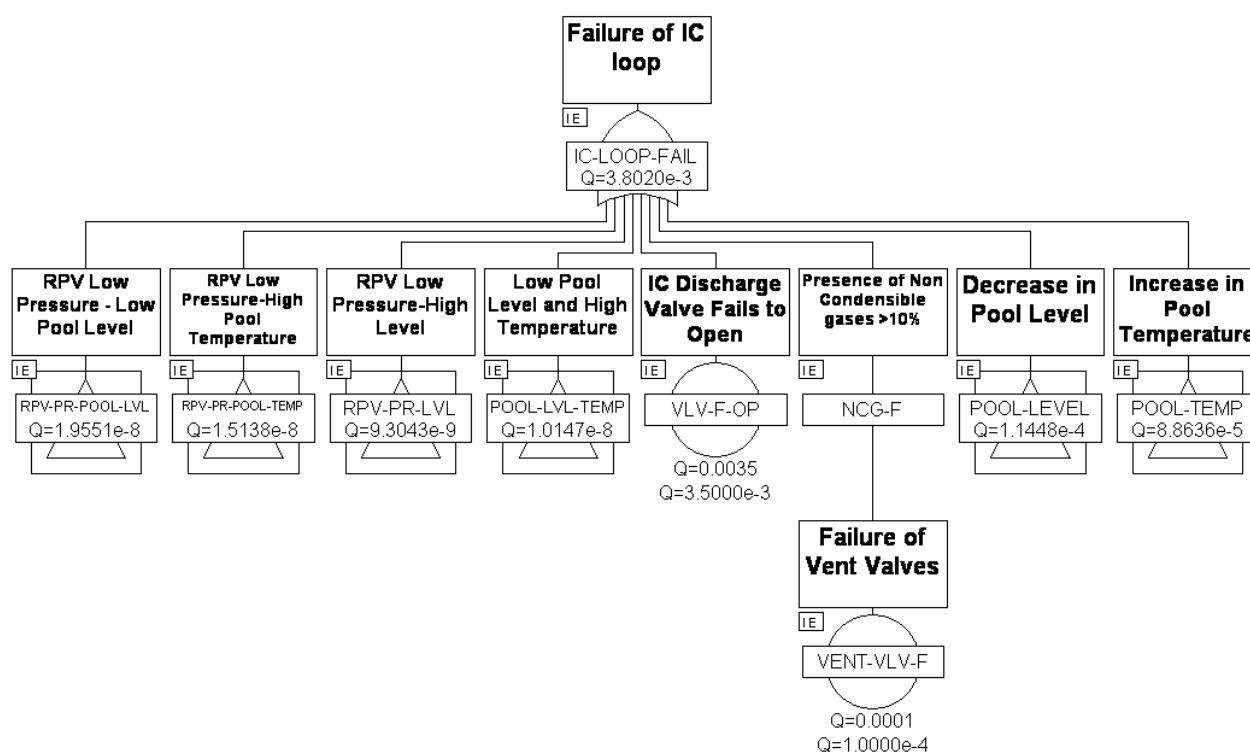


FIG. 118. Fault Tree for deviation of process parameters.

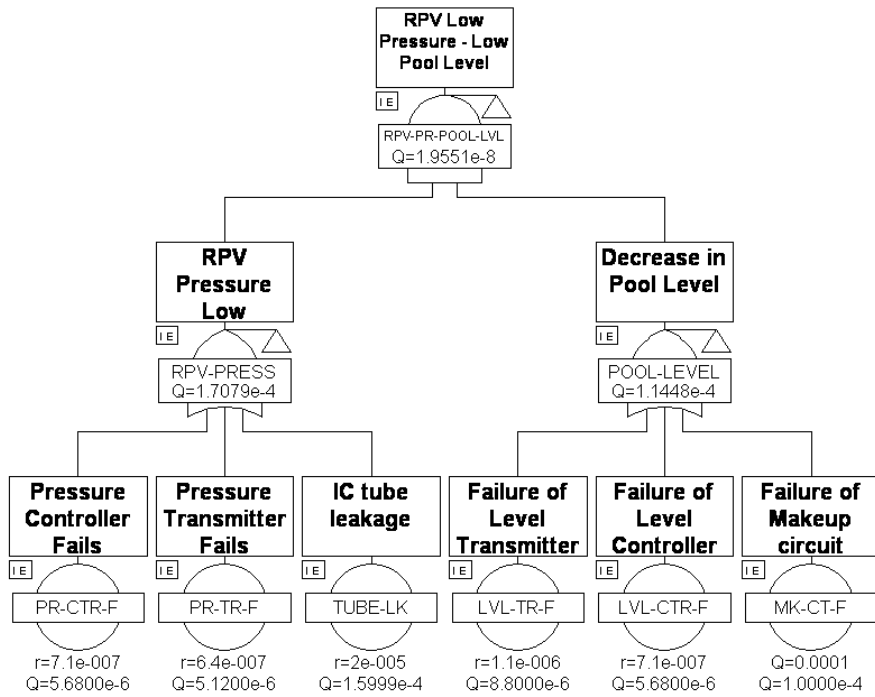


FIG. 119. Fault Tree for Low RPV pressure and low pool level.

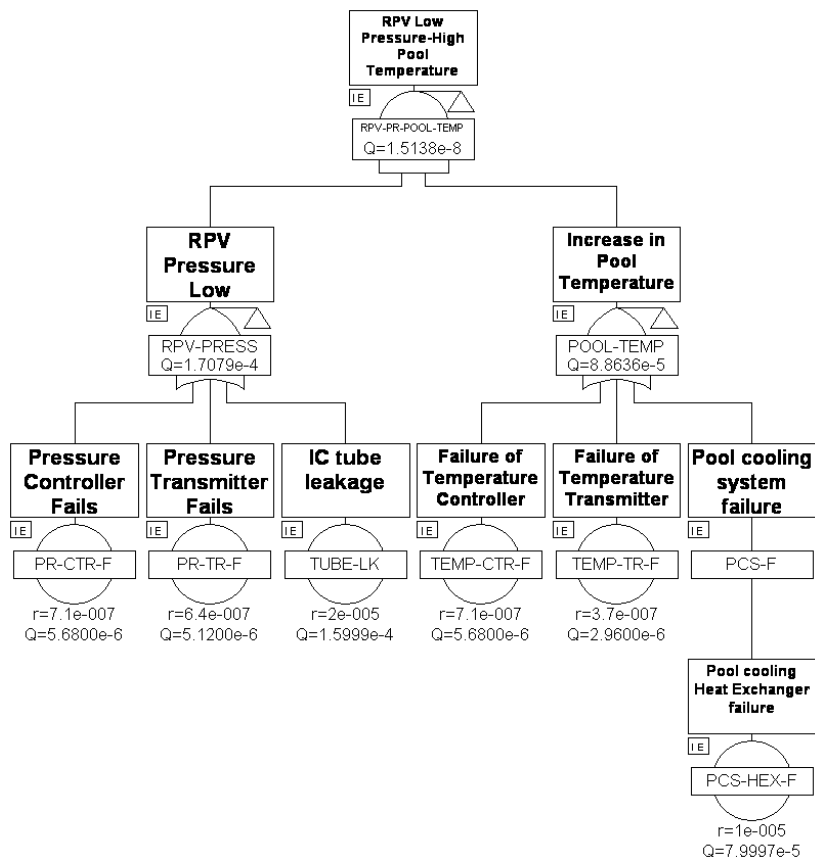


FIG. 120. Fault tree for low RPV pressure and high pool temperature.

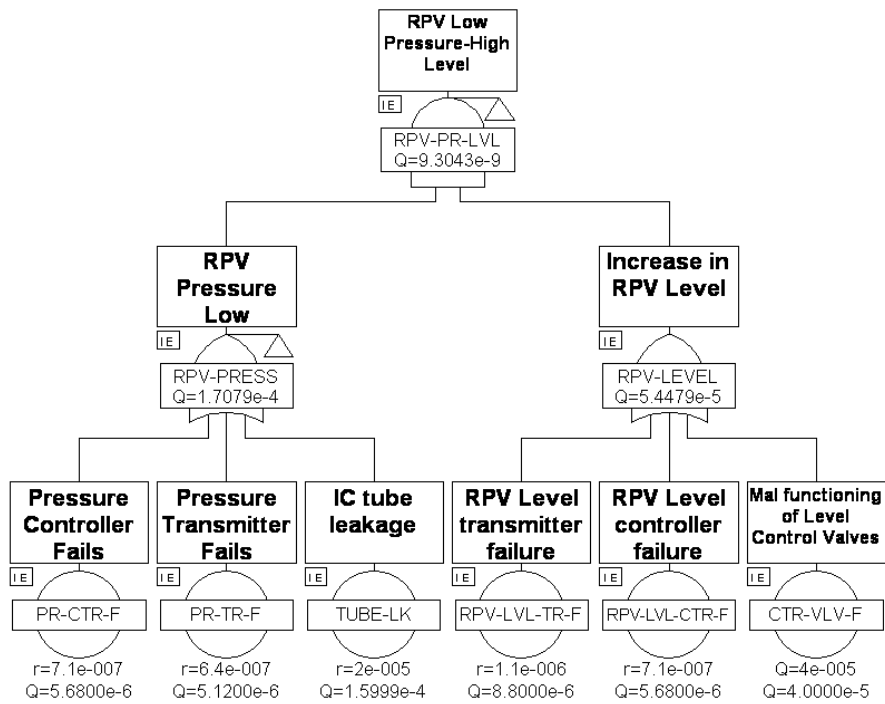


FIG. 121. Fault tree for low RPV pressure and high RPV level.

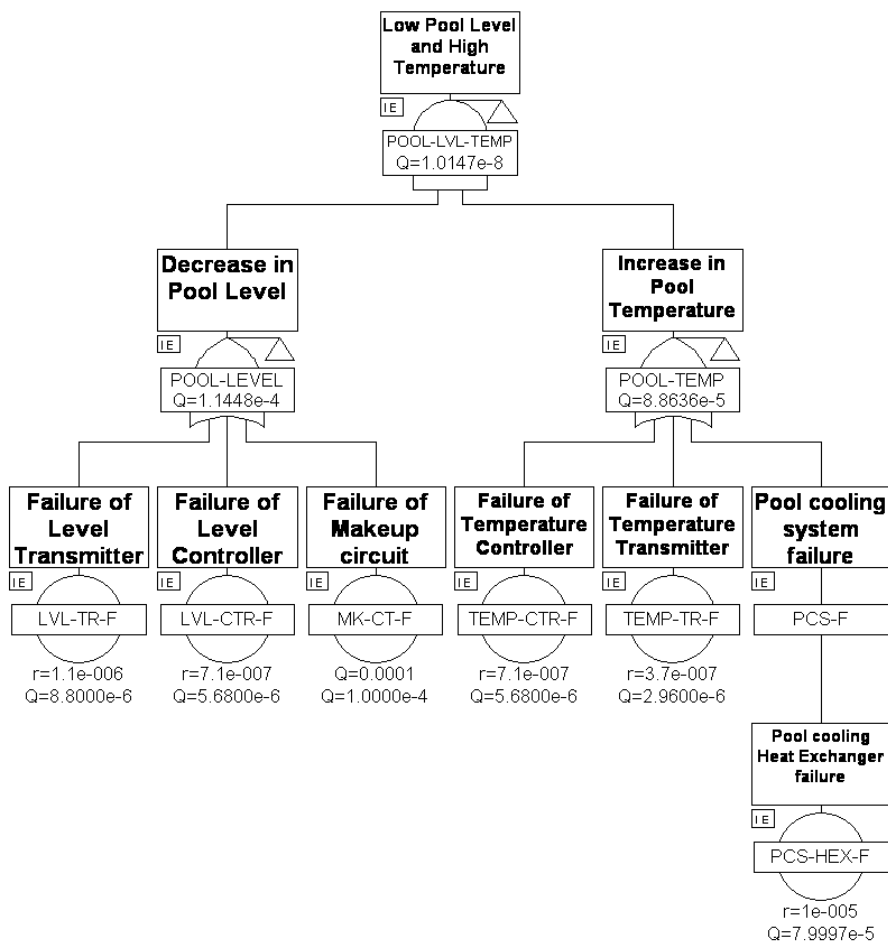


FIG. 122. Fault tree for low pool level and high pool temperature.

Step VII: Evaluation of failure probability of components causing the failure

The failure frequency of the system is calculated based on the generic data [70] available for components governing variation of key process parameters. The analysis shows that the unavailability of decay heat removal system to perform successfully is found to be $3.8E-03/\text{demand}$.

Conclusion

Evaluation of passive system reliability is a challenging task. It involves a clear understanding of the operation and failure mechanism and failure criteria for the system which the designer must identify prior to prediction of its reliability. Besides, applicability of the existing best estimate codes to the reliability assessment of passive systems is neither proven nor understood enough due to lack of sufficient plant/experimental data. Thus, assessing the uncertainties of the best estimate codes when applied to passive system safety analysis further add to the complexity. However, the best estimate code RELAP5/MOD3.2 has been used to demonstrate the application of APSRA methodology for reliability assessment of passive decay heat removal system of ALWR. The failure frequency is found to be $3.8E-3/\text{demand}$.

6.3. BENCHMARKING PERFORMED BY ENEA, ITALY

6.3.1. Approach based on independent failure modes

The primary step of this approach is the identification of system modes of failure and corresponding drivers, referred to as critical parameters.

In general the reliability of passive systems should be seen from two main aspects:

- systems/components reliability (e.g. piping, valves)
- physical phenomena reliability (e.g. natural circulation stability)

The first facet calls for well-engineered safety components with at least the same level of reliability of the active ones.

The second aspect is concerned with the way the natural physical phenomena operate in a particular system and the long-term effect of the surrounding on their performance/stability. It calls for the identification of modes/causes of failures and assessment of the relative uncertainties.

A qualitative analysis is required in order to identify all the potential failure modes affecting the system and their consequences associated with the passive system operation. The aim of this analysis is to identify the parameters critical for the natural circulation performance/stability, allowing associating to each of the failure modes a proper parameter direct indicator of the failure cause.

Thus well-structured procedures, commonly used for hazard identification in risk analysis, like FMEA and hazard and operability (HAZOP) for instance are considered, as suitable means for such an analysis. These approaches are presented and discussed and the relative results compared.

6.3.1.1. Failure mode and effect analysis (FMEA)

FMEA is a bottom-up procedure conducted at component level by which each failure mode in a system is investigated in terms of failure causes, preventive actions on causes, consequences on the system, corrective/preventive actions to mitigate the effects on the system and eventually classification according to its severity

The FMEA approach application implies the introduction, in addition to mechanical components of the system (piping, drain valve, heat exchanger), of a 'virtual' component - which refers to the characteristic phenomenology for the passive system, unidentifiable as a classic component - recognized as natural circulation and its evaluation in terms of potential 'phenomenological' factors (the list of these includes e.g. non-condensable gas build-up, thermal stratification, surface oxidation, cracking, etc.), the consequences of which can impair or stop the natural circulation, and the identification of the relative critical parameters (non-condensable fraction, undetected leakage, heat loss, etc.).

Failure modes are ranked according to a severity index related to the estimated range of frequency of occurrence of the fault, in accordance with Table 24, which categorizes the events by likelihood of occurrence.

In Table 25 a sample of FMEA sheet is reported, together with the assessed critical parameters associated to the failure modes and the tentatively assigned severity ranks. Reflecting the qualitative nature of the present analysis, ranking process is based upon a sort of 'rough' subjective/engineering judgment, aiming at providing a preliminary classification of the events, following the grading scheme stated in Table 24.

TABLE 24. EVENT CATEGORIZATION BY EVENT LIKELIHOOD OF OCCURRENCE

Category	Events likelihood	Frequency of occurrence
I	Operational Events	More than one per year
II	Likely Events	10^{-2} -1/y
II	Unlikely Events	10^{-4} - 10^{-2} /y
IV	Extremely Unlikely Events	10^{-6} - 10^{-4} /y

The analysis pointed out several factors leading to disturbances in the IC system; the list of these includes:

- Unexpected mechanical/thermal loads, challenging the primary boundary integrity;
- Heat exchanger plugging;
- Mechanical component malfunction, i.e. drain valve;
- Non-condensable gas build-up;
- Heat exchange process reduction: surface oxidation, thermal stratification, piping layout, thermal insulation degradation, etc.

Finally, as previously assumed, this qualitative analysis points out a set of critical parameters affecting the natural convection reliability and to be accounted for in further probabilistic analysis:

- Non-condensable fraction;
- Undetected leakage;
- POV (partially opened valve) in the discharge line;

- Heat loss;
- Piping inclination;
- HX plugged pipes.

6.3.1.2. Hazard and operability (HAZOP) studies

The HAZOP approach is taken into consideration in order to compare and 'endorse' the results coming from the FMEA analysis. This procedure considers any parameters characteristic of the system (among pressure, temperature, flow rate, heat exchanged through the HX, opening of the drain valve) and by applying a set of 'guide' words, which imply a deviation from the nominal conditions as for instance undesired decrease or increase, determines the consequences of operating conditions outside the design intentions.

In Table 26 some of the HAZOP sheets are reported.

6.3.1.3. Results

The main difference between the two approaches consists in the fact that while the former is performed at component level, the latter is conducted on a parameter basis (e.g. flow, temperature). For this reason the HAZOP application seems to be more suitable for functional reliability assessment as defined earlier.

Looking at the tables the HAZOP analysis confirms what assessed in the previous FMEA analysis: in fact in general the possible causes of the deviation of the characteristic parameter from the nominal conditions, which result in the natural circulation impairment, imply the occurrence of the aforementioned failure modes individuated by the previous analysis.

TABLE 25. FMEA TABLE FOR IC SYSTEM

Component	Failure Mode	Causes	Prev. Actions on Causes	Consequences	Corr./Prev. Act. on Consequences	Comment	Severity Rank
System piping	Rupture	Material defects and aging; Corrosion; Abnormal operation conditions; Vibrations; Local. Stresses; Impact of heavy loads (missile)	Adequate welding process quality; Water chemistry control; In Service inspect; Design against missile generation	LOCA in the Drywell; Instantaneous loss of natural circulation; Emptying of the circuit; Loss of heat removal capability; Loss of reactor coolant inventory	Isolate the breached loop; Safety relief valves actuation; Automatic reactor depressurisation; Gravity Driven Cooling System actuation;	Includes both steam line and drain line Critical Parameter: Undetected Leakage	V
	Leak	Material defects and aging; Corrosion; Abnormal operating conditions; Vibrations; Local. stresses	Adequate welding process quality; Water chemistry control; In Service inspect.	Small LOCA in the Drywell; Slow emptying of the circuit and natural circulation arrest for long periods of operation; Reduced heat removal capability	Leak monitoring; Isolate the breached loop; Safety relief valves actuation	Critical Parameter: Undetected Leakage	III
Tube Bundle of the heat exchangers of the IC	Single pipe rupture	Wearing due to vibration and corrosion	Preventive maintenance; Water chemistry control; Leak monitoring	Release of primary water to the pool; Slow emptying of the circuit and natural circulation arrest for long periods of operation; Reduced heat removal capability	Flow monitoring; Isolate the breached loop; Safety relief valves actuation	Critical Parameter: Undetected Leakage	IV
	Multiple pipe rupture	Wearing due to corrosion, vibration and pressure transient	Preventive maintenance; Water chemistry control; Leak monitoring	Release of primary water to the pool; Natural circulation stop; Emptying of the circuit;	Isolate the breached loop; Safety relief valves actuation; Automatic reactor depressurization;	Critical Parameter: Undetected Leakage	V

Component	Failure Mode	Causes	Prev. Actions on Causes	Consequences	Corr./Prev. Act. on Consequences	Comment	Severity Rank
				Loss of reactor coolant inventory; Loss of heat removal capability	Gravity Driven Cooling System actuation		
Tube Bundle of the heat exchangers of the IC	Single pipe plugging	Crud in the cooling loop; Foreign object in the cooling loop	Water chemistry control; Yearly test of pipes flow; Preventive maintain.	No consequences		Critical Parameter: HX Plugged Pipes	II
Tube Bundle of the heat exchangers of the IC	Multiple pipe plugging	Violent pressure and vibration transient detaching large amount of crud from pipes walls	Water chemistry control; Use of suitable materials for cooling loop pipes; Preventive maintenance	Natural circulation stop; Loss of heat removal capability; Reactor pressure and temperature increase	Safety relief valves actuation	Critical Parameter: HX Plugged Pipes	III
Drain valve on the return condensate line	Valve fails to open	Control circuit failure; Loss of electric power to motor; Electric motor failure	Redundancy of control devices; Signal to the operator; In Service inspect.	Non triggering of Isolation Condenser if bypass valve does not operate; Loss of heat removal capability; Reactor pressure and temperature increase	Reactor pressure and temperature control; Safety relief valves actuation; Realignment by the operator; Corrective maintenance	Critical Parameter: Partially Open Valve	III
	Inadvertent valve closing	Spurious signal; Control circuit failure; Human error	Redundancy of control devices; Signal to the operator; Actions based on procedure	Natural circulation stop in case bypass valve does not operate; Loss of heat removal capability; Reactor pressure and temperature increase	Reactor pressure and temperature control; Safety relief valves actuation; Realignment by the operator; Corrective maintenance	Critical Parameter: Partially Open Valve	IV

Component	Failure Mode	Causes	Prev. Actions on Causes	Consequences	Corr./Prev. Act. on Consequences	Comment	Severity Rank
Natural Circulation	Envelope failure	Material defects and aging; Corrosion; Abnormal operating conditions; Vibrations; Local. Stresses; Impact of heavy loads (missile)	Adequate welding process quality; Water chemistry control; In Service inspect; Design against missile generation	LOCA in the Drywell; Instantaneous loss of natural circulation; Emptying of the circuit; Loss of heat removal capability; Loss of reactor coolant inventory	Isolate the breached loop; Safety relief valves actuation; Automatic reactor depressurization; Gravity Driven Cooling System actuation	Includes both steam line and drain line Critical Parameter: Undetected Leakage	V
Natural Circulation	Cracking	Material defects and aging; Corrosion; Abnormal operating conditions; Vibrations; Local. stresses	Adequate welding process quality; Water chemistry control; In Service inspect.	Small LOCA in the Drywell; Slow emptying of the circuit and natural circulation arrest for long periods of operation; Reduced heat removal capability	Leak monitoring; Isolate the breached loop; Safety relief valves actuation	Critical Parameter: Undetected Leakage	IV
	Modification of surface characteristics	Oxidation; Aerosol deposits	Water chemistry control	Reduction in heat exchange efficiency; Reduced heat removal capability	Flow monitoring	Critical Parameter: Oxide Layer	II
Natural Circulation	Thermal stratification	Temperature dishomogeneity; Density variations; Onset of local thermal hydraulic phenomena	Process control (pressure, flow, temperature)	Reduction of heat convection; Natural circulation blockage; Loss of heat removal capability; Reactor pressure and temperature	Flow monitoring; Reactor pressure and temperature control; Safety relief valves actuation	Critical Parameter: Piping Layout, Heat Loss	IV

Component	Failure Mode	Causes	Prev. Actions on Causes	Consequences	Corr./Prev. Act. on Consequences	Comment	Severity Rank
				increase			
	Non condensable build-up	Onset of chemical phenomena; Radiolysis products; Impurities	Water chemistry control (PH, O2, H2)	Reduction in heat exchange efficiency; Reduction of heat convection; Natural circulation blockage; Loss of heat removal capability; Reactor pressure and temperature increase	Flow monitoring; Reactor pressure and temperature control; Purging through vent lines Safety relief valves actuation	Critical Parameter: Non-Condensables Fraction	II
	Heat dissipation	Thermal insulation degradation; Inaccurate material assembly	In Service inspect.	Reduction of heat convection; Natural circulation impairment	Flow monitoring;	Critical Parameter: Heat Loss	III

TABLE 26. HAZOP TABLES FOR THE ISOLATION CONDENSER SYSTEM

Guide Word	Deviation	Possible Causes	Consequences	Safeguards/Interlocks	Actions Required
PARAMETER: flow rate					
More of ¹	High Flow	N/A			
Less of	Low Flow	Modifications of surface characteristics (crud deposition, oxidation); Non-condensable build-up; Thermal stratification; Pipe partial plugging; Pipe leak; HX single pipe plugging; HX single pipe rupture Drain valve partial opening	Natural circulation degradation and reduced heat transfer capability; T and P increase	Safety relief valve actuation; Vent line valve actuation	Corrective maintenance; Operator action
No/None	No Flow	Non-condensable build-up; Thermal stratification; Pipe plugging;	Natural circulation stop and loss of heat transfer capability; T and P increase	Safety relief valve actuation; Vent line valve actuation; Automatic Depressurisation	Corrective maintenance; Operator action

Guide Word	Deviation	Possible Causes	Consequences	Safeguards/Interlocks	Actions Required
PARAMETER: flow rate					
		Pipe rupture; HX Multiple pipe plugging; HX Multiple pipe rupture; Drain valve closed		System actuation; Gravity Driven Cooling System actuation	

PARAMETER: Pressure

Guide Word	Deviation	Possible Causes	Consequences	Safeguards/Interlocks	Actions Required
More of	High Pressure	Non-condensable build-up; Surface modifications (crud, oxidation); HX tube plugging; HX tube rupture Partial valve opening	Natural circulation degradation and reduced heat transfer capability; T increase	Safety relief valve actuation; Vent line valve actuation	Corrective maintenance; Operator action
Less of ^l	Low Pressure	N/A			
No/None	No Pressure	N/A			

PARAMETER: Drain valve opening

Guide Word	Deviation	Possible Causes	Consequences	Safeguards/Interlocks	Actions Required
More of	N/A				
Less of	Reduced Opening	Partial blockage	Natural circulation degradation and reduced heat transfer capability; T and P increase	Safety relief valve actuation;	Corrective maintenance; Operator action
No/None	No Opening	Loss of electrical power; Circuit control failure;	Natural circulation stop and loss of heat transfer capability;	Safety relief valve actuation; Vent line valve actuation;	Corrective maintenance; Operator action

Guide Word	Deviation	Possible Causes	Consequences	Safeguards/Interlocks	Actions Required
		Electrical motor failure; Valve stuck	T and P increase	Automatic Depressurisation System actuation; Gravity Driven Cooling System actuation	

PARAMETER: Exchanged heat flux

Guide Word	Deviation	Possible Causes	Consequences	Safeguards/Interlocks	Actions Required
More of ¹	High flux	N/A			
Less of	Low Flux	Non-condensable build-up; Surface modifications (crud, oxidation); HX single tube plugging; HX single tube rupture	Natural circulation degradation and reduced heat transfer capability; T and P increase	Safety relief valve actuation; Vent line valve actuation	Corrective maintenance; Operator action
No/None	No Flux	Non-condensable build-up; HX multiple tube plugging; HX multiple tube rupture	Natural circulation stop and loss of heat transfer capability; T and P increase	Safety relief valve actuation; Vent line valve actuation; Automatic Depressurisation System actuation; Gravity Driven Cooling System actuation	Corrective maintenance; Operator action

¹ This deviation is not evaluated, even if it implies an overcooling of the system that could potentially induce to thermal stresses on core structures and reactor components, like the heat exchanger.

N/A: Not Available

A further improvement of this study proposes the quantification of the failure probabilities of the mechanical components, through a quantitative FMEA assessment. Table 27 lists all the system components under consideration.

TABLE 27. COMPONENT LIST FOR THE ISOLATION CONDENSER

Code	Description	Comment	No of Units for System	No of Systems	Note
IC-SPipe	Steam pipe connection between the RPV and the IC in the cooling pool		1	3	
IC-LPipe	Drain line (liquid phase) connecting the IC and the RPV		1	3	
IC-HX-UH	Upper Header of the heat exchangers of the IC	Two heat exchangers for each system (circuit)	2	3	
IC-HX-LH	Lower Header of the heat exchangers of the IC	Two heat exchangers for each system (circuit)	2	3	
IC-HX-TB	Tube Bundle of the heat exchangers of the IC	Two straight tube bundle heat exchangers for each system (circuit) (120 tubes/each exchanger)	2	3	
IC-DV	Drain valve on the condensate return line	One main and one redundant bypass valve on the drain line	1	3	Two component (main and bypass valve) unit
IC-VL	Vent line from the Lower Header of the IC		1	3	
IC-VL-V	Valve on the vent line of the IC	Two groups of valves in parallel: each group consisting of two valves in series	2	3	Two component (two valves in series) unit
IC-Makeup-V	Makeup valve of the IC cooling pool		1	1	

For each one of the scrutinized components all the possible failure modes that could occur in the different operating states are evaluated in terms of: accident frequencies and relative category classification, failure causes and possible actions to prevent the failure, consequences and actions to prevent and mitigate the consequences. Also, each elementary accident initiator is classified in an Initiating Event (IE), since it is not practical to consider each basic failure as an accident initiator. In this way a defined IE will be characterized by:

- A representative event, which usually is the most challenging from the safety point of view;
- A set of elementary accident initiators grouped under this IE taking into account the similarity of accident development in terms of mitigating features and possible consequences;
- An overall frequency obtained by adding the ones for the elementary initiators.

Existing data deriving from operating experiences in fission nuclear plants are used to determine frequency values; the grace time of 72 hours/year has been considered for the calculation of the frequencies.

As an example, as regards the drain valve on the return pipe the possible failure modes individuated are: valve failure to open (single fault and common cause failure, CCF), inadvertent valve closure (single fault and CCF), and case external leakage. The valve failure to open could be caused by electric motor failure, or loss of electric power to motor, or control circuit failure. To prevent and/or reduce the effect of these causes the following actions could be performed: for the electric motor failure, in-service inspection and preventive maintenance; for control circuit failure, arrange redundancy of control devices. The possible consequences due to valve failure to open and the actions to prevent and/or mitigate each consequence are shown in Tables 28 and Table 29 (as regards, respectively, the single and the intersystem CCF modes of failure). The frequencies evaluated for these kind of valve failures are evaluated respectively as $1,4E-6/y$ and $1,2E-4/y$ corresponding to event of category IV and III, and the IEs associated are 'Loss of Flow in one unit of the Isolation Condenser' and 'loss of flow in the IC', labelled as 'FF1' and 'FF'.

In some cases the assessment of subsystems or sets of components instead of single components is necessary, and schematic fault trees are built in order to take into account the overall component failures that could concur in the subsystem failure (e.g. parallel components, as drain valves).

Table 30 lists the complete set of initiating events, together with the estimated frequency values, as outcome of the analysis, consistent with the procedure outlined in the previous section and the event classification provided in Table 24.

For each IE a complete list of elementary failures that could contribute to cause the event, with related total frequencies, is included

TABLE 28. FMEA TABLE FOR DRAIN VALVE (FAILURE TO OPEN)

Failure Mode	Causes	Prev. Action on Causes	Consequences	Corr./Prev. Act. on Consequence	IE	Comment
Valve fails to open	Control circuit failure	Redundancy of control devices; Signal to the operator	No triggering of Isolation Condenser if bypass valve does not actuate	Reactor pressure and temperature control; Safety relief valves actuation	FF	Only the single faulted circuit is involved in the accident. Redundant circuit operation allows temperature and pressure values to be kept within acceptable values, not requiring the actuation of the automatic depressurization system.
	Loss of electric power to motor		Loss of heat removal capability; Reactor pressure and temperature increase.	Realignment by the operator; Corrective maintenance.		
	Electric motor failure	In-Service inspection; Preventive maintenance.				

TABLE 29. FMEA TABLE FOR DRAIN VALVE (CCF FAILURE TO OPEN)

Failure Mode	Causes	Prev.Action on Causes	Consequences	Corr./Prev. Act. on Consequence	IE	Comment
Valve fails to open (CCF)	Control circuit failure;	Redundancy of control devices; Signal to the operator,	No triggering of Isolation Condenser;	Reactor pressure and temperature control; Safety relief valves actuation;	FF	All the 3 circuits (therefore the whole system) are interested to the accident
	Loss of electric power to motor;		Loss of heat removal capability; Reactor pressure and temperature increase.	Automatic reactor depressurization;		
	Electric motor failure.	In-Service inspect.; Preventive maintenance.		Gravity Driven Cooling System actuation;		
				Realignment by the operator;		
				Corrective maintenance.		

TABLE 30. LIST OF IES RELATED TO FAILURES IN ISOLATION CONDENSER SYSTEM

IE	Description	Frequency (ev/y)	Category
FF1	Loss of flow in one unit of the isolation Condenser	3.0E-2	II
FF	Loss of flow in the Isolation Condenser	1.4E-3	III
LP	Liquid release in the pool	1.6E-6	IV
SLP	Small liquid release in the pool	1.6E-5	IV
LDW	LOCA in the Drywell	3.7E-7	V
SLDW	Small LOCA in the Drywell	3.7E-5	IV

In Table 31 a sample related to two IEs that could occur during IC operation due to cooling loop fault conditions is reported: loss of flow in one unit of the IC (FF1) and loss of flow in the whole IC (FF). In the columns are indicated: IE code, code and description of components whose failure will induce the IE, component failure mode, number of component units in a loop and number of loops in the plant, failure frequencies and related category classification. Specifically, as regards the IE FF1, the values reported in the fifth and ninth columns of the table show the frequencies referring respectively to a single unit and the total number of units (that is the values in ninth column are obtained by multiplying the single frequency values by the number of units for each system and the number of systems themselves). Conversely, since the contributors to the IE named FF are due to CCFs, the values are the same for either columns.

To verify the fulfillment of the safety goals in probabilistic terms a reduced set of the identified IEs will be considered as reference accident initiators of accident sequences, which have to undergo probabilistic quantification by event tree modeling.

In fact effects of an IE could be similar to or enveloped by the effect of other IEs, already taken into account in the reactor analysis, in terms of consequences and plant response to the accident evolution.

Looking at the results one infers that IEs are suitable to be grouped into two classes. The first one is relative to the so-called loss of coolant accident for which the relative frequency is rather low. The IE SLP ‘Small liquid release in the pool’, due to the heat exchanger headers or tubes leak can be disregarded, because of the low consequences affecting the system operation; the same consideration is not valid for the IE ‘LP liquid release in the pool’, for which the potential of the consequences is more severe. Lastly 'LOCA in the Drywell' IE is not worth attention, being its frequency negligible (less than 1.0E-6).

The second family of IEs pertains to the loss of function of the system due to the loss of flow in the circuit, involving only one unit or the whole system: in the first case redundant circuits operation allows temperature and pressure values to remain within acceptable limits, in the other case the accident consequences are more severe because they imply the loss of the whole system. This consideration allows us to overlook the IE named 'loss of flow in one unit of the IC' (FF1).

TABLE 31. ELEMENTARY FAILURES GROUPED ON IES

IEs	Comp Code	Component Description	Failure Mode	Freq.	Cat.	No of unit for system	No of systems	Total Freq.	Tot Cat.
FF1	IC-HX-TB	Tube Bundle of the heat exchangers of the IC	Multiple pipe plugging	4.9E-3	III	2	3	2.9E-2	II
	IC-DV	Drain valve on the return condensate line	Valve fails to open	1.4E-6	IV	1	3	4.2E-6	IV
	IC-DV	Drain valve on the return condensate line	Inadvertent valve closing	8.6E-9	V	1	3	2.6E-8	V
	IC-VL	Vent line from the Lower Header of the Isolation Condenser	Tube rupture	6.1E-7	V	1	3	1.8E-6	IV
	IC-VL-V	Valves on the vent line of the isolation Condenser	Valve fails to open	2.9E-6	IV	2	3	1.7E-5	IV
	IC-VL-V	Valves on the vent line of the Isolation Condenser	Inadvertent valve closing	1.7E-8	V	2	3	1.0E-7	V
								3.0E-2	II
FF	IC-DV	Drain valve on the return condensate line	Valve fails to open (CCF)	1.2E-4	III	1	3	1.2E-4	III
	IC-DV	Drain valve on the return condensate line	Inadvertent valve closing (CCF)	7.2E-7	V	1	3	7.2E-7	V
	IC-VL-V	Valves on the vent line of the Isolation Condenser	Valve fails to open (CCF)	1.2E-4	III	2	3	1.2E-4	III
	IC-VL-V	Valves on the vent line of the Isolation Condenser	Inadvertent valve closing (CCF)	7.2E-7	V	1	3	7.2E-7	V
	IC-Makeup-V	Makeup valve of the Isolation Condenser pool	Valve fails to open	1.2E-3	III	1	1	1.2E-3	III
								1.4E-3	III

7. UNCERTAINTY CALCULATIONS ON PHENIX NATURAL CONVECTION TEST

The sodium reactor PHENIX is the French semi-industrial prototype of sodium reactor. After 35 years of successful service, this experimental reactor has been shut down in mid-2009. Before shutdown and the decommissioning process, several challenging tests, called ‘Ultimate Tests’, have been performed. Regarding the thermal hydraulics field, an ambitious test of natural convection has been carried out. The IAEA has selected this thermal hydraulics test for an international benchmark i.e. CRP on PHENIX end of life tests. The objective of this benchmark was to compare several codes in their ability to simulate the PHENIX NC test

performed in June 2009. For these calculations, the CEA has used the CATHARE system code.

7.1. PHENIX REACTOR

PHENIX [71] is a pool type reactor composed of a main primary vessel, three sodium secondary circuits, three tertiary water/steam circuits and one turbine, as depicted in FIG. 123. PHENIX nominal power was 560 MW(th)/250 MW(e). However, during the ultimate tests in 2009, one secondary and tertiary circuit was out of operation and the reactor was operating at a lower power of 350 MW(th)/145 MW(e). The reactor vessel shown in FIG. 124 is 11.8 m in diameter and 9.8 m height. The main internal structures in the reactor vessel are the core support structure, the diagrid structure feeding the core, the above core structure, the handling machine and the internal vessel separating the hot pool and the cold pool. The main components are the three primary pumps and the six intermediate heat exchangers. Only four intermediate heat exchangers were in operation during the ultimate tests, while the other two being replaced by inactive components. The core is composed of three main regions: an inner core, an outer core and a fertile zone. Reflector and shielding zones are surrounding the main core region, with very low power release and low flow rate. A small flow rate of sodium (less than 10%) is taken at the core inlet to cool the main vessel and it is returned into the cold pool via a weir. At the core outlet, the flow rate through the above core structure is very low. Each secondary circuit consists of two intermediate heat exchangers, a steam generator, a secondary pump and an expansion tank. The steam generator is composed of three main parts: the evaporator, the heater and the super-heater. The whole steam generator is surrounded by a casing which can be opened if required to ensure an air cooling in case of a steam generator dry out. Another decay heat removal possibility is the heat radiation of the reactor vessel towards the emergency cooling system.

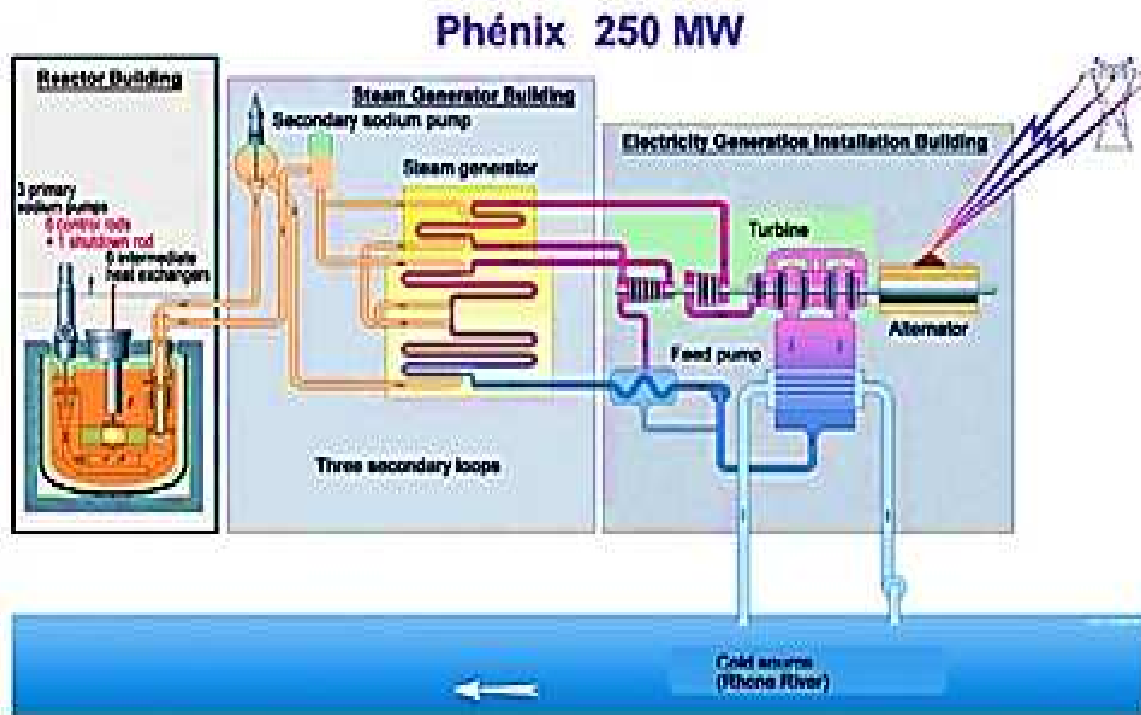


FIG. 123. Phenix power plant [71].

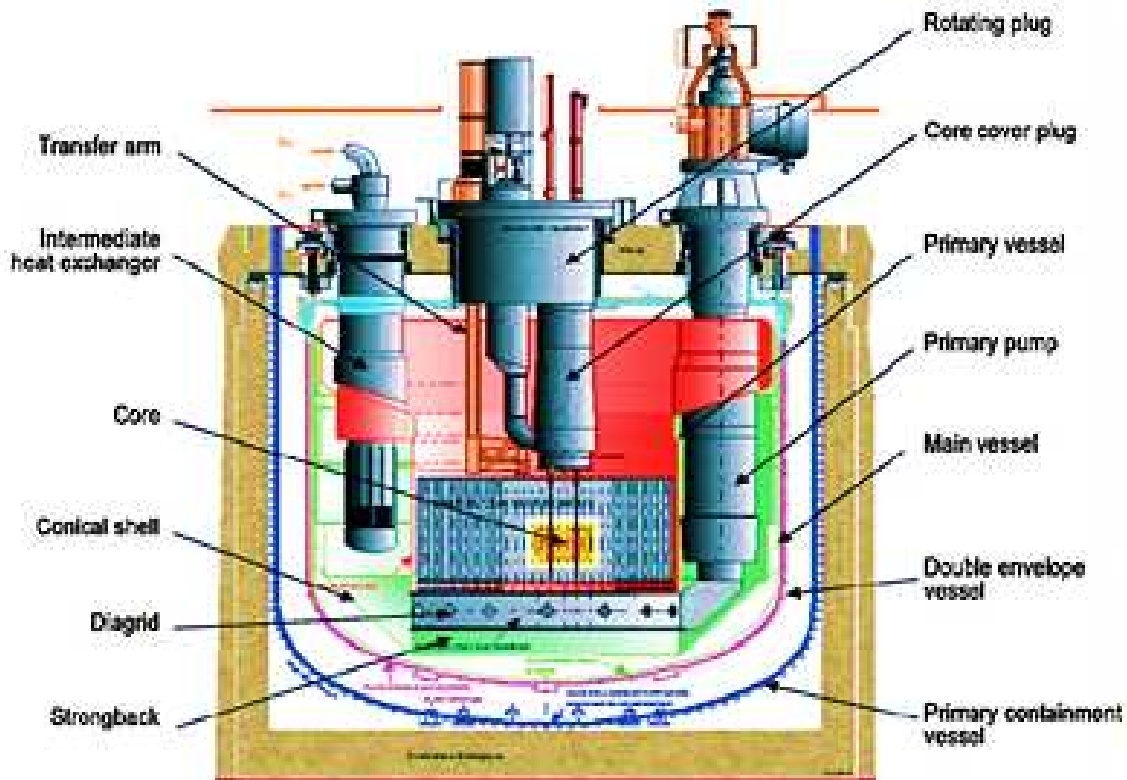


FIG. 124. Phenix reactor vessel [71].

Transient description

According to Ref. [72], the scenario of the natural convection test is the following:

- *First step: secondary loop dry-out*
 - Reactor initially stabilized at 120 MW(th).
 - At $t=0s$, dry out of steam generators (SG) 1 and 3.
 - About 6 minutes after the beginning of the transient (at $t=466s$), manual scram, followed by an automatic linear decrease of the two secondary pumps to 110 rpm within 60s (the corresponding flow rate at a pump speed of 110 rpm is around 100 kg/s).
 - 5 seconds later, manual stop of the three primary pumps. Due to primary pump inertia, the primary pump speed decreases roughly from nominal speed to zero within 3 minutes.
- *Second step: natural convection on secondary circuit heat losses*
 - During nearly 3 hours (until $t=10500s$), there are no actions. The secondary loops stabilize at a mean temperature of $430^{\circ}C$, with heat losses estimated at around 500kW.
- *Third step: natural convection with increase of heat losses on SG*
 - After nearly 3 hours ($t=10500s$), the two steam generator containments casing open. There is a natural circulation of air in the SG casing (air mass flow rate of 7 kg/s and air inlet temperature of $20^{\circ}C$) and therefore, a more efficient cooling of the secondary side.

- The cooling of the secondary side leads to a decrease of the secondary temperature at the inlet of the IHX (intermediate heat exchanger) and therefore to a most efficient cooling of the primary circuit (primary vessel).

For the benchmark problem, the boundary conditions (temperature and flow rate) at the inlet of the secondary side of the IHX are fixed to the values measured in the PHENIX test (FIG. 125).

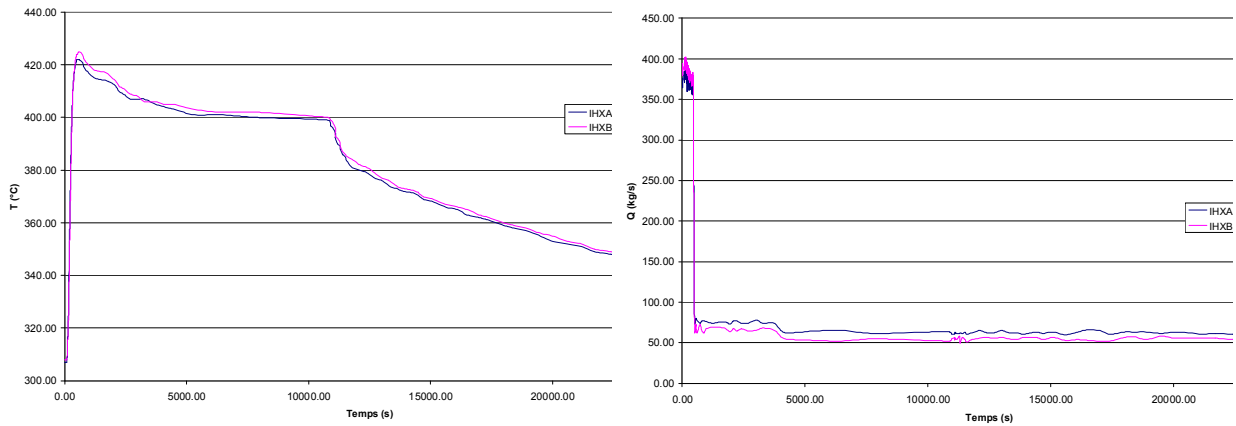


FIG. 125. Boundary conditions: IHX secondary inlet T and Q (PHENIX NC test).

The evolution of the power during the transient is also a boundary condition given by the power measured during the PHENIX test. We can point out that before the scram (at 466s), there is a drastic fall of the core power, due to the neutronics feedback effects (FIG. 126).

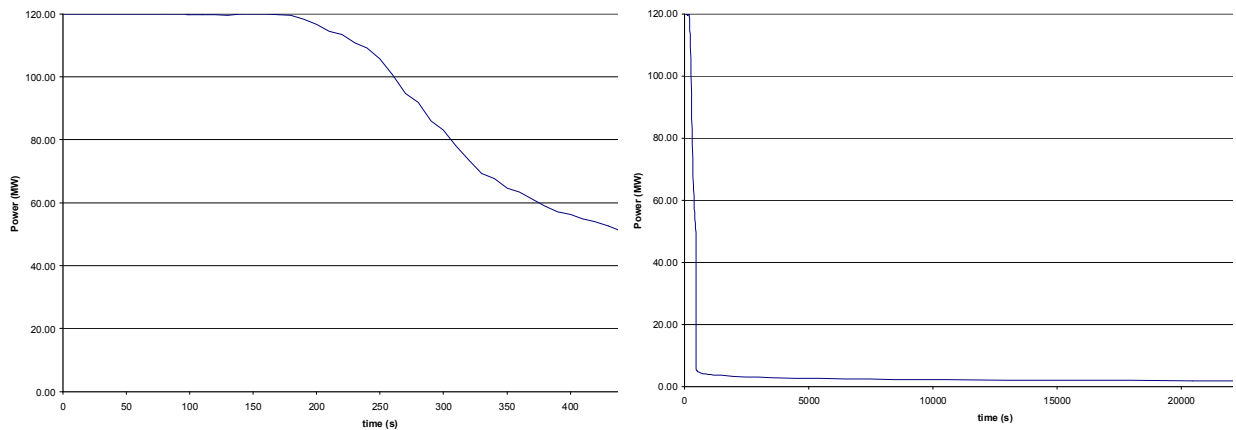


FIG. 126. Boundary condition: core power (PHENIX NC test).

7.2. VALIDATION PERFORMED BY CEA, FRANCE

The data input deck used to model PHENIX reactor with the CATHARE code is described in [72]. The modeling of the vessel with the CATHARE is described in [71]. The different modules of the vessel modeled by CATHARE are presented in (FIG. 127).

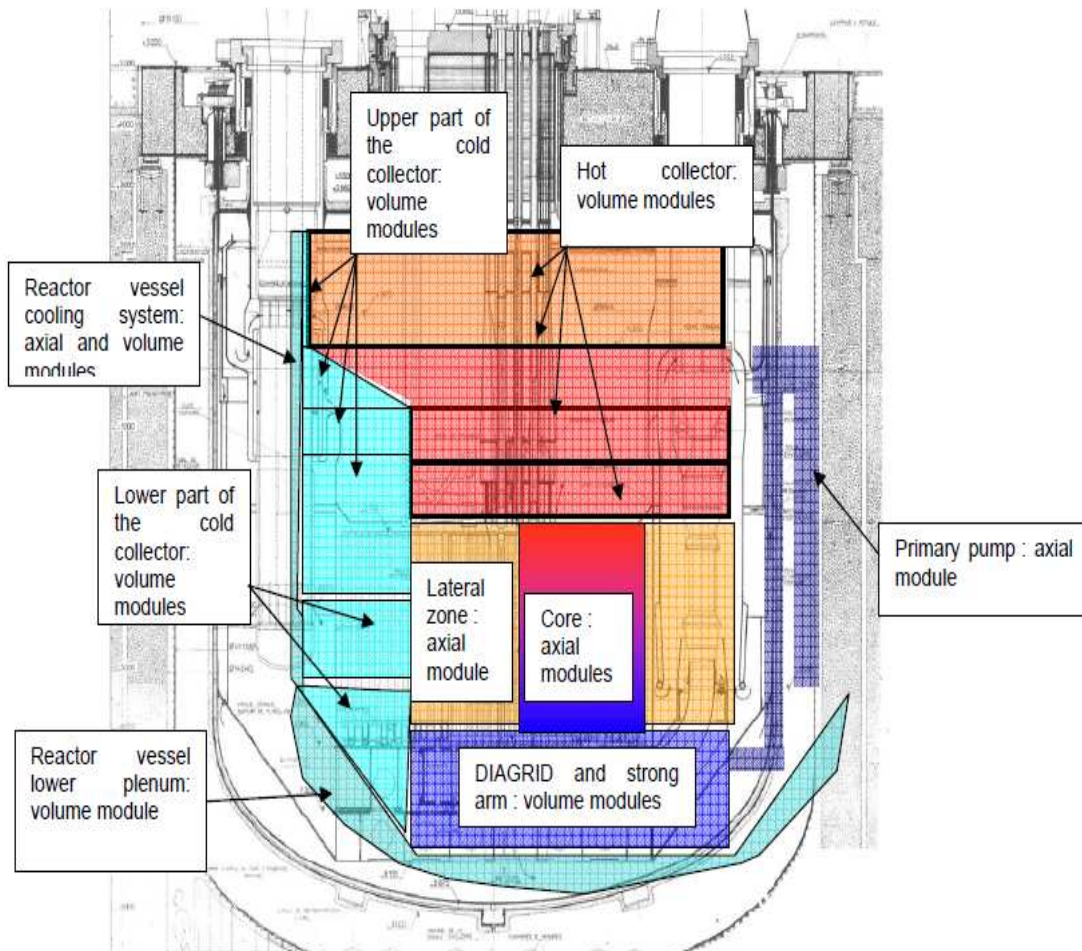


FIG. 127. CATHARE modules in the vessel [73].

Uncertain parameters

Table 32 lists the input parameters considered as uncertain by the CEA experts. The choice of their corresponding uncertainty ranges relies on the analysis of some reports given in the column 'references'.

7.2.1. Probabilistic model

Normal distributions have been considered for all the 13 parameters. Standard deviation has been calculated with the assumption that the lower and the upper bounds of the uncertainty range correspond respectively to the quartiles 2.5% and 97.5% (i.e. the confidence to be inside the uncertainty range is 95%). The normal distributions are truncated to ± 3 standard-deviations except for the parameter 8 for which the lower truncation is 0.

7.2.2. Uncertainty propagation

Latin hypercube sampling has been performed on the 13 parameters. 100 samples have been generated and for each sample a CATHARE simulation of the PHENIX test has been carried out. The stochastic input parameters are assumed to be independent of one another.

7.2.3. Characteristics of the output distribution

7.2.3.1. Diagrid inlet temperature

Plots of 100 curves of the diagrid inlet temperature are shown in FIG. 128 and plots of mean values and percentiles in FIG. 129.

Comparison of the percentiles observed and the percentiles of the normal distribution suggests that the normal distribution may be a reasonable approximation to the probability distribution for the diagrid inlet temperature. The difference between the 95 and the 5 percentile (i.e. 90% confidence interval) is always less than 8°C.

TABLE 32. LIST OF UNCERTAIN INPUT PARAMETERS WITH THEIR SELECTED UNCERTAINTY RANGES

No	Parameter	Nominal	Uncertainty range	References
1	Pump inertia	1545 kg.m ²	+/- 20%	[73] → + ou - 25%
2	Operating power	PTOT	+/- 5 MW (+/- 4.2%)	[72]
3	Decay power	From the scram : PHENIX data curve	+/- 10%	[72]
4	IHX secondary inlet T	PHENIX data curve	+/- 5°C	[72]
5	IHX secondary inlet Q	PHENIX data curve	+/- 5%	[72]
6	Core pressure drop ¹	-	+/- 10%	[72]
7	IHX pressure drop	-	+/- 20%	[72]
8	IHX heat transfer area (number of blocked tubes)	N tubes = 2279 blocked tubes = 0	0-40 blocked tubes	[72]
9	Hot pool Na mass	-	+/- 10%	-
10	Cold pool na mass	-	+/- 10%	-
11	Roof heat loss	-	+/-10%	-
12	Vessel heat loss	-	+/- 10 %	-
13	Core flowrate ²	-	+/- 5%	[72]

7.2.3.2. Core flow rate

Figure 130 shows the mean values and percentiles for the core flow rate. The core flow rate which is equal to 1240 kg/s in average at the beginning of the transient, drop to 26 kg/s, then increases up to 36 kg/s at the end of the second step (10500s) and after increases more sharply

¹ The pressure drop coefficients at the inlet of the three derivations are modified by the same percentages.

²The pressure drop coefficients at the inlet of the derivation 1 and 2 (inner core) are increased by certain percentage when in the same time the pressure drop coefficients at the inlet of the derivation 3 (blanket) is decreased by the same percentage.

in the third step up to 62 kg/s at the end. The width of the 90% confidence interval is less than 20 kg/s except during the pumps rundown where it is more than 100 kg/s.

7.2.3.3.IHX primary inlet and outlet temperatures

Plots of 100 curves of the diagrid inlet and outlet temperatures are shown in FIG. 131.

Comparison of these curves to the measurement performed in the PHENIX reactor during the NC test suggests that the CATHARE code under-predicts the IHX primary inlet temperature during the major part of the transient except at the beginning and at the end of the transient, and over-predicts the IHX primary outlet temperature at the beginning of the transient between 500s and 2000s and then under-predicts it after 11000s.

Plots of mean values and percentiles are shown in FIG. 132. The width of the 90% confidence interval is less than 8°C for the outlet temperature and less than 10°C for the inlet temperature.

7.2.3.4.IHX secondary outlet temperature

Plots of 100 curves of the IHX secondary outlet temperatures are shown in FIG. 133. Comparison of these curves to the measurement performed in the PHENIX reactor during the NC test shows a good agreement except after 15000s, where the CATHARE code over-predicts slightly the secondary output temperature.

7.2.3.5.Fuel maximum temperature

Figure 134 shows the mean values and percentiles for the fuel maximal temperature. The width of the 90% confidence interval is close to 25°C at the beginning of the transient before 200s, and during the scram and then decreases down to 10°C after 5000s.

7.2.3.6.Na maximum temperature at core outlet

Plots of 100 curves of the maximum temperature of the sodium at core outlet are shown in Figure 135 and Figure 136. These temperatures are calculated in the hottest derivation modeled by the CATHARE code (see [73]) and at the outlet of the assemblies. These curves are compared to the measurement performed in the PHENIX reactor during the NC test:

- at the hottest sub-assembly(1)
- at the outlet of the hottest part of the core(2)
- at the outlet of the entire core(3)

It can be shown that the CATHARE calculations plus uncertainties are well bounded by (2) and (3) measurements except around the peak of temperature at 930s, which is over-predicted by the code.

Figure 137 shows the mean values and percentiles for the Na maximal temperature. The width of the 90% confidence interval is maximal around 700s (21°C) and less than 10°C in the major part of the transient.

Comparison of the percentiles observed and the percentiles of the normal distribution (FIG. 138) suggests that the normal distribution may be a reasonable approximation to the probability distribution for the Na maximum temperature.

7.2.4. Global sensitivity analysis

The objective of this analysis is to evaluate the importance of each input uncertain parameter in contributing to the overall uncertainty of each response of interest. A global sensitivity analysis has been carried out by the way of standard regression coefficients. Considering that the response Y is a linear function of the random input variables X_i , the standardized regression coefficients (SRC) are obtained from the regression model:

$$Y = \beta_0 + \sum_{i=1}^p \beta_i X_i$$

They quantify the effect of varying each input variable away from its average by a fixed fraction of its variance. They are given by:

$$SRC(Y, X_i) = \beta_i \sqrt{\frac{Var(X_i)}{Var(Y)}}$$

The quality of the fitness of the assumed linear model, in comparison with the actual code response, is given by the coefficient of determination R^2 , which must be close to 1.

The sign of the SR coefficients indicates if the response increases (+) or decreases (-) when the variable increases. The sum of the SRC^2 is equal to the coefficient of determination R^2 .

The SR coefficients are calculated each 50s at the beginning of the transient, up to 1000s, each 100s up to 5000s and after each 200s.

7.2.4.1. Diagrid inlet temperature

Figure 139 and Figure 140 show R^2 and SRC^2 between the diagrid inlet temperature and the input parameters. The hypothesis of a linear relation between the output and the input parameters is valid, because the values of R^2 are between 0.9 and 1 throughout the transient. So the SR coefficients can be used as sensitivity indices.

At the beginning of the transient (FIG. 139), the uncertainty of the output, the diagrid inlet temperature, is fully due to the uncertainties on the operating power and to a lesser extent on the core pressure drop. After the start of secondary loop dry-out and before the scram, the relative influence of the operating power goes down and the influence of three parameters, namely IHX secondary input temperature, flow rate and cold pool Na mass, increases.

After the scram and the manual stop of the three primary pumps, the influence of the pump inertia slightly increases. This influence of the pump inertia remains after that the primary pumps are fully stopped and up to 4000s.

At the level of the peak of the output, around 570s, the most influential parameters are IHX secondary input temperature (45%), the cold pool Na mass (17%), the operating power (13%) and the IHX secondary input flow rate (9%).

At the long term, the relative influence of the operating power increases again up to 5000s and then decreases. The influence of the decay power increases up to 7000s and decrease after, conversely to the IHX secondary input temperature whose influence is minimal at 5000s and then increase up to the end of the transient where its uncertainty explains about 99% of the uncertainty of the output.

7.2.4.2. Core flowrate and IHX primary flowrate

Plots of the R^2 and the SRC^2 for the core flow are shown in FIG. 141 and FIG. 142. The hypothesis of a linear relation between the output and the input parameters is quite valid ($0.8 < R^2 < 1$) up to 7000s with the exception of a short period after the scram where the influence is distributed among several parameters. Before the scram, the uncertainty of the core flow rate is fully due to the uncertainties on the core pressure drop. During the pumps rundown the major influence is due to the pump inertia, influence which decreases when the pumps are stopped. Then (up to 7000s) the most influential parameters are IHX secondary input temperature, the operating power and the decay power.

Logically the same influences are observed for the IHX primary flow rate.

7.2.4.3. IHX primary inlet and outlet temperatures

Plots of the R^2 and the SRC^2 for the IHX primary inlet temperature are shown in FIG. 143 and FIG. 144. Up to 200s, the major influence is due to the operating power and to a lesser extent to the core pressure drop. After 200s, the influences of IHX secondary temperature and flow rate increase. At the long term, the main influence is due to IHX primary inlet temperature, operating power and decay power.

Plots of the the R^2 and the SRC^2 for the IHX primary outlet temperature are shown in FIG. 145. The influence of the operating power and the core pressure drop is only sensitive in the 50 first second and after, the influences of IHX secondary temperature and flow rate increase. After 600s and up to the end of the transient, the uncertainty of IHX primary outlet temperature is fully due to the uncertainties on the IHX secondary input temperature.

7.2.4.4. IHX secondary outlet temperature

Logically influences observed for the IHX secondary outlet temperature are quite identical to the ones of the IHX primary inlet temperature.

7.2.4.5. Fuel maximum temperature

Plots of the the R^2 and the SRC^2 for the fuel maximum temperature are shown in FIG. 146 and FIG. 147. The hypothesis of a linear relation between the output and the input parameters is valid, because the values of the R^2 are between 0.9 and 1 all over the transient, except around 450s.

At the beginning of the transient, the only influent parameter is the operating power. Then after 150s the influences of IHX secondary input temperature and flow rate increase. During the pumps rundown the most influent parameter is the pump inertia.

At the long term, the most influential parameters are the IHX secondary input temperature, the decay power which pass by a maximum just before the third step and the operating power.

7.2.4.6. Na maximum temperature at core outlet

For the sodium maximum temperature at core outlet, plots of the SRC are shown in FIG. 148 and FIG. 149 and plots of the SRC^2 in FIG. 150 and FIG. 151. The hypothesis of a linear relation between the output and the input parameters is valid, because the values of the R^2 are close to 1.

At the beginning of the transient, the uncertainty of the output (Na maximum T) is fully due to the uncertainties on the operating power and to a lesser extent on the core pressure drop. After the starting of the secondary loop dry-out and before the scram, the relative influence of the operating power goes down and three parameters have their influence increasing: IHX secondary input temperature and flow rate and cold pool Na mass.

After the scram and the manual stop of the three primary pumps, there is a relative sharp increase of the influence of the decay power and the pump inertia. This last influence logically disappears when the primary pumps are fully stopped.

At the level of the peak of the output, around 930s, the most influential parameters are IHX secondary input temperature (73%) and the decay power (25%).

At the long term, the relative influence of the decay power increases up to 11000s and decrease after, conversely to the IHX secondary input temperature.

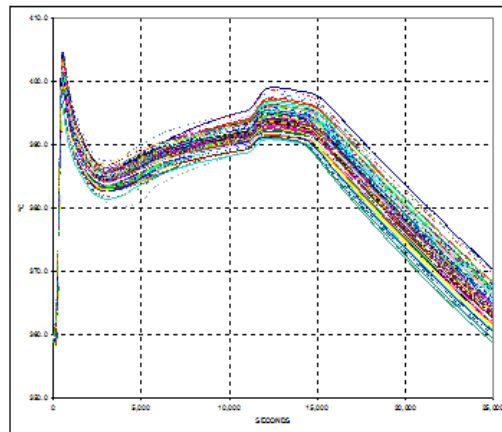


FIG. 128. 100 curves of evolution of diagrid inlet temperature.

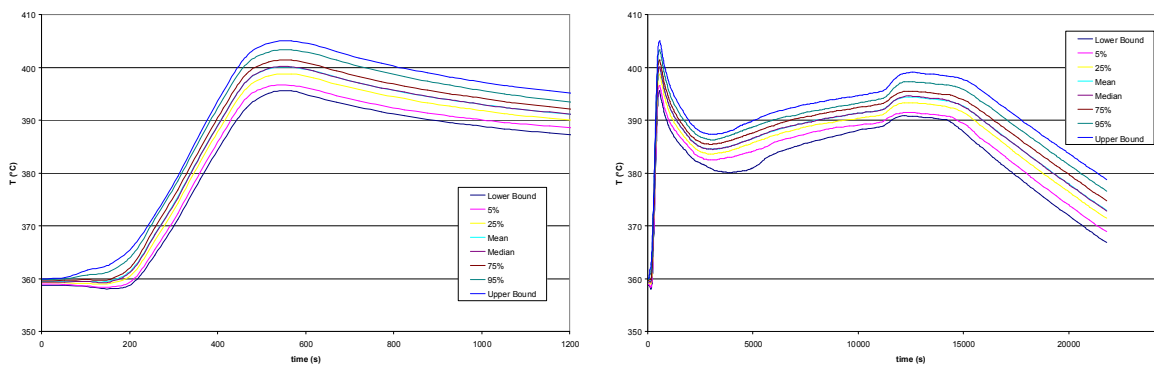


FIG. 129. Mean, percentiles and upper and lower bounds for the diagrid inlet temperature (short term-left, long term-right).

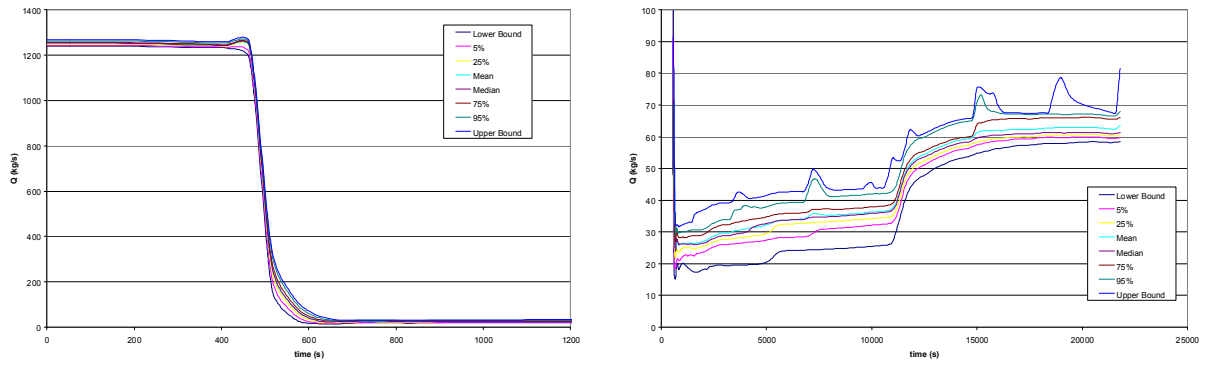


FIG. 130. Mean, percentiles and upper and lower bounds for the core flow rate (short term-left, long term-right).

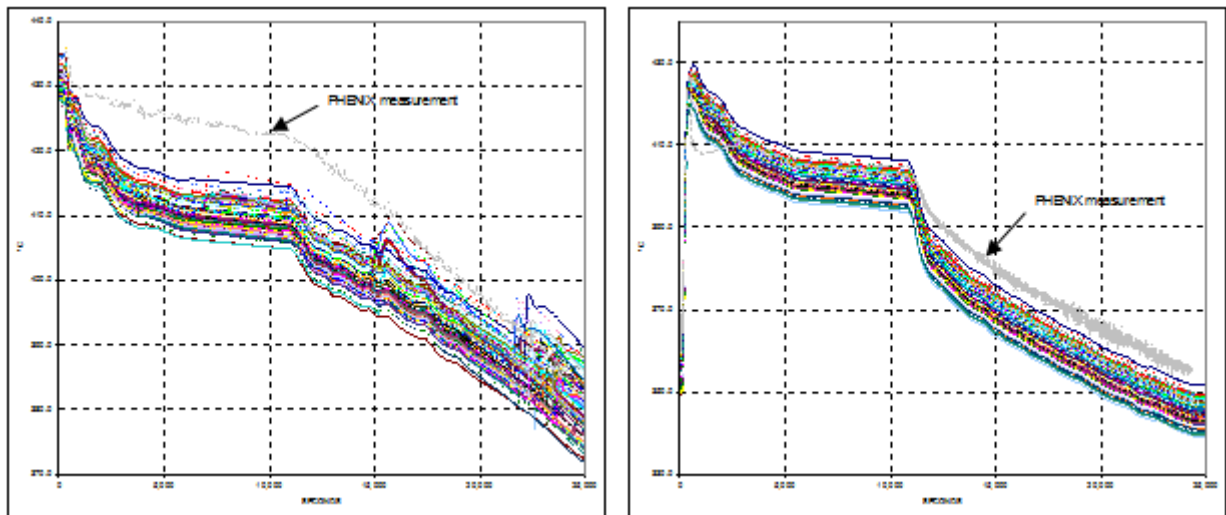


FIG. 131. 100 curves of IHX primary temperature (inlet – left and outlet – right. Comparison with PHENIX measurements).

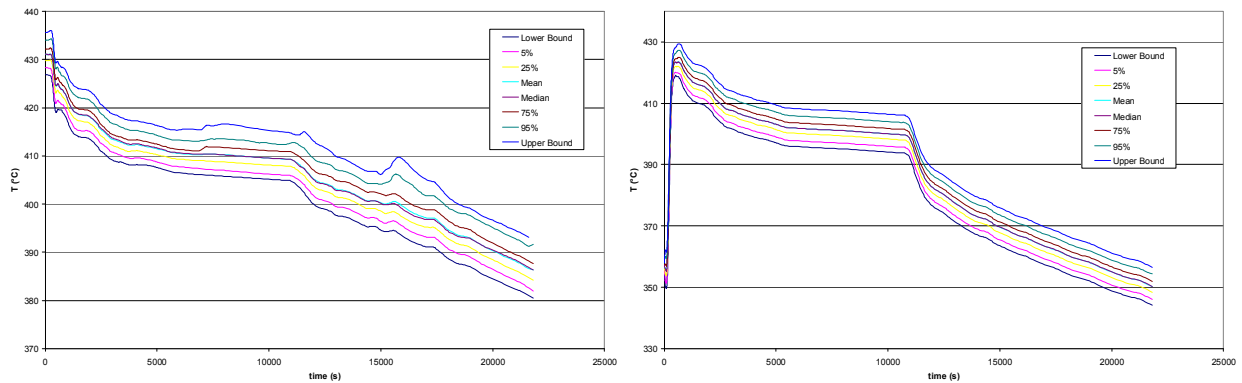


FIG. 132. Mean, percentiles and upper and lower bounds for the IHX primary temperature (inlet – left and outlet – right).

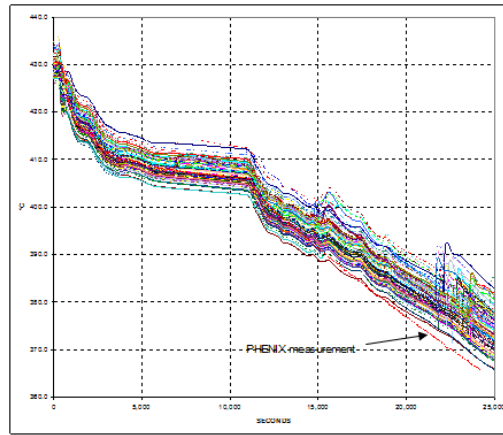


FIG. 133. 100 curves of IHX secondary outlet temperature. Comparison with PHENIX measurement.

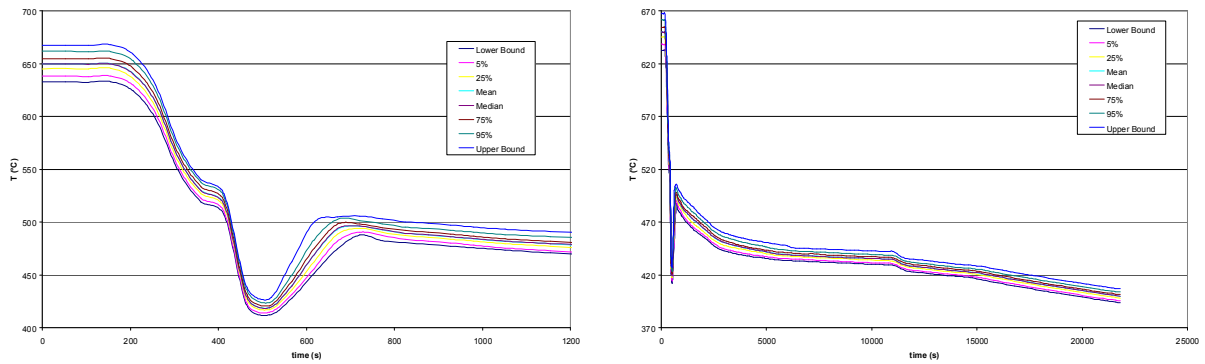


FIG. 134. Mean, percentiles and upper and lower bounds for the fuel maximum temperature (short-term-left and long term-right).

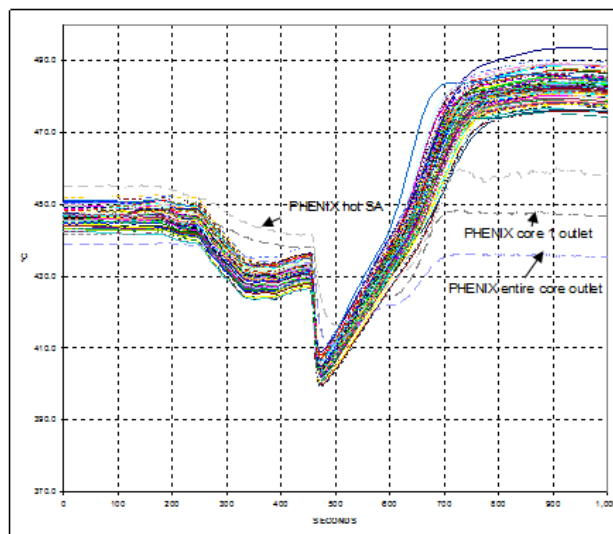


FIG. 135. 100 curves of Na maximum temperature at core outlet (short term).

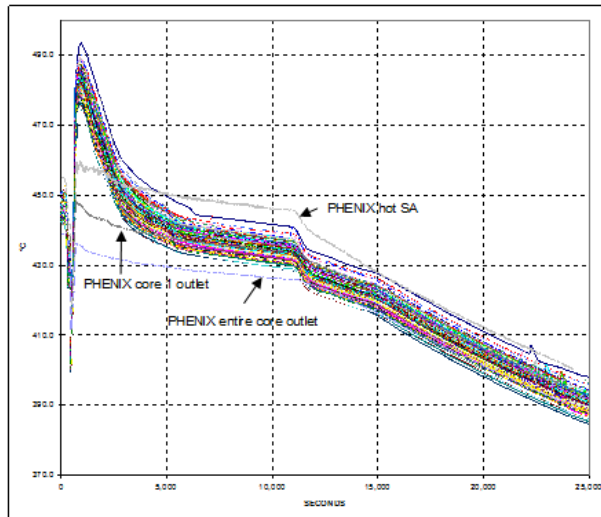


FIG. 136. 100 curves of Na maximum temperature at core outlet (long term).

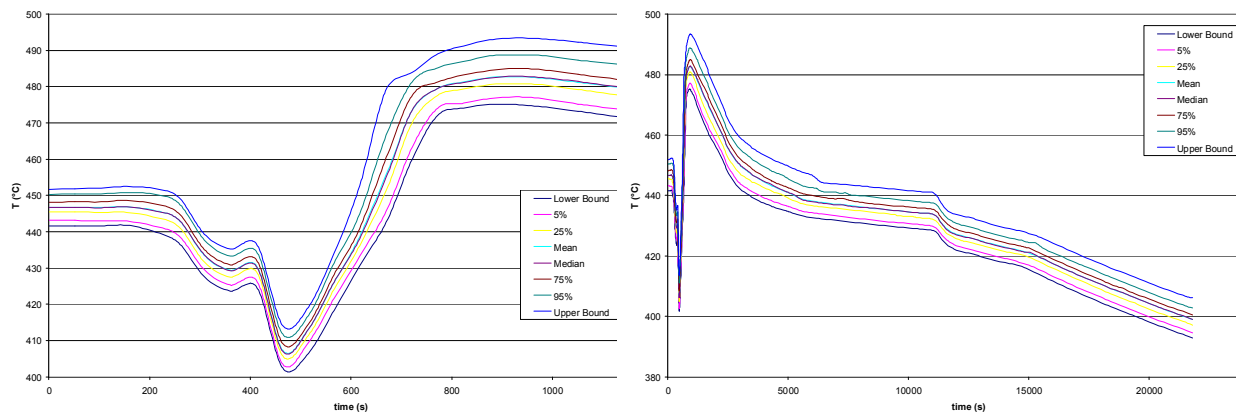


FIG. 137. Mean, percentiles and upper and lower bounds for the Na maximum temperature (short term-left and long-term right).

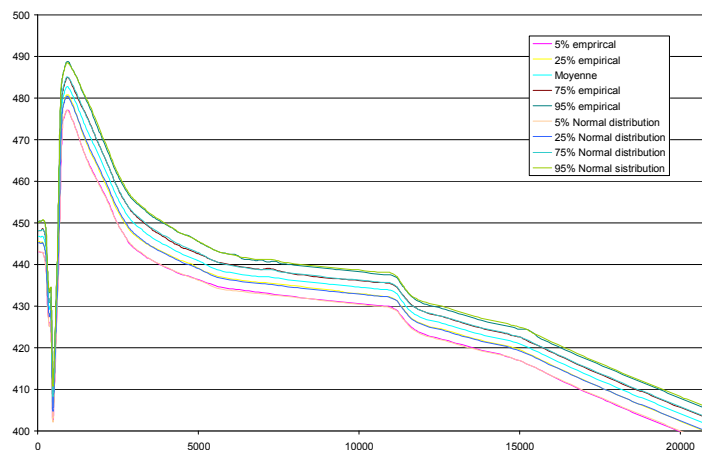


FIG. 138. Comparison of the percentiles observed and the percentiles of the normal distribution for the Na maximum temperature.

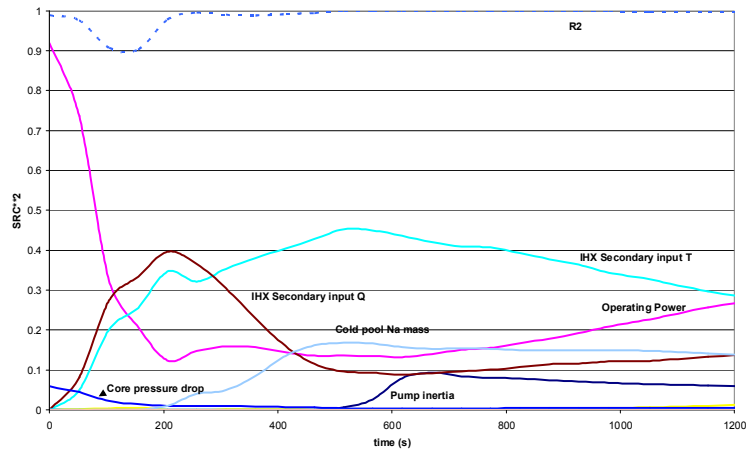


FIG. 139. R^2 and square of standard regression coefficients (SRC^2) between the diagrid inlet T and the input parameters (short term).

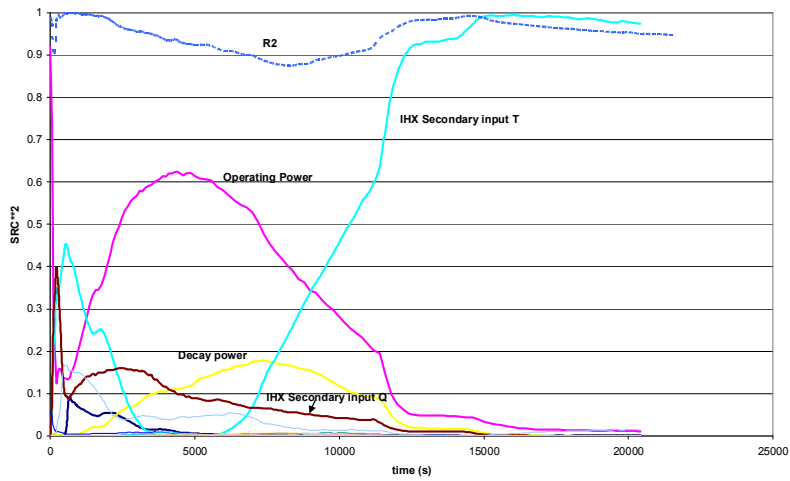


FIG. 140. R^2 and square of standard regression coefficients (SRC^2) between the diagrid inlet T and the input parameters (long term).

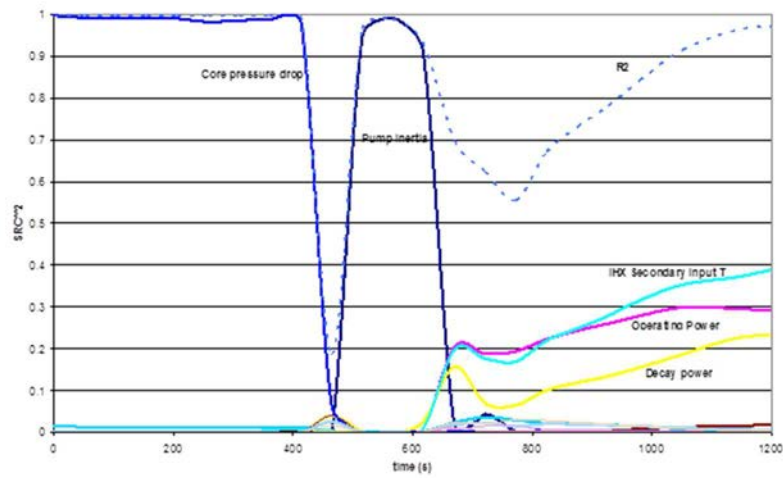


FIG. 141. R^2 and square of standard regression coefficients (SRC^2) between the core flowrate and the input parameters (short term).

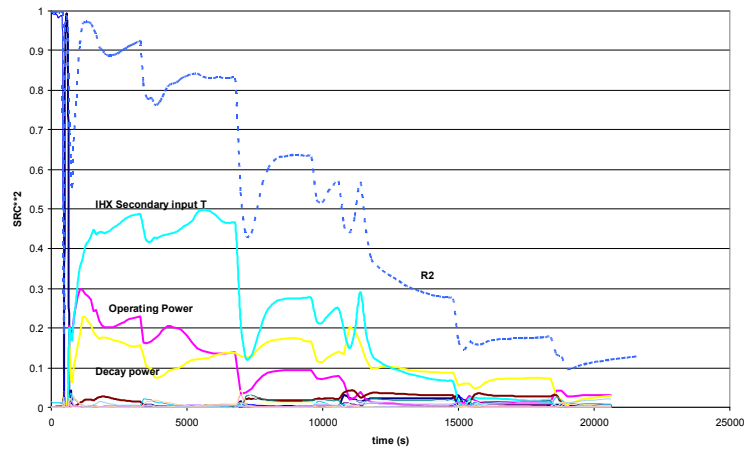


FIG. 142. R^2 and square of standard regression coefficients (SRC^2) between the core flowrate and the input parameters (long term).

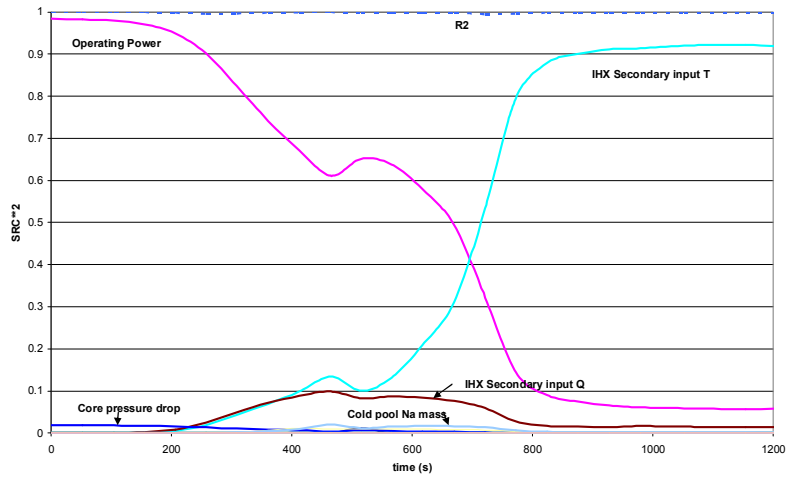


FIG. 143. R^2 and square of standard regression coefficients (SRC^2) between IHX primary inlet temperature and the input parameters (short term).

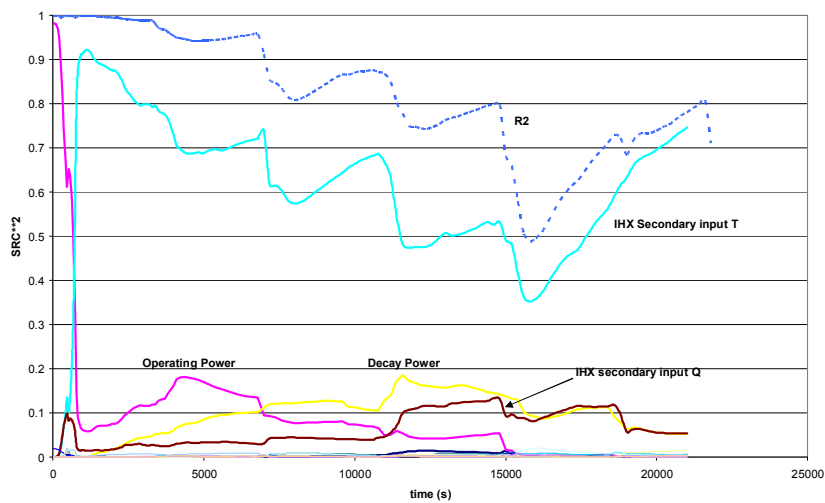


FIG. 144. R^2 and square of standard regression coefficients (SRC^2) between IHX primary inlet temperature and the input parameters (long term).

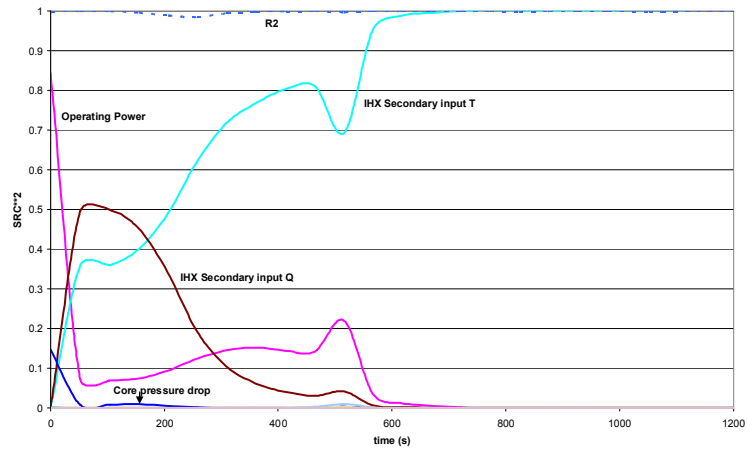


FIG. 145. R^2 and square of standard regression coefficients (SRC^2) between IHX primary outlet temperature and the input parameters (short term).

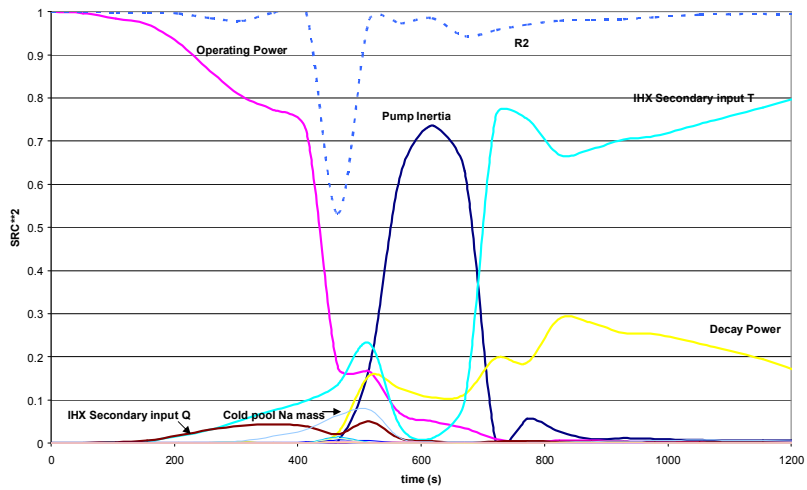


FIG. 146. R^2 and square of standard regression coefficients (SRC^2) between fuel maximum temperature and the input parameters (short term).

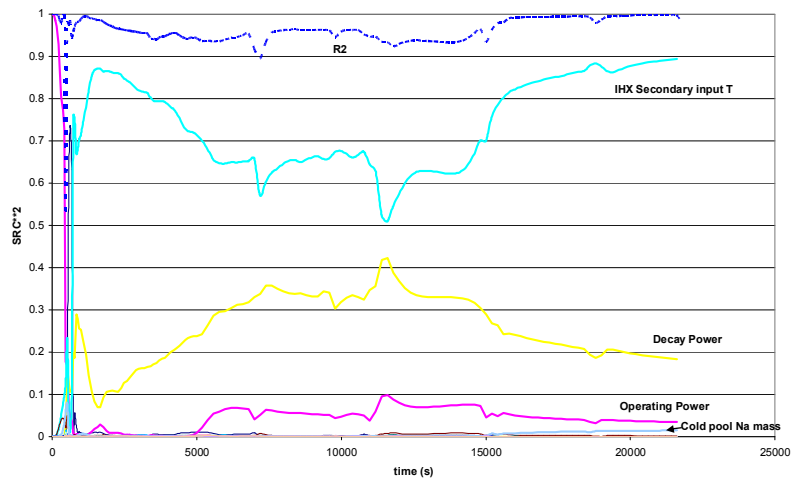


FIG. 147. R^2 and square of standard regression coefficients (SRC^2) between fuel maximum temperature and the input parameters (long term).

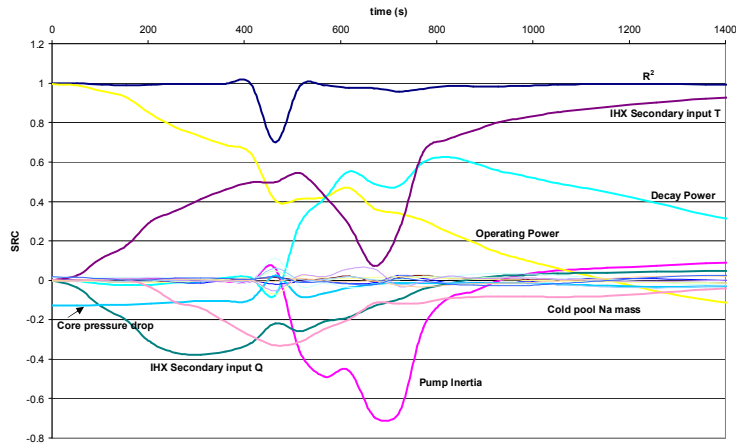


FIG. 148. R^2 and standard regression coefficients (SRC) between Na maximum temperature and the input parameters (short term).

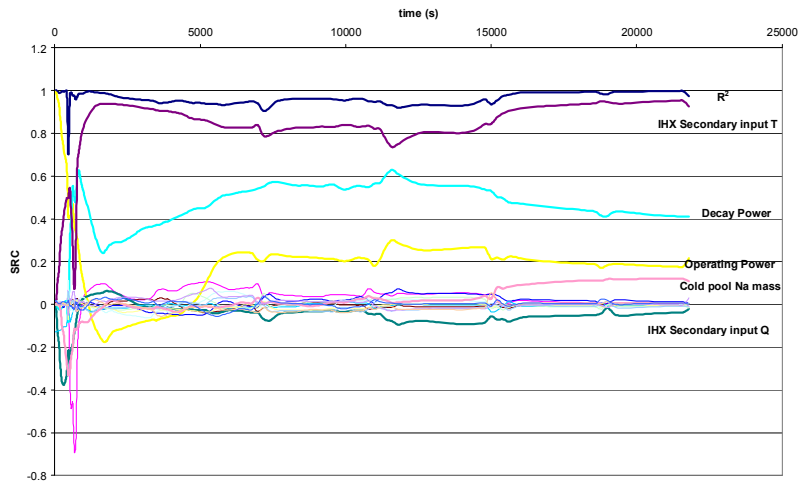


FIG. 149. R^2 and standard regression coefficients (SRC) between Na maximum temperature and the input parameters (long term).

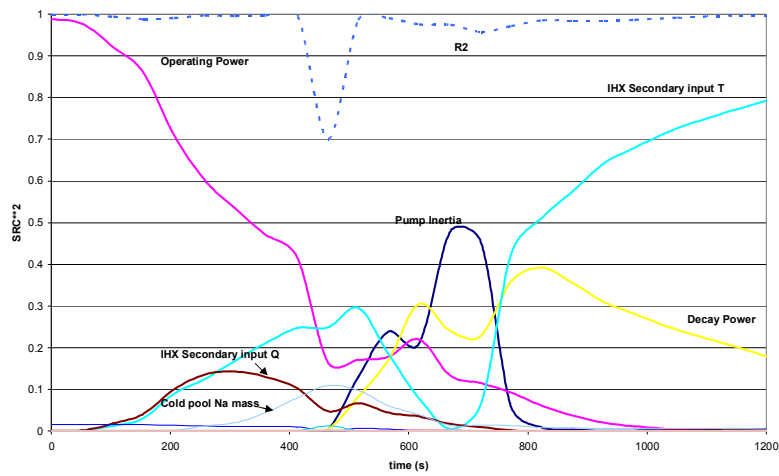


FIG. 150. R^2 and square of standard regression coefficients (SRC^2) between Na maximum temperature and the input parameters (short term).

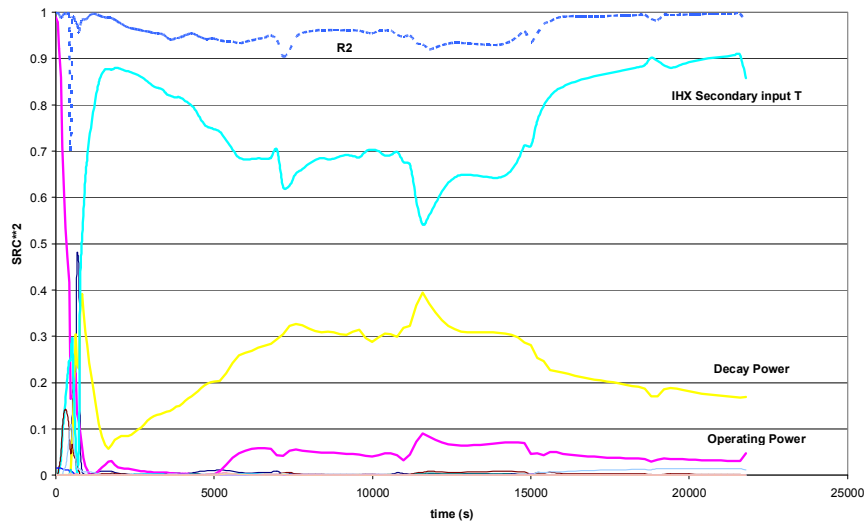


FIG. 151. R^2 and square of standard regression coefficients (SRC^2) between Na maximum temperature and the input parameters (long term).

Conclusion

The propagation of the uncertainties of selected input parameters has been carried out through the CATHARE code. The results of this propagation on several output parameters show a relative low influence of the input uncertainties on the temperatures (IHX, fuel, sodium at core exit) with variation interval often less than 10°C ; the uncertainty on the flow rate is also small (less than 2%) in the major part of the transient but it can reach 8% during the pumps stop.

The global sensitivity analysis enables to quantify the relative importance of the uncertain input parameters to some outputs. The fact that the relation between each analyzed output and the input parameters are generally linear has allowed the use of linear sensitivity indices (standard regression coefficients). This analysis which has been carried out all over the transient enables to evaluate the most influential parameters at each time important step.

The conclusion of this sensitivity analysis is that at long term during the second and the third step of the transient, the most influential parameter is the temperature at the inlet of the secondary side of the IHX, and to a lesser extent the operating power and the decay power. In the absence of modeling of the secondary circuits, the temperature and flow rate at the inlet of the secondary side of the IHX have been taken as boundary conditions. So a good precision on these conditions appears essential to an accurate evaluation of the transient at long term.

During the first step of the transient (from the beginning up to 700s), the pump inertia plays an important role on the flow rate and accordingly on the fuel temperature and on the sodium temperature at core outlet but it does not seem to affect the peak of sodium temperature at 1000s, whose uncertainty is mainly due to the secondary input temperature and to the decay power.

Among the selected input parameters, some have a very small influence on the outputs: the IHX pressure drop, the core flow rate, the hot pool sodium mass and the roof and vessel heat losses.

7.3. VALIDATION PERFORMED BY IGCAR, INDIA

7.3.1. 1-D Modelling features

An in-house developed Plant dynamics code has been modified as PHENIX-DYN to model primary circuit of PHENIX. Perfect mixing for all discrete volumes is assumed. Hot and cold pools are modeled as single mixing volumes and reactor core is modeled as 10 radial channels. 18 CVs are considered in axial direction for core. Radial power distribution in various zones is considered as per the supplied data and axial power distribution is considered according to flux distribution supplied. Hydraulic inertia of various segments is modeled as per the length and area data provided. Hydraulic resistance of various paths is modeled as per the flow and pressure drop data supplied. IHX is subdivided into 19 CVs.

Pump characteristics have been modeled using homologous characteristics corresponding to the given rated conditions. Pump coast down characteristics is modeled through inertia and drive resistance. Main vessel cooling circuit is not considered in the present analysis. Thermal inertia of cold pool region in the annulus between main vessel and inner vessel is considered as a part of the hot pool. Thermal inertia of diagrid is considered along with that of hot pool. Thermal inertia of shielding subassemblies is not considered. The secondary circuit is simulated with the boundary conditions of experimental data for IHX secondary inlet temperature and flow rate. Core power evolution is also used as input. The important uncertain parameters identified are listed in Table 33.

TABLE 33. IDENTIFIED UNCERTAIN PARAMETERS

Parameter	Distribution type	uncertainty
IHX pressure drop	normal	20%
Core pressure drop	normal	15%
Reactor operating power	normal	2.50%
Decay power	normal	5%
Flow through core	normal	5%
Heat transfer coefficient (fuel-clad)	normal	10%
Primary pumps trip delay time	normal	10%
Pump flow halving time	discrete	7-11 s
Clad thermal conductivity	normal	5%
Gap conductance	normal	10%
Specific heat of sodium	normal	5%
Viscosity of sodium	normal	5%
Density of sodium	normal	5%
IHX heat transfer area	discrete	10 – 40 tubes blocked

7.3.2. Analysis of results

The frequency plots for maximum hot pool temperature, fuel temperature, clad hot spot temperature and SA outlet temperature are shown from FIG. 152 to FIG. 155.

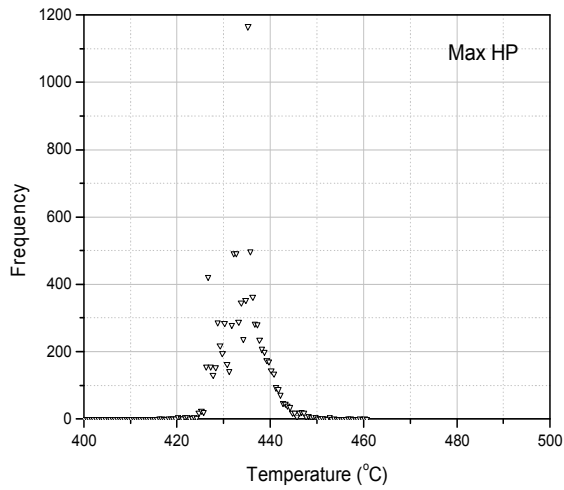


FIG. 152. Frequency distribution of maximum hot pool temperature.

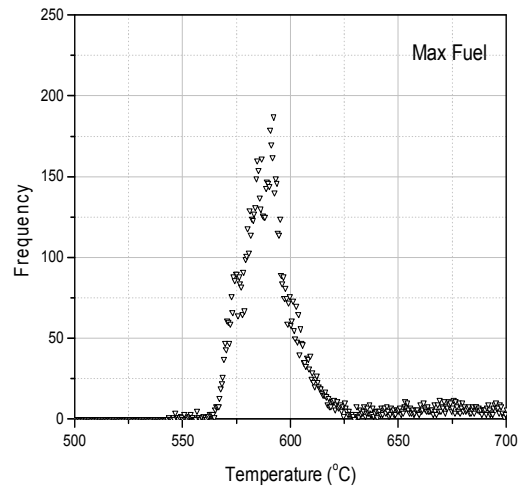


FIG. 153. Frequency distribution of maximum fuel temperature.

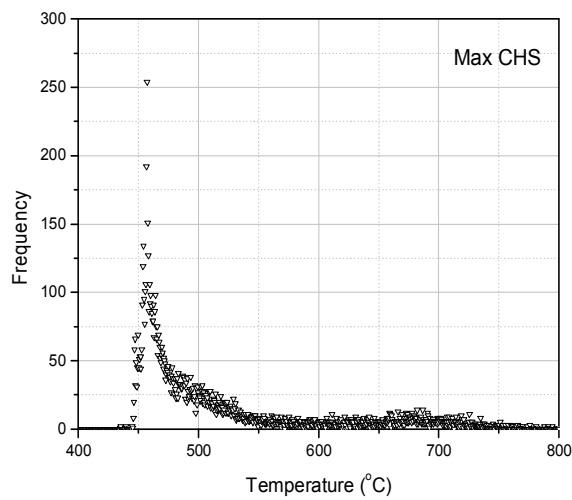


FIG. 154. Frequency distribution of maximum clad hot spot temperature.

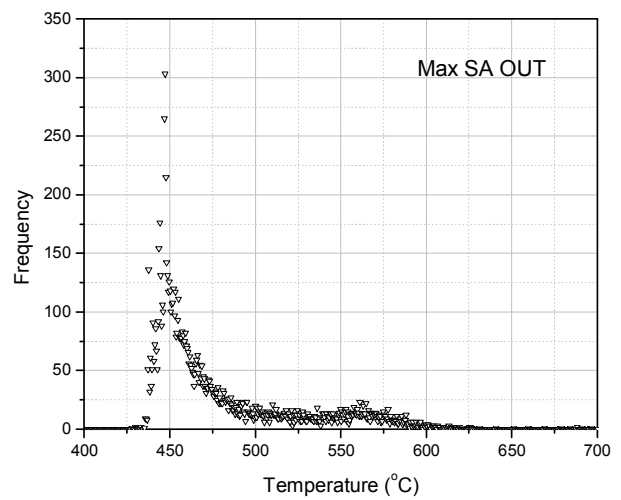


FIG. 155. Frequency distribution of maximum SA outlet temperature.

The frequency distribution of hot pool temperature, fuel temperature, clad hot spot temperature and SA outlet temperature at different instances are shown from FIG. 156 to FIG. 159.

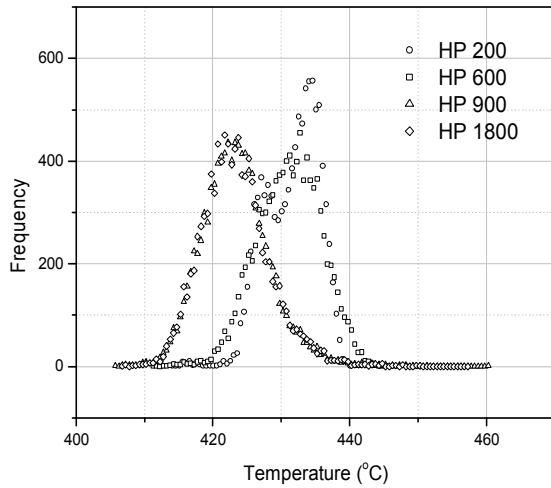


FIG. 156. Frequency distribution of hot pool temperature at different instances.

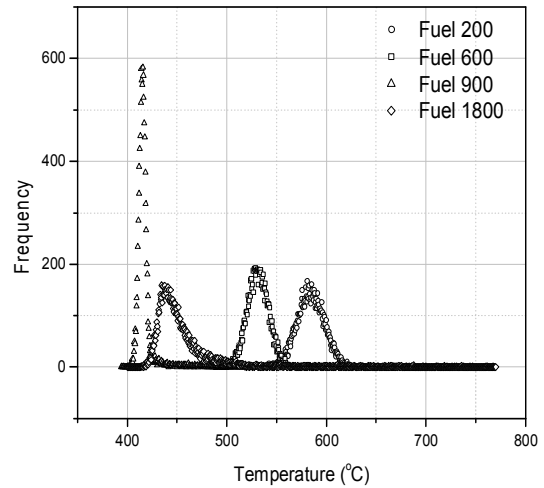


FIG. 157. Frequency distribution of fuel temperature at different instances.

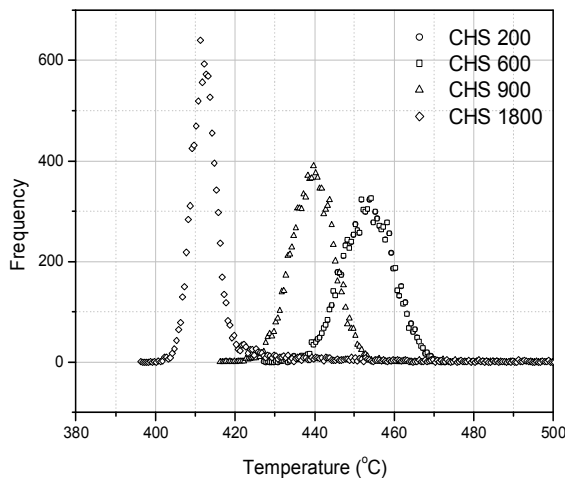


FIG. 158. Frequency distribution of clad hot spot temperature at different instances.

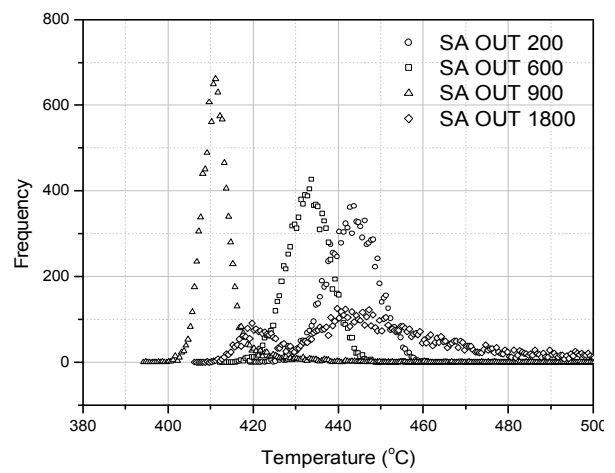


FIG. 159. Frequency distribution of SA outlet temperature at different instances.

Uncertainty in hot pool temperature prediction, fuel temperature prediction, clad hot spot temperature prediction and SA outlet temperature prediction are shown from FIG. 160 to FIG. 163.

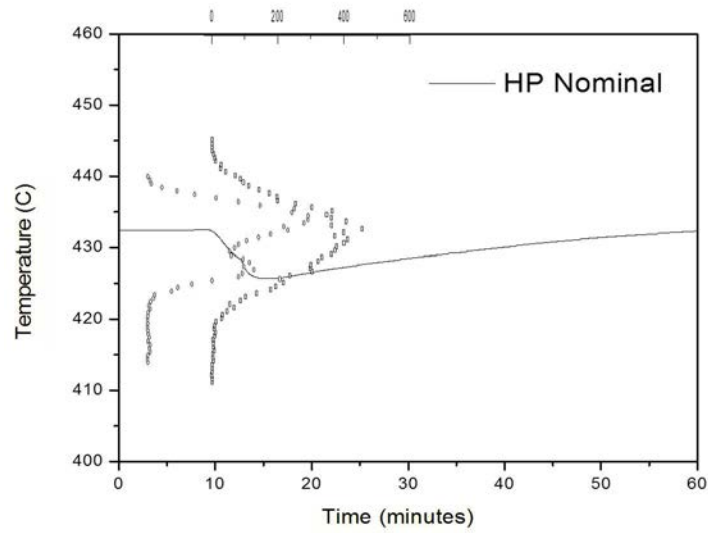


FIG. 160. Uncertainty in hot pool temperature prediction at various instances.

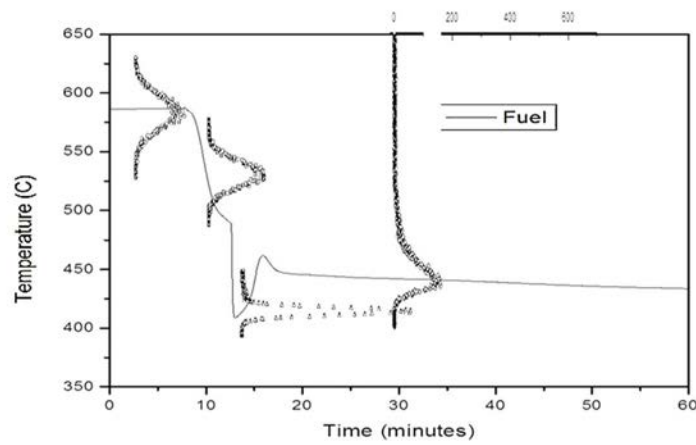


FIG. 161. Uncertainty in fuel temperature prediction at various instances.

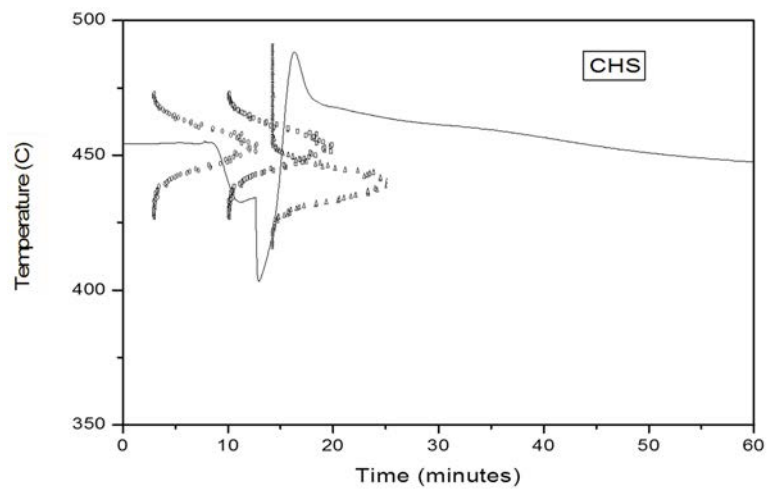


FIG. 162. Uncertainty in clad hot spot temperature prediction at various instances.

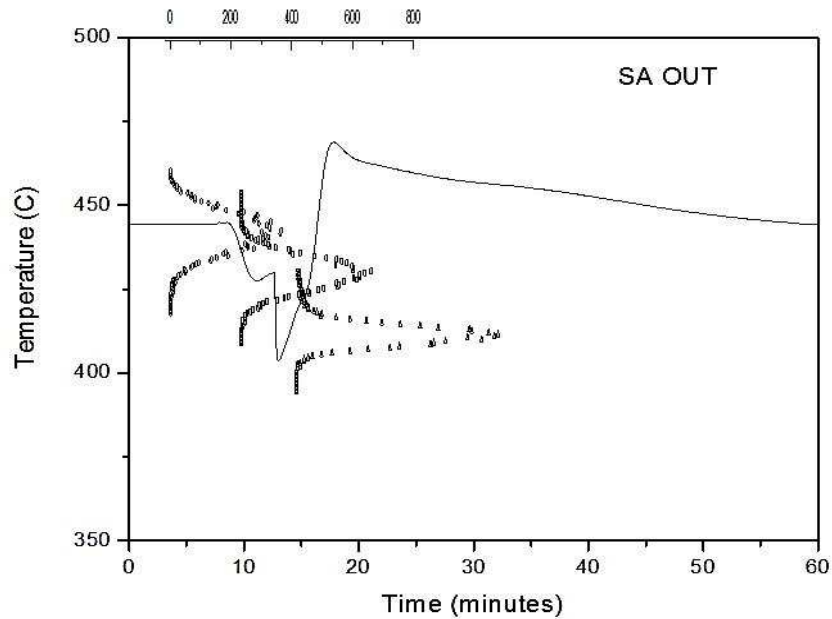


FIG. 163. Uncertainty in SA outlet temperature prediction at various instances.

Typical variation in temperature predicted by various codes is shown in FIG. 164.

Uncertainty in the response variables, especially maximum clad hot spot temperature and SA outlet temperature is asymmetric (skewed to right). Only fuel temp is asymmetric for 1800s. The 95 % range is 20°C. The variation observed due to 'other factors' is 50°C. This result indicates that there is need to identify and estimate the magnitude of deviations from 'other factors' (not considered in the usual list of parameters) and include into reliability predictions.

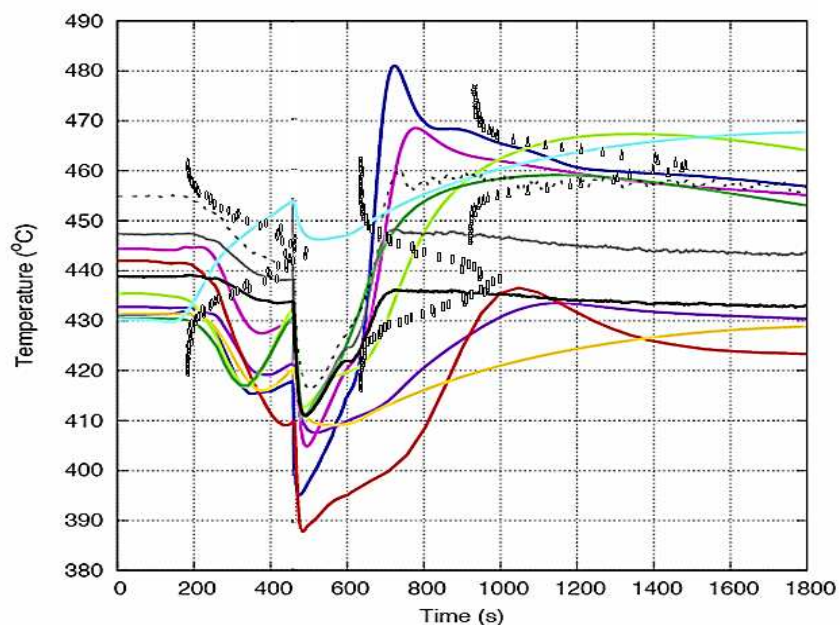


FIG. 164. Variation in temperature predicted by various codes.

8. CONCLUSIONS

The passive safety features have to be the new standard for all advanced reactors. This study has analysed the current state of the art for the assessment of the reliability of passive systems for extensive use in advanced small reactors. This study uncovers the insights on the technological issues associated with the assessment of reliability of the safety systems based on thermal – hydraulics, for which, methods are still in developing phase.

The principal conclusion of the CRP is that there is a clear need to obtain more data, especially related to thermal hydraulics. This necessitated additional development, testing and research. It is essential that passive and evolutionary components, Common Cause Failures (CCF) of high redundancy systems and intersystem CCF of such reactors are adequately addressed. The technical challenges for advanced reactors also include the potential need to address very different systems and phenomenology, the potential unavailability of important reliability and experimental data, the potential unavailability of knowledge on new key phenomena, and the potential unavailability of accident analysis models. Previously accepted modelling simplifications may no longer be appropriate for the advanced small reactor reliability assessment.

The other broad based conclusions are derived from the CRP are as follows:

- Failure of passive components and structures now more important in advanced reactor designs. The new and advanced Methodologies described in the report for the assessment of passive safety system reliability are considered as important tools and approaches to achieve improved safety for the future advanced nuclear power plants and particular attention should be paid to the status of development of the methodologies and the obtained results.
- The general consensus was that a more practical approach would be very helpful for the robust design and qualification of advanced nuclear reactors. The further promotion of international collaboration which needs to be enhanced in order to model the unique features of new reactors in key areas such as digital/software based I&C reliability and passive system high degree reliability modelling.
- Passive systems and passive PSA are becoming more and more important as technology evolves. The key element as to furthering development and use of passive systems is the decision to proceed with licensing and construction of an advanced reactor design.
- Facilitate information exchange and promote international collaborative research and development in the area of advanced nuclear reactor technologies needed to meet, in a sustainable manner, the increasing energy demands of the 21st century.

The following is the specific conclusions of the specific analysis/studies or individual country/institution participated in the CRP.

8.1. CONCLUSIONS FROM BARC, INDIA REGARDING VALIDATION OF METHODOLOGIES USING TESTS ON L2 NATURAL CIRCULATION LOOP

Dynamic behaviour of loop as a function of heat sink temperature, power transferred to the fluid and the vertical inclination was analysed. It was observed that with increasing power and heat sink temperature the natural circulation flow tends to be more stable. While the stability characteristics improve with power transferred to fluid, it seemed to be rather random with

heat sink temperature. Simulation results show that effects of inclination angle on the flow stability is minimal. Different flow regimes such as stable flow, unstable flow, mono directional pulsing and bidirectional pulsing have been observed during the investigation. Comparison between numerical predictions and experiment show that while the results of numerical study are in good agreement at low power and low heat sink temperature but differ at high power and/or high heat sink temperature.

8.2. CONCLUSIONS FROM THE UNIVERSITY OF PISA, ITALY REGARDING VALIDATION OF METHODOLOGIES USING TESTS ON L2 NATURAL CIRCULATION LOOP

The application of the REPAS/RMPS has shown that the methodology is able to calculate the reliability of the system, while from the experimental point of view, the lack of some information as the real thickness of the tubes of the facility and the measurement of the power is the reason why the performance indicator of the system cannot be evaluated properly.

At the end is possible to conclude that this activity has a relevant scientific value because the capability of the REPAS/RMPS to simulate the behaviour of the natural circulation loop L2 has been highlighted and from the experimental point of view represents a good test for the design of new future qualification activities.

8.3. CONCLUSIONS REGARDING APPLICATION OF RESPONSE CONDITIONING METHOD TO SGDHRs

Functional reliability analysis is carried out for the SGDHRs using the overall approach reported in the RMPS. Important parameters that affect the performance of the SGDHRs are identified. Probable ranges of variation of the parameters are estimated and suitable probability distributions were assigned based on experimental data analysis and expert judgment. System failure criteria were identified consistent with the conditions defined for probabilistic safety analysis. The uncertainty in the critical parameters was propagated using the DHDYN code to get the variation in the system response. From a set of 100 code runs multi response surface model for five important responses were constructed. By considering the uncertainties associated with high dimension response surfaces while evaluating small probabilities, here response surfaces are not used directly to evaluate system failure probability. On the other hand, the information obtained from the response surfaces about the system failure region is used to make conditional stratified samples. The system failure probability is evaluated from these conditional samples. The conditional samples are generated by subset simulation of response surfaces.

The probability of functional failure of SGDHRs to limit temperatures of critical structures to their DSL, is dependent on the number and duration of loop availability during the initial few hours of mission. The evaluated functional failure probabilities on various possible hardware system configurations vary from $1.0E-2/de$ to $<1.0E-7/de$ for category 4 design safety limits. Functional failure probabilities are also evaluated with respect to category 3 design safety limits.

8.4.CONCLUSIONS FROM CNEA, ARGENTINA REGARDING COMPARISON OF DIFFERENT METHODOLOGIES FOR A BENCHMARK PROBLEM OF ISOLATION CONDENSER

The RMPS methodology was improved, tested and used to probabilistically quantify the performance of passive safety systems in order to verify the fulfilment of design criteria.

A sensitive point observed in the methodology is the selection of the performance indicator (i.e. output observable). Its adequacy sustains the results from direct Monte Carlo simulations and the calculations based on surrogate model; therefore, the performance indicator must be strictly linked to the design failure criteria and its definition have to assure that the correct system's phenomenology is encompassed. Then the performance indicator definition is not a straight forward task, and is important to dedicate them a considerably effort.

Finally we can conclude that the improved methodology (RMPS+) was very useful in order to accomplish the objectives proposed for the present work.

8.5.CONCLUSIONS FROM BARC, INDIA REGARDING COMPARISON OF DIFFERENT METHODOLOGIES FOR A BENCHMARK PROBLEM OF ISOLATION CONDENSER

Evaluation of passive system reliability is a challenging task. It involves a clear understanding of the operation and failure mechanism and failure criteria for the system which the designer must identify prior to prediction of its reliability. Besides, applicability of the existing best estimate codes to the reliability assessment of passive systems is neither proven nor understood enough due to lack of sufficient plant/experimental data. Thus, assessing the uncertainties of the best estimate codes when applied to passive system safety analysis further add to the complexity. However, the best estimate code RELAP5/MOD3.2 has been used to demonstrate the application of APSRA methodology for reliability assessment of passive decay heat removal system of ALWR. The failure frequency is found to be $3.8e-3/\text{demand}$.

8.6.CONCLUSIONS REGARDING UNCERTAINTY CALCULATIONS ON THE PHENIX NATURAL CONVECTION TEST

The propagation of the uncertainties of selected input parameters has been carried out through the CATHARE code. The results of this propagation on several output parameters show a relative low influence of the input uncertainties on the temperatures (IHX, fuel, sodium at core exit) with variation interval often less than 10°C ; the uncertainty on the flow rate is also small (less than 2%) in the major part of the transient but it can reach 8% during the pumps stop.

The global sensitivity analysis enables to quantify the relative importance of the uncertain input parameters to some outputs. The fact that the relation between each analyzed output and the input parameters are generally linear has allowed the use of linear sensitivity indices (standard regression coefficients). This analysis which has been carried out all over the transient enables to evaluate the most influential parameters at each time important step.

The conclusion of this sensitivity analysis is that at long term during the second and the third step of the transient, the most influential parameter is the temperature at the inlet of the secondary side of the IHX, and to a lesser extent the operating power and the decay power. In the absence of modelling of the secondary circuits, the temperature and flow rate at the inlet

of the secondary side of the IHX have been taken as boundary conditions. So a good precision on these conditions appears essential to an accurate evaluation of the transient at long term.

During the first step of the transient (from the beginning up to 700s), the pump inertia plays an important role on the flow rate and accordingly on the fuel temperature and on the sodium temperature at core outlet but it does not seem to affect the peak of sodium temperature at 1000s, whose uncertainty is mainly due to the secondary input temperature and to the decay power.

APPENDIX I PASSIVE SAFETY SYSTEMS IN ADVANCED SMALL MODULAR REACTORS

This section describes the passive safety systems employed in the following advanced small modular reactors:

- AHWR 300 LEU
- CAREM-25
- SMART
- NuScale
- mPower
- ACP100
- IRIS

The reader should consider that the description of passive safety systems of selected designs does not imply a preference relative to other advanced small reactors that are not described.

I.1. AHWR300-LEU (Bhabha Atomic Research Centre, India)

The advanced heavy water reactor (AHWR) is a 300 MW(e) boiling light water cooled, heavy water moderated, vertical pressure tube type reactor designed to produce most of its power from thorium with an associated 500 m³/day capacity desalination plant. The core consists of (Th-U₂₃₃) O₂ and (Th-Pu)O₂ fuel. A simplified sketch of the reactor is depicted in FIG. 165. A number of passive systems that utilize natural circulation have been incorporated in AHWR.

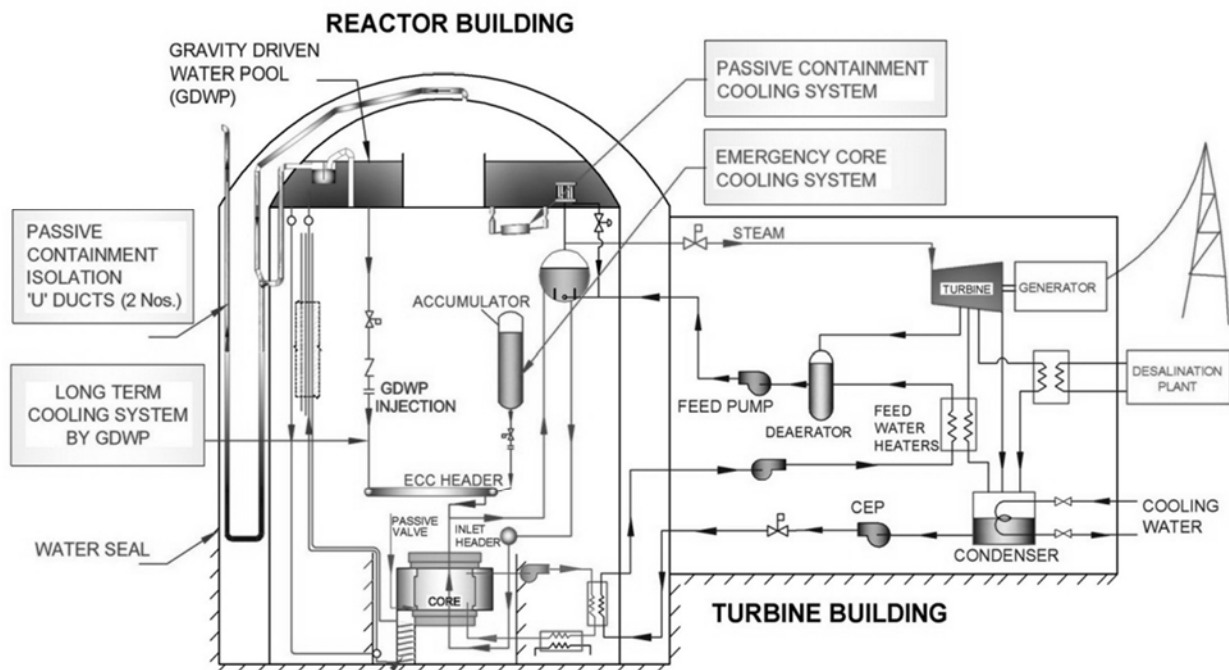


FIG. 165. Simplified flow sheet of AHWR.

Some of them are briefly described.

Passive core cooling system

In AHWR, natural circulation is used to remove heat from the reactor core under normal as well as shutdown conditions. Figure 166 shows the main heat transport (MHT) System and the passive decay heat removal system of AHWR. The two-phase steam water mixture generated in the core flows through the tail pipes to the steam drum, where steam gets separated from water. The separated water mixes with the sub-cooled feed water and flows down the downcomers to the reactor inlet header. From the header it flows back to the core through inlet feeders.

Larger density differences between hot and cold legs are possible to be achieved in two-phase flow systems compared to single-phase natural circulation flow systems. The absence of pumps not only reduces operating cost, but also eliminates all postulated transients and accidents involving failure of pumps and pump power supply.

Steady state flow prevails in a natural circulation loop when the driving buoyancy force is balanced by the retarding frictional forces. However, the driving force in a natural circulation system is much lower compared to a forced circulation system. With a low driving force, measures are needed to reduce the frictional losses. The methods adopted to reduce frictional losses include, elimination of mechanical separators in the steam drum and the use of large diameter piping. The larger pipes increase the amount of coolant needed in the primary system.

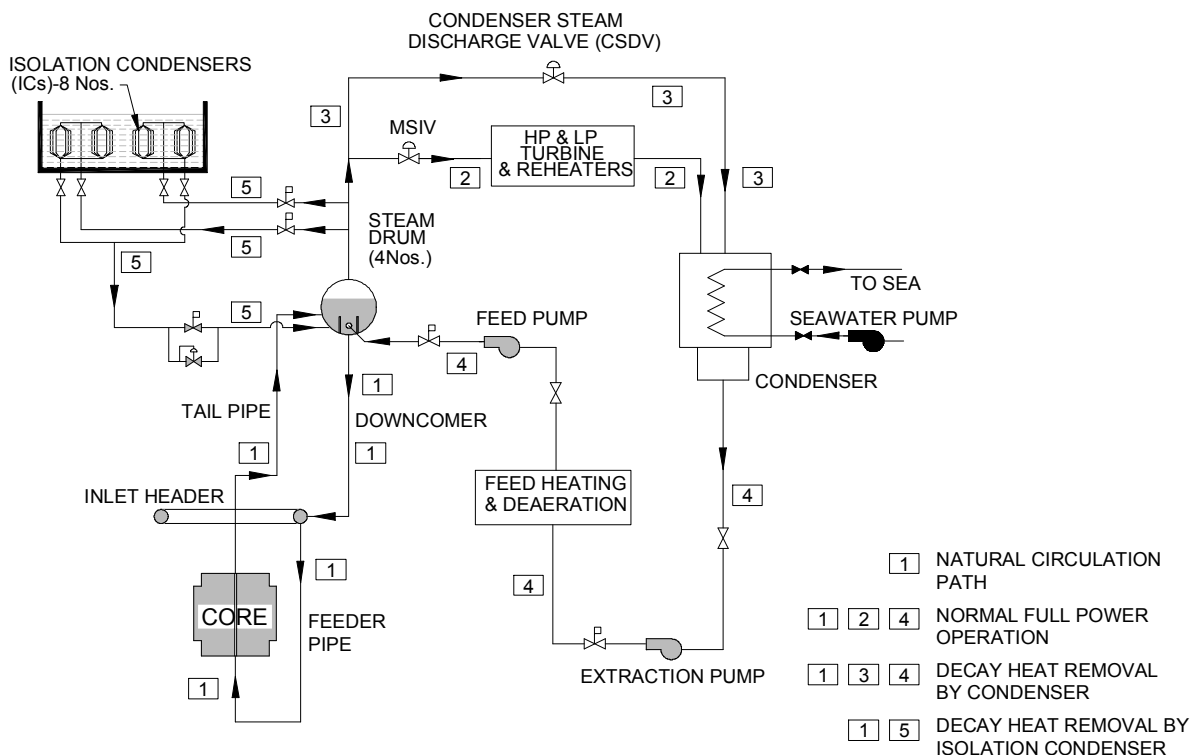


FIG. 166. MHT and decay heat removal system.

Elimination of mechanical separators makes the system dependent on natural gravity separation at the surface in the steam drum, which may increase carryover and carryunder. Carryover is the fraction of the liquid entrained by the steam, whereas carryunder is the fraction of vapor that is carried by the liquid flowing into the downcomer. Excessive carryover can damage the turbine blades due to erosion, whereas carryunder can significantly reduce the driving buoyancy force and hence the natural circulation flow rate. The steam drum size is chosen to keep carryunder and carryover within acceptable limits.

A rational start-up procedure of the AHWR has been worked out for low pressure and temperature conditions. For this, after the MHT is filled with water to a desired level in the steam drum, the MHT system is pressurized to an initial desired pressure by using steam generated from an external boiler. Subsequently, the control rods are partially withdrawn and coolant heating up continues at about 2 % full power. Core boiling will start only after the steam drum pressure reaches 70 bar and the coolant temperature attains 285°C. The reactor power is increased gradually with controlled sub-cooling at the inlet of the reactor core until full power is reached.

Emergency core cooling system (ECCS) is designed to remove the core heat by passive means in case of a postulated loss of coolant accident (LOCA). In the event of rupture in the primary coolant pressure boundary, the cooling is initially achieved by a large flow of cold water from high pressure accumulators. Later, cooling of the core is achieved for three days by low pressure injection of cold water from gravity driven water pool (GDWP) located near the top of the reactor building. The emergency core cooling system is shown in FIG. 165.

Core decay heat removal system

During normal reactor shut down core decay heat is removed by passive means utilizing isolation condensers (ICs) immersed in a gravity driven water pool (GDWP) located above the steam drum. Core decay heat, in the form of steam enters the IC tube bundles. The steam condenses inside the tubes and heat is transferred to the surrounding water pool. The condensate returns by gravity to the steam drum. The water inventory in the GDWP is adequate to cool the core for more than 3 days without any operator intervention and without boiling of GDWP water. Figure 166 depicts the core decay heat removal system comprising isolation condensers. A separate GDWP cooling system is provided to cool the GDWP inventory in case the temperature of GDWP inventory rises above a set value.

GDWP as ultimate heat sink

Isolation condensers (ICs) for removal of decay heat are immersed in the gravity driven water pool (GDWP). The pool is having a capacity of 6000 m³ of water and is divided into 8 symmetry sectors, each containing one IC. In normal operation the pool water circulates through heat exchangers to maintain the pool temperature. Figure 165 shows the recirculation and cooling system of GDWP water. The decay heat generated in the reactor during shut down is stored in the form of sensible heat of water. However, stratification may influence heat transfer to pool to a great extent and heat storage capacity of the pool in the form of sensible heat is significantly reduced. The GDWP also acts as heat sink for passive containment cooling system (FIG. 167).

Passive containment cooling system

Containment is a key component of the mitigation part of the defence in depth philosophy, since it is the last barrier designed to prevent large radioactive release to the environment.

In advanced heavy water reactor (AHWR), a passive containment cooling system (PCCS) is envisaged which can remove long term heat from containment following loss of coolant accident (LOCA). Immediately following LOCA, steam released is condensed in water pool by vapor suppression system. For subsequent long term cooling, PCCS is provided. PCCS, by definition is able to carry out its function with no reliance on external source of energy.

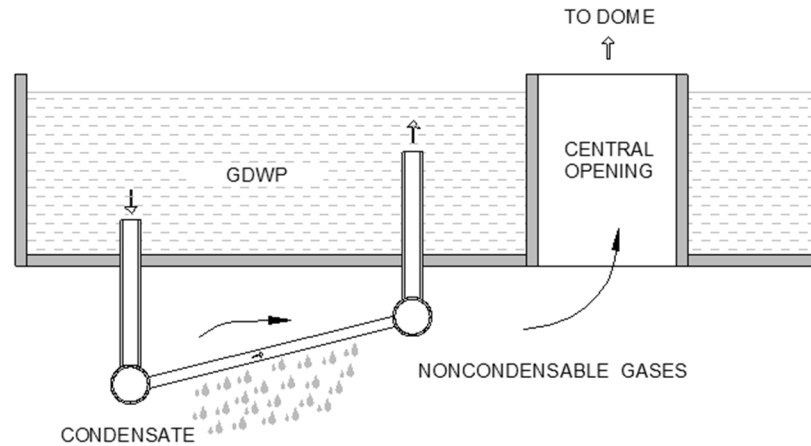


FIG. 167. Schematic of passive external condenser.

As mentioned earlier, gravity driven water pool acts as the heat sink for a number of passive heat removal systems including the PCCS. The passive external condensers (PECs) of the PCCS are connected to the pool as shown in FIG. 167. The containment steam condenses on the outer surface of the tubes of PEC. The water inside the tubes takes up heat from air/vapor mixture and gets heated up. Due to the heating up of water, the natural circulation of water from the pool to PEC and from PEC to pool is established.

One important aspect of PCCS functioning is the potential degradation of heat transfer on PEC outer surface due to the presence of noncondensable gases in the containment. The presence of noncondensable (NC) gases in vapor can greatly inhibit the condensation process. Extensive R&D work is in progress to address this issue. Another aspect of PCCS functioning is the blockage of passive external condenser by noncondensable gas due to the stratification of noncondensable gas/vapor in the containment. In case of AHWR, the noncondensable gas is likely to escape through the central opening provided in the GDWP to the dome region. Experiments are planned to confirm this.

I.2. CAREM-25 (National Atomic Energy Commission, Argentina)

CAREM-25 is an Argentine project to achieve the development, design, and construction of an innovative simple and small NPP, which is jointly developed by CNEA (National Atomic Energy Commission) and INVAP. This nuclear plant has an indirect cycle reactor with some distinctive and characteristic features that greatly simplify the design, and contributes to a higher safety level. Some of the high level design characteristics of the plant are: integrated primary cooling system, self-pressurized primary system and safety systems relying on passive features.

The CAREM concept was first presented in March 1984 in Lima, Peru, during the IAEA conference on small and medium size reactors. CAREM was, chronologically, one of the first of the present new generation of reactor designs. The first step of this project is the

construction of the prototype of about 27 MW(e) (CAREM-25). CAREM has been recognized as an international near term deployment (INTD) reactor by the Generation IV International Forum (GIF).

Description of passive core cooling system

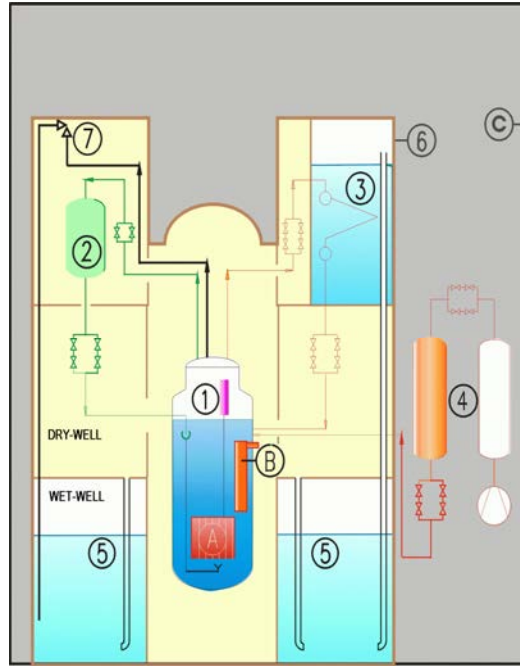
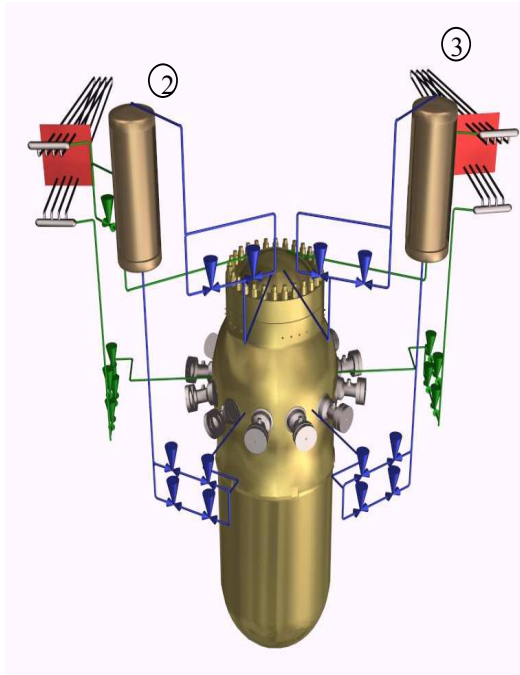
The CAREM nuclear power plant design is based on a light water integrated reactor. The whole high-energy primary system, core, steam generators, primary coolant and steam dome, is contained inside a single pressure vessel (FIG. 168).

For low power modules (below 150 MW(e)), the flow rate in the reactor primary systems is achieved by natural circulation. Figure 168 shows a diagram of the natural circulation of the coolant in the primary system. Water enters the core from the lower plenum. After it's heated the coolant exits the core and flows up through the riser to the upper dome. In the upper part, water leaves the riser through lateral windows to the external region. Then it flows down through modular steam generators, decreasing its enthalpy. Finally, the coolant exits the steam generators and flows down through the down-comer to the lower plenum, closing the circuit. The driving forces obtained by the differences in the density along the circuit are balanced by the friction and form losses, producing the adequate flow rate in the core in order to have the sufficient thermal margin to critical phenomena. Reactor coolant natural circulation is produced by the location of the steam generators above the core.

Description of the residual heat removal system

CAREM safety systems are based on passive features that don't require active actions to mitigate accidents for a long period. They are duplicated to fulfil the redundancy criteria. One of them that relies on natural circulation is the residual heat removal system (RHRS) shown in FIG. 168. It has been designed to mitigate a loss of heat sink, reducing the pressure of the primary system to values lower than the values at hot shutdown, by removing the decay heat. The RHRS is a simple and reliable system that operates condensing steam from the reactor dome in the emergency condensers. This establishes a stratified two-phase natural circulation loop with the primary system.

The emergency condensers are heat exchangers consisting of an arrangement of parallel horizontal U tubes between two common headers. The top header is connected to the reactor vessel steam dome, while the lower header is connected to the reactor vessel at a position below the reactor water level. The condensers are located in a pool filled with cold water inside the containment building. The inlet valves in the steam line are always open, while the outlet valves are normally closed, therefore the tube bundles are filled with condensate. When the system is triggered, the outlet valves open automatically. The water drains from the tubes and steam from the primary system enters the tube bundles and condenses on the cold surface of the tubes. The condensate is returned to the reactor vessel forming a natural circulation circuit. In this way, heat is removed from the reactor coolant. During the condensation process the heat is transferred to the pool water by boiling process. This evaporated water is then condensed in the suppression pool of the containment. The pool of the RHRS has a volume sufficient to provide autonomy greater than the grace period for the prototype (48 hrs).



1: First shutdown system

2: Second shutdown system

3: Residual heat removal system

4: Emergency injection system

5: Pressure suppression pool

6: Containment

7: Safety valves

A: Core; B: Steam generator; C: Reactor building

FIG. 168. Safety systems of CAREM-25.

The RHRS main characteristics are listed in Table 34.

TABLE 34. RESIDUAL HEAT REMOVAL SYSTEM–EMERGENCY CONDENSER FOR CAREM PROTOTYPE

Operation Mode	Steam Condensation
Maximum Power of one module (at reactor nominal operational conditions)	2 MW
Tube length	13.3 m
Tube external diameter	60.3 mm
Tube inner diameter	42.8 mm
Redundancy	Condenser 2 x 100%
Valves	4 x 100 %
Autonomy	> 48 hours

In case of a very small LOCA (smaller than 3/4 in) the RHRS is also demanded by the reactor protection system to depressurize the primary system to allow the emergency injection system to act.

I.3. SMART (Korea Atomic Energy Research Institute, Republic of Korea)

The SMART (System Integrated Modular Advanced Reactor) is an advanced pressurized light water reactor that is being continuously studied at KAERI (Korea Atomic Energy Research Institute) with a rated thermal power of 330 MW. The reactor is proposed to be utilized as an energy source for sea water desalination as well as for small scale power generation. Advanced technologies such as inherent and passive safety features are incorporated in establishing the design concepts to achieve inherent safety, enhanced operational flexibility, and good economy. The SMART is designed to supply 40000 tons of fresh water per day and 90MW of electricity to an area with an approximate population of 100000 or an industrialized complex. In order to demonstrate the relevant technologies incorporated in the SMART design, the SMART-P (i.e. a pilot plant of the SMART) project is currently underway at KAERI. SMART received standard design approval (SDA) on 4 July 2012.

The prominent design feature of SMART is the adoption of integral arrangement. The major components of the NSSS such as the core, steam generators, main coolant pumps, and pressurizer are integrated into a reactor vessel without any pipe connections between those components. The schematic diagram of the SMART NSSS is shown in FIG. 169.

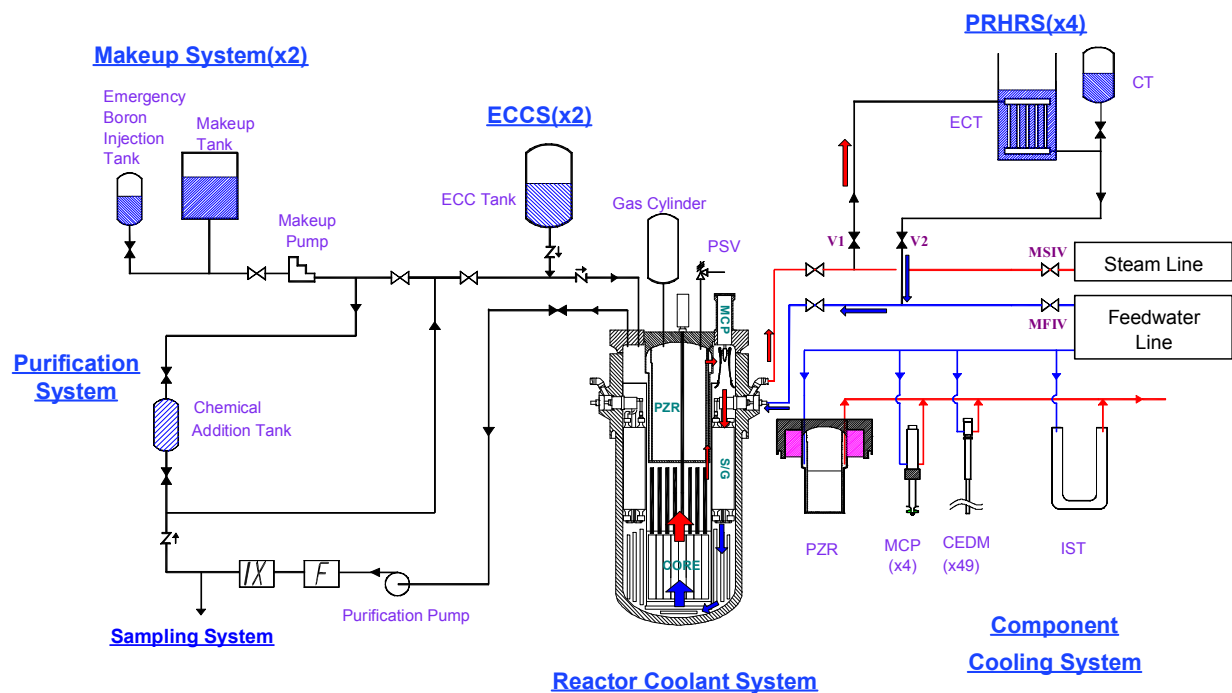


FIG. 169. Schematic diagram of the SMART NSSS.

The SMART core is currently being designed with the fuel design based on existing Korea optimized fuel assembly (KOFA) which is in 17x17 rectangular rod arrays. The SMART core design is characterized by an ultra long operation cycle with a single or modified single batch reload scheme, low core power density, soluble boron-free operation, enhanced safety with a large negative moderator temperature coefficient (MTC) at any time during the fuel cycle, a large thermal margin, inherently free from xenon oscillation instability, and minimum rod motion for the load follow with coolant temperature control. Due to soluble boron-free operation, an important design requirement for the SMART CRDM is a fine maneuvering capability to control the excess core reactivity. A linear step motor type CRDM is employed

for easy maintenance. The minimum step length is 4mm that is short enough for the fine reactivity control. 49 CRDMs are installed in 57 fuel assemblies of the SMART core.

Twelve identical steam generators (SGs) cassettes are located in the annulus formed by the reactor pressure vessel (RPV) and the core support barrel. Each SG cassette is a once-through type with helically coiled tubes wound around the inner shell. The primary coolant flows downward in the shell side of the SG tubes, while the secondary feedwater flows upward in the tube side. Therefore, the tubes are under compressive loads from the greater primary pressure, reducing the stress corrosion cracking and thus reducing the probability of tube rupture. The 40°C superheated steam at the exit of the helically coiled tubes eliminates the necessity of a steam separator during normal operations. The twelve SGs are divided into four sections. Each section consists of the neighboring three steam generator cassettes which are connected together with the steam and feedwater pipes. If there is a leakage in one or more of the tubes, the relevant section is isolated and SMART can be operated with reduced power until the scheduled shutdown.

The SMART adopted an in-vessel self-controlled pressurizer (PZR) located in the upper space of the RPV. The volume of the PZR is filled with water, steam, and nitrogen gas. The self-pressurizing design eliminates the active mechanisms such as spray and heater. The system pressure is determined by a sum of the steam and nitrogen partial pressures. In order to minimize the contribution of the steam partial pressure, a PZR cooler is installed for maintaining the low PZR temperature, and wet thermal insulator is installed to reduce the heat transfer from the primary coolant. The coolant temperature of the core outlet is controlled during a power maneuvering so as to minimize the system pressure variation by counterbalancing the increase of the coolant volume of the hot part with the decrease of the coolant volume of the cold part.

The SMART MCP is a canned motor type pump that eliminates the problems connected with conventional seals and associated systems. Four MCPs are installed vertically on the RPV annular cover. MCP is an integral unit consisting of a canned asynchronous 3-phase motor and an axial flow single-stage pump. The motor and pump are connected through a common shaft rotating on three radial and one axial thrust bearings. The impeller draws the coolant from above and discharges downward directly to the SG. This design minimizes the pressure loss of the flow.

There are many inherent safety features in the SMART design. Those include a large negative moderator temperature coefficient due to the boron-free operation, a low core power density, and the reduced xenon oscillations. Furthermore, enhanced safety of the SMART is accomplished with highly reliable engineered safety systems. The engineered safety systems consist of a reactor shutdown system, passive residual heat removal system, emergency core cooling system, safety vessel, reactor overpressure protection system and containment overpressure protection system. As the result of the probabilistic safety assessments for 10 internal events, the core meltdown frequency is predicted as 8.56×10^{-7} .

Description of passive residual heat removal system

The passive residual heat removal system (PRHRS) is designed to remove the core decay heat during the accident conditions when the active systems are not available. In the case of a normal shutdown of the SMART, the residual heat is removed through the steam generators by a turbine bypass system. During accident conditions, the coolant temperature of the primary system goes down to a certain lower level due to the heat transfer through steam

generators that is attained by the natural circulation flow paths established in the primary and the secondary systems of the SMART. The PRHRS consists of four independent trains with 50% of the heat removal capacity for each train. Two trains are sufficient to remove the decay heat generated in the primary system after the reactor trip. Each train is composed of an emergency cool down tank (ECT), a condensation heat exchanger, a compensating tank (CT), and several valves, pipes, and instrumentations as shown in the FIG. 169. The condensation heat exchanger consists of inlet and outlet headers connected with several straight tubes for the heat exchange with the inner diameter of 13 mm. The compensating tank is filled with the water and pressurized nitrogen gas, which can be used to make up the losses of initial inventory in the PRHRS. The system is designed to prevent core damage for 72 hours after the postulated design basis accidents without any corrective actions by operators.

Three natural circulation circuits are involved in the operation of the PRHRS. In case of design basis events, the main steam isolation valve (MSIV) and the main feed water isolation valve (MFIV) are closed automatically according to the reactor trip signal. After the automatic opening of the cut-off valves (V1 and V2), a natural circulation path is established between the heat exchanger in ECT and the steam generator due to the density difference of the two elevations. The ECT is located high enough relative to the steam generator in order to retain the heat removal capability during the events by supplying sufficient driving forces to the natural circulation flow. In the primary system, after the RCP trip, a natural circulation path is established between the reactor core and the steam generators. The decay heat generated in the reactor core is transported to the steam generators by the natural circulation flow. The third natural circulation path is established around the heat exchanger inside the ECT. The heat carried by the natural circulation flow in the primary and secondary systems is transferred to the ultimate heat sink through the natural convection at the vicinity of the heat exchanger.

I.4. NUSCALE (NuScale Power, Inc., USA)

In 2003, Oregon State University, in collaboration with the Idaho National Engineering Laboratory, and Nexant-Bechtel, completed a project to develop a preliminary design for an innovative reactor called the 'Multi-Application Small Light Water Reactor', or 'MASLWR'. The final results were published by the project sponsor, the U.S. Department of Energy and a description of the MASLWR design was included in Ref. [4]. Since then Oregon State University continued to advance the concept with proprietary modifications for which US and international patents are currently being reviewed.

In 2007, NuScale Power Inc. was formed to commercialize the concept, and MASLWR was renamed to the NuScalePlant to reflect the significant improvements made to the original design. In early 2008, NuScale Power notified the U.S. Nuclear Regulatory Commission of its intent to begin Pre-Application discussions aimed at submitting an application for Design Certification of a twelve module NuScale Power Plant.

A NuScale plant consists of 1 to 12 independent modules, each capable of producing a net electric power of 45 MW(e). Each module includes a Pressurized Light Water Reactor operated under natural circulation primary flow conditions. Each reactor is housed within its own high pressure containment vessel which is submerged underwater in a stainless steel lined concrete pool. The cross-sectional view of NuScale reactor building is shown in FIG. 170.



FIG. 170. Cross sectional view of NuScale reactor building.

Description of NuScale passive safety systems

The NuScale plant includes a comprehensive set of engineered safety features designed to provide stable long term nuclear core cooling under all conditions, as well as severe accident mitigation. They include a high pressure containment vessel, two passive decay heat removal and containment heat removal systems, a shutdown accumulator, and severe accident mitigation.

Each NuScale module has its own set of independent passive safety systems. The entire nuclear steam supply system (NSSS) including its containment, is immersed in a pool of water capable of absorbing all decay heat generated following a reactor shutdown for 72 hours without exceeding a bulk fluid temperature of 93°C (200°F). The water is contained in a stainless steel lined concrete structure that is entirely below grade.

Each NuScale module includes two redundant passive safety systems to provide pathways for decay heat to reach the containment pool: the decay heat removal system (DHRS) and the containment heat removal system (CHRS). These systems do not require external power for actuation.

The DHRS, shown in FIG. 171, uses either of the two independent helical coil steam generator tube bundles to transfer heat generated within the core to the containment pool. Feedwater accumulators provide initial feed flow while DHRS transitions to natural circulation flow

The CHRS, shown in FIG. 172, provides a means of removing core decay heat in the event the steam generator tube bundles are not available. It operates by opening the vent valves located on the reactor head. Primary system steam is vented from the reactor vessel into the containment where it condenses on the containment surfaces. The condensate collects in the lower containment region (sump). When the liquid level in the containment sump rises above the top of the recirculation valves, the recirculation valves are opened to provide a natural circulation path from the sump through the core and out of the reactor vent valves.

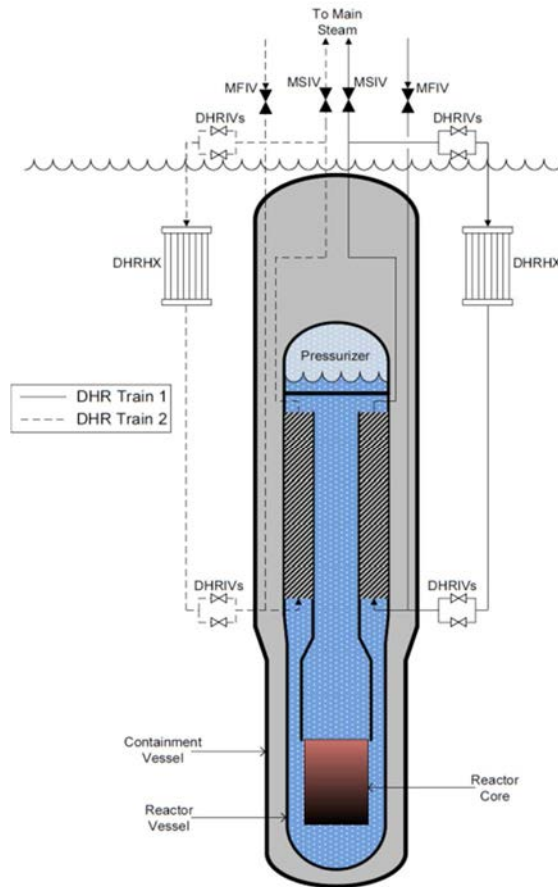


FIG. 171. Passive decay heat removal system (DHR).

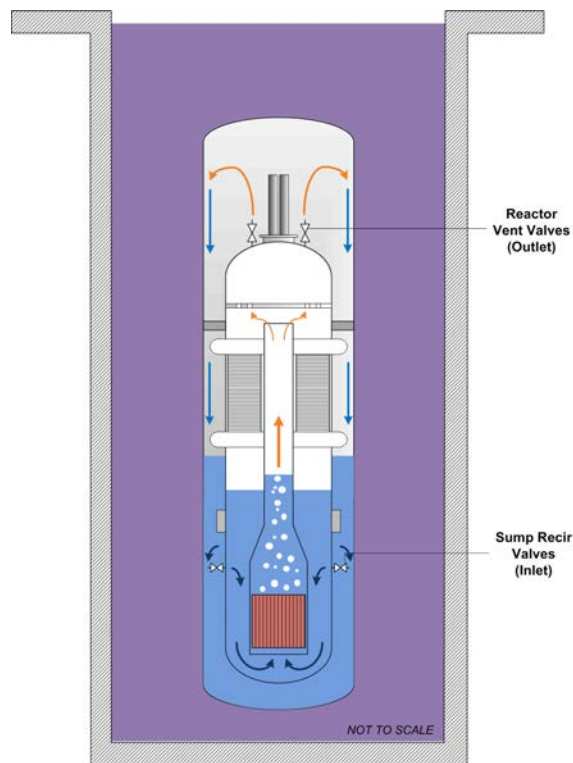


FIG. 172. Passive containment heat removal system (CHRS).

I.5. MPOWER (B&W Generation mPower Inc., USA)

The B&W mPower™ reactor module is an integral PWR designed by B&W to generate an output of 180 MW(e).

Description of passive safety systems

The inherent safety features of the reactor design include a low core linear heat rate which reduces fuel and cladding temperatures during accidents, a large reactor coolant system volume which allows more time for safety system responses in the event of an accident, and small penetrations at high elevations, increasing the amount of coolant available to mitigate a small break LOCA. The emergency core cooling system is connected with the reactor coolant inventory purification system and removes heat from the reactor core after anticipated transients in a passive manner, while also passively reducing containment pressure and temperature. The plant is designed without taking credit for safety related emergency diesel generators, and a design objective is no core uncovering during design basis accidents.

A large pipe break LOCA is not possible because the primary components are located inside the pressure vessel and the maximum diameter of the connected piping is less than 7.6 cm.

The mPower reactor deploys a decay heat removal strategy (shown in FIG. 173) with a passive heat exchanger connected with the ultimate heat sink, an auxiliary steam condenser on the secondary system, water injection or cavity flooding using the reactor water storage tank, and passive containment cooling.

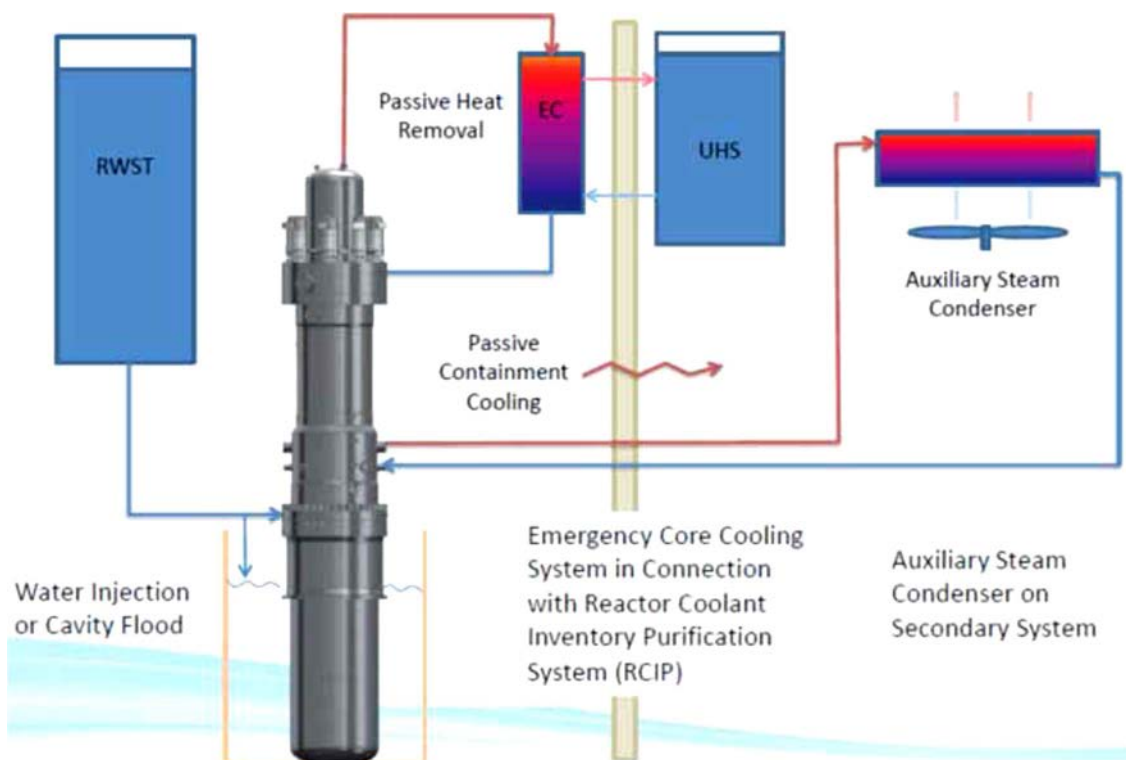


FIG. 173. Decay heat removal strategy.

I.6. ACP100 (China National Nuclear Corporation, China)

The ACP100 is being developed by China National Nuclear Corporation (CNNC). It is an integral pressurized water reactor (iPWR) with a rated power of 100 MW(e). The reactor is proposed to be utilized for electricity generation, heat or desalination. A plant utilizing the design will have a flexible configuration, with between one and eight modules. A number of passive systems have been incorporated in ACP100. Some of them are described below.

Passive residual heat removal system

The passive residual heat removal system (PRHRS) of ACP100 consists of PRHR heat exchanger (HX) and injection water storage tank (IWST) as shown in FIG. 174. The PRHR HX is mounted in IWST. The temperature and elevation of PRHR HX provides thermal driving head. Due to natural circulation or forced flow (if reactor coolant pumps (RCPs) are running) through HX, the heat is transferred to IWST. PRHRS prevents core meltdown in case of design basis (DBA) as well as beyond design basis (BDBA) events.

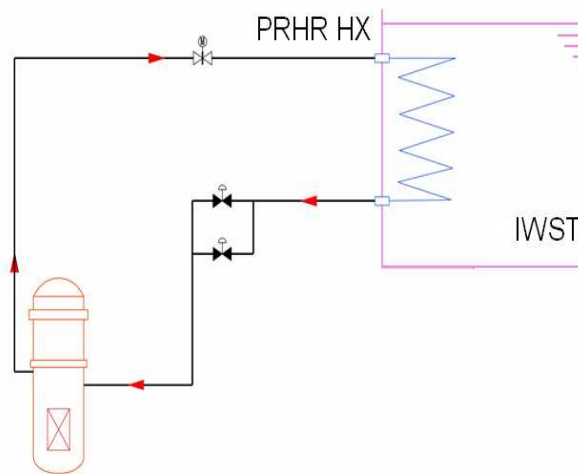


FIG. 174. Passive residual heat removal system of ACP100.

Passive core cooling system (PCCS)

This system, as shown in FIG. 175, provides the reactor coolant system emergency makeup and boration for steam system pipe failure. The safety injection provides adequate core cooling for small break LOCA (SBLOCA) i.e. steam generator tube rupture (SGTR) by core makeup tanks (CMTs), accumulators, and IWST. After CMTs, accumulators, and IWST have been injected, the containment is flooded sufficiently to provide recirculation flow. The PCCS maintains safe shutdown conditions for 72 hours or more, after an event without operator action or non-safety related power.

Passive containment cooling system (PCCS)

The PCCS, as shown in FIG. 176, provides long term heat removal from the containment in case of any DBA and BDBA including those associated with blackout and spray system failure. It limits containment pressure by containment HX-condenser-IWST, convective heat transfer or heat conduction, and IWST or sump recirculation. The steam condensed on containment HX and condensate collects in IWST/Sump via gutter arrangement.

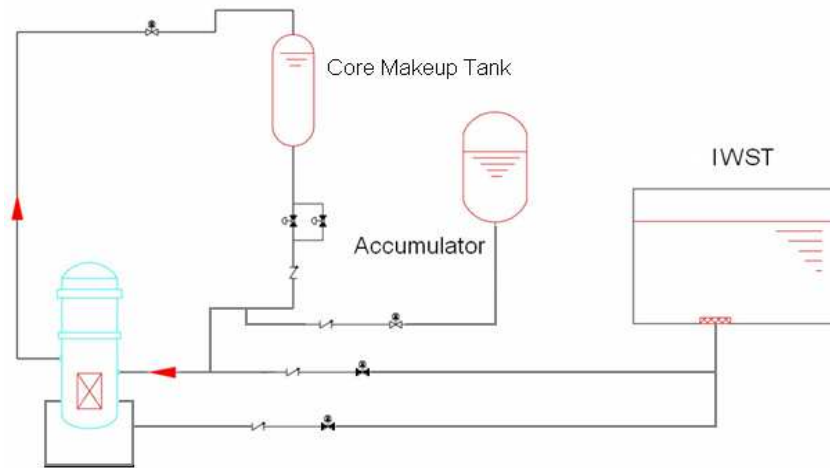


FIG. 175. Passive core cooling system of ACP100.

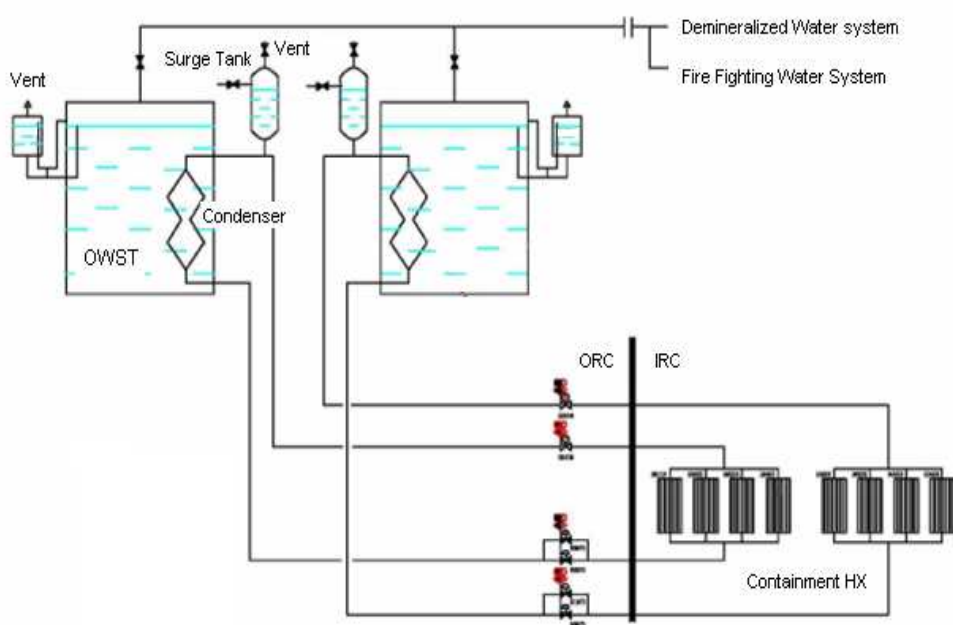


FIG. 176. Passive containment cooling system of ACP00.

I.7. INTERNATIONAL REACTOR INNOVATIVE AND SECURE (IRIS International Consortium)

IRIS is an integral, modular PWR design with a rated power of 335 MW(e). IRIS has been primarily focused on achieving design with innovative safety characteristics. The first line of defence in IRIS is to eliminate event initiators that could potentially lead to core damage. In IRIS, this concept is implemented through the 'safety-by-design'™ IRIS philosophy, which can be simply described as 'design the plant in such a way as to eliminate accidents from occurring, rather than coping with their consequences.' If it is not possible to eliminate certain accidents altogether, then the design inherently reduces their consequences and/or decreases

their probability of occurring. To complement its safety-by-design™, IRIS features limited and simplified passive systems as shown in FIG. 177. They include:

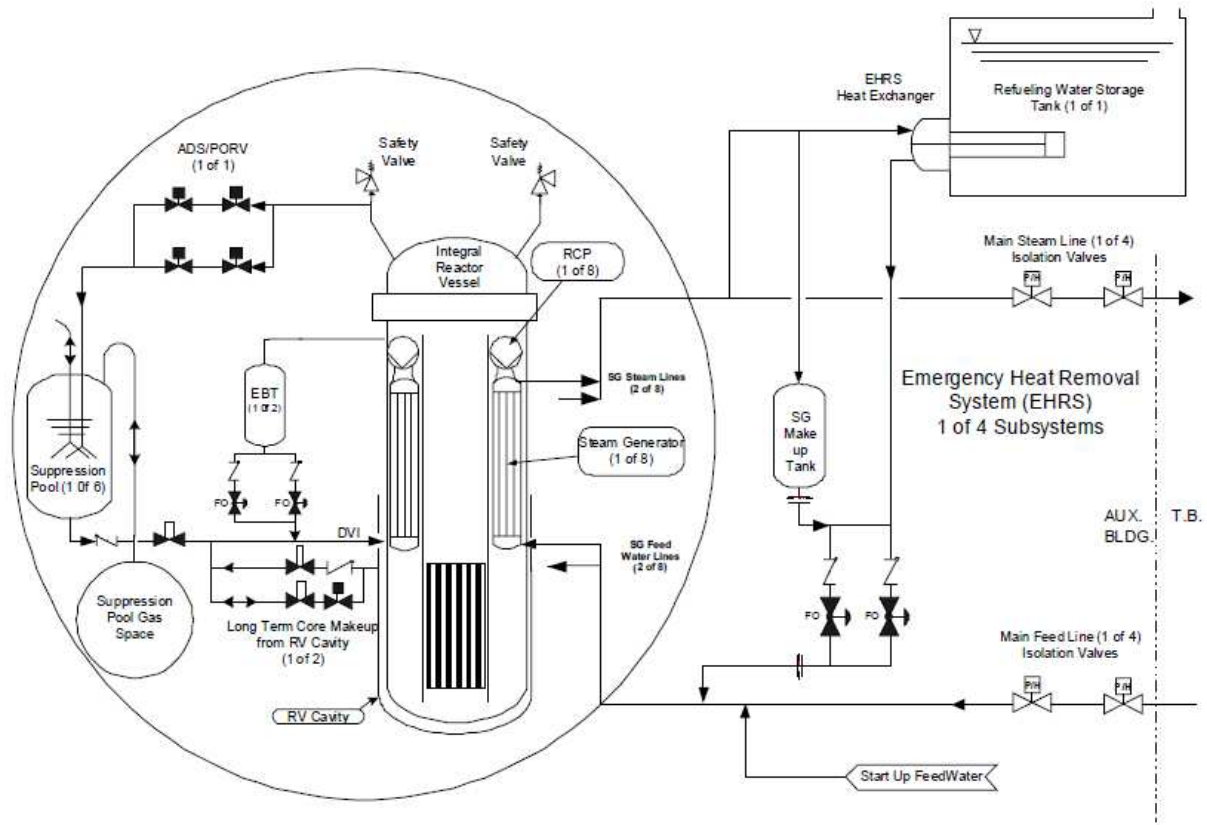


FIG. 177. IRIS passive safety system schematic.

Passive emergency heat removal system (EHRS) made of four independent subsystems, each of which has a horizontal, U-tube heat exchanger connected to a separate SG feed/steam line. These heat exchangers are immersed in the refuelling water storage tank (RWST) located outside the containment structure. The RWST water provides the heat sink to the environment for the EHRS heat exchangers. The EHRS is sized so that a single subsystem can provide core decay heat removal in the case of a loss of secondary system heat removal capability. The EHRS operates in natural circulation, removing heat from the primary system through the steam generators heat transfer surface, condensing the steam produced in the EHRS heat exchanger, transferring the heat to the RWST water, and returning the condensate back to the SG. The EHRS provides both the main post-LOCA depressurization (depressurization without loss of mass) of the primary system and the core cooling functions. It performs these functions by condensing the steam produced by the core directly inside the reactor vessel. This minimizes the break flow and actually reverses it for a portion of the LOCA response, while transferring the decay heat to the environment.

Two full-system pressure emergency boration tanks (EBTs) to provide a diverse means of reactor shutdown by delivering borated water to the RV through the direct vessel injection (DVI) lines. By their operation these tanks also provide a limited gravity feed makeup water to the primary system.

A small automatic depressurization system (ADS) from the pressurizer steam space, which assists the EHRS in depressurizing the reactor vessel when/if the reactor vessel coolant inventory drops below a specific level. This ADS has one stage and consist of two parallel 4

in. lines, each with two normally closed valves. The single ADS line downstream of the closed valves discharges into the pressure suppression system pool tanks through a sparger. This ADS function ensures that the reactor vessel and containment pressures are equalized in a timely manner, limiting the loss of coolant and thus preventing core uncover following postulated LOCAs even at low RV elevations.

A containment *pressure suppression system (PSS)* consists of six water tanks and a common tank for non-condensable gas storage. Each suppression water tank is connected to the containment atmosphere through a vent pipe connected to a submerged sparger so that steam released in the containment following a loss of coolant or steam/feed line break accident is condensed. The suppression system limits the peak containment pressure, following the most limiting blowdown event, to less than 1.0 MPa (130 psig), which is much lower than the containment design pressure. The suppression system water tanks also provide an elevated source of water that is available for gravity injection into the reactor vessel through the DVI lines in the event of a LOCA.

APPENDIX II

SET OF DEFINITIONS FOR RELIABILITY ASSESSMENT OF PASSIVE SAFETY SYSTEMS

Term	Definition
Actual components	A physical component of the system having material existence such as pipes, valves, heat exchangers, etc.
Adjoint algorithm	A numerical algorithm to evaluate derivatives in the reverse direction.
Adjoint equation	An equation involving adjoint operators and operands.
Adjoint operator	An operator B such that the inner product (Ax,y) and (x,By) are equal for a given operator A and for all elements x and y of a Hilbert space (mathematical space endowed with a property of inner product).
Aleatory uncertainty	Uncertainty due to variability of input and/or model parameters when the characterization of the variability is available (e.g. with probability density function, PDF).
Availability	The probability that a component, system, or structure is performing intended function at given time and under given conditions.
Available	The state of a system, structure or component being able to perform its intended function, under given conditions and at a given time.
Benchmark(ing)	Comparative exercise in which predictions of different computer codes and users for a given physical problem are compared with each other or with the results of a carefully controlled experimental study.
Code uncertainty	Uncertainties in the results of code prediction due to the approximations of physical models, correlations, numerical solution schemes, etc.
Conditional probability	The probability of an event, given that another event is known to have occurred.
Continuous probability density function	Probability density function of a continuous random variable.
Continuous random variable	A random variable takes values from an uncountable set, and the probability of any one value is zero, but a set of values can have positive probability.
Cumulative distribution function	Function giving, for all value x, the probability that the random variable X will be less than or equal to x.
Discrete probability density function	A list of probabilities associated with each possible values of the discrete random variable
Discrete random variable	A random variable which takes values from a countable set of specific values, each with some probability greater than zero
Dynamic PSA	PSA that utilises dynamic methods, such as dynamic fault trees, Markov models, and the dynamic flowgraph methodology, that can account for the coupling between systems through explicit consideration of time in system evolution and interaction
Elicitation process	A heuristic process for gathering evidence and data or answering questions on issues/problems of concern
Epistemic uncertainty	Uncertainty due to variability of input and/or model parameters when the corresponding variability characterization is not available or uncertainty due to any lack of knowledge or information in any phase or activity of

Term	Definition
	the modeling process.
Expert judgement	An approach for soliciting informed opinions from individuals with particular expertise.
Failure	The loss of ability of a system, structure or component to perform a required function during required time.
Failure Analysis	The logical, systematic examination of a system to identify the probability, causes, and consequences of potential failures.
Failure Cause	The circumstances during design, manufacturing or use which have induced or activated a failure mechanism.
Failure criteria	Logical and/or numerical relationships which define the system failure or physical conditions that define the component or structure failure.
Failure effect	The consequences a failure has on the operation, function, or status of a system.
Failure mechanism	The physical, chemical, electrical, thermal or other process that causes a failure.
Failure mode	Distinguishing physical or behavioural characteristic that can be associated with a failure.
Failure mode and effect analysis (FMEA)	Procedure by which each potential failure mode in a system is analyzed to determine its effect on the system and classify them according to its severity.
Failure point	The most probable point of the failure surface which is at the minimal distance of the origin in a Gaussian space.
Failure Rate	A function that describes the number of failures to a system, device or component that can be expected to take place over a given unit of time.
Failure surface	The surface defined by limit state function in multi-dimensional space that demarcates the state of failure from the state of success of the system, where the limit state function is zero.
Fault Tree	A graphical representation of an undesired event caused by a combination of factors arising from equipment failure, human error, or environmental events.
Fault Tree Analysis	A deductive technique in which an undesired state of a system is analysed using boolean logic to combine a series of lower-level events.
First-order reliability method (FORM)	Method of evaluation of the failure probability where the failure surface is approximated by a tangent hyper-plane passing through the design point.
Functional failure (in a passive safety system)	Failure of the passive system to perform its intended function due to deviations of process parameters or unknown phenomena's.
Fuzzy logic	An extension of the concept of a set in which the characteristic function which determines membership of an object in the set is not limited to 1 (a member) or 0 (not a member), but can take on any value between 0 and 1 as well.
Fuzzy set	The logic of approximate reasoning bearing the same relation to approximate reasoning that two valued logic to precise reasoning.
Global sensitivity	Sensitivity analysis which apportions the output variability to the variability of the input parameters when they vary in their whole uncertainty domains. This uncertainty is generally described using probability densities for factors.

Term	Definition
Hardware failure (in a passive safety system)	Failure of a component or structure that can impact operation of the passive system.
HAZOP – Hazard and operability study	Structured and systematic examination of all credible deviations from normal conditions in a process or operation in order to identify and evaluate potential hazards and operability problems.
Human error	An inappropriate or undesirable human decision or behaviour that reduces, or has the potential for reducing, effectiveness, safety, or system performance.
Limit state	The condition beyond which a safety system or structure is deemed to have failed.
Limit state function	A mathematical expression that divides an n-dimensional probability space into failure domain and safe domain.
Local sensitivity	Sensitivity analysis performed by estimating the partial derivatives of the output with respect to each input parameter around given nominal values. It gives a local measure of the output sensitivity which may vary with the nominal value.
Mission time	Time interval during which a system has to carry out its safety function after it is demanded.
Passive component	A component whose operation does not depend on operation of other systems or components, e.g. control system, energy source etc.
Passive system	Either a system which is composed of passive components and structures or a system which uses active components in a very limited way to initiate subsequent passive operation.
Performance indicator	A numerical value representing the performance of a safety system.
Perturbation theory	The study of solution to differential equations based on the assumption that perturbations in the given conditions of a problem cause only small changes in the solution.
Probabilistic safety assessment	A comprehensive, structured approach to identifying failure scenarios, constituting a conceptual and mathematical tool for deriving numerical estimates of risk.
Probability density function	Derivative, if exists, of the cumulative distribution function of a random variable.
Propagation of uncertainty	Evaluation of the effects of the input parameters uncertainty on the output uncertainty.
Reliability	The probability that a system will perform its intended function in a satisfactory manner for a given period of time $[0, t]$, when used under specified operating conditions.
Reliability Analysis	A quantification of the sources of failures in a system, with emphasis on the most significant contributors towards the overall system unreliability, in order to correct them and therefore improve the reliability of the fielded system.
Reliability index	A measure of the distance that the mean is away from the zero of the limit state function.
Response surface	Simplified mathematical expression as a function of input variables

Term	Definition
	designed to approximate outcomes of complex mathematical model or possible experimental outcomes.
Risk	<p>A multi-attribute quantity expressing hazard, danger or chance of harmful or injurious consequences associated with actual or potential exposures. It relates to quantities such as the probability that specific deleterious consequences may arise and the magnitude and character of such consequences.</p> <p>In mathematical terms, this can be expressed generally as a set of triplets, $R = \{S_i ; P_i ; X_i\}$, where S_i is an identification or description of a scenario i, P_i is the probability of that scenario and X_i is a measure of the consequence of the scenario.</p>
Risk-informed approach	A safety focused approach aimed at consideration of risk insights together with other factors effecting safety with the main goal to ensure that any decision that affecting safety is sound
Second order reliability method (SORM)	Method of evaluation of the failure probability where the failure surface is approximated by a tangent hyper-parabolic surface passing through the design point.
Unavailability	The complement of availability.
Uncertainty	<p>General:</p> <ol style="list-style-type: none"> 1. A state of having limited knowledge where it is impossible to exactly describe existing state or future outcome 2. The extent of our knowledge or ignorance <p>Statistics: The estimated amount by which an observed or calculated value may depart from true value</p>
Uncertainty analyses	An analysis to estimate the uncertainties and error bounds of the quantities involved in, and the results from, the solution of a problem.
Unreliability	The complement of reliability.
Virtual components	A phenomenological component of the system having no material existence which functions based on natural laws such as gravity, buoyancy, etc.

APPENDIX III

FRAMEWORK FOR CREATING A DATABANK TO GENERATE PROBABILITY DENSITY FUNCTIONS

III.1. INTRODUCTION

PSA analysis should be based on the best available data for the types of equipment and systems in the plant. In some cases very limited data may be available for evolutionary designs or new equipment, especially in the case of passive systems.

It has been recognized that difficulties arise in addressing the uncertainties related to the physical phenomena and characterizing the parameters relevant to the passive system performance evaluation due to the unavailability of a consistent operational and experimental data base. This lack of experimental evidence and validated data forces the analysts to resort to expert/engineering judgment to a large extent, hence making the results strongly dependent upon the expert elicitation process.

This prompts the need for the development of a framework for constructing a database to generate probability distributions for the parameters influencing the system behaviour.

III.2. OBJECTIVE OF THE TASK

The objective of the task was to develop a consistent framework aimed at creating probability distributions for the parameters relevant to the passive system performance evaluation.

In order to achieve this goal considerable experience and engineering judgement were also required to determine which existing data are most applicable to the new systems or which generic data bases or models provide the best information for the system design.

Eventually in case of absence of documented specific reliability data, documented expert judgement coming out from a well-structured procedure could be used to envisage sound probability distributions for the parameters under interest.

III.3. DESCRIPTION OF THE TASK

A table that lists the data collected on probability distribution functions was generated. The table consists of the following details:

Parameter Type

Parameters can be categorized as:

- Design parameters: These refer to the initial and boundary conditions (for instance the values taken by the design parameters, like the pressure in the reactor pressure vessel, the collapsed level in the vessel, etc.)
- Critical parameters: These refer to the factors driving the modes of failure of the system(e.g. non-condensable gas, undetected leak, heat loss)

- Process parameters: These are the physical variables to be adopted for the system under analysis. These include parameters such as flow rate, temperature, power, pressure, heat flux, thermal energy.
- Geometrical properties parameters: They can affect the system performance, as the heat exchange area and the system layout. Thus, they should be included in the list of parameters consistent with system reliability. These include parameters such as HX area, piping diameter, length.
- Material properties parameters: They can affect the system failure, for instance, to the failure modes related to the undetected leakages and heat losses. Thus, they should also be included in the list of parameters consistent with system reliability.
- T-H parameters: These parameters refer to the parameters and models adopted in the T-H analysis by T-H code simulation, including also T-H correlations defining, for instance, Reynolds number, Nusselt number and so on.

In the present study, however, the distinction of the parameters according to above categorization is not accomplished.

Type of distribution

This describes the choice of the distribution.

Distribution parameters

This specifies the parameters (mean, standard deviation, etc.) of the distribution, according to the available information.

Estimated range

The range of the distribution is assigned.

Typical system application

Obviously the parameters will have to be consistent with the specificities of the system under examination. Therefore, the table includes a specific passive system.

Basis

The rationale is aimed at supporting the values in the cells, as:

- Subjective assessment
- Engineering assessment
- Expert panel elicitation
- Experimental and/or operational inference

III.4. RECOGNIZED ISSUES

A major issue for this task is associated with the availability of scientific and engineering evidence of the effectiveness of the selected safety provisions (i.e. their physical performances and expected reliability). It might be expected that available operational and test data are inadequate to support the judgments on the reliability of the innovative solutions. It is expected to start the evaluation with qualitative expert judgements, which eventually, with the evolution of the design solutions and progressive research and development, will be replaced with quantitative measures.

III.5. Results

No indication of development of probabilistic distributions based on experimental investigation or operating experience comes out as a result of a literary survey. The PDFs assigned to the parameters to address the relative uncertainties are almost exclusively either based on engineering assessment or elicited from an expert panel.

As outlined before, this adds additional uncertainty in the sought reliability figure to be qualified.

III.6. Examples for specific cases

According to the task content, some examples, coming out from journal papers, are presented and conveniently integrated within the format provided above.

As reported, the earliest significant effort to quantify the reliability of such systems is represented by a methodology known as REPAS (Reliability Evaluation of Passive Safety Systems), which has been developed in late 1990s, cooperatively by ENEA, the University of Pisa, the Polytechnic of Milan and the University of Rome, that was later incorporated in the EU (European Union) RMPS (Reliability Methods for Passive Systems) project. This methodology is based on the evaluation of a failure probability of a system to carry out the desired function from the epistemic uncertainties of those physical and geometric parameters, which can cause a failure of the system.

Thus, first example (Table III-1) refers to the REPAS methodology application to the isolation condenser system of a SBWR, given in [74]. In that work, design and critical parameters are considered and both are assigned discrete values.

TABLE III- 1. EXAMPLE FROM REPAS APPLICATION

Parameter	Type of distribution	Distribution parameters	Estimated range	Typical system application	Basis	References
RPV pressure (MPa)	Discrete	Nominal* = 7	0.2-9	Isolation Condenser	REPAS/ Engineering judgement	Journal publication [74, 75]
RPV collapsed level (m)	Discrete	Nominal* = 8.7	12-May	Isolation Condenser	REPAS/ Engineering judgement	Journal publication [74, 75]
Pool level (m)	Discrete	Nominal* = 4.3	2-5 m	Isolation Condenser	REPAS/ Engineering judgement	Journal publication [74, 75]
Pool initial temperature (K)	Discrete	Nominal* = 303	280-368	Isolation Condenser	REPAS/ Engineering judgement	Journal publication [74, 75]
RPV non-condensable fraction	Discrete	Nominal* = 0	0-1	Isolation Condenser	REPAS/ Engineering judgement	Journal publication [74, 75]
Non-condensable fraction at the inlet of the IC piping	Discrete	Nominal* = 0	0-1	Isolation Condenser	REPAS/ Engineering judgement	Journal publication [74, 75]
Inclination of the IC piping on the suction side (deg)	Discrete	Nominal* = 0	0-10	Isolation Condenser	REPAS/ Engineering judgement	Journal publication [74, 75]
Heat Losses piping –IC suction (Kw)	Discrete	Nominal* = 5	0-100	Isolation Condenser	REPAS/ Engineering judgement	Journal publication [74, 75]
Initial condition liquid level –IC tubes, inner side (%)	Discrete	Nominal* = 100	0-100	Isolation Condenser	REPAS/ Engineering judgement	Journal publication [74, 75]
Undetected leakage (m ²)	Discrete	Nominal* = 0	0-10e ⁻⁵	Isolation Condenser	REPAS/ Engineering judgement	Journal publication [74, 75]
Partially opened valve in the IC discharge line (%)	Discrete	Nominal* = 100	1-100	Isolation Condenser	REPAS/ Engineering judgement	Journal publication [74, 75]

* Nominal value is assigned the highest probability

The RMPS methodology was successfully applied to several passive systems, such as the isolation condenser system of boiling water reactor as in Ref. [75] where again design and critical parameters are assigned discrete distributions, as shown in Table III-1.

Another example is provided by the residual passive heat removal system on the primary circuit (RP2) system. The RP2 system is an innovative passive system designed by the CEA, which is supposed to be implemented on a 900MWe pressurized water reactor, as described in [6]. This passive system is composed of three circuits dedicated for heat removal, each one being connected to a loop in the primary circuit. Each circuit includes an exchanger immersed in a cooling pool located inside the containment, and a valve to allow it to start. Table III-2 gives an example from RMPS application for pressurized water reactor.

A set of 24 parameters likely to be more or less uncertain at the time of the RP2 passive system start-up and significantly influencing the performances of the system was identified by expert judgment. These parameters are called the characteristic parameters.

TABLE III- 2. EXAMPLE FROM RMPS APPLICATION (PWR)

Parameter	Type of distribution	Distribution parameters	Estimated range	Typical system application	Basis	Reference
$I_{i=1,2,3}$ Instant at which the isolation valve opens	Composed			RP2	RMPS/Expert judgement	Journal publication Ref. [6]
$X_{i=1,2,3}$ Rate of non-condensable at the inlet of the exchanger	Exponential	$\lambda = 182$ $\mu = 0$		RP2	RMPS/Expert judgement	Journal publication Ref. [6]
$L_{i=1,2,3}$ Initial pool water level	Truncated normal	$\mu = 4.5$ $\sigma = 0.6$		RP2	RMPS/Expert judgement	Journal publication Ref. [6]
$T_{i=1,2,3}$ Initial pool water temperature	Truncated normal	$\mu = 303$ $\sigma = 20$	280-368	RP2	RMPS/Expert judgement	Journal publication Ref. [6]
$C_{i=1,2,3}$ Fouling of exchanger tubes	Truncated normal	$\mu = 15$ $\sigma = 5$	0-30	RP2	RMPS/Expert judgement	Journal publication (III)
$R_{i=1,2,3}$ Number of broken tubes in the exchanger	Exponential	$\lambda = 7$ $\mu = 0$		RP2	RMPS/Expert judgement	Journal publication Ref. [6]
PUI Percentage of nominal core power	Truncated normal	$\mu = 100$ $\sigma = 1$	98-102	RP2	RMPS/Expert judgement	Journal publication Ref. [6]
PP Pressure in the pressurizer	Truncated normal	$\mu = 155$ $\sigma = 4$	153-166	RP2	RMPS/Expert judgement	Journal publication Ref. [6]
ANS Decay of residual power (ANS law)	Truncated normal	$\mu = 10$ $\sigma = 5$	0-20	RP2	RMPS/Expert judgement	Journal publication Ref. [6]
$NGV_{i=1,2,3}$ Real secondary level in the three steam generators	Truncated normal	$\mu = 12.78$ $\sigma = 0.30$	12.08-13.91	RP2	RMPS/Expert judgement	Journal publication Ref. [6]

RMPS methodology is used for estimating the uncertainties in the fulfilment of a target related with the design of the Isolation Condenser of a 'CAREM-like' integral reactor. The passive-system assessment is made on a basis of a loss of heat sink transient. Given this scenario, the safety function is to remove the core decay heat after the actuation of the shutdown system, thus reducing the primary system pressure and leading the plant to a safe condition.

Table III-3 shows the selected parameters and their corresponding distributions. These parameters have been established from an expert panel, to duly find and justify the assumptions on the relevant parameters.

TABLE III- 3. RELEVANT SELECTED PARAMETERS AND THEIR DISTRIBUTIONS FOR THE CAREM-LIKE INTEGRAL REACTOR ISOLATION CONDENSER

Parameter	Type of distribution	Distribution parameters	Estimated range	Typical system application	Basis	Reference
Operational power	Normal			Isolation Condenser for CAREM-like reactor	RMPS/Expert judgement	Journal publication Ref. [76]
Scram delay	Lognormal			Isolation Condenser for CAREM-like reactor	RMPS/Expert judgement	Journal publication Ref. [76]
Safety rods total drop time	Lognormal			Isolation Condenser for CAREM-like reactor	RMPS/Expert judgement	Journal publication Ref. [76]
Decay power factor	Lognormal			Isolation Condenser for CAREM-like reactor	RMPS/Expert judgement	Journal publication Ref. [76]
Nominal Pressure	Normal			Isolation Condenser for CAREM-like reactor	RMPS/Expert judgement	Journal publication Ref. [76]
SCRAM: pressure set-point	Normal			Isolation Condenser for CAREM-like reactor	RMPS/Expert judgement	Journal publication Ref. [76]
IC: pressure set point	Normal			Isolation Condenser for CAREM-like reactor	RMPS/Expert judgement	Journal publication Ref. [76]
RPV dome water level	Normal			Isolation Condenser for CAREM-like reactor	RMPS/Expert judgement	Journal publication Ref. [76]
PCS mass flow rate	Normal			Isolation Condenser for CAREM-like reactor	RMPS/Expert judgement	Journal publication Ref. [76]
IC valves opening time	Normal			Isolation Condenser for CAREM-like reactor	RMPS/Expert judgement	Journal publication Ref. [76]
PHRHS pool temperature	Lognormal			Isolation Condenser for CAREM-like reactor	RMPS/Expert judgement	Journal publication Ref. [76]
IC tube thickness	Normal			Isolation Condenser for CAREM-like reactor	RMPS/Expert judgement	Journal publication Ref. [76]
Heat losses in IC vapor line	Normal			Isolation Condenser for CAREM-like reactor	RMPS/Expert judgement	Journal publication Ref. [76]
IC tube thickness: fouling	Lognormal			Isolation Condenser for CAREM-like reactor	RMPS/Expert judgement	Journal publication Ref. [76]

Parameter	Type of distribution	Distribution parameters	Estimated range	Typical system application	Basis	Reference
				reactor		
RPV dome heat losses (in steam zone)	Normal			Isolation Condenser for CAREM-like reactor	RMPS/Expert judgement	Journal publication Ref. [76]
IC friction	Normal			Isolation Condenser for CAREM-like reactor	RMPS/Expert judgement	Journal publication Ref. [76]

One more application of the RMPS methodology is offered in Ref. [16]. The aim of this exercise is ultimately to determine the performance reliability of the 2400MWth gas-cooled fast reactor DHR system operating in a ‘passive’ mode, taking into account the uncertainties of parameters retained for thermal-hydraulic calculations performed with the CATHARE 2 code. The DHR system consists of three dedicated DHR loops (redundancy) with secondary oops connected to an external water pool (the ultimate heat sink); the list of critical parameters is shown here below in Table III-4.

Ref. [77] presents the functional reliability analysis carried out for the passive decay heat removal system known as safety grade decay heat removal system (SGDHR) of Indian 500 MW(e) pool-type prototype fast breeder reactor. The analysis is carried out based on the overall approach reported in the reliability methods for passive system project.

Due to lack of adequate data, the uncertainty intervals were elicited from experts. The nature of probability distributions was determined from the information on variability from experimental data whenever they are available. Otherwise expert judgment is used. The probability density functions assigned are given in Table III- 5.

TABLE III-4. EXAMPLE FROM RMPS APPLICATION (GAS COOLED FAST REACTOR, GCFR)

Parameter	Type of distribution	Distribution parameters	Estimated range	Typical system application	Basis	Reference
T2DHR Initial pool water temperature	Normal	$\mu = 50^{\circ}\text{C}$	42.5°C-47.5°C	DHR for GCFR	RMPS/Engineering judgement	Journal publication Ref. [16]
P2DHR Secondary side pressure	Normal	$\mu = 1.0 \text{ MPa}$	0.85 MPa-1.15 MPa	DHR for GCFR	RMPS/Engineering judgement	Journal publication Ref. [16]
FRPLAQ Core regular pressure drop in laminar conditions	Normal	$\mu = 15\%$	0 %-30 %	DHR for GCFR	RMPS/Engineering judgement	Journal publication Ref. [16]
ECPLAQ Multiplicative factor to fluid heat transfer coefficient	Normal	$\mu = 5\%$	0 %-10 %	DHR for GCFR	RMPS/Engineering judgement	Journal publication Ref. [16]
REPLAQ Turbulent-to-laminar transition Reynolds number	Normal	$\mu = 5000$	4000-6000	DHR for GCFR	RMPS/Engineering judgement	Journal publication Ref. [16]
ECDHX1 DHX water convective heat transfer	Normal	$\mu = 5\%$	0 %-10 %	DHR for GCFR	RMPS/Engineering judgement	Journal publication Ref. [16]
ECDHX2 Exchange coefficient between secondary and ternary circuits	Normal	$\mu = 5\%$	0 %-10 %	DHR for GCFR	RMPS/Engineering judgement	Journal publication Ref. [16]
DPSUOF Pressure drop provided by the stopped DHR blower	Normal	$\mu = 15\%$	0 %-30 %	DHR for GCFR	RMPS/Engineering judgement	Journal publication Ref. [16]
FUITE Primary circuit natural leakage	Triangular	max = 2e-04 lower bound = 2e-5 upper bound = 2e-3	2e-5-2e-3	DHR for GCFR	RMPS/Engineering judgement	Journal publication Ref. [16]

TABLE III- 5. EXAMPLE FROM RMPS APPLICATION (FAST BREEDER REACTOR)

Parameter	Type of distribution	Distribution parameters	Estimated range	Typical system application	Basis	Reference
K_{PRI} Primary circuit pressure drop coefficient	Normal	$P1^* = 1, P2^* = 0.085$ Nominal = 0.148 (kgm) ⁻¹	-15% - +15%	DHR for FBR	RMPS/Expert judgement	Journal publication Ref. [77]
K_{DHXP} DHX pressure drop coefficient	Normal	$P1^* = 1, P2^* = 0.09$ Nominal = 0.473 (kgm) ⁻¹	-20% - +20%	DHR for FBR	RMPS/Expert judgement	Journal publication Ref. [77]
K_{IC} Intermediate circuit pressure drop coefficient	Normal	$P1^* = 1, P2^* = 0.085$ Nominal = 14 (kgm) ⁻¹	-15% - +15%	DHR for FBR	RMPS/Expert judgement	Journal publication Ref. [77]
K_{AIR} AHX pressure drop coefficient	Normal	$P1^* = 1, P2^* = 0.085$ Nominal = 0.16 (kgm) ⁻¹	-15% - +15%	DHR for FBR	RMPS/Expert judgement	Journal publication Ref. [77]
h_{DHX} DHX overall heat transfer coefficient	Normal	$P1^* = 1, P2^* = 0.06$ Nominal = 6211 W/(m ² K)	-10% - +10%	DHR for FBR	RMPS/Expert judgement	Journal publication Ref. [77]
h_{AHX} AHX overall heat transfer coefficient	Normal	$P1^* = 1, P2^* = 0.06$ Nominal = 57.3 W/(m ² K)	-10% - +10%	DHR for FBR	RMPS/Expert judgement	Journal publication Ref. [77]
A_{DHX} Surface area (number of tubes n)	Discrete	$P2^* = 0.05, 0.15, 0.8$ Nominal = 108	106 - 108	DHR for FBR	RMPS/Expert judgement	Journal publication Ref. [77]
A_{AHX} Surface area (number of tubes n)	Discrete	$P2^* = 0.05, 0.15, 0.8$ Nominal = 116	114 - 116	DHR for FBR	RMPS/Expert judgement	Journal publication Ref. [77]
Air inlet temperature	Normal	$P1^* = 1, P2^* = 0.1553$ Nominal = 30°C	18 - 42	DHR for FBR	RMPS/Expert judgement	Journal publication Ref. [77]
Decay heat	Normal	$P1^* = 1, P2^* = 0.05$	-10% - +10%	DHR for FBR	RMPS/Expert judgement	Journal publication Ref. [77]
FHT (flow halving time)-PSP (Primary Sodium Pump)	Discrete	$P2^* = 0.1677$ Nominal = 8 s	7 - 11	DHR for FBR	RMPS/Expert judgement	Journal publication Ref. [77]
FHT-SSP (Secondary Sodium Pump)	Discrete	$P2^* = 0.205$ Nominal = 4 s	3 - 6	DHR for FBR	RMPS/Expert judgement	Journal publication Ref. [77]
SCRAM delay	Normal	$P1^* = 1, P2^* = 0.05$ Nominal = 41 s	37 - 45	DHR for FBR	RMPS/Expert judgement	Journal publication Ref. [77]
Damper opening delay	Gamma	$P1^* = 16.0 (\alpha), P2^* = 16.724 (\eta)$ Nominal = 30 min	20 - 45	DHR for FBR	RMPS/Expert judgement	Journal publication Ref. [77]

REFERENCES

- [1] INTERNATIONAL ATOMIC ENERGY AGENCY, Safety Related Terms for Advanced Nuclear Plants, IAEA-TECDOC-626, IAEA, Vienna (1991).
- [2] INTERNATIONAL ATOMIC ENERGY AGENCY, Natural Circulation in Water Cooled Nuclear Power Plants. Phenomena, Models, and Methodology for System Reliability Assessments, IAEA-TECDOC-1474, Vienna (2005).
- [3] INTERNATIONAL ATOMIC ENERGY AGENCY, Status of Innovative Small and Medium Sized Reactor Designs 2005: Reactors with Conventional Refuelling Schemes, IAEA-TECDOC-1485, IAEA, Vienna (2006).
- [4] INTERNATIONAL ATOMIC ENERGY AGENCY, Status of Small Reactor Designs without On-site Refuelling: 2007, IAEA-TECDOC-1536, IAEA, Vienna (2007).
- [5] INTERNATIONAL ATOMIC ENERGY AGENCY, Status of Advanced Light Water Reactor Designs 2004, IAEA-TECDOC-1391, IAEA, Vienna (2004).
- [6] MARQUES, M., PIGNATEL, J. F., SAIGNES, P., D'AURIA, L., MULLER, C., BOLADO-LAVIN, C., KIRCHSTEIGER, C., LA LUMINA, V., IVANOV, L., Methodology for the reliability evaluation of a passive system and its integration into a probabilistic safety assessments, Nuclear Engineering and Design 235 (2005) 2612–2631.
- [7] NAYAK, A.K., GARTIA, M.R., ANTONY, A., VINOD, G., SINHA, R.K., Passive system reliability analysis using the APSRA methodology, Nuclear Engineering and Design 238 (2008) 1430–1440.
- [8] DELANEY, M.J., APOSTOLAKIS, G.E., and DRISCOLL, M.J., Risk-informed design guidance for future reactor systems, Nuclear Engineering and Design 235 (2005) 1537-1556.
- [9] INTERNATIONAL ATOMIC ENERGY AGENCY, Safety of Nuclear Power Plants: Design, Safety Standards Series, No. NS-R-1, IAEA, Vienna (2000).
- [10] INTERNATIONAL ATOMIC ENERGY AGENCY, Safety Assessment and Verification for Nuclear Power Plants, IAEA Safety Guide NS-G-1.2, IAEA, Vienna (2002).
- [11] PAGANI, L.P., APOSTOLAKIS, G.E., and HEJZLAR, P., The impact of uncertainties on the performance of passive systems, Nuclear Technology 149 (2005) 129-140.
- [12] GLÄSER, H., Experience in application of uncertainty methods and review of methods used in licensing, Exploratory OECD meeting of experts on best estimate calculations and uncertainty analysis, Aix-en-Provence, France, 13–14 May (2002).
- [13] D'AURIA, F., GIANNOTTI, W., Development of a code with internal assessment of uncertainty, Nuclear Technology 131 (2000) 159–196.
- [14] SAATY, T., Mathematical Methods of Operations Research, Dover Publications, Inc. (1988).
- [15] ZIO, E., CANTARELLA, M., CAMMI, A., The analytic hierarchy process as a systematic approach to the identification of important parameters for the reliability assessment of passive systems, Nuclear Engineering and Design 226 (2003) 311–336.
- [16] BASSI, C. & MARQUES, M., Reliability assessment of 2400 MW(th) Gas-cooled Fast Reactor natural circulation Decay Heat Removal in pressurized situations, Science and Technology of Nuclear Installations, Special issue “Natural Circulation in Nuclear Reactor Systems”, 2008.
- [17] BURGAZZI, L., Passive system reliability analysis: a study on the isolation condenser, Nuclear Technology 139 (2002) 3–9.
- [18] SALTELLI, A., et al., Sensitivity Analysis, John Wiley & Sons (2000).

- [19] RUBINSTEIN, R.Y., Simulations and Monte-Carlo method, Wiley Series in Probability and Mathematical Statistics, J. Wiley & Sons (1981).
- [20] MADSEN, H., et al., Methods of Structural Safety, Prentice Hall (1986).
- [21] RACKWITZ, R., et al., Structural reliability under combined random load sequences, Computers and Structures, 9 (1979) 489–494.
- [22] MELCHERS, R.E., Structural Reliability Analysis and Prediction, J.Wiley & Sons (1999).
- [23] DEVICTOR, N., Advances in methods for uncertainty and sensitivity analysis, Proceedings of the Workshop on Level 2 PSA and Severe Accident Management, OECD/NEA/CSNI/WGRISK, Köln, March (2004).
- [24] BOLADO, L. R., DEVICTOR, N., Uncertainty and sensitivity methods in support of PSA level 2, Workshop on Evaluation of uncertainties in Relation to Severe Accidents and Level 2 PSA, OECD Nuclear Energy Agency, 2006.
- [25] GUBA, A., MAKAI, M., PAL, L., Statistical aspects of best estimate method, Reliability Engineering and System Safety, 80 (2003) 217-232.
- [26] BURGAZZI, L., Addressing the uncertainties related to passive system reliability, Progress in Nuclear Energy 49 (2007) 93-102.
- [27] BURGAZZI, L., Evaluation of uncertainties related to passive systems performance, Nuclear Engineering Design 230 (2004) 93-106.
- [28] BURGAZZI, L., Reliability evaluation of passive systems through functional reliability assessment, Nuclear Technology 144 (2003) 145-151.
- [29] MISALE, I. M., Single phase natural circulation loops: Effects of geometry and heat sink temperature on dynamic behaviour and stability, DIPTeM/tec, Università degli Studi di Genova.
- [30] FERRERI, J.C., AMBROSINI, W., Verification of RELAP/Mod3 with Theoretical and Numerical Stability Results on Single-Phase, Natural Circulation in a Simple Loop, Autoridad Regulatoria Nuclear – Argentine , 1998.
- [31] D'AURIA, F., FROGHERI, M., MISALE, M., System Codes Capabilities in Predicting Instabilities in Single-Phase Natural Circulation, 4th Regional Meeting Nuclear Energy in Central Europe – Bled, Slovenia – September 7-10, 1997.
- [32] AMBROSINI, W., D'AURIA, F., PENNATI, J., FERRERI, C., Numerical Effects in the Prediction of Single-phase Natural Circulation Stability, UIT 2001 Conference, Modena, Italy, 2001.
- [33] GARIBALDI, P., Single-Phase Natural Circulation Loops: Effects of Geometry and Heat Sink Temperature on Dynamic Behaviour and Stability, PhD Thesis of the DIPTeM/Tec at the Università degli Studi di Genova , 2010.
- [34] OLOFSEN, E., The identification of strange attractors using experimental time series Master Thesis, Twente University Netherlands, 1991.
- [35] THEILER, J., Estimating the Fractal Dimension of Chaotic Time Series, The Lincoln Laboratory Journal 3 (1990).
- [36] WILKS, S., Determination of Sample Size for Setting Tolerance Limits, Annals of Mathematical Statistics (1941) 91-96.
- [37] GUBA, A.M., PÁL, L., Statistical aspects of best estimate method, Reliability Engineering & System Safety 80 (2003) 217-232.
- [38] ROSENSTEIN, M.T., COLLINS, J.J., DE LUCA, C.J., A practical method for calculating largest Lyapunov exponents from small data sets, Boston University, 1992.
- [39] COSCARELLI, E., RAIMATO, A., ARANEO, D., CHERUBINI, M., MUELLNER, N., AND D'AURIA, F., Accuracy Assessments with Fast Fourier Transform Based Method (FFTBM), 14th International Topical Meeting on Nuclear Reactor Thermal- Hydraulics (NURETH-14), Hilton Toronto Hotel, Toronto, Ontario, Canada, 25-29, September, 2011.

- [40] PROŠEK, A., D'AURIA, F., MAVKO, B., Review of quantitative accuracy assessments with fast Fourier transform based method (FFTBM), *Nuclear Engineering and Design* 217 (2002) 179-206.
- [41] AMBROSINI, W., BOVALINI, F., D'AURIA, F., Evaluation of accuracy of thermal hydraulic code calculations, *Energia Nucleare* 7 (1990) 5-16.
- [42] D'AURIA, F., DEBRECIN, N., GALASSI, G.M., Outline of the Uncertainty Methodology based on Accuracy Extrapolation, *Nuclear Technology* 109 (1995), p.21.
- [43] D'AURIA, F., GIANNOTTI, F.W., Development of Code with capability of Internal Assessment of Uncertainty. *Nuclear Technology* 131 (2000) p.159.
- [44] MADSEN, H. O., KRENK, S. AND LIND, N. C., *Methods of Structural Safety*, Prentice Hal Inc, New Jersey (1986).
- [45] MELCHERS, RE., *Structural reliability analysis and prediction*. 2nd ed. Wiley, New York (1999).
- [46] BURGAZZI L, FIORINI G.L, DE MAGISTRIS F, et al., Reliability assessment of passive safety systems. In Proc. 6th Int Conf. on Nucl Eng (ICONE-6), S. Diego, USA, 6340 (1998).
- [47] Durga Rao, K, et. al., Quantification of epistemic and aleatory uncertainties in level-1 probabilistic safety assessment studies. *Reliab Eng Syst Saf.* 92 (2007) 947-956.
- [48] OBLOW, E. M., Sensitivity theory for reactor thermal-hydraulics problems. *Nuclear Science and Engineering*, 68 (1978) 322-337.
- [49] PARKS, C.V., MAUDLIN, P.J., Application of differential sensitivity theory to a neutronic/thermal hydraulic reactor safety code. *Nuclear Technology* 54 (1981) 38-53.
- [50] GILES, M.B., AND PIERCE, N.A., An introduction to the adjoint approach to design. *Flow Turbulence and combustion*. 65 (2000) 393-415.
- [51] GILES, M.B., AND PIERCE, N.A., Analytic adjoint solutions for the quasi-1d Euler equations. *J. Fluid Mech.* 426 (2001) 327-345.
- [52] REUTHER, J., JAMESON, A., ALONSO, J..J., REMLINGER, M.J, SAUNDERS, D., Constrained multipoint aerodynamic shape optimization using and adjoint formulation and parallel computers, Part 2. *J. Aircraft* 36 (1999) 61–74.
- [53] GILKS, W. R., et al., *Markov Chain Monte Carlo in Practice: Interdisciplinary Statistics*, Chapman and Hall, New York (1996).
- [54] ZIO, E., AND PEDRONI, N., Estimation of the functional failure probability of a thermal-hydraulic passive system by Subset Simulation. *Nuclear Engineering and Design* 239 (2009) 580-599.
- [55] AU, S.K., Augmenting approximate solutions for consistent reliability analysis. *Probabilistic Engineering Mechanics* 22 (2007) 77-87.
- [56] JOHN, L.A., KANNAN, I, N., AND VELUSAMY, K., Adjoint operator approach to functional reliability analysis of passive fluid dynamical systems. *Reliab Eng & Syst Safety* 94 (2009) 1917-1926.
- [57] TERRENCE, J.A., *Applied numerical methods for engineers*. New York: John Wiley & Sons Inc (1994).
- [58] JOHN, A., KANNAN, I.N., AND VELUSAMY, K., Efficient reliability estimate of passive thermal hydraulic safety system with automatic differentiation, *Nuclear Engineering and Design* 240 (2010) 2768-2778.
- [59] GIERING, R. AND KAMINSKI, T., Recipes for adjoint code construction. *ACM Trans. Math. Software*. 24 (1998) 437–474.
- [60] GRIEWANK, A., *Evaluating Derivatives: Principles and Techniques of Algorithmic Differentiation*, *Frontiers in Applied Mathematics* 19 (2000), SIAM, Philadelphia.
- [61] AU, S.K. AND BECK, J. L., Estimation of small failure probabilities in high dimensions by subset simulation. *Probab. Eng. Mech* 16 (2001) 263-77.

- [62] ATHMALINGAM, S., AND VIJAYAKUMARAN, P.M., Operation Note for Safety Grade Decay Heat Removal Circuit, PFBR/3400/ON/1001, Dec-2000.
- [63] SCHUELLER, G.I., PRADLWARTER, P., Methods for reliability assessment of nonlinear systems under stochastic dynamic loading-a review. In proceedings of EURO DYN'93, Balkema; 751-9.
- [64] GOVINDARAJAN, S., Temperature Limits for Fuel Elements During Transients, PFBR/31110/DN/1012/Rev-A, 1995.
- [65] ANDRE, I.K., JOHN, A.C., Response Surfaces-Designs and Analyses, Marcel Dekker Inc, New York, USA, (1996).
- [66] ZANOCCO, P., GIMÉNEZ, M., DELMASTRO, D., D'AURIA, F., Self-pressurization behavior in integrated reactors, Heat and Technology 21(2003) 149-158.
- [67] MEZIO, F., "Evaluación de la fenomenología termohidráulica de un Condensador de Aislamiento y su impacto desde el punto de vista de la Seguridad Nuclear", Master Thesis of the "Instituto Balseiro", Bariloche-Argentina (2010).
- [68] MANACHE, G., MELCHING, C., Identification of reliable regression- and correlation-based sensitivity measures for importance ranking of water-quality model parameters, Environmental Modeling & Software, 23 (2008) 549-562.
- [69] D'AURIA, F., GALASSI, G.M., Methodology for the evaluation of the reliability of passive systems, PISA, DIMNP NT 420 (2000).
- [70] INTERNATIONAL ATOMIC ENERGY AGENCY, Component Reliability Data for Use in Probabilistic Safety Assessment, IAEA-TECDOC-478, IAEA, Vienna (1988).
- [71] TENCHINE D. et al. Status of CATHARE code for sodium cooled fast reactor, Nuclear Engineering and Design 245 (2012) 140-152.
- [72] PIALLA, D., Computation of PHENIX ultimate test (Natural Convection) with CATHARE code – post-calculation, Ref. DEN/CAD/DER/SSTH/LDAS/NT/2010-151/A.
- [73] MARQUÈS M., Reliability analysis of 2400 MW(th) gas-cooled fast reactor natural circulation decay heat removal system, PSA 2011, Wilmington (USA), 13-17 March (2011).
- [74] PIERRO, F., ARANEO, D., GALASSI, G., AND D'AURIA, F., Application of REPAS Methodology to Assess the Reliability of Passive Safety Systems by, Hindawi Publishing Corporation Science and Technology of Nuclear Installations Volume 2009, Article ID 768947, 18 pages, doi:10.1155/2009/768947.
- [75] MARQUES, M., et. al., Reliability Methods for Passive Safety Functions. Proceedings of the International Conference ICONE 10, Arlington, VA, USA, 14–18 April 2002.
- [76] LORENZO, G., BURGAZZI, L., MARQUES, M., GIMENEZ, M, et al., Assessment of an Isolation Condenser of an Integral Reactor in View of Uncertainties in Engineering Parameters, Science and Technology of Nuclear Installations 2011 (2011), Article ID 827354.
- [77] MATHEWS, T., RAMAKRISHNAN, M., PARTHASARATHY, U., JOHN, A., SENTHIL, K. C., Functional Reliability Analysis of Safety Grade Decay Heat Removal System of Indian 500 MW(e) PFBR. Nuclear Engineering and Design 238 (2008), 2369–2376.

ABBREVIATIONS

ADS	Automatic Depressurization System
AHWR	Advanced Heavy Water Reactor
ALWR	Advanced Light Water Reactor
APSRA	Assessment of Passive System Reliability
BDBA	Beyond Design Basis Accident
BE	Best Estimate
CCF	Common Cause Failure
CHF	Critical Heat Flux
CHRS	Containment Heat Removal System
CRDM	Control Rod Drive Mechanism
CMT	Core Makeup Tank
CT	Compensating Tank
CRP	Coordinated Research Project
DBA	Design Basis Accident
DHRS	Decay Heat Removal System
DMCS	Direct Monte Carlo Simulation
DSL	Design Safety Limit
DVI	Direct Vessel Injection
ECCS	Emergency Core Cooling System
EBT	Emergency Boron Tank
ECT	Emergency Cooldown Tank
EJ	Expert Judgement
EHRS	Emergency Heat Removal System
FAST	Fourier Amplitude Sensitivity Test
FFTBM	Fast Fourier Transformation Based Method
FMEA	Failure Mode and Effect Analysis
FT	Fault Tree
GDWP	Gravity Driven Water Pool
HAZOP	Hazard and Operability
HS	Heat Sink
HX	Heat Exchanger
iPWR	integral Pressurized
IC	Isolation Condenser

IE	Initiating Event
I&C	Instrumentation and Control
IHX	Intermediate Heat Exchanger
IWST	Integral Water Storage Tank
KOFA	Korean Optimized Fuel Assembly
L2	L2 Test Facility
LEU	Low Enriched Uranium
LOCA	Loss of Coolant Accident
LWCR	Light Water Cooled Reactor
MC	Monte Carlo
MFIV	Main Feedwater Isolation Valve
MHT	Main Heat Transport
MSIV	Main Steam Isolation Valve
NC	Natural Circulation or Natural Convection
NCL	Natural Circulation Loop
NPP	Nuclear Power Plant
NSSS	Nuclear Steam Supply System
PCC	Partial Correlation Coefficients
PCCS	Passive Containment Cooling System
PDF	Probability Density Function
PI	Performance Indicator
POV	Pressure Operated Valve
PRA	Probabilistic Risk Assessment
PRC	Partial Regression Coefficient
PRHR	Passive Residual Heat Removal
PSA	Probabilistic Safety Assessment
PSP	Primary Sodium Pump
PSS	Pressure Suppression System
PZR	Pressurizer
RCM	Response Conditioning Method
REPAS	Reliability Evaluation of Passive Safety System
RIDM	Risk Informed Decision Making
RHRS	Residual Heat Removal System
RMPS	Reliability Methods for Passive Systems
RPV	Reactor Pressure Vessel

SB-LOCA	Small Break Loss of Coolant Accident
SBO	Station Blackout
SBWR	Simplified Boiling Water Reactor
SDA	Standard Design Approval
SDHR	Safety Decay Heat Removal
SG	Steam Generator
SGTR	Steam Generator Tube Rupture
SGDHRS	Safety Grade Decay Heat Removal System
SMR	Small and Medium-sized Reactors or Small Modular Reactors
SRC	Standardized Regression Coefficient
SRS	Simple Random Sampling
T-H	Thermal Hydraulics

CONTRIBUTORS TO DRAFTING AND REVIEW

Araneo, D.	University of Pisa, Italy
Arul, J.	Indira Gandhi Centre for Atomic Research (IGCAR)
Burgazzi, L.	National Agency for New Technologies, Energy and Sustainable Economic Development (ENEA), Italy
Bykov, M.A.	OKB Gidropress, Russian Federation
Gimenez, M.	Comisión Nacional de Energía Atómica (CNEA), Argentina
Hidayatullah, H.	International Atomic Energy Agency
Jain, V.	Bhabha Atomic Research Centre (BARC), India
Kryuchkov, M.E.	OKB Gidropress, Russian Federation
Kuznetsov, V. V.	International Atomic Energy Agency
Lyubarskiy, A.	International Atomic Energy Agency
Marques, M.	French Atomic Energy Commission (CEA), France
Mezio, F.	Comisión Nacional de Energía Atómica (CNEA), Argentina
Nayak, A.K.	Bhabha Atomic Research Centre (BARC), India
Qureshi, K.R.	International Atomic Energy Agency
Saha, D.	Bhabha Atomic Research Centre (BARC), India
Subki, M.H.	International Atomic Energy Agency
Susyadi, S.	International Atomic Energy Agency

Research Coordination Meetings (RCMs)

Vienna, Austria: 31 March – 3 April 2009, 16 – 19 March 2010,
26 – 28 April 2011, and 24 – 26 April 2012



IAEA

International Atomic Energy Agency

No. 23

ORDERING LOCALLY

In the following countries, IAEA priced publications may be purchased from the sources listed below or from major local booksellers.

Orders for unpriced publications should be made directly to the IAEA. The contact details are given at the end of this list.

AUSTRALIA

DA Information Services

648 Whitehorse Road, Mitcham, VIC 3132, AUSTRALIA

Telephone: +61 3 9210 7777 • Fax: +61 3 9210 7788

Email: books@dadirect.com.au • Web site: <http://www.dadirect.com.au>

BELGIUM

Jean de Lannoy

Avenue du Roi 202, 1190 Brussels, BELGIUM

Telephone: +32 2 5384 308 • Fax: +32 2 5380 841

Email: jean.de.lannoy@euronet.be • Web site: <http://www.jean-de-lannoy.be>

CANADA

Renouf Publishing Co. Ltd.

5369 Canotek Road, Ottawa, ON K1J 9J3, CANADA

Telephone: +1 613 745 2665 • Fax: +1 643 745 7660

Email: order@renoufbooks.com • Web site: <http://www.renoufbooks.com>

Bernan Associates

4501 Forbes Blvd., Suite 200, Lanham, MD 20706-4391, USA

Telephone: +1 800 865 3457 • Fax: +1 800 865 3450

Email: orders@bernan.com • Web site: <http://www.bernan.com>

CZECH REPUBLIC

Suweco CZ, spol. S.r.o.

Klecakova 347, 180 21 Prague 9, CZECH REPUBLIC

Telephone: +420 242 459 202 • Fax: +420 242 459 203

Email: nakup@suweco.cz • Web site: <http://www.suweco.cz>

FINLAND

Akateeminen Kirjakauppa

PO Box 128 (Keskuskatu 1), 00101 Helsinki, FINLAND

Telephone: +358 9 121 41 • Fax: +358 9 121 4450

Email: akatilaus@akateeminen.com • Web site: <http://www.akateeminen.com>

FRANCE

Form-Edit

5 rue Janssen, PO Box 25, 75921 Paris CEDEX, FRANCE

Telephone: +33 1 42 01 49 49 • Fax: +33 1 42 01 90 90

Email: fabien.boucard@formedit.fr • Web site: <http://www.formedit.fr>

Lavoisier SAS

14 rue de Provigny, 94236 Cachan CEDEX, FRANCE

Telephone: +33 1 47 40 67 00 • Fax: +33 1 47 40 67 02

Email: livres@lavoisier.fr • Web site: <http://www.lavoisier.fr>

L'Appel du livre

99 rue de Charonne, 75011 Paris, FRANCE

Telephone: +33 1 43 07 50 80 • Fax: +33 1 43 07 50 80

Email: livres@appeldulivre.fr • Web site: <http://www.appeldulivre.fr>

GERMANY

Goethe Buchhandlung Teubig GmbH

Schweitzer Fachinformationen

Willstätterstrasse 15, 40549 Düsseldorf, GERMANY

Telephone: +49 (0) 211 49 8740 • Fax: +49 (0) 211 49 87428

Email: s.dehaan@schweitzer-online.de • Web site: <http://www.goethebuch.de>

HUNGARY

Librotade Ltd., Book Import

PF 126, 1656 Budapest, HUNGARY

Telephone: +36 1 257 7777 • Fax: +36 1 257 7472

Email: books@librotade.hu • Web site: <http://www.librotade.hu>

INDIA

Allied Publishers

1st Floor, Dubash House, 15, J.N. Heredi Marg, Ballard Estate, Mumbai 400001, INDIA
Telephone: +91 22 2261 7926/27 • Fax: +91 22 2261 7928
Email: alliedpl@vsnl.com • Web site: <http://www.alliedpublishers.com>

Bookwell

3/79 Nirankari, Delhi 110009, INDIA
Telephone: +91 11 2760 1283/4536
Email: bkwell@nde.vsnl.net.in • Web site: <http://www.bookwellindia.com>

ITALY

Libreria Scientifica "AEIOU"

Via Vincenzo Maria Coronelli 6, 20146 Milan, ITALY
Telephone: +39 02 48 95 45 52 • Fax: +39 02 48 95 45 48
Email: info@libreriaaeiou.eu • Web site: <http://www.libreriaaeiou.eu>

JAPAN

Maruzen Co., Ltd.

1-9-18 Kaigan, Minato-ku, Tokyo 105-0022, JAPAN
Telephone: +81 3 6367 6047 • Fax: +81 3 6367 6160
Email: journal@maruzen.co.jp • Web site: <http://maruzen.co.jp>

NETHERLANDS

Martinus Nijhoff International

Koraalrood 50, Postbus 1853, 2700 CZ Zoetermeer, NETHERLANDS
Telephone: +31 793 684 400 • Fax: +31 793 615 698
Email: info@nijhoff.nl • Web site: <http://www.nijhoff.nl>

Swets Information Services Ltd.

PO Box 26, 2300 AA Leiden
Dellaertweg 9b, 2316 WZ Leiden, NETHERLANDS
Telephone: +31 88 4679 387 • Fax: +31 88 4679 388
Email: tbeysens@nl.swets.com • Web site: <http://www.swets.com>

SLOVENIA

Cankarjeva Založba dd

Kopitarjeva 2, 1515 Ljubljana, SLOVENIA
Telephone: +386 1 432 31 44 • Fax: +386 1 230 14 35
Email: import.books@cankarjeva-z.si • Web site: http://www.mladinska.com/cankarjeva_zalozba

SPAIN

Diaz de Santos, S.A.

Librerias Bookshop • Departamento de pedidos
Calle Albasanz 2, esquina Hermanos Garcia Noblejas 21, 28037 Madrid, SPAIN
Telephone: +34 917 43 48 90 • Fax: +34 917 43 4023
Email: compras@diazdesantos.es • Web site: <http://www.diazdesantos.es>

UNITED KINGDOM

The Stationery Office Ltd. (TSO)

PO Box 29, Norwich, Norfolk, NR3 1PD, UNITED KINGDOM
Telephone: +44 870 600 5552
Email (orders): books.orders@tso.co.uk • (enquiries): book.enquiries@tso.co.uk • Web site: <http://www.tso.co.uk>

UNITED STATES OF AMERICA

Bernan Associates

4501 Forbes Blvd., Suite 200, Lanham, MD 20706-4391, USA
Telephone: +1 800 865 3457 • Fax: +1 800 865 3450
Email: orders@bernan.com • Web site: <http://www.bernan.com>

Renouf Publishing Co. Ltd.

812 Proctor Avenue, Ogdensburg, NY 13669, USA
Telephone: +1 888 551 7470 • Fax: +1 888 551 7471
Email: orders@renoufbooks.com • Web site: <http://www.renoufbooks.com>

United Nations

300 East 42nd Street, IN-919J, New York, NY 1001, USA
Telephone: +1 212 963 8302 • Fax: 1 212 963 3489
Email: publications@un.org • Web site: <http://www.unp.un.org>

Orders for both priced and unpriced publications may be addressed directly to:

IAEA Publishing Section, Marketing and Sales Unit, International Atomic Energy Agency
Vienna International Centre, PO Box 100, 1400 Vienna, Austria
Telephone: +43 1 2600 22529 or 22488 • Fax: +43 1 2600 29302
Email: sales.publications@iaea.org • Web site: <http://www.iaea.org/books>

International Atomic Energy Agency
Vienna
ISBN 978-92-0-108614-3
ISSN 1011-4289